

Isolation and Characterisation of
Muscle Satellite Cells from Differentiating
Human Embryonic Stem Cells

James Parris

PhD Thesis

A thesis submitted for the degree of Doctor of Philosophy in
the Institute of Human Genetics, Newcastle University

Abstract

Muscular dystrophies are a category of diseases in which the muscle fibres degrade over time. At present there is no known cure, however a great deal of promise exists in cell replacement therapy, which has been successful in alleviating animal models of muscular dystrophy. Unfortunately, attempts to use stem cell therapy to cure or treat muscular dystrophies in humans have been unsuccessful, despite many different approaches to isolating and transplanting potentially myogenic cells. While skeletal muscle differentiation of embryonic stem cells has previously been reported, a simple and efficient method for the isolation of myogenic precursors from human ES cells has not been established. Recently, advances in induced pluripotent stem cell technology have brought the possibility of patient-specific pluripotent cell lines within reach, though a great deal of work needs to be done to understand the reprogramming process and the differentiation potential of these cells. This technology provides another avenue for cell therapy treatment of muscular dystrophies.

Aims: The primary goals of the work described in this thesis were to develop a novel method of differentiating human embryonic stem cells to muscle satellite cells or comparable myogenic precursors and to isolate them using fluorescence activated cell sorting based on the expression of satellite cell-specific genes or surface proteins.

Results: Myoblast conditioned medium was used as the primary means of driving myogenic differentiation of hES cells, measured by flow cytometry analysis of surface marker expression and quantitative PCR analysis of myogenic gene expression. During ES cell differentiation, isolation of a pure, differentiated population of cells can be difficult. A variety of satellite cell surface markers were examined in human adult and foetal myoblast lines to test potential targets for FACS isolation. In addition, a reporter construct was developed with the intent of having the *PAX7* promoter drive expression of GFP and a line of hES cells containing this construct was established. The differentiation strategy developed for hES cells was also tested on a line of iPS cells and a new line of iPS cells were generated from a patient with Duchenne muscular dystrophy.

Conclusions: Several viable candidates for surface marker selection of satellite cells were identified including CD56, CD106, and M-cadherin. However, despite trying a number of different approaches of differentiating hES cells, none resulted in a highly efficient method for generating myogenic precursors. The small number of myogenic cells produced was confirmed by flow cytometry, qPCR, and immunostaining analysis.

Acknowledgements

I would like to take this opportunity to thank a few of the many people who supported me, both in work and in life, throughout my doctoral study.

First, I would like to thank my advisor, Dr Lyle Armstrong, for his knowledge and insight. He kept both me and my project focused and did an excellent job balancing my need for guidance with my desire for independence. His door was always open and I always left his office with words of encouragement. I also wish to thank Dr Majlinda Lako for her help and support throughout my time in Newcastle.

Second, I wish to thank my lab, the Stem Cell Group, as well as Ian Dimmick and Rebecca Stewart for all of their help on my project. The people in lab were a constant source of inspiration, entertainment, and friendship and I am fortunate to have had the pleasure of working with them. I would especially like to thank my dear friend, Kasia, for helping me get through each day, no matter how tired or frustrated I was. And I will always be grateful to Sun, for his help in all the little things.

Finally, I want to thank my family and my fiancé, Ritika, for their never-ending support, love, and encouragement.

Contents

Abstract.....	I
Acknowledgements.....	II
Contents.....	III
Declaration.....	VI
Table of Figures.....	VII
Table of Tables.....	XV
Abbreviations.....	XVI
Chapter 1: Introduction.....	1
1.1 <i>Skeletal Muscle Development</i>	1
1.2 <i>The Muscle Satellite Cell and Regeneration</i>	2
1.2.1 Origin of the Satellite Cell.....	2
1.2.2 The Satellite Cell Niche.....	3
1.2.3 Molecular Signature of Satellite Cells.....	4
1.2.4 Adult Muscle Regeneration.....	4
1.3 <i>Stem Cell-Based Therapeutic Muscle Regeneration</i>	7
1.3.1 Early Attempts to Alleviate DMD.....	7
1.3.2 Transplantation of Isolated Satellite Cells.....	8
1.3.3 Alternative Sources of Myogenic Cells.....	8
1.3.4 Calculation of the Number of Cells Needed for Therapeutic Trials.....	9
1.4 <i>Embryonic Stem Cells</i>	10
1.4.1 Derivation of Embryonic Stem Cells.....	10
1.4.2 Embryonic Stem Cell Pluripotency.....	11
1.4.3 Differences between Mouse and Human Embryonic Stem Cells.....	15
1.4.4 Culture and Characterisation of Embryonic Stem Cells.....	16
1.4.5 Differentiation of Embryonic Stem Cells to Skeletal Muscle.....	18
1.5 <i>Induced Pluripotent Stem Cells</i>	20
1.5.1 A Brief History of Reprogramming.....	20
1.5.2 The Events of iPS Cell Reprogramming.....	22
1.6 <i>Project Aims</i>	24
Chapter 2: Materials and Methods.....	25
2.1 <i>Cell Culture</i>	25
2.1.1 Adult and Foetal Myoblast Culture.....	25

2.1.2	hES Cell Culture.....	26
2.1.2.1	Feeder Preparation.....	26
2.1.2.2	hES Cell Maintenance and Passaging.....	26
2.1.2.3	hES Cell Monolayer Differentiation.....	28
2.1.2.4	hES Cell Co-culture Differentiation.....	29
2.1.3	Culture and Differentiation of iPS Clone IV Cells.....	30
2.1.4	Culture of DMD Fibroblast Cells.....	30
2.2	<i>Generation of the Pax7P-GFP Construct</i>	30
2.2.1	PCR Isolation of the PAX7 Promoter.....	30
2.2.2	Cloning of the PAX7 Promoter into pCR 2.1-TOPO and pEGFP-1 Vectors.....	31
2.2.3	Nucleofection of the Pax7P-GFP Construct into Adult Human Myoblasts.....	32
2.2.4	Nucleofection of the Pax7P-GFP Construct into H9 Cells.....	33
2.3	<i>Generation and Culture of DMD Induced Pluripotent Stem Cells</i>	35
2.3.1	Preparation of hES Conditioned Medium.....	35
2.3.2	Attempted Generation of DMD iPS Cells using Multi-gene <i>OCT4/SOX2/KLF4/MYC (OSKM) Construct</i>	35
2.3.3	Generation of DMD iPS Cells from Stemgent <i>OCT4/SOX2/LIN28/NANOG</i> (OSLN) Reprogramming Lentivirus Set.....	36
2.3.4	Freezing Down and Thawing F055 iPS Cells.....	37
2.3.5	Differentiation of F055 iPS Cells.....	38
2.4	<i>Flow Cytometry and Fluorescence Activated Cell Sorting (FACS)</i>	38
2.4.1	Staining and Flow Cytometry of Myoblasts.....	38
2.4.2	Staining and Flow Cytometry of Differentiated hES Cell Cultures.....	38
2.4.3	FACS of BMP-4 Co-culture and H9 Pax7-GFP Differentiations.....	39
2.4.4	Flow Analysis of MyoD Expression in the BMP4 D21 Differentiation.....	40
2.5	<i>Quantitative Polymerase Chain Reaction (qPCR) Analysis</i>	40
2.5.1	RNA Isolation and cDNA Preparation.....	40
2.5.2	Quantitative Polymerase Chain Reaction.....	41
2.6	<i>Cell Staining Procedures</i>	43
2.6.1	Immunostaining of Differentiated hES Cells.....	43
2.6.2	Immunostaining of Undifferentiated and Differentiated F055 iPS Cells.....	43
2.6.3	Alkaline Phosphatase Staining of Undifferentiated F055 iPS Cells.....	43
2.7	<i>Microarray Analysis of Differentiated H9 Pax7-GFP Cells</i>	44
Chapter 3: Expression of Myogenic Genes and Cell Surface Markers in Adult and Foetal Myoblast Lines.....		45
3.1	<i>Introduction</i>	45
3.2	<i>Results</i>	47
3.2.1	Flow Cytometry Analysis of Myoblast Surface Markers.....	47

3.2.2 qPCR Analysis of Myoblast Lines for Myogenic Gene Expression.....	50
3.3 Discussion.....	51
Chapter 4: Myogenic Differentiation of hES Cells.....	55
4.1 Introduction.....	55
4.2 Results.....	57
4.2.1 Monolayer Differentiation using Horse Serum and Conditioned Medium.....	57
4.2.2 Modified Conditioned Medium Differentiation.....	60
4.2.3 Conditioned Medium from Various Myoblast Lines.....	63
4.2.4 Differentiation with Activin A and Conditioned Medium.....	65
4.2.5 Myoblast Co-culture and BMP-4 Treatment.....	67
4.3 Discussion.....	74
Chapter 5: Isolation of Differentiated hES Cells Using a Pax7-GFP Reporter Construct.....	80
5.1 Introduction.....	80
5.2 Results.....	82
5.2.1 Creation of the Pax7P-GFP Construct.....	82
5.2.2 Generation of the H9 Pax7-GFP Cell Line.....	84
5.2.3 Differentiation of H9 Pax7-GFP Cells.....	84
5.2.4 FACS of Differentiated H9 Pax7-GFP Cells.....	88
5.3 Discussion.....	92
Chapter 6: Myogenic Differentiation of iPS Cells and Generation of a DMD iPS Cell Line.....	95
6.1 Introduction.....	95
6.2 Results.....	98
6.2.1 Myogenic Differentiation of iPS Cells.....	98
6.2.2 Generation of a DMD iPS Cell Line.....	101
6.2.3 Differentiation Potential of F055 iPS Cells.....	109
6.3 Discussion.....	111
Chapter 7: Conclusions.....	115
References.....	118

Declaration

I, James J. Parris, confirm that no part of the material offered has previously been submitted by me for a degree in this or any other University. Material generated through joint work has been acknowledged and the appropriate publications cited. In all other cases, material from the work of others has been acknowledged, and quotations and paraphrases suitably indicated.

Signature:

A handwritten signature in black ink that reads "James J. Parris". The signature is written in a cursive style with a large, prominent initial "J" and "P".

Date: 5/23/2011

Table of Figures

Figure 1.1.....1

Embryonic Somitogenesis: A schematic showing the location of early myogenesis in the developing embryo. Somites are formed from paraxial mesoderm on each side of the neural tube and form the dermomyotome, myotome, and sclerotome. Reproduced from (Buckingham, Bajard et al. 2003).

Figure 1.2.....5

Adult Muscle Regeneration: An outline of adult muscle regeneration showing the growth factors which promote (green) and inhibit (red) satellite cell activation, myoblast proliferation, and differentiation as well as some of the key genes expressed in each population of cells (green). After muscle injury (A), satellite cells are activated (B) and begin proliferating. Some of these cells will reoccupy the satellite cell niche (F) while others will differentiate and fuse (C) forming an early myofibre with central nuclei (D) before maturing (E). Reproduced from (Charge and Rudnicki 2004).

Figure 1.3.....10

Human ES Cell Derivation: Derivation of human embryonic stem cell lines from the ICM of a blastocyst cultured from a surplus IVF embryo. Modified from (Hasegawa, Pomeroy et al. 2010).

Figure 1.4.....12

Lineage development during early mouse embryogenesis: The blastocyst is formed from the late cleavage stage embryo. As the blastocyst develops, cells of the ICM become specified to either epiblast (green) or primitive endoderm (yellow) fates while the trophectoderm (red) will become the trophoblast. The epiblast eventually develops into the embryo proper, the primitive endoderm into components of the yolk sac, and the trophoblast into the placenta. Reproduced from (Ralston and Rossant 2010).

Figure 1.5.....14

Control of Transcription by Oct4, Sox2, and Nanog: Genes involved in the maintenance of pluripotency and early differentiation bound by Oct4/Sox2 and Nanog. Reproduced from (Boyer, Lee et al. 2005).

Figure 1.6.....16

Differences in Signaling Pathways between (a) Mouse and (b) Human ES cells: The most notable differences are the effects of BMP-4, which promotes pluripotency in mouse ES cells but differentiation in human ES cells, and LIF, which prevents differentiation in mouse but not human ES cells. Modified from (Hyslop, Armstrong et al. 2005).

Figure 1.7.....21

Methods of Reprogramming Cells to a Pluripotent State: Cells can be reprogrammed using (a) nuclear transfer of a differentiated cell into an enucleated oocyte, (b) by fusing a somatic cell with an undifferentiated cell (or multiple undifferentiated cells), and (c) by the introduction of exogenous transcription factors important in establishing and maintaining pluripotency. Reproduced from (Yamanaka and Blau).

Figure 2.1	27
Human Embryonic Stem Cell Colonies: A colony of H9 hES cells at (A) 5x and (B) 10x magnification prior to cleaning. *Undifferentiated H9 cells at the centre of the colony can be seen amongst **differentiated H9 cells and ***MEFs.	
Figure 2.2	30
H9-GFP Cells: A colony of undifferentiated H9-GFP cells at 10x magnification. GFP expression in the colony is clearly distinguishable from the surrounding MEFs.	
Figure 3.1	48
Myoblast Analysis by Flow Cytometry: Flow cytometry analysis of satellite cell surface markers in myoblast cell lines. There was very little expression of any surface markers in the S31/05 line (A) and CD34 was absent in all four cell lines. 17/01 cells expressed high levels of CD56 and CD106 and moderate amounts of M-cadherin (B). The FHM line expressed high levels of CD56 but very few cells were CD106 or M-cadherin positive (C). Fewer HFM cells were CD56+ than in the previous two lines and it had a moderate amount of CD106 and M-cadherin expression (D). n=3 for each cell line.	
Figure 3.2	49
Myoblast Analysis by Flow Cytometry (Quantification): Co-expression of CD56, CD106, and M-cadherin in myoblast lines. Both the 17/01 and HFM lines had cells positive for both CD56 and CD106 however only the HFM line had a population of CD106+/CD56- cells (top graph). In the three myogenic lines, most M-cadherin+ cells were also CD56+ while much fewer were positive for CD106. The only substantial population of triple positive cells was in the 17/01 line (bottom). Error bars indicate SEM, n=3 for each cell line.	
Figure 3.3	50
Myoblast Analysis by qPCR: qPCR analysis of myogenic genes in myoblast cell lines. Gene expression results confirm the flow cytometry data suggesting that the S31/05 line has lost its myogenic character. Of the remaining three lines, <i>PAX7</i> expression is highest in the foetal lines while <i>MYF5</i> expression shows the opposite trend. <i>MYOD</i> expression is similar in all three lines suggesting that all are equally myogenic in nature. 17/01 cells have the highest level of <i>MYOGENIN</i> followed by HFM and FHM cells. n=3 for each cell line.	
Figure 4.1	58
Initial Myogenic Differentiation Medium Analysis by Flow Cytometry: Representative dot plots from the flow cytometry analysis of the initial differentiation strategy. (A) Unstained cells were used as a control for autofluorescence in all experiments. (B) Populations of cells stained for CD133, CD56, M-cadherin, and Pax7 are shown along with the gates used to determine population percentages. Dot plots are representative of both trials of multiple time points in the differentiation experiment.	
Figure 4.2	59
Initial Myogenic Differentiation Medium Analysis by Flow Cytometry: Consistently high levels of CD56 are seen at all time points. CD133 expression is much lower and more variable between the two trials and the different time points as is M-cadherin and Pax7 expression. Co-expression of satellite cell markers suggests that between 1 and 5% of cells may be myogenic. The high degree of variability was thought to be a product of the fixation and permeabilization procedure, thus only one repeat was conducted before the staining strategy was modified.	

Figure 4.3.....60

Diff:CM Differentiation Analysis by Flow Cytometry: Representative dot plots from the flow cytometry analysis of the HFM time course differentiation. Plots show populations of cells staining for CD106 and CD56 (first plot), CD133 (second plot), and M-cadherin (third plot).

Figure 4.4.....61

Diff:CM Differentiation Time Course Analysis by Flow Cytometry: Flow cytometry analysis of the HFM differentiation time-point experiments. (Top Graph) Cultures grown only in Diff medium (no conditioned medium) showed higher levels of CD56 and CD56/CD133 staining, indicative of neurogenesis, as compared to the cells grown in conditioned medium. All cultures displayed similar levels of CD133 (a broadly expressed stem cell marker). Two trials were conducted. (Middle Graph) Staining for satellite cell markers show similar levels of CD106 between all cultures but a significant increase of M-cadherin expression in the cells grown with conditioned medium. (Bottom Graph) Co-expression of CD56/CD106 and M-cad/CD56 are similar among the different differentiation conditions, however M-cad/CD106 expression is significantly lower in the Diff D12 culture than in the HFM cultures. Very few triple positive cells were seen in any of the cultures, however the highest average was in the HFM D12 differentiation. Middle and Bottom Graphs give the average +/- SEM of three trials.

Figure 4.5.....63

Diff:CM Differentiation Analysis by qPCR: The highest level of expression for *PAX3* and *PAX7* occurred after 12 days of differentiation, after which point expression declined steadily. *MEF2* transcript levels were comparable among all three time points of the HFM differentiation, though significantly lower in the Diff control. Expression of both *MYF5* and *MYOD* peaked at 16 days of differentiation, though *MYOD* expression remained high at day 20 while *MYF5* had decreased.

Figure 4.6.....64

Flow Cytometry Analysis of Conditioned Medium from Various Myoblast Lines: Representative dot plots from the flow cytometry analysis of the media conditioned using various myoblast lines. A 12 day differentiation in 17/01 conditioned medium is shown, with populations staining for CD56 and CD106 (first plot), CD133 (second plot), and M-cadherin (third plot).

Figure 4.7.....65

Quantification of Flow Cytometry Analysis by Various Conditioned Media: The effect of conditioning medium with various myoblast cell lines on myogenic differentiation. Two foetal (HFM and FHM) and two adult (S31/05 and 17/01) cell lines were compared. (Top Graph) There was not a substantial difference between the cell lines in terms of neurogenesis markers, however HFM conditioned medium yielded the highest expression of CD56 in both trials. However, this did not correlate to a lower level of myogenic markers. (Bottom Graph) All cultures showed comparable levels of CD106 and M-cadherin, in addition to the co-expression of CD56/CD106 and CD56/M-cad. Two trials were conducted for this experiment.

Figure 4.8.....66

Activin A Medium Differentiation Analysis by Flow Cytometry: Representative dot plots from the flow cytometry analysis of the Activin A gradient differentiations. The plots show the results from adding 30 ng/mL of Activin A to the differentiation medium. A significant reduction in the number of cells stained for CD56 can be seen (first plot), while a large increase in CD133 staining is observed (second plot).

Figure 4.9.....67

Activin A Medium Differentiation Analysis by Flow Cytometry: Effect of ectopic expression of Activin A (at concentrations of 10, 30, 50, and 100 ng/mL) on myogenic differentiations. (Top Graph) Activin A was found to reduce CD56 expression and increase CD133 expression in a dose-dependent manner when compared to the HFM D12 differentiation. The percent of cells expressing CD56 decreased by roughly two-thirds, while the expression of CD133 increased by between 10-30%, when Activin A was added to the differentiation medium. (Bottom Graph) Activin A had a much less noticeable effect on CD106 and M-cadherin expression, however M-cadherin and CD56/M-cad expression were higher in the HFM D12 than at any concentration of Activin A. Only one trial was conducted for this experiment.

Figure 4.10.....68

H9 Cell GFP Staining during Co-culture Differentiation Experiment: H9-GFP cells differentiating alongside inactivated myoblasts. At day 2, most GFP-positive cells are found in the hES colony that settled after plating, with only a few cells beginning to migrate among the myoblasts. By day 7, GFP-positive cells have further dispersed throughout the myoblast networks and by day 20 the vast majority of the cells are GFP-positive.

Figure 4.11.....69

BMP4 Differentiation Analysis by Flow Cytometry: Representative dot plots from the flow cytometry analysis of the BMP4 differentiation. Only GFP+ cells were used for analysis and FACS (first plot). GFP+ cells also stained for CD56, CD106 (second plot), and M-cadherin (third plot). Similar gates were used when sorting cells.

Figure 4.12.....70

BMP4 Differentiation Analysis by Flow Cytometry (Quantified): Expression of GFP in BMP4 differentiation cultures and satellite cell surface markers in GFP+ cells determined by flow cytometry. GFP was expressed in approximately 80% of the cultures. The expression of CD56 was compared between GFP+ BMP4 cells and HFM D12 cells. All of the BMP4 cultures expressed higher levels of CD56 than the HFM D12 cells (Top Graph). The expression of CD106 was comparable between HFM D12 and BMP4 days 17 and 21, with higher levels seen in BMP4 day 12 and lower levels seen in BMP4 day 28. M-cadherin expression was consistently low in all of the BMP4 cultures (Middle Graph). The co-expression of multiple markers was also observed (Bottom Graph). HFM D12 cells were more likely to expression multiple markers than the BMP4 cultures, with the exception of the BMP4 day 12 M-cad/CD106+ population which was comparable to the same population in the HFM D12 culture.

Figure 4.13.....71

BMP4 Differentiation Analysis by qPCR: qPCR analysis from GFP+ cells isolated from the BMP4 differentiations showed an increase in the expression of myogenic genes when compared to the HFM D12 differentiation. *PAX3* and *PAX7* were most highly expressed on days 12 and 21 during the BMP4 differentiation, however these genes also showed a high degree of variability between trials. In contrast, *MEF2* was most highly expressed on day 17, gradually decreasing to a minimum on day 20, with similar results observed of *MYOD*. *MYF5* and *MYOGENIN* expression peaked at day 12, with significant levels also seen at day 21.

Figure 4.14.....72

BMP4 Differentiation Analysis of Sorted Populations by qPCR: Several different populations of BMP4 day 21 differentiated cells were sorted and analyzed by qPCR. They were compared to the baseline BMP4 results for GFP+ cells. *PAX3*, *PAX7*, and *MEF2* expression were highest in the GFP+

population with significant levels also seen in the M-cad⁺ cells. However, *MYOD* expression was highest in the M-cad⁺ and CD56/106⁺ populations, with only a very small level seen in the GFP⁺ and the CD106⁺ cells.

Figure 4.15.....73

BMP4 Differentiation Immunostaining for Desmin and M-cadherin: Immunostaining of BMP4 day 21 cultures showed GFP-positive cells expressing the intermediate filament marker desmin (top row) as well as the skeletal muscle-specific transmembrane protein M-cadherin (bottom row). Left panels show GFP expression in the differentiation cultures, middle panels show desmin and M-cadherin positive cells stained with AlexaFluor 594 and Rhodamin Red-X secondaries, respectively. The right panels show the merged image along with DAPI staining.

Figure 4.16.....74

BMP4 Differentiation Analysis by Flow Cytometry for MyoD Expression: Flow cytometry analysis of BMP4 day 21 cells stained for MyoD. Unstained cells are seen on the left while MyoD-stained cells are on the right. Approximately 0.7% of GFP⁺ cells were positive for MyoD.

Figure 4.17.....78

Surface Marker Expression during Mesoderm Differentiation: A schematic showing the surface markers expressed during the formation of mesoderm-derived cell types from embryonic stem cells. Note the interconversion between lateral and paraxial mesoderm cells, the ability of CD73⁺ cells to become myogenic, and the lack of a myoblast-specific surface marker. PDGFR α – platelet derived growth factor receptor-alpha, VEGFR – vascular endothelial growth factor receptor, Mesen. – mesenchymal

Figure 5.1.....82

Generation of the Pax7P-GFP Construct: (A) Schematic of the *PAX7* gene and the region of the promoter, marked in green, isolated to drive GFP expression in the pEGFP-1 vector. The enzymes Sac I and Pst I were used to excise the promoter from the purified PCR product. As a comparison, the region of the promoter used in Syagailo et al. is marked in red (Syagailo, Okladnova et al. 2002). (B) The region of the *PAX7* promoter (green) ligated into the pEGFP-1 vector. The promoter drives eGFP (orange) expression while an SV40 promoter drives expression of the kanamycin/neomycin resistance gene (red).

Figure 5.2.....83

Sequencing the Pax7P-GFP Construct: Shown is the overlap between the sequencing results from the forward primer 5'-GCTCACATGTTCTTCTGCG-3' (Fwd) and the reverse complement of the reverse primer 5'-CATGGCGGACTTGAAGAAGTC-3' (Rev) aligned with theoretical sequence of the *PAX7* promoter ligated into the pEGFP-1 vector (Pax7P). Highlighted areas show the restriction sites for Sac I (blue) and Pst I (red) used for the insertion. Sequence overlap on both sides of the insertion sites demonstrates the successful ligation.

Figure 5.3.....84

Pax7P-GFP Construct Validation by Flow Cytometry: GFP expression in non-transfected (left) and Pax7P-GFP transfected (right) adult human myoblasts analyzed by flow cytometry. Approximately 5% of the cells are GFP⁺ in the transfected myoblasts.

Figure 5.4.....85

Differentiated Pax7GFP Cells Analyzed by Flow Cytometry: Representative dot plots from flow cytometry analysis of Pax7-GFP HFM differentiation cultures are shown. Unstained cells were used as

a control (top row). Cells were analyzed for GFP expression (bottom left) and stained for CD56, CD106 (bottom middle), and M-cadherin (bottom right). GFP was more widely expressed than anticipated, while the surface markers showed similar levels of expression as previous HFM differentiations.

Figure 5.5.....86

Expression Dynamics of Differentiated Pax7GFP Cells: For all four time points, the total GFP expression (top graph) and the expression of CD56, CD106, and M-cadherin as well as their co-expression with GFP (middle graph) are shown. The bottom graph illustrates the percent of GFP+ cells in each of the populations of CD56+, CD106+, and M-cadherin+ cells. The CD106 population has the highest percentage of GFP+ cells followed by the CD56 and M-cadherin populations. In all three populations, GFP expression decreases as the differentiation progressed to 20 days.

Figure 5.6.....87

Analysis of Marker Co-expression in Differentiated Pax7GFP Cells: Comparison of different populations positive for multiple satellite cell markers and GFP (Top and Middle Graphs). Each of the four time points is shown for a given population and then compared to the same population also expressing GFP. The populations containing CD106 (CD56/CD106+ and CD106/M-cad+) tended to have the highest percentage of GFP+ cells (Bottom Graph). GFP expression also decreased in each of the populations as differentiation progressed.

Figure 5.7.....88

Pax7GFP Cell Differentiation Analysis by qPCR: qPCR analysis of the Pax7-GFP HFM differentiations show that the expression of *BRACHYURY* peaks at day 6 and is expressed only at very low levels at other time points and in the undifferentiated H9 control cells. In contrast, myogenic genes such as *PAX3*, *MYF5*, and *MYOD* are all most highly expressed after 12 days of differentiation and then begin to decrease until day 20.

Figure 5.8.....89

Pax7GFP Cell Differentiation Analysis of Sorted Populations by qPCR: qPCR analysis of sorted populations for *NESTIN*, *PAX3*, *MYF5*, and *MYOD* expression. *NESTIN* is most highly expressed in the GFP+ population, indicating that it has a significant percent of neurogenic cells. *PAX3* and *MYF5* expression are also highest in the GFP+ population, suggesting that it also contains myogenic cells, although no *MYOD* transcript was detectable. In contrast, the CD56/GFP+ population expresses low levels of *NESTIN* but moderate levels of *PAX3*, *MYF5*, and *MYOD*. The CD56/M-cad/GFP+ population did not contain enough cells to test for *PAX3* and *MYF5*, but it did express the highest level of *MYOD* in all four populations.

Figure 5.9.....91

Microarray Analysis of Sorted Differentiated Pax7GFP Cells: Microarray results were chosen for selected genes expressed during myogenesis and neuroectoderm differentiation. A positive sloped line indicates that the gene is more highly expressed in the CD56/GFP+ population than the Negative population. Most genes marking myogenic differentiation (*MYF5*, *MYOD*, *MYOGENIN*) or satellite cells (*PAX7*, *FOXK1*, *M-CADHERIN*) were not more highly expressed in the CD56/GFP+ population than the Negative control cells (top three rows). *PAX3* did show an increase in expression, however, like *PAX6* and many of the other up-regulated genes, it is expressed during neuroectoderm formation (bottom row).

Figure 5.10.....92

Evaluation of Pax7 Expression in Pax7GFP Cells: (A) FACS analysis of different populations of GFP negative and positive cells. Left Graph shows the range of GFP expression while the right graph shows the gates used to sort negative (Blue), moderately positive (Green), and brightly positive (Purple) cells. (B) qPCR analysis of *PAX7* in the sorted populations. GFP-negative cells showed the highest expression of *PAX7* while GFP+ and GFP++ cells expressed similarly low levels.

Figure 6.1.....98

iPS Clone IV Cells: A colony of iPS Clone IV cells on MEF feeders at (A) 10x, (B) 20x, and (C) 40x magnification showing hES cell-like morphology and colony structure.

Figure 6.2.....98

Myogenic iPS Differentiation Analysis by Flow Cytometry: Flow cytometry analysis of iPS clone IV cells differentiated in Diff:CM. Data for day 20 of the differentiation is representative of all time points. (Top Row) Unstained cells were used as a control for autofluorescence. (Bottom Row) Cells were stained for CD56 and CD106 (Left Plot) as well as M-cadherin (Right Plot). CD106 expression was surprisingly high, while expression M-cadherin was significantly lower than hES cell differentiations.

Figure 6.3.....99

Comparison of Flow Cytometry Data after Myogenic Differentiation of iPS and H9 Cells: The iPS cells showed significantly higher levels of CD56 and CD106 as well as the CD56/CD106 dual positive population (Top Graph). However, they expressed significantly lower levels of M-cadherin (Bottom Graph). Other dual and triple positive populations were comparable between the two cell types. Only one trial was conducted for iPS D16 and D20. All other time points were performed in triplicate.

Figure 6.4.....100

iPS Cell Myogenic Differentiation Analysis by qPCR: The qPCR analysis of differentiated iPS cells was compared to differentiated H9s. *PAX3* was more highly expressed in the iPS cultures, while *PAX7* did not show a significant difference in expression. The iPS cultures expressed slightly lower *MEF2* but very low levels of *MYF5* (with none detectable at day 16). Considering the large difference in *MYF5* expression, it was somewhat surprising that *MYOD* expression was similar between the two cell types.

Figure 6.5.....101

OSKM Construct Failed to Reprogramme DMD Fibroblasts: Incomplete reprogramming of F055 fibroblast cells after transduction with the OSKM construct. Cells in large colonies with a very distinct morphology could be observed after 16 days (A) and 19 days (B) on MEF feeders. After removing MEFs surrounding colonies, a new type of proliferating cells could be seen 21 days plating (C). Even as late as 25 days post plating, small colonies of partially reprogrammed cells could be found. However, no hES cell-like colonies were observed. All pictures were taken at 5x magnification. A 200 mm scale bar can be seen in (C).

Figure 6.6.....102

Reprogramming DMD Fibroblasts after Transduction with OCT4, LIN28, NANOG, and SOX: Images were taken 6, 9, and 16 days after plating on MEF feeders. The left column shows transduced F055 fibroblasts while the right column shows F029 fibroblasts. Early colonies can be seen by day 6 (top row) and continue to expand through day 16 (bottom rule). Morphological changes, predominantly a decrease in cell size, can be seen as the colonies expand. Pictures were taken at 5x magnification.

Figure 6.7.....103

F055 iPS Cell Colony: An early colony of fully reprogrammed cells from transduced F055 fibroblasts showing hES cell morphology at 5x (A) and 10x (B) magnification. Round cells can be seen with a large, central nucleolus and a small cytoplasm surrounded by differentiated cells and MEF feeders.

Figure 6.8.....104

Immunostaining of F055 iPS Cells: Colonies of F055 iPS cells were stained for markers of pluripotency. The left column shows brightfield images of the colonies, the middle column shows the cells stained for each protein, and the right column shows the merged image of the marker and DAPI. The colonies showed strong expression of the pluripotency genes OCT4 and NANOG as well as the surface markers SSEA4, TRA-1-60, and TRA-1-81. Cells also stained positive for alkaline phosphatase activity (bottom row).

Figure 6.9.....106

Analysis of F055 iPS Cell Pluripotency by qPCR: The expression of pluripotency-related genes was analyzed by qPCR and compared between three different samples of F055 iPS cells and H9s. FHM cells were used as a negative control. *NANOG*, *OCT4*, *KLF4*, and *GDF3* transcripts were all more highly expressed in the iPS cells than the H9s. Similar levels of *LIN28*, *SOX2*, *TERT*, and *MYC* were seen in both cell types. However, *REX1* was much more highly expressed in H9s than the iPS line.

Figure 6.10.....107

Endogenous Transcript Analysis of F055 iPS Cells by qPCR: In order to distinguish between total mRNA expression and endogenous expression, primers were designed to amplify only endogenous transcript for *LIN28*, *NANOG*, *SOX2*, and *OCT4*. Expression levels of *LIN28*, *NANOG*, and *SOX2* were comparable between the F055 iPS line and H9 cells, however *OCT4* levels were lower in the iPS cells. Endogenous expression of each gene was also found to be higher in the iPS3 sample (the latest sample tested) than in earlier iPS samples.

Figure 6.11.....109

Immunostaining of F055 iPS Cells: F055 iPS cells were differentiated and stained for markers of each germ layer to test for pluripotency. Cells were positive for AFP (top row, endoderm), β 3-TUBULIN (middle row, ectoderm), and weakly positive for NKX-2.5 (bottom row, mesoderm). Brightfield images of the differentiated cells are shown at 10x magnification (left column). The three proteins were stained green (middle column) while nuclei were stained with DAPI (merged, right column).

Figure 6.12.....110

F055 iPS Cell Differentiation Analysis by qPCR: Differentiated F055 iPS cultures (Diff) were also analyzed by qPCR for genes involved in early lineage formation and compared to undifferentiated F055 iPS cells and H9 cells. Both ectoderm markers (*NESTIN* and *PAX6*) were expressed at higher levels in some of the H9 samples than the differentiated iPS cells, however the Diff sample expressed higher levels of *PAX6* than the undifferentiated iPS cells. *AFP* and *BRACHYURY* were expressed much more highly in the differentiated cultures than any other samples and *MIXL1* expression was significantly increased.

Table of Tables

Table 2.1: Monolayer Differentiations of hES and iPS Cells 28

Table 2.2: Primers Used for Quantitative PCR 42

Table 4: Summary of hES Cell Myogenic Differentiations 75

Table 6: Pluripotency Marker Expression in F055 iPS and H9 Cells 108

Abbreviations

AFP	alpha-fetoprotein
ALK	activin receptor-like kinase
ALS	amyotrophic lateral sclerosis
APC	allophycocyanin
AT	annealing temperature
BDNF	brain-derived neurotrophic factor
bFGF	basic fibroblast growth factor
BIO	6-bromoindirubin 3'-oxime
BMP	bone morphogenic protein
bp	base pair
BrdU	bromodeoxyuridine
BSA	bovine serum albumin
cDNA	complementary DNA
CM	conditioned medium
cRNA	complementary RNA
CTR	calcitonin receptor
Cy5	cyanine 5
DAPI	4',6-diamidino-2-phenylindole
Diff	differentiation
DMD	Duchenne muscular dystrophy
DMEM	Dulbecco's modified Eagle's medium
DMSO	dimethyl sulfoxide
DNA	deoxyribonucleic acid
Dnmt3b	DNA methyltransferase
dNTPs	deoxyribonucleotides
dpc	days post coitum
EB	embryoid body
EC Cells	embryonal carcinoma cells
ECM	extracellular matrix
EDTA	ethylenediaminetetraacetic acid
EG Cells	embryonic germ cells
EGF	epidermal growth factor
EpiSC	epiblast stem cell
ES Cells	embryonic stem cells
FA	Fanconi anemia
FACS	fluorescence activated cell sorting
FBS	foetal bovine serum
FGF	fibroblast growth factor
FHM	foetal human myoblast
FITC	fluorescein isothiocyanate
FRV	Fast Red Violet
GAPDH	glyceraldehydes-3-phosphate dehydrogenase

GDF	growth differentiation factor
GFP	green fluorescent protein
GSK	glycogen synthase kinase
H3K27me3	trimethylation of lysine 27 of histone H3
H3K4me3	trimethylation of lysine 4 of histone H3
HAC	human artificial chromosome
HEK Cells	human embryonic kidney cells
HEPES	2-[4-(2-hydroxyethyl)piperazin-1-yl]ethanesulfonic acid
hES Cell	human embryonic stem cell
HFM	human foetal myoblast
HGF	hepatocyte growth factor (scatter factor)
HMGA2	high mobility group type A-2
ICM	inner cell mass
IGF	insulin-like growth factor
Ig	immunoglobulin
iPS Cell	induced pluripotent stem cell
ITS	insulin transferrin selenium
IVF	<i>in vitro</i> fertilisation
JAK	janus-associated kinase
kb	kilobase
KLF	Kruppel-like factor
KOSR	knock out serum replacement
LB	lysogeny broth
LIF	leukaemia inhibitory factor
MEF	mouse embryonic fibroblast
MEF2	myocyte enhancer factor 2
mES Cell	mouse embryonic stem cell
MRF	myogenic regulatory factor
mRNA	messenger RNA
MT	melting temperature
NCAM	neural cell adhesion molecule
NEAA	non-essential amino acids
NHDF	normal human dermal fibroblast
NOS	nitric oxide synthase
NT	neurotrophin
OSKM	OCT4/SOX2/KLF4/MYC
OSLN	OCT4/SOX2/LIN28/NANOG
OSN	OCT4-SOX2 and NANOG
PBS	phosphate buffered saline
PBST	PBS tween-20
PCR	polymerase chain reaction
PDGFR α	platelet-derived growth factor receptor-alpha
PE	phycoerythrin
PECAM	platelet endothelial cell adhesion molecule
QCPN	quail non-chick perinuclear antigen
qPCR	quantitative PCR
RCF	relative centrifugal force

RNA	ribonucleic acid
ROCKi	RHO kinase inhibitor
RPL13A	ribosomal protein L13
rpm	revolutions per minute
RPMI	Roswell Park Memorial Institute medium
RT-PCR	reverse transcriptase PCR
SCID	severe combined immunodeficiency
SEM	standard error of the mean
SFM	serum-free medium
SMA	spinal muscular atrophy
SSEA	stage-specific embryonic antigen
Stat	signal transducer and activator of transcription
TAE	tris-acetate-EDTA
TERT	telomerase reverse transcriptase
TGF	transforming growth factor
TRA	tumour rejection antigen
TRIM	tripartite motif-containing
UTF-1	undifferentiated embryonic cell transcription factor 1
VCAM	vascular cell adhesion molecule
VEGFR	vascular endothelial growth factor receptor

Chapter 1: Introduction

1.1 Skeletal Muscle Development

Muscles of the trunk and limbs are originally formed on each side of the embryo from the paraxial mesoderm positioned next to the neural tube and notochord. The paraxial mesoderm becomes segmented and develops into the somites, the dorsal portion of which becomes the dermomyotome. The dermomyotome has both an epaxial region near the neural tube which develops into the back muscles and a more peripheral hypaxial region which will form the muscle for the rest of the body and limbs (**Figure 1.1**). Somites near the limb buds produce migratory myogenic cells to populate the limbs and develop into muscle. In contrast, head muscles can be formed from prechordal mesoderm in addition to paraxial mesoderm via the anterior somites (Buckingham, Bajard et al. 2003; Buckingham 2006).

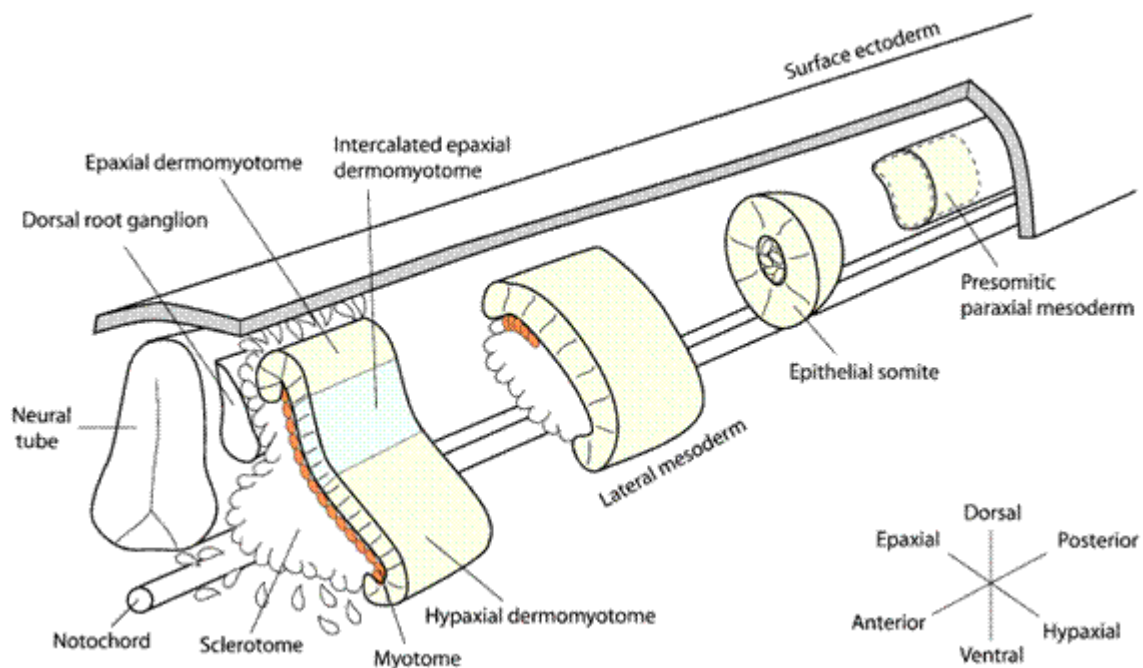


Figure 2.1: Embryonic Somitogenesis. A schematic showing the location of early myogenesis in the developing embryo. Somites are formed from paraxial mesoderm on each side of the neural tube and form the dermomyotome, myotome, and sclerotome. Reproduced from (Buckingham, Bajard et al. 2003).

Myogenic development is largely controlled by a family of basic helix-loop-helix genes known as myogenic regulatory factors (MRFs), most importantly *Myf5* and *MyoD*. These genes are activated by

Wnt and Sonic hedgehog signals from surrounding tissue (Cossu and Biressi 2005). Once myogenic capacity has been established by Myf5 and MyoD, muscle differentiation is initiated by the presence of myogenin, MRF4, and MEF2 (Buckingham, Bajard et al. 2003; Chen and Goldhamer 2003).

The first muscle tissue to form is the myotome, located on the ventral face of the dermomyotome. By 11-12 days post coitum (dpc) in the mouse, primary muscle fibres will have formed by the fusion of myoblasts derived from the dermomyotome (embryonic myogenesis). While some myoblasts form primary fibres, others continue to proliferate until around 15-17 dpc when they form secondary fibres (foetal myogenesis). A basal lamina develops around these secondary fibres and from this time forward satellite cells can be identified based on their location between the basal lamina and the muscle fibre (Mauro 1961; Cossu and Biressi 2005).

1.2 The Muscle Satellite Cell and Regeneration

1.2.1 Origin of the Satellite Cell

Until recently, the origin of satellite cells had not been confirmed. Although they were largely suspected to be derived from somites along with other muscle cells, the ability of cells from other tissues to regenerate muscle has made people skeptical of the satellite cell origin (Chen and Goldhamer 2003; Cossu and Biressi 2005). However, several recent studies have eliminated most doubts and it is now accepted that satellite cells originate in the central portion of the dermomyotome (Buckingham 2006). Satellite cells are thought to be the progeny of a population of Pax3/Pax7+ cells first found in the dermomyotome. During myogenesis, as these cells leave the dermomyotome and begin to express MRFs they lose their Pax3/Pax7 expression. However a small population of Pax3/Pax7+ cells, some of which do not express MRFs, can still be found in skeletal muscle masses of the embryo. These cells are thought to be a source of embryonic and foetal myoblasts during development. As myogenesis progresses, these cells seem to downregulate Pax3 but maintain Pax7 expression and also express Myf5. The Pax7+ cells eventually take up a satellite cell position residing between the basal lamina and the muscle fibre (Kassar-Duchossoy, Giaccone et al. 2005; Relaix, Rocancourt et al. 2005).

A study by Gros et al. (2005) used quail-chick grafting experiments to trace the fate of cells during myogenesis. The central region of quail dermomyotome was excised and used to replace the same region in chick somites. Quail cells were then tracked by staining for the quail cell perinuclear antigen (QCPN) and, in doing so, any cells and their progeny from the central dermomyotome could be monitored. They found that 95% of satellite cells in the hatched chimeras stained for QCPN, demonstrating that the vast majority, if not all, satellite cells originate in the somite (Gros, Manceau

et al. 2005). While some transplantation studies have shown that cells such as foetal mesoangioblasts (Minasi, Riminucci et al. 2002; Sampaolesi, Torrente et al. 2003), neonatal bone marrow, and foetal liver cells (Fukada, Miyagoe-Suzuki et al. 2002) can occupy the satellite cell niche, this does not appear to occur under normal circumstances.

1.2.2 *The Satellite Cell Niche*

Satellite cells are defined based on their position between a myofibre and its basal lamina. In this location, three crucial factors help establish the satellite cell niche: the interaction between a satellite cell and its host myofibre on its apical side, the interaction between the satellite cell and the basal lamina on its basal side, and the signals and nutrients received by the microvasculature and interstitial cells near to the satellite cell. For example, it has been shown that nitric oxide signals from muscle fibres is important in both the maintenance of pluripotency and the activation of satellite cells (Wozniak and Anderson 2007). In normal muscle fibres, inhibition of nitric oxide synthase (NOS) increased satellite cell activation. However, while stretching individual fibres *in vitro* (to induce activation), inhibition of NOS reduced activation of satellite cells and promoted quiescence. Important signals involved in the activation of satellite cells also come from the surrounding ECM. Hepatocyte growth factor (HGF, scatter factor) is found in the ECM of normal muscle tissue and upregulated at sites of damage. Its receptor, c-Met is present on quiescent satellite cells. Abolishing HGF signaling using an anti-HGF antibody prevents satellite cell activation in damaged muscle (Tatsumi, Anderson et al. 1998). Finally, calcitonin reaches the satellite cell from the circulation and promotes satellite cell quiescence. Calcitonin receptor (CTR) is only present on quiescent satellite cells and a CTR agonist, elcatonin, suppresses the activation and migration of satellite cells in *in vitro* single myofibre experiments (Fukada, Uezumi et al. 2007).

In regenerating muscle, the satellite cell niche contains heterogeneous Pax7⁺ cells, most notably distinguished based on the expression of Myf5 at some point in their lineage. The Pax7⁺/Myf5⁻ cells (i.e. cells that have never expressed Myf5 and also have not had ancestors who expressed Myf5) are thought to represent a population capable of self-renewal and differentiation into the Pax7⁺/Myf5⁺ cells. Once Myf5 expression has occurred in a cell, it and its decedents are thought to be committed to proliferation and differentiation (Kuang, Kuroda et al. 2007). These differences are achieved via asymmetric cell division governed by the physical properties of the satellite cell niche. Each satellite cell has a basal side in contact with the basal lamina and an apical side in contact with the host myofibre. When a satellite cell divides, the daughter cell next to the basal lamina is responsible for self renewal (Pax7⁺/Myf⁻) while the daughter cell in contact with the myofibre (which becomes Pax7⁺/Myf⁺) will undergo transient amplification and differentiation. In addition, BrdU labeling studies showed that with each satellite cell division the older, “immortal” DNA strands are segregated into a self-renewal cell, which expresses the stem cell marker Sca1, while the newly

synthesized strands are segregated into the differentiating cell, which expresses desmin (Conboy, Karasov et al. 2007).

1.2.3 *Molecular Signature of Satellite Cells*

Because the satellite cell is defined based on its anatomical position relative to a muscle fibre, the molecular characterisation of these cells is somewhat limited. The most definitive marker of satellite cells is Pax7, which is present in all satellite cells and expressed in proliferating myoblasts until they begin to differentiate (Chen and Goldhamer 2003; Dhawan and Rando 2005; Zammit, Partridge et al. 2006). Pax7^{-/-} mice develop muscle normally but lose their satellite population after birth, suggesting a role for Pax7 in cell maintenance or apoptosis inhibition (Seale, Sabourin et al. 2000; Oustanina, Hause et al. 2004). Other transcription factors common to quiescent satellite cells include Foxk1 (Garry, Meeson et al. 2000), which is thought to regulate cell cycle progression of myogenic cells (Hawke, Jiang et al. 2003); Pax3, although it is not present in all muscle tissue (Montarras, Morgan et al. 2005); and Myf5 (Beauchamp, Heslop et al. 2000). MyoD expression begins once satellite cells become activated and the presence of myogenin, desmin, and MRF4 (Cornelison and Wold 1997) indicates a commitment to differentiation. These events are discussed in more detail below.

The surface markers of satellite cells are especially important when using a fluorescence activated cell sorting (FACS)-based isolation strategy. A number of different cell-surface proteins have been identified, however their expression is not always consistent and many only label a subset of the satellite cell population (Shi and Garry 2006). The most common marker used to distinguish satellite cells from surrounding tissue is the hepatic growth factor (HGF) receptor, c-Met (Andermarcher, Surani et al. 1996). However, because of its broad expression during development it is of limited usefulness when trying to isolate cells from a heterogeneous mix of differentiated human embryonic stem (hES) cells. M-cadherin is present in most but not all quiescent satellite cells and upregulated once they become activated (Donalies, Cramer et al. 1991; Irintchev, Zeschnigk et al. 1994; Cornelison and Wold 1997). Other markers include CD106 (VCAM-1), CD56 (NCAM), CD34, and syndecans 3 and 4 (Covault and Sanes 1986; Jesse, LaChance et al. 1998; Beauchamp, Heslop et al. 2000; Cornelison, Filla et al. 2001; Cornelison, Wilcox-Adelman et al. 2004). Satellite cell surface markers are discussed in more detail in Chapter 3.

1.2.4 *Adult Muscle Regeneration*

The adult muscle fibre is a multinucleated syncytium grouped into bundles to form skeletal muscle tissue. When muscle tissue is damaged it undergoes a two-step repair process: first the tissue becomes necrotic eliciting an inflammatory response and then regeneration begins. Regeneration requires the proliferation of myogenic cells which then may either fuse with damaged fibres or create de novo fibres to replace lost muscle (Charge and Rudnicki 2004).

The first step in regeneration is the activation of normally quiescent muscle satellite cells in response to signals from damaged muscles. Upon injury, HGF is released from the extracellular matrix of muscle and causes satellite cells to enter the cell cycle and begin proliferating (Miller, Thaloor et al. 2000; Tatsumi and Allen 2004; Lluís, Perdiguero et al. 2006). This process is complemented by the release of several fibroblast growth factors (FGFs) which are recognized by any of four FGF receptors found in satellite cells (Johnson and Allen 1995). Activation also induces the expression of MRFs responsible for the transition from satellite cells to proliferating myoblasts. Myoblast proliferation is promoted by additional extracellular signals including insulin-like growth factor (IGF-I), interleukin-6, and leukaemia inhibitory factor while it is inhibited by transforming growth factor- β (Figure 1.2, (Charge and Rudnicki 2004)).

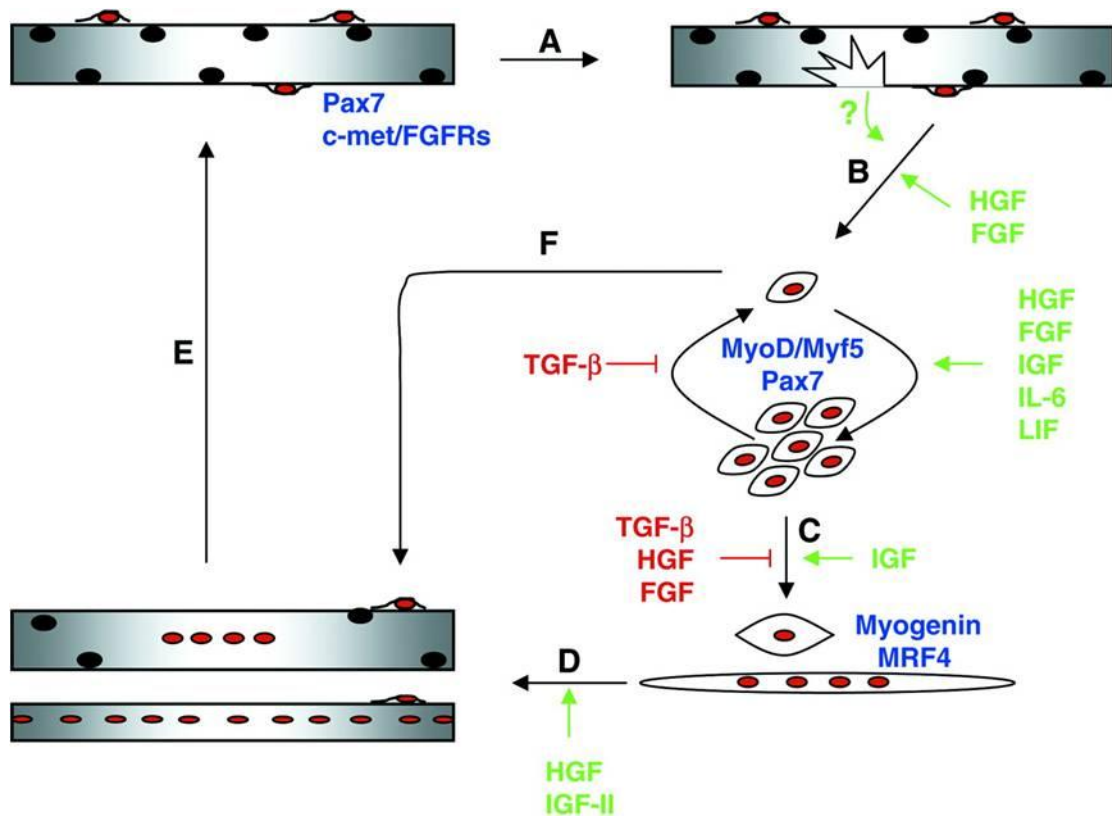


Figure 1.2: Adult Muscle Regeneration. An outline of adult muscle regeneration showing the growth factors which promote (green) and inhibit (red) satellite cell activation, myoblast proliferation, and differentiation as well as some of the key genes expressed in each population of cells (green). After muscle injury (A), satellite cells are activated (B) and begin proliferating. Some of these cells will reoccupy the satellite cell niche (F) while others will differentiate and fuse (C) forming an early myofiber with central nuclei (D) before maturing (E). Reproduced from (Charge and Rudnicki 2004).

At this point there are two possible fates for these cells: terminal differentiation and fusion to form muscle fibres or replenishment of the satellite cell population. Studies in the rat suggest that roughly

80% of satellite cells divide rapidly and contributed to myonuclei (and thus underwent differentiation and fusion) while the other 20% divide relatively slowly and were thought to be the source of replacement satellite cells (Schultz 1996). It is believed that the decision is made based on the initial expression of either MyoD or Myf5, although both become expressed as the myogenic pathway progresses (Cornelison and Wold 1997). Myoblasts in MyoD^{-/-} mice will continue to proliferate and produce increased levels of IGF-I but muscle regeneration is severely diminished (Megeney, Kablar et al. 1996). These cells also express lower levels of M-cadherin (Sabourin, Girgis-Gabardo et al. 1999; Cornelison, Olwin et al. 2000). These data suggest that MyoD is necessary for myoblasts to exit the proliferative stage, differentiate, and fuse to form muscle fibres. In contrast, Myf5 expression is thought to promote satellite cell replenishment as there is a natural population of self-renewing Myf5⁺/MyoD⁻ cells when satellite cells are forced to differentiate (Baroffio, Hamann et al. 1996). These cells may then dedifferentiate and reoccupy the satellite cell niche, consistent with the finding that Myf5 is present in quiescent satellite cells (Beauchamp, Heslop et al. 2000).

The final stage of muscle regeneration is myoblast differentiation and fusion. Differentiation is marked by the upregulation of myogenin and MRF4 and the continued expression of MyoD and Myf5 (Smith, Janney et al. 1994; Yablonka-Reuveni and Rivera 1994; Cornelison and Wold 1997). This leads to cell cycle arrest through the activation of p21 and, eventually, expression of muscle-specific proteins like myosin heavy chain (Charge and Rudnicki 2004). Myoblast fusion is guided by a number of adhesion and cytoskeletal-reorganization proteins. M-cadherin, which is upregulated as satellite cells differentiate, is important in forming cytoplasmic complexes found in fusing myogenic cells (Kuch, Winnekendonk et al. 1997) and ablation of M-cadherin activity by antagonistic peptides or anti-sense RNA disrupts myotube formation (Zeschnigk, Kozian et al. 1995). The intracellular cysteine protease m-capsin behaves in a similar manner, being upregulated during myoblast fusion and preventing fusion when inhibited by calpastatin or anti-sense RNA treatment (Kwak, Chung et al. 1993; Balcerzak, Poussard et al. 1995; Temm-Grove, Wert et al. 1999). Intermediate filament proteins are also important in the final stages of differentiation. Desmin^{-/-} mice show normal muscle development but delayed regeneration (Smythe, Davies et al. 2001). The expression patterns of vimentin and nestin suggest that they also have a role in myoblast fusion, albeit at an earlier time-point than desmin (Vaittinen, Lukka et al. 2001). Thus, adult muscle regeneration is a multi-step process that begins with activation of the muscle satellite cell and ends with the formation of a mature, multinucleated myofibre.

1.3 Stem Cell-Based Therapeutic Muscle Regeneration

There is a great deal of promise in the use of myogenic stem cells in therapies directed toward muscular dystrophies. These disorders are characterised by skeletal muscle degeneration often due to a mutation in one of the structural proteins found in muscle. In extreme forms, like Duchenne muscular dystrophy (DMD), the muscle degradation will eventually lead to paralysis, cardiac dysfunction, respiratory failure, and death in the late teens or early twenties (Emery 2002; Negroni, Butler-Browne et al. 2006). DMD is caused by a mutation in the dystrophin gene found on the X-chromosome. Functional dystrophin is necessary to properly form the structural network joining the cytoskeleton of a myofibre to the extracellular matrix. When dystrophin is absent, muscle fibres degrade over time and eventually will no longer be replaced by normal muscle regeneration as available satellite cells become exhausted (Blau, Webster et al. 1983; Matsumura and Campbell 1994). Stem cell research offers the possibility of replacing lost myogenic cells with new ones containing functional dystrophin.

1.3.1 Early Attempts to Alleviate DMD

Transplantation studies in the late 1970s and early 1980s first showed that donor myogenic cells can contribute to muscle regeneration (Watt, Lambert et al. 1982; Blau, Webster et al. 1983; Morgan, Watt et al. 1988). Interestingly, the most efficient rates of regeneration were found when whole muscle fibres containing attached satellite cells were transplanted (Hansen-Smith and Carlson 1979; Collins, Olsen et al. 2005; Price, Kuroda et al. 2007). One of the most common animal models used to study DMD is the mdx mouse, which has X chromosome-linked muscular dystrophy and displays a similar pattern of muscle degeneration and fibre necrosis as in humans. Unlike humans, the mice are capable of regenerating lost muscle indefinitely without any signs of interstitial fibrosis or adipose tissue replacement (Tanabe, Esaki et al. 1986). It was not until the late 1980s that myoblast transplant was first used as a treatment in mdx mice (Partridge, Morgan et al. 1989). After several more positive studies using both mouse and human myoblasts, the first clinical trials were attempted to alleviate DMD in humans through cell transplantation (Negroni, Butler-Browne et al. 2006). Unfortunately, these efforts were largely ineffective. While there were occasional signs of dystrophin+ muscle fibres, it was later found that these were the result of a rare reversion of the initial mutation in host cells, not due to the presence of transplanted myoblasts. On the whole, there were low levels of donor cell incorporation, generally attributed to poor survival of transplanted cells or a lack of dispersion from the injection site. As a result there was only a minimal improvement in the recipients (Partridge, Lu et al. 1998; Peault, Rudnicki et al. 2007).

1.3.2 *Transplantation of Isolated Satellite Cells*

Due to the difficulty in isolating large numbers of pure satellite cells, their use in transplantation studies has been limited. More often, a mixed population of muscle derived stem cells is used to obtain proliferating myoblasts for injection. These myoblasts are either obtained by culturing satellite cells *in vitro* or by using collagen-coated flasks to plate mixtures of cells from enzyme-dissociated muscle. In the latter case, known as the pre-plate method, it was found that various populations of myogenic cells had different affinities to the flask and could be purified based on that characteristic (Montarras, Morgan et al. 2005; Peault, Rudnicki et al. 2007). Both of these methods have the drawback of requiring significant expansion *in vitro*, which is known to lead to cell senescence (Decary, Mouly et al. 1996).

These problems have been cleverly avoided in a recent study by Montarras et al. (2005). Using a mouse strain that contained green fluorescence protein (GFP) under control of the Pax3 gene, they were able to use a FACS-based strategy to isolate adult satellite cells from mouse muscle without needing an intermediate step of *in vitro* cell culture. These cells were capable of both contributing to new muscle fibres and repopulating the satellite cell pool in mdx mice. Further, they showed that expanding the cells in culture substantially reduced their regenerative ability. This was partially attributed to the onset of MyoD expression, which occurred in cultured cells but was largely absent in freshly sorted cells (Montarras, Morgan et al. 2005). This method shows a great deal of promise but it is severely limited, especially for use in clinical trials, by the amount of muscle needed to obtain sufficient numbers of fresh satellite cells.

1.3.3 *Alternative Sources of Myogenic Cells*

Recently people have begun looking for alternative sources of myogenic cells to use in transplantation. Muscle side population cells, identifiable based on their exclusion of the nuclear dye Hoechst 33342, have been found and are distinguishable from resident satellite cells (Asakura, Seale et al. 2002). These cells are also capable of replacing dystrophin-null fibres when transplanted into mdx mice. Similar cells isolated from bone marrow (again based on the exclusion of Hoechst 33342) also have myogenic potential (Gussoni, Soneoka et al. 1999). Both bone marrow- and muscle-derived side population cells have the desirable characteristic of being able to populate muscle when injected into the blood stream, thus showing promise for systemic repopulation. Unfortunately these cells do not seem to contribute to long term muscle regeneration despite taking up a position in the satellite cell niche (Price, Kuroda et al. 2007). Haematopoietic stem cells from bone marrow transplantation and stem cells isolated from blood based on AC133 (CD133) expression also show limited myogenic capacity and regenerative ability (Torrente, Belicchi et al. 2004) although it is

doubtful that either cell population will be a practical therapeutic tool. Mesenchymal stem cells isolated from foetal (Chan, O'Donoghue et al. 2006) or adult (Dezawa, Ishikawa et al. 2005) bone marrow readily differentiate into muscle cells, including Pax7+ cells, with efficiencies of greater than 60% in some culture conditions and are capable of regenerating muscle in vivo.

One novel approach to alleviate DMD involves using blood vessel-derived stem cells called mesoangioblasts. A recent study by Sampaolesi et al. (2006) explored their potential using the golden retriever dog model for muscular dystrophy, which contains a mutation in the dystrophin gene resulting in the complete absence of the protein and a pathological condition very similar to humans with DMD. Mesoangioblasts were isolated from blood vessels in muscle biopsy outgrowths and, in the case of autologous transplantation, transduced with a lentivirus containing human microdystrophin. Donor-derived mesoangioblasts were transplanted both with and without immunosuppressive drugs. In addition to showing that canine mesoangioblasts could form myotubes in culture and in SCID (severe combined immunodeficiency)-mdx mice, they reported a remarkable improvement in dogs that received donor mesoangioblasts with immune suppression (Sampaolesi, Blot et al. 2006). While promising, their results may be due to the immunosuppressive treatment more than the cell transplantation. Dogs that did not receive immunosuppressants did not show much improvement and several studies including a clinical trial suggest that treatment with only cyclosporine, one of the immunosuppressive drugs used by Sampaolesi et al., is capable of alleviating some symptoms of DMD (Miller, Sharma et al. 1997; Sampaolesi, Blot et al. 2006; Radley, De Luca et al. 2007).

1.3.4 Calculation of the Number of Cells Needed for Therapeutic Trials

Clinical trials in DMD patients vary in the extent of muscles injected and the number of myoblasts that are used. One study injected 110 million cells into the biceps brachii muscle once a month for 6 months (Mendell, Kissel et al. 1995) while another study showed that injections of between 25 and 30 billion myoblasts into multiple muscle sites (20 to 30 total sites per patient) are safe and could lead to clinical improvement (Law, Goodwin et al. 1997). The latter study showed that 50 billion myoblasts could be expanded in vitro from a 2-gram muscle biopsy. This represents a very large number of population doublings from a small number of isolated cells, which should be avoided in primary cell lines.

The benefit of using ES cells to generate myoblasts is that they do not show the genetic wear-and-tear upon extensive expansion in vitro that most cell types exhibit. In the work described herein, 10 million differentiated hES cells were obtained for each individual time point in one experiment. This could be scaled up to 1 billion differentiated hES cells and maintained by a single person without being prohibitively difficult. Generously assuming that 10% of the differentiated cells could be

converted to isolatable myoblasts, one experiment could yield 100 million cells capable for direct injection or subsequent expansion. This number is sufficient for single-muscle clinical trials as described above, or could be expanded in vitro for multiple injection site studies.

In conclusion, there are a number of alternative sources of cells for muscle regeneration, most of which have some degree of therapeutic potential but all have significant drawbacks that must be addressed. The final source for obtaining myogenic stem cells is through the differentiation of either mouse or human embryonic stem cells, discussed below and in Chapter 4.

1.4 Embryonic Stem Cells

1.4.1 Derivation of Embryonic Stem Cells

The inner cell mass (ICM) of the blastocyst is composed of immortal, pluripotent stem cells capable of generating non-trophoblast extraembryonic tissues and all the cell types of the developing embryo proper. Embryonic stem (ES) cells are derived from the ICM (**Figure 1.3**).

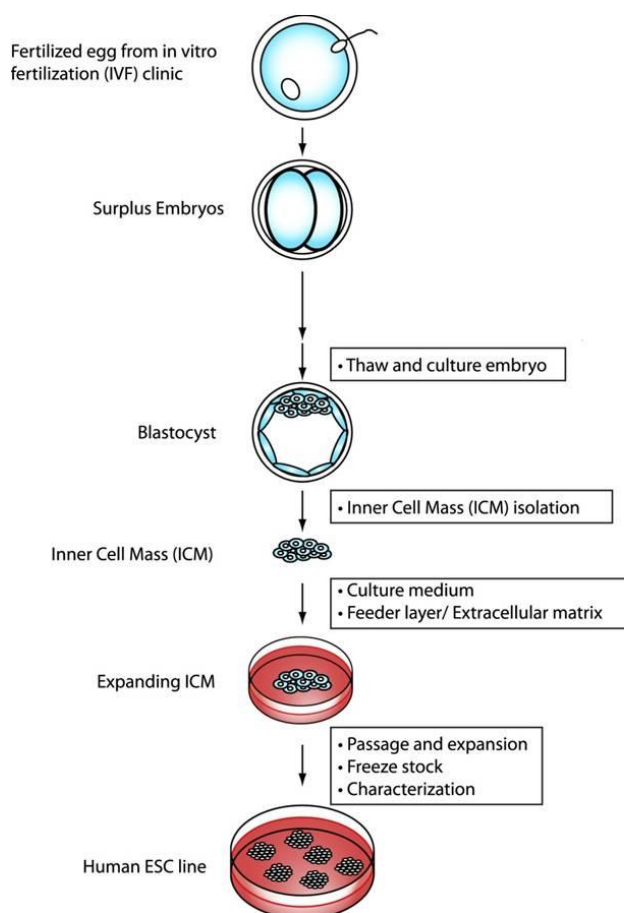


Figure 1.3: Human ES Cell Derivation. Derivation of human embryonic stem cell lines from the ICM of a blastocyst cultured from a surplus IVF embryo. Modified from (Hasegawa, Pomeroy et al. 2010).

To qualify as a bona fide pluripotent ES cells several criteria need to be met: they must maintain a normal karyotype after extensive passaging, they must be capable of differentiating into cells representative of all three germ layers both *in vivo* (as teratomas or chimeric mice) and *in vitro*, and they must possess both of these qualities after indefinite propagation. The first mouse ES (mES) cell lines were derived independently by two groups in 1981. Evans and Kaufman isolated delayed blastocysts from mice that had been impregnated and injected with Depo-Provera (Depot medroxyprogesterone acetate) to stimulate diapause. The blastocysts were allowed to adhere to Petri dishes with trophoderm and endodermal cells growing attached to the dish surrounding an egg cylinder-like structure. This structure was removed, trypsinized, and passaged onto mitotically inactivated mouse embryonic fibroblasts (MEFs). The cells, termed “EK cells” (as opposed to embryonal carcinoma, or EC cells) were transplanted into syngeneic mice and found to form teratocarcinomas (Evans and Kaufman 1981). Similarly, Martin showed that mouse ICMs isolated from normal blastocysts by immunosurgery could be seeded to form cultures of “embryonic stem cells” that could be maintained in medium conditioned by undifferentiated EC cells. These ES cells and subclonal cultures established from single cells were found to form teratocarcinomas *in vivo* and to differentiate similarly to EC cells *in vitro* (Martin 1981).

Human ES cell lines were first derived in 1998 from blastocysts cultured from *in vitro* fertilization (IVF) cleavage stage embryos. The ICM of these embryos was isolated by immunosurgery and plated on MEFs. Outgrowths from the ICM were dissociated into clumps mechanically, enzymatically, or using EDTA in PBS and replated. These hES cells were cultured in the presence of MEFs and found to express stage-specific embryonic antigen (SSEA)-3, SSEA-4, TRA-1-60, TRA-1-81, and alkaline phosphatase similar to human EC cells. They formed teratomas with representative tissues from all three germ layers when injected into immunocompromised mice and could be passaged repeatedly without losing their pluripotency or normal karyotype, a characteristic attributed to their high telomerase activity (Thomson, Itskovitz-Eldor et al. 1998). More recently, ES cell lines have also been developed from cleavage stage embryos including individual blastomeres, later blastocyst stage embryos, and parthenogenetic embryos (Yu and Thomson 2008).

1.4.2 Embryonic Stem Cell Pluripotency

ES cell pluripotency is governed primarily by three master regulators: Oct3/4 (also called Pou5f1, herein referred to as Oct4), Sox2, and Nanog. Oct4 is a POU transcription factor expressed in blastomeres, pluripotent cells of the early embryo (present in the ICM and epiblast), and germ line cells *in vivo*, while it is found in embryonic germ (EG), EC, and ES cells *in vitro*. Oct4 is thought to act through transactivation and in a complex with Sox2 to regulate the transcription of genes such as

FGF4 and Utf-1 (Pesce and Scholer 2001). The importance of Oct4 in the establishment and maintenance of pluripotent stem cells of the early embryo is well established. Oct4^{-/-} embryos are capable of developing into a blastocyst, however the cells of the ICM are not pluripotent and are only able to form trophoblast-derived cells (Nichols, Zevnik et al. 1998). In ES cells, Oct4 expression must be carefully regulated to prevent differentiation. Even a 50% increase in Oct4 expression will promote the differentiation of ES cells to primitive endoderm or mesoderm, while a similar decrease in Oct4 expression leads to the formation of trophectoderm (**Figure 1.4**, (Niwa, Miyazaki et al. 2000)).

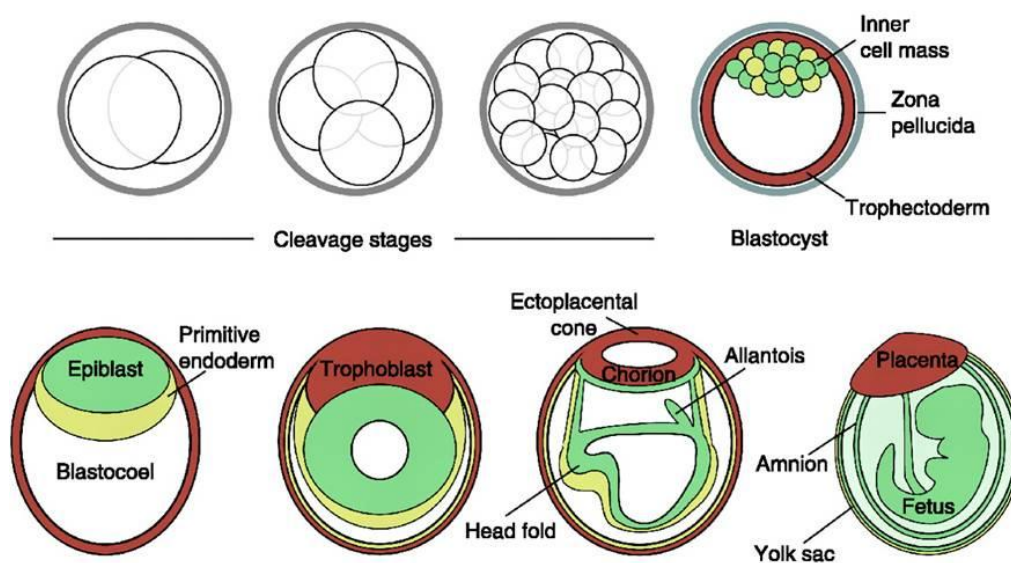


Figure 1.4: Lineage Development during Early Mouse Embryogenesis. The blastocyst is formed from the late cleavage stage embryo. As the blastocyst develops, cells of the ICM become specified to either epiblast (green) or primitive endoderm (yellow) fates while the trophectoderm (red) will become the trophoblast. The epiblast eventually develops into the embryo proper, the primitive endoderm into components of the yolk sac, and the trophoblast into the placenta. Reproduced from (Ralston and Rossant 2010).

Sox2 is a member of the SRY-related HMG box (Sox) family of transcription factors. It is expressed in the ICM, extraembryonic ectoderm, neuroectoderm, and in various tissues during development including the brain, brachial arches, gut endoderm, and germ cells. The importance of Sox2 in the maintenance of pluripotency was first established when it was identified as the binding partner of Oct4 on the *FGF4* enhancer in EC cells (Yuan, Corbi et al. 1995; Ambrosetti, Basilico et al. 1997). In Sox2^{-/-} embryos, the blastocyst forms but the epiblast is disrupted. Similar to Oct4^{-/-} embryos, ICM cells from Sox2^{-/-} blastocysts were found to form trophectoderm; however they also could form primitive endoderm. It was concluded that Sox2 was necessary for the proper formation of the epiblast and its derivatives (Avilion, Nicolis et al. 2003). Upregulation of Sox2 in ES cells using a tetracycline-inducible promoter lead to differentiation and an increase in ectoderm, mesoderm, and

extraembryonic genes. Interestingly, there was no increase extra- or embryonic endoderm genes. There was also a corresponding decrease in pluripotency-related genes targeted by the Oct4-Sox2 complex such as *Oct4*, *Lefty1*, *BMP-4*, *Utf-1*, *FGF4*, *Nanog*, and *Sox2* (Kopp, Ormsbee et al. 2008).

Nanog was first described as an ES cell associated transcript which, when constitutively expressed is capable of maintaining mES cell pluripotency in the absence of leukaemia inhibitory factor (LIF). Nanog is largely restricted to pluripotent cell populations: it is expressed in the morula, ICM, epiblast (but not primitive endoderm), and primordial germ cells *in vivo*, and expressed in ES, EC, EG cell lines. ES cells deficient in Nanog were capable of differentiating to extraembryonic endoderm lineages but not to trophoctoderm, mesoderm or neuroectoderm. Similar to Oct4 and Sox2, no epiblast is formed in Nanog^{-/-} embryos, however, unlike Oct4, Nanog^{-/-} ICMs form parietal endoderm rather than trophoctoderm. Nanog was further found to be unable to maintain pluripotency in the absence of Oct4, even when overexpressed (Chambers, Colby et al. 2003; Mitsui, Tokuzawa et al. 2003).

While Oct4 and Sox2 had been shown to interact to affect the expression of ES cell-specific genes, it was only relatively recently that Nanog was examined alongside of them. In a genome wide study of hES cells, it was found that 50% of Oct4 binding sites were also occupied by Sox2, as expected. Strikingly, over 90% of the Oct4/Sox2 sites were also occupied by Nanog, often in close proximity. Individually and as a trio, Oct4, Sox2, and Nanog (OSN) bound both active and inactive genes relatively equally. Many active genes bound by OSN were important in the maintenance of pluripotency including Oct4, Sox2, Nanog, Stat3, and components of the transforming growth factor (TGF)- β and Wnt signaling pathways. Additionally, the inactive genes bound by OSN were often transcription factors with important roles in differentiation and embryonic development (**Figure 1.5**). It was concluded that Oct4, Sox2, and Nanog compose a central regulatory control of pluripotency and differentiation in ES cells (Boyer, Lee et al. 2005).

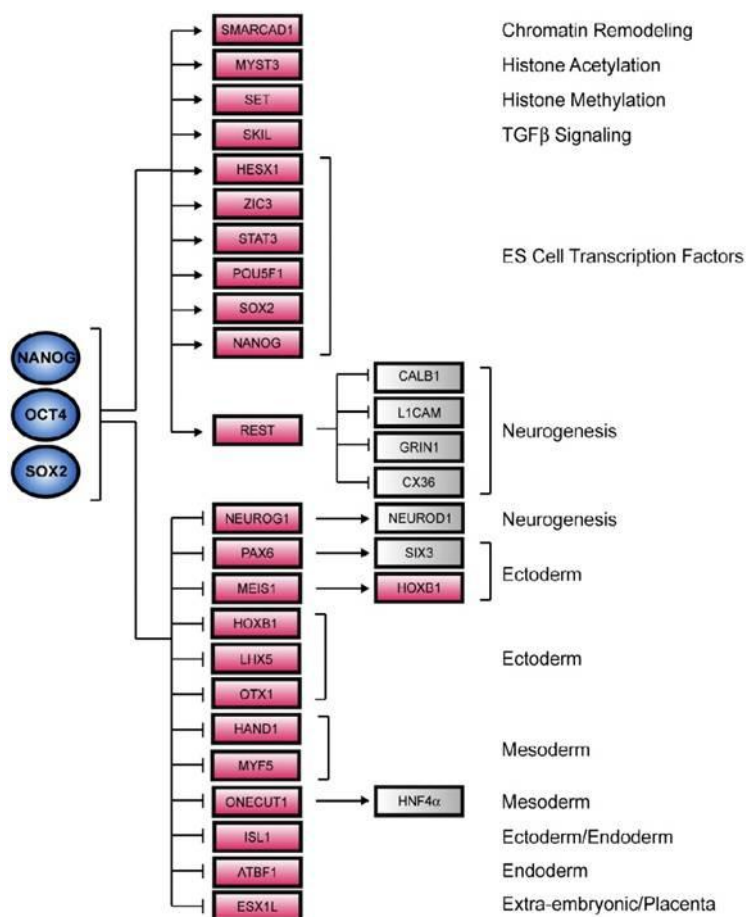


Figure 1.5: Control of Transcription by Oct4, Sox2, and Nanog. Genes involved in the maintenance of pluripotency and early differentiation bound by Oct4/Sox2 and Nanog. Reproduced from (Boyer, Lee et al. 2005).

Two signaling pathways are especially important in maintaining hES cell pluripotency. The TGF- β pathway is split into two components: TGF β /Activin/Nodal signaling which activates SMAD2/3 via activin receptor-like kinase (ALK)-4, 5, and 7 and bone morphogenic protein/growth differentiation factor (BMP/GDF) signaling which activates SMAD1/5 via ALK1-3 and 6. In the undifferentiated state, the TGF β /Activin/Nodal pathway is active and SMAD2/3 is phosphorylated and localized to the nucleus. As differentiation occurs, SMAD1/5 becomes phosphorylated and replaces SMAD2/3 in the nucleus. Chemical inhibition of SMAD2/3 phosphorylation decreased the expression of Oct4 and Nanog and resulted in differentiation. Similarly, differentiation can be induced by activated SMAD1/5 using BMP-4. Upon BMP-4 treatment, Oct4 levels decreased and changes in hES cell morphology were observed (James, Levine et al. 2005).

The canonical Wnt pathway is also crucial for the maintenance of ES cell pluripotency. Wnt activation is characterized by the inactivation of glycogen synthase kinase (GSK)-3 and by the accumulation of β -catenin in the nucleus, which activates the transcription of Wnt target genes. Wnt signaling in cells can be activated by treatment with 6-bromoindirubin 3'-oxime (BIO), an inhibitor of GSK-3. Undifferentiated ES cells express nuclear β -catenin, which is lost upon differentiation. However,

under conditions which would normally promote differentiation, cells treated with BIO preserved undifferentiated cell morphology, showed nuclear β -catenin staining, and maintained expression levels of Oct4, Nanog, and Rex1, another marker of pluripotency (Sato, Meijer et al. 2004).

1.4.3 Differences between Mouse and Human Embryonic Stem Cells

While the defining characteristics of ES cells derived from mice and humans are shared, a number of differences exist between the two cell types (Hyslop, Armstrong et al. 2005). When grown on feeders, hES cells form thinner colonies (2-4 cells thick) than mES cells (4-10 cells thick) and show a substantially longer doubling time (36-45 hours for hES cells compared to 12 hours for mES cells). Differences in surface marker expression between mES and hES cells can also be found. For instance, undifferentiated hES cells, but not mES cells, express SSEA3, SSEA4, TRA-1-60, TRA-1-81, and TRA-2-54 while undifferentiated mES cells express high levels of SSEA1, PECAM (CD31), and LIF receptor (Ginis, Luo et al. 2004). In contrast, both hES cells and mES cells show a similar expression pattern of pluripotency-related genes including *Oct4*, *Nanog*, *Sox2*, *Utf1*, *Rex1*, *Foxd3*, *Tert* and others (Hyslop, Armstrong et al. 2005).

There are also significant differences in the signaling pathways responsible for maintaining pluripotency (**Figure 1.6**). Most notably, mES cells can be grown in the absence of feeders in medium supplemented with LIF, which activates the janus-associated tyrosine kinase/signal transducer and activator of transcription (Jak/Stat3) pathway (Niwa, Burdon et al. 1998). In contrast, attempted activation of Stat3 in hES cells by LIF or interleukin-6 and soluble IL-6 receptor does not prevent differentiation. Further, LIF treatment resulted in a much lower increase in Stat-3 activation in hES cells than in mES cells (Sato, Meijer et al. 2004). As discussed above, in hES cells activation of SMAD1/5 leads to differentiation while SMAD2/3 activation promotes pluripotency. In mES cells, however, SMAD1/5 (activated by BMP-4) inhibits neuroectoderm formation and, along with LIF, will prevent differentiation even in serum-free conditions (Ying, Nichols et al. 2003). Further, mES cells do not require SMAD2/3 activation to maintain pluripotency when cultured in the presence of LIF or BIO, though neither factor is capable of preventing hES cell differentiation if SMAD2/3 is inactive (James, Levine et al. 2005).

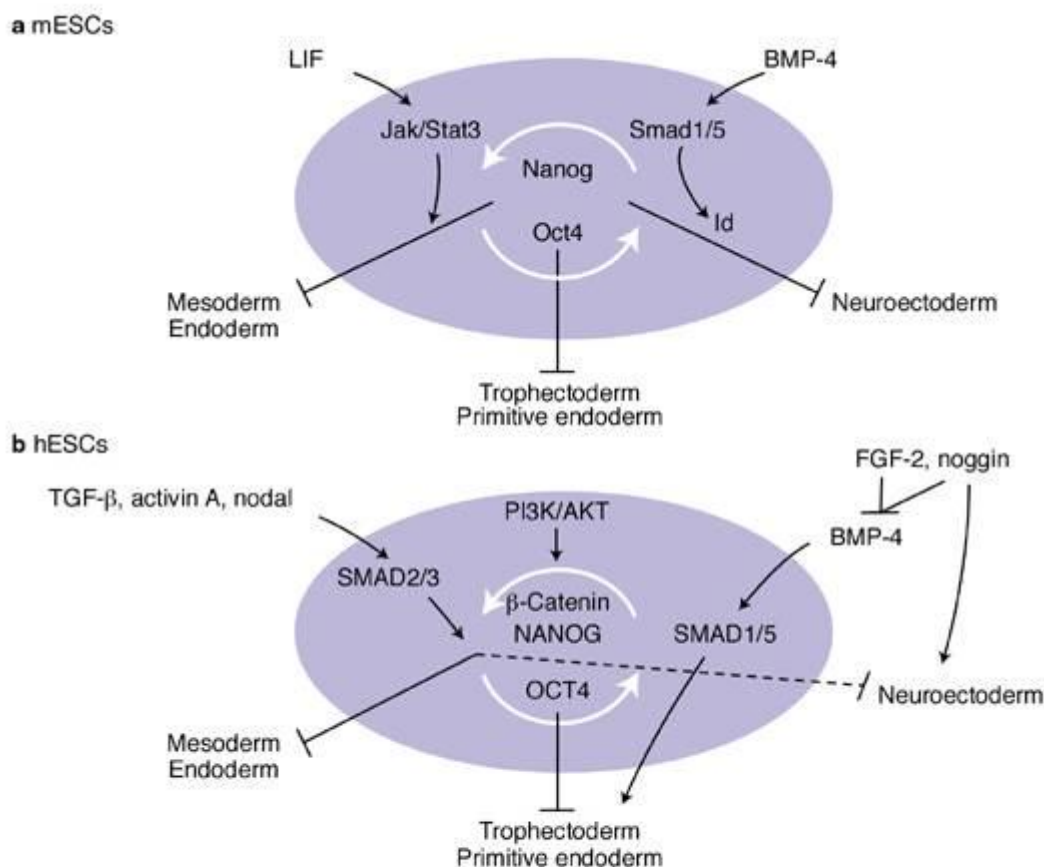


Figure 1.6: Differences in Signaling Pathways between (a) Mouse and (b) Human ES Cells. The most notable differences are the effects of BMP-4, which promotes pluripotency in mouse ES cells but differentiation in human ES cells, and LIF, which prevents differentiation of mouse but not human ES cells. Modified from (Hyslop, Armstrong et al. 2005).

Interestingly, a recent report describing the derivation of pluripotent cells from the mouse epiblast (termed EpiSCs) has shed some light on the differences between mouse and human ES cells. It was observed that hES, but not mES, cell culture conditions supported EpiSC growth and that EpiSCs formed thin, flat colonies more reminiscent of hES cells than mES cells. Further, epigenetic patterns, TGF-β pathway signaling, pluripotency regulatory pathways, and differentiation patterns were found to be more similar between EpiSCs and hES cells than mES cells (Tesar, Chenoweth et al. 2007). This strongly suggests that hES cells may fundamentally differ from mES cells: hES cells represent a developmental population more akin to the epiblast while mES cells are more truly correspond to cells from the early ICM.

1.4.4 Culture and Characterization of Embryonic Stem Cells

Culture techniques for the propagation of undifferentiated hES cells are constantly being developed to ensure pluripotency, genetic stability, and minimize the presence of xenomaterials (reviewed in (Draper, Moore et al. 2004; Hasegawa, Pomeroy et al. 2010)). Traditionally, hES cells are grown as

colonies several cell layers thick plated on MEF feeder cells in medium containing knockout serum replacement (KOSR, Invitrogen) and 4-10 ng/mL basic fibroblast growth factor (bFGF). Human feeders, including human foreskin fibroblasts and human foetal fibroblasts, as well as MEF-conditioned medium can replace the need for MEF co-culture. Additionally, xeno-free serum replacements are available to replace KOSR. However, in cases where feeder cells are not used another source of extracellular matrix (ECM) is needed, such as Matrigel (BD Biosciences) or purified ECM components. Due to the growing understanding of important signaling pathways in pluripotency (discussed above), recent advances have been made in serum-free, defined media that do not require feeder cells. Finally, small molecule inhibitors of histone deacetylase, GSK3 β , and BMP-4 receptor type 1 have been shown to prevent spontaneous differentiation and may be integral in designing relatively inexpensive defined media. High-throughput screening assays have also been developed to identify small molecules from chemical libraries that promote hES cell pluripotency and self-renewal (Desbordes, Placantonakis et al. 2008). This would support the goal of establishing xeno-free, fully defined culture media and would potentially be much cheaper than the use of recombinant proteins.

Ludwig et al. 2006 were able to derive two hES cell lines from blastocysts using the non-xenogenic TeSR1 medium with fully defined human factors (with the exception human serum albumin) supplemented with bFGF, LiCl, GABA, pipercolic acid, and TGF- β . The cells were grown on recombinant collagen IV, fibronectin, laminin, and vitronectin (Ludwig, Levenstein et al. 2006). Currently there are commercial media available that are xeno-free, serum-free, and allow the growth of hES cells without feeder cells. For instance, StemPro hESC SFM (Invitrogen) has been shown to be effective in the growth and maintenance of hES cells when using the defined, xeno-free matrix CELLstart as a replacement for Matrigel. The medium is supplemented with recombinant bFGF and 2-mercaptoethanol (Wagner and Vemuri 2010).

In addition to changes in medium, advances are also be made in culture systems. Recently, a novel system was reported in which hES cells could be derived from embryos and propagated in suspension (Steiner, Khaner et al. 2010). Cells were grown in Neurobasal medium with Nurtidoma-CS (a serum replacement) and supplemented with neurotrophic factors (NT-3, NT-4, and brain-derived neurotrophic factor, BDNF), Activin A, and bFGF along with dissolved ECM components such as laminin, fibronectin, and gelatin. The cells grew as floating, spheroid aggregates with comparable rates of proliferation, cell death, and apoptosis as adherent cultures. However, the suspended cultures had a lower rate of expansion, which was attributed to cell loss during passaging, performed by trituration of the spheroid aggregates. The cells also showed maintained pluripotency and could undergo directed differentiation. This method avoided the use of feeder cells (though it did not use

defined components) and, most significantly, showed a great potential in the ability to effectively scale up hES cell culture.

Passaging of hES cells is generally done mechanically or by enzymatic dissociation using collagenase IV or dispase (discussed in Chapter 2 Materials and Methods). Complete dissociation into single cells generally results in very low survival and is thought to accelerate the formation of chromosomal abnormalities. hES cells are characterized based on their morphology and expression of specific surface markers (such as SSEA3/4, TRA-1-60/81), pluripotency-related proteins (OCT4, NANOG, SOX2), and other enzymes (alkaline phosphatase, telomerase) using assays, immunofluorescence, flow cytometry, and quantitative PCR (qPCR). Additionally, their differentiation potential must be demonstrated *in vitro*, often by the formation of differentiating embryoid bodies (EBs) containing markers from each germ layer, and *in vivo*, based on the formation of teratomas in immunocompromised mice (Draper, Moore et al. 2004; Hasegawa, Pomeroy et al. 2010).

1.4.5 Differentiation of Embryonic Stem Cells to Skeletal Muscle

The early experiments involving ES cell differentiation towards the muscle lineage showed that the pattern of myogenic gene activation during EB culture mimics that of *in vivo* myogenesis. EBs are spherical aggregates of ES cells that resemble the early embryo and are commonly used to study differentiation during early development. When EBs are plated and allowed to produce outgrowths, some cells naturally differentiate into muscle fibres. In the mouse ES cell line BLC6, the genes *Myf5*, *myogenin*, *MyoD*, and *Myf6* are all activated in the order seen during early muscle formation *in vitro*. Further, myocytes derived from these cells were also shown to express functional nicotinic acetylcholine receptors and have Ca^{2+} currents that mirror normal skeletal muscle cells (Rohwedel, Maltsev et al. 1994). Thus, *in vitro* ES cell-derived myocytes are physiologically indistinguishable from normal muscle cells.

Subsequent work, also in mouse ES cell lines, was able to decipher the role of various MRF genes during myogenesis without needing to produce knockout mice that may not survive early development or may express complicated phenotypes. *Myf5* is the first myogenic gene expressed in differentiating EBs (Rohwedel, Maltsev et al. 1994). *Myf5*^{-/-} ES cells were found to still produce skeletal muscles after being differentiated as EBs for 5-7 days and plated at low density for 3-5 days. However, closer examination showed that while control ES cells produced both MyoD⁺ and MyoD⁻ cells, *Myf5*^{-/-} ES cells only produced MyoD⁺ muscle cells and began to express MyoD earlier than their wildtype counterparts (Braun and Arnold 1994). This suggests that MyoD is capable of compensating for a lack of *Myf5* expression during myogenic development. Conversely, ES cells that are homozygous null for the *desmin* gene showed a total inhibition in skeletal and smooth muscle formation (but not cardiac muscle formation) after EB differentiation for 4.5 days and subsequent

plating. ES cells heterozygous for the *desmin* gene showed an increase in the number of myocytes but a dramatic decrease in secondary myotube formation indicative of the important role of desmin in myocyte fusion (Weitzer, Milner et al. 1995). Similarly, myogenin^{-/-} ES cells failed to produce skeletal muscles when differentiated for 5 days as EBs. Their ability to form muscle was restored when myogenin was constitutively expressed in the cells by transfecting them with a myogenin-expression plasmid. This was not the case when myogenin^{-/-} cells were transfected with a MyoD-expression plasmid, which led to an increase in myoblast formation but only a marginal increase in mature myocytes (Myer, Olson et al. 2001). This confirms results found in developing myogenin^{-/-} mice which show proper myoblast migration and commitment but not fusion to form myofibres (Hasty, Bradley et al. 1993; Nabeshima, Hanaoka et al. 1993). Thus myogenin and MyoD have distinct roles in the differentiation of myoblasts and the final formation of myofibres. The same group later goes to show that unlike MyoD, constitutive MRF4 expression in myogenin^{-/-} ES cells will rescue proper myotube formation, suggesting that the roles of MRF4 and myogenin are closely related (Sumariwalla and Klein 2001).

The effects of genes outside the MRF family have also been studied in relation to ES cell myogenesis. Knockout embryos lacking the $\beta 1$ integrin subunit die just after implantation occurs, making it difficult to assess the function of $\beta 1$ in development (Fassler and Meyer 1995; Stephens, Sutherland et al. 1995). However, ES cells lacking $\beta 1$ can form EBs which, after being grown and plated to allow outgrowths, show a delay in myogenic differentiation and myofibre organization. Reverse transcriptase (RT)-PCR analysis shows a slower onset of transcript expression in MRF genes of $\beta 1$ -null cells compared to wildtype or heterozygous controls. $\beta 1$ -null outgrowths from EBs also tended to form myoblasts but were less likely to fuse into myofibres (Rohwedel, Guan et al. 1998). A delay in myogenesis has also been shown when the basic helix-loop-helix protein M-twist is overexpressed in ES cells. EBs overexpressing M-twist were grown for 5 days and plated for both morphological and RT-PCR analysis. Myocyte and myotube formation occurred approximately 3 days later than in wildtype cells and the expression of several MRFs and M-cadherin were delayed anywhere from 1 to 4 days relative to control cells (Rohwedel, Horak et al. 1995).

Other genes have been found to enhance myogenic differentiation of ES cells. IGF-II is known to induce differentiation in myoblasts by promoting myogenin expression (Stewart, James et al. 1996; Stewart and Rotwein 1996). Overexpression of IGF-II in ES cells accelerates and enhances myogenic differentiation in 7 day cultured EBs. After the EBs were plated and cultured for 7 days, immunostaining for M-cadherin and several myotube-specific proteins showed an increased number of myocytes which had matured more quickly in IGF-II-overexpressing cells compared to control cells. RT-PCR analysis showed an increase in Myf5, myogenin, and MyoD mRNA in the IGF-II cultures (Prele, Wobus et al. 2000). Similarly, overexpression of an activated mutant of the high mobility

group type A-2 (HMGA2) protein increases myogenic differentiation of ES cells. After EB formation and approximately 21 days in culture, differentiated HMGA2 cells showed more than a five-fold increase in myotubes than control cells. Teratocarcinomas from these cells also contained large areas of muscle fibres unlike control tumours. Interestingly, this increase was not accompanied by a corresponding increase in the levels of Myf5, MyoD, or myogenin mRNA, as determined by RT-PCR or northern blot analysis. These data led the authors to conclude that HMGA2 acted through an unknown myogenic differentiation mechanism most likely to be involved in the later stages of muscle differentiation (Caron, Bost et al. 2005).

While there has been a good deal of work studying the differentiation of ES cells to muscle, most of the effort has focused on illuminating the roles of various genes in the early decisions leading to myogenesis. Relatively little time has been devoted to the therapeutic aspect of ES cells in regards to muscular dystrophy. Several reports, discussed in Chapter 4, describe the derivation of cells with myogenic potential from ES cells.

1.5 Induced Pluripotent Stem Cells

1.5.1 A Brief History of Reprogramming

Differentiated cells (or nuclei) can be reprogrammed to pluripotency through several methods. These include nuclear transfer (or cloning), cell fusion, and transcription factor transduction (**Figure 1.7**, (Yamanaka and Blau)). Nuclear transfer is the transfer of a somatic cell nucleus into an enucleated oocyte or zygote and was the earliest means of reprogramming. The first experiments involved the transfer of nuclei from frog blastocysts into oocytes, resulting in clones that could be grown to the tadpole stage (Briggs and King 1952) and, later, into adult frogs. These experiments were then successfully repeated with more differentiated tadpole intestinal cells (Gurdon 1962). Crucially, this work showed that differentiation did not require irreversible genetic changes in cells. The work was later extended to mammals when a mammary cell was fused with an unfertilized enucleated oocyte resulting in the first cloned mammal, Dolly the sheep (Wilmut, Schnieke et al. 1997). Shortly thereafter the first mice were successfully cloned (Wakayama, Perry et al. 1998).

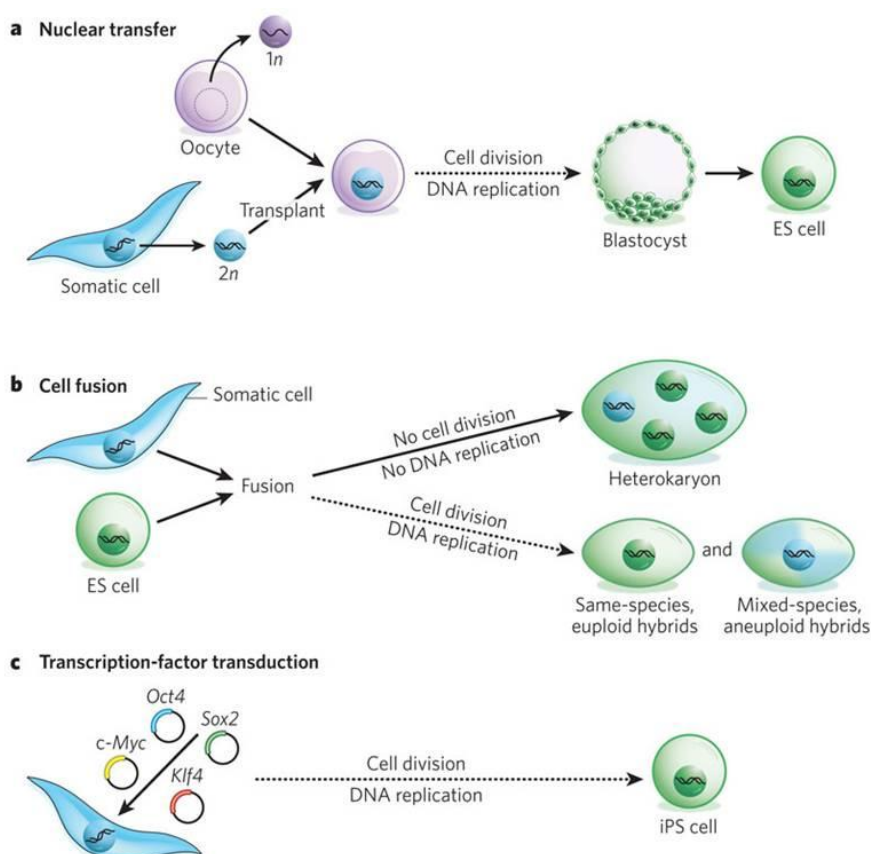


Figure 1.7: Methods of Reprogramming Cells to a Pluripotent State. Cells can be reprogrammed using (a) nuclear transfer of a differentiated cell into an enucleated oocyte, (b) by fusing a somatic cell with an undifferentiated cell (or multiple undifferentiated cells), and (c) by the introduction of exogenous transcription factors important in establishing and maintaining pluripotency. Reproduced from (Yamanaka and Blau).

Cell fusion is another route towards reprogramming. Early experiments had shown that genes, in this case responsible for pigmentation, expressed in differentiated cells such as hamster melanoma cells could be turned off by fusion with mouse fibroblasts (Davidson, Ephrussi et al. 1966). Subsequent studies went on to show that malignancy in transformed cells could be suppressed by fusion with normal cells expressing tumour repressors (Harris, Miller et al. 1969). However, the most important early studies that demonstrated the activation of silenced genes used heterokaryons, multinucleate, non-dividing products of cell fusion. Human muscle proteins were observed when human amniotic cells were fused to mouse muscle fibres (Blau, Chiu et al. 1983). Studies with heterokaryons also demonstrated the importance of epigenetics in reprogramming, as mitosis did not occur.

In order to achieve nuclear reprogramming and the expression of pluripotency markers by cell fusion, pluripotent cells must be used. This was first demonstrated when mouse EG cells were fused with adult thymocytes. The resultant cells showed significant epigenetic reprogramming including widespread DNA demethylation and were capable of contributing to all three germ layers in chimeric

embryos (Tada, Tada et al. 1997). Similar results were found when mES cells were fused to thymocytes. In this case, the thymocytes contained a GFP construct driven by the *Oct4* promoter, and GFP expression was observed in fused cells (Tada, Takahama et al. 2001).

The use of exogenously expressed transcription factors to achieve reprogramming was preceded by experiments showing that the overexpression of certain genes in *D. melanogaster* larvae could alter the fate of specific tissues or structures in the adult. In one study, *Antennapedia* overexpression was capable of replacing antennae with legs from the second thoracic segment (Schneuwly, Klemenz et al. 1987), while in another experiment, ectopic expression of *Pax6* was found to induce eye formation on the legs, wings, and antennae (Gehring 1996). Similarly, the *MyoD* gene in mice was the first “master regulator” found in mammals capable of converting one cell type to another. Several transcripts expressed in fibroblasts which had been converted to myoblasts using 5-azacytidine were used to generate cDNAs. The transfection of one of these, representing the *MyoD* gene, was capable of converting fibroblasts to myoblasts (3690668). These findings led to the work by Yamanaka et al. which showed that the expression of only four factors (*Oct4*, *Sox2*, *Klf4*, and *c-Myc*) was sufficient to reprogram differentiated cells to undifferentiated “induced pluripotent stem” (iPS) cells similar in nature to ES cells (Takahashi and Yamanaka 2006). This work is discussed in detail in Chapter 6.

1.5.2 The Events of iPS Cell Reprogramming

The series of events culminating in pluripotency of reprogrammed cells is incompletely understood. However, several studies in mouse fibroblast reprogramming have started to outline the sequence of molecular and epigenetic changes which take place. Using doxycycline-inducible promoters driving expression of *Oct4*, *Sox2*, *Klf4*, and *c-Myc* in MEFs, Brambrink et al. showed that alkaline phosphatase was the first mES cell-specific marker to be expressed, followed by SSEA1. It was not until significantly later in the reprogramming process that the classic pluripotency factors *Oct4* and *Nanog* were first expressed. They further demonstrated that reprogramming efficiency increased the longer the reprogramming factors were expressed, but expression of the four factors prevented proper differentiation of iPS cells (Brambrink, Foreman et al. 2008). A similar set of experiments by Stadtfeld et al. confirmed that the induction of SSEA1 expression occurred early in the process, while expression of *mTert* and *Sox2* as well as X chromosome reactivation are later steps in reprogramming. Another characteristic of ES cells, the ability to silence viral genes, was also examined. They found that viral genes were progressively silenced as reprogramming occurred and that this process corresponded to the gradual increase in expression of genes important in epigenetic silencing such as *DNA methyltransferase 3b* (*Dnmt3b*) and *TRIM28* (Stadtfeld, Maherali et al. 2008).

A more in depth study of changes in gene expression revealed that as reprogramming occurs MEF-specific genes (*Snai1/2*) are downregulated while genes involved in DNA replication and cell cycle

progression were upregulated, consistent with the observed increase in proliferation and with c-Myc expression. However, an increase in anti-proliferative genes was also observed, attributed to Klf4 expression and deregulated c-Myc expression. Genes involved in lineage-specific functions such as axon guidance or glomerular proteins were also observed during the reprogramming process, suggesting that the introduction of the four transcription factor has broad effects on gene expression beyond the induction of pluripotency. ES cells are characterized by a very specialized epigenetic landscape such as a broad enrichment of H3K4me3 (indicating gene activation) on high-CpG promoters, a subset of which is also enriched with H3K27me3 (indicating gene repression). These “bivalent” domains are usually associated with the repression of genes involved in early development. The epigenetic patterning was largely replicated in fully reprogrammed iPS cells. In contrast, partially reprogrammed cells will express genes conducive to self-renewal and proliferation but not pluripotency. The number of bivalent domains in partially reprogrammed cells is somewhere between that seen in iPS cells or MEFs and most pluripotency genes were found to be hypermethylated, indicating gene repression (Mikkelsen, Hanna et al. 2008).

These reports suggest that reprogramming is largely a stochastic process of epigenetic rearrangement. There are general trends in gene activation which have been observed, for instance, SSEA1 will be expressed early in the transition while pluripotency genes are not expressed until much later, but reprogramming does not seem to occur in a consistent, step-wise manner between or even within cell lines. As a result, the vast majority of cells exposed to the exogenous factors do not complete reprogramming: many halt along the way or revert back to a fibroblast-like cell type. Further work is needed to elucidate the important steps in this process. Much of the work to date has focused on the method of gene delivery, the flexibility in which pluripotency genes are used, and applying the technique to disease models. These aspects of iPS cell technology are discussed in more detail in Chapter 6.

1.6 Project Aims

The lack of suitable treatments for muscular dystrophies may be addressed through the differentiation of human embryonic stem cells to muscle satellite cells or similar myogenic precursors. However, an efficient and simple protocol for the differentiation and isolation of skeletal muscle tissue from hES cells has not been reported. Further, the recent advancement of reprogramming through transcription factor transduction provides an avenue for the generation of patient-specific pluripotent cell lines. With these considerations in mind, the goals of this project were to:

1. Develop a simple and efficient method for the differentiation of hES cells to muscle satellite cells.
2. Develop a method to isolate myogenic cells from differentiated hES cells using fluorescence activated cell sorting based on myogenic-specific protein expression.
3. Confirm the myogenic nature of differentiated and isolated cells using protein and gene expression analysis.
4. Test the ability of iPS cells to undergo myogenic differentiation.
5. Generate a line of iPS cells from patients with Duchenne muscular dystrophy.

Chapter 2: Materials and Methods

2.1 Cell Culture

2.1.1 *Adult and Foetal Myoblast Culture*

Adult and foetal human myoblast cells were used to examine the gene and surface marker expression of myogenic cells, for conditioning medium for hES cell differentiation, and for co-culture differentiations. The foetal myoblast line, HFM, was obtained from Dr Jennifer Morgan at the Centre for Neuromuscular Diseases at University College, London. The adult myoblast lines, S31/05 and 17/01, and the foetal myoblast line, FHM, were obtained from Dr Steve Laval at the Institute of Human Genetics at Newcastle University.

Cells were grown in T25, T75, or T150 culture flasks (Iwaki) at 37°C and 5% CO₂ using a recipe for Myogenic medium provided by Dr Morgan. The medium consisted of Dulbecco's modified Eagle's medium:F12 (DMEM:F12) with glutamine (PAA) with 20% foetal bovine serum (FBS, Bioclear), penicillin-streptomycin (100 units/mL of penicillin and 100 µg/mL streptomycin, Gibco), 0.4 µg/mL dexamethasone (Sigma), 10 µg/mL recombinant human insulin (Sigma), 10 ng/mL recombinant human epidermal growth factor (EGF, Sigma), and 1 ng/mL recombinant human bFGF (Invitrogen). All medium was sterile filtered and stored in filter bottles (Nalgene) prior to use. Medium was changed every two days. Cells were passaged 1:2 or 1:3 when they reached 80-90% confluency, generally after 2-3 days. To passage cells, the medium (5 mL/T25, 15 mL/T75, and 30 mL/T150) was aspirated and the flask was washed with an equal volume of phosphate buffered saline (PBS, PAA). Approximately 0.15 volumes of Trypsin-EDTA (0.5 g/L Trypsin and 0.2 g/L EDTA, Gibco) were added and the flask was incubated at 37°C for 4-5 minutes. The cells were then washed and resuspended with at least 0.5 volumes of Myogenic medium to dislodge adherent cells and neutralize the trypsin. The cell suspension was transferred to a 15 mL Falcon tube (BD Falcon), centrifuged for 4 minutes at 900 rpm in a tabletop centrifuge (Eppendorf), the supernatant was aspirated and the pellet was resuspended in 0.5-1 mL of medium per flask seeded. To freeze cells for cryopreservation, the pellet was resuspended in 0.5 mL of cold cryopreservation medium containing 90% FBS and 10% dimethyl sulfoxide (DMSO, Sigma), transferred to a cryovial (Nunc) and frozen slowly at -80°C in a 5100 Cryo 1°C Freezing Container ("Mr. Frosty," Nalgene). Cells could be stored at -80°C for several months before being transferred to liquid N₂. Cells were thawed by warming the cryovial in a 37°C water bath until the suspension was completely liquid then transferring it drop-wise into 8 mL of pre-warmed Myogenic medium in a 15 mL Falcon tube. The suspension was then centrifuged and seeded as

described above. Cells were seeded onto the same sized flask that they were frozen down from and allowed to adhere overnight at 37°C and 5% CO₂.

2.1.2 *hES Cell Culture*

The human embryonic stem cell line, H9 (WiCell), was used between passages 30 and 70 for all experiments.

2.1.2.1 *Feeder Preparation*

H9 cells were grown on either human or mouse embryonic fibroblast (H/MEF) cells. MEFs were cultured in T150 or T300 flasks at 37°C and 5% CO₂ using high glucose DMEM (PAA) containing 10% FBS (Bioclear), 1:100 non-essential amino acids (NEAA, Gibco), 1:100 Glutamax (Gibco), and Penstrep (Gibco). Feeders were passaged up to five times after being harvested and generally seeded at a 1:3 or 1:4 dilution. The protocol for passaging and freezing/thawing cells is described above. To prepare MEFs for use as feeders, non-confluent cells in a T300 flask containing 50 mL of medium were inactivated by adding 500 µL of 1 mg/mL mitomycin C (Sigma) in Knockout (KO) DMEM (Gibco) and incubating at 37°C for 2.5 hours. The medium was removed, the cells were rinsed three times with PBS and then trypsinized by adding 8 mL of Trypsin-EDTA and incubating at 37°C for 4-5 minutes. The cells were resuspended in 25 mL of medium, transferred to a 50 mL Falcon tube, and centrifuged at 900 rpm for 3 minutes. The supernatant was aspirated and cells were suspended in 20 mL of medium before being counted using a hemocytometer. Cells were seeded onto 6-well plates at 120-140,000 cells/well in 2 mL of medium and allowed to settle overnight. Plates had been treated with 0.1% Gelatin in distilled water (1 mL per well) for at least one hour and then aspirated prior to cell seeding.

2.1.2.2 *hES Cell Maintenance and Passaging*

H9 cells were grown at 37°C and 5% CO₂ using hES medium consisting of KO DMEM (Gibco) with 20% KO Serum Replacement (KOSR, Gibco), 8 ng/mL bFGF (Invitrogen), Glutamax, NEAA, and Penstrep. Cells grew as adherent colonies alongside MEFs and required cleaning approximately every other day. To clean cells, they were transferred to an IVF workstation (K systems) and examined under a dissection microscope (Nikon SMZ800). Differentiated cells were removed from colonies (**Figure 2.1**) using a 200 µL pipette tip and medium was changed after cleaning or whenever it began to appear yellowish in colour. Every 4-7 days the cells were passaged either mechanically, using a 1000 µL pipette tip to divide and remove colonies, or by collagenase treatment. For the latter, the medium is aspirated, replaced with 1 mg/mL collagenase, type IV (Gibco) in KO DMEM and incubated at 37°C for 15-20 minutes. The collagenase solution is then carefully aspirated to avoid removing adherent colonies and replaced with 3 mL/well of hES medium. The cells are incubated at 37°C for 10-15 minutes and then removed by gently pipetting up and down with approximately 300 µL of medium in a 1000 µL pipette to dislodge and break apart the colonies. Once the colonies are divided and

floating, the medium can be transferred to 6-well plates containing fresh MEFs and new hES medium. Cells are usually seeded 1:3 when passaged mechanically or 1:4 or higher when passaged with collagenase. The colony pieces are allowed to settle for 2-3 days without medium changes or cleaning.

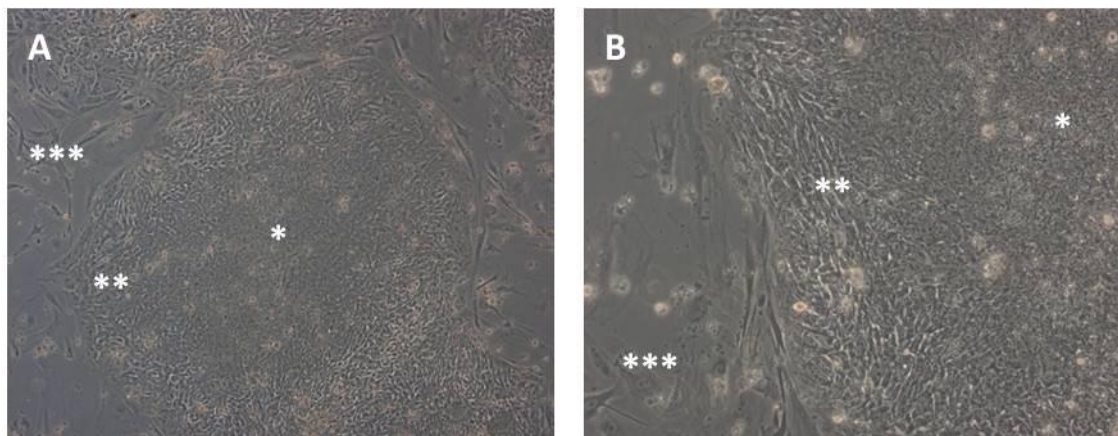


Figure 2.1: Human Embryonic Stem Cell Colonies. A colony of H9 hES cells at (A) 5x and (B) 10x magnification prior to cleaning. *Undifferentiated H9 cells at the centre of the colony can be seen amongst **differentiated H9 cells and ***MEFs.

hES cells were frozen in cryovials. When freezing down cells, colonies were treated with collagenase and removed as if passaging, however the colonies were generally kept as larger pieces. The cells were then transferred to a 15 mL Falcon tube and centrifuged at 300 rpm for 1 minute. The supernatant was carefully aspirated (as the pellet was very loose) and the cells were resuspended in 1 mL hES medium per 6-well plate. An equal volume of hES cryopreservation medium (60% KOSR, 20% DMSO, 20% hES medium) was added drop-wise to the falcon tube while gently mixing and 1 mL of the mixed solution was transferred to a cryovial for overnight freezing at -80°C in a “Mr. Frosty” (Nalgene).

Cells were thawed by incubating the cryovials in a 37°C water bath until the medium was completely liquid. The cryovial was then mixed gently to suspend the colonies and the medium was added drop-wise to a 15 mL Falcon tube containing 8 mL of pre-warmed high-bFGF (16-24 ng/mL) hES medium. The colonies were allowed to settle at the bottom of the tube and the medium was gently aspirated, replaced with another 3 mL of hES medium, and centrifuged at 300 rpm for 1 minute. Again, the medium was aspirated and 1.5 mL of hES medium was added to resuspend the colonies and transfer them to a 6-well plate. 0.5 mL of the suspension was added to each of three wells in a 6-well containing 1.5 mL of pre-incubated high-bFGF hES medium. Colonies were allowed to settle for at least two days before changing medium and grown in high-bFGF hES medium for at least one passage.

2.1.2.3 hES Cell Monolayer Differentiation

A number of hES cell differentiations were set up with the intention of promoting skeletal myogenesis primarily using combinations of differentiation medium and myoblast conditioned medium for various lengths of time. They are summarized in **Table 2.1** and described in detail below.

Table 2.1 Monolayer Differentiations of hES and iPS Cells

Differentiation	Medium Used	Cells	Time Points
D(X)CM(Y)	Diff 20% Horse Serum, then HFM Conditioned Medium	H9s	Diff: 3, 5, 7 days CM: 7, 10 days
HFM	1:1 Diff(20% FBS):CM (Diff:CM)	H9s, H9 Pax7-GFP, iPS cells	6, 12, 16, 20 days
Activin A	Diff:CM with 10, 30, 50, 100 ng/mL Act. A, then Diff:CM	H9s	10 days with Act. A, 6 days without
Myoblast media	Diff:CM with conditioned medium from 17/01, S31/05, and FHM lines	H9s	12 days
BMP-4 Co-culture	SFM* with BMP-4, then SFM, then increasing concentrations of Diff:CM	H9-GFP	12, 17, 21, 28 days
Control	Diff (20% FBS)	H9s, H9 Pax7-GFP, DMD iPS	12 days

*SFM – Serum-free medium

For the monolayer differentiation strategies, hES cells were seeded on tissue culture treated 6-well plates as described above. The medium was changed to the various types of differentiation medium prior to colony removal. Cultures were grown in incubators at 37°C and 5% CO₂.

In the initial differentiation strategy, hES cells were seeded at a 1:3 dilution and the differentiation medium contained KO DMEM with 20% Horse Serum, Glutamax, NEAA, and Penstrep (as above). The conditioned medium was simply myogenic medium (described above) which had been filtered after it was conditioned by HFM cells for 2 days. Conditioned medium was stored in the dark because of the presence of light-sensitive dexamethasone. The cells were grown in differentiation medium for 3, 5, or 7 days before being switched to conditioned medium for 7 or 10 days (each time point was thus named D3CM7, D5CM10, etc.). The day the hES cells were plated was considered day 0. Early in the differentiation, 2 mL of medium per well was used, increasing to 3 mL/well after 12 to 14 days. Medium was changed every two days until the cells were harvested for staining and flow cytometry.

Subsequent differentiations used hES cells seeded at a 1:6 dilution and used a 1:1 ratio of Diff medium (KO DMEM with 20% FBS, Glutamax, NEAA, and Penstrep) and conditioned medium (called Diff:CM) from the HFM, FHM, 17/01, or S31/05 myoblast line. HFM cells were used to condition the medium unless otherwise noted. Diff:CM medium was added from day 0 of the differentiation and changed every two days until the cells were harvested. For the set of experiments using Activin A, cells were differentiated in Diff:CM containing either 10, 30, 50, or 100 ng/mL Activin A (PeproTech)

for 10 days, followed by 6 days in Diff:CM without Activin A. For H9 Pax7-GFP cells (described below), the differentiation medium contained 100 µg/mL neomycin.

2.1.2.4 hES Cell Co-culture Differentiation

To further promote myogenesis, a new differentiation method was designed using BMP-4 to induce mesoderm formation early in the differentiation (Zhang, Li et al. 2008) and myoblast co-culture and conditioned medium to stimulate myogenesis.

In order to prepare plates for co-culture differentiations, an optimal seeding density for differentiating FHM cells had to be determined. Densities of 20, 40, 80, and 120,000 cells per well in 6-well plates were tested. Myoblasts were differentiated in KO DMEM with 2% horse serum, Penstrep, and 10 ng/mL insulin for up to 12 days. Lower densities resulted in sparsely populated cells that did not proliferate, elongate, or form networks of myofibres while higher densities prevented cells from differentiating. Thus, for the hES differentiation experiments, FHM cells were seeded at 60-70,000 cells per well and differentiated for 7 to 10 days. However, upon re-exposure to myogenic (growth) medium, residual myoblasts in the differentiated cultures would begin proliferating. It was therefore necessary to mitotically inactivate cells using mitomycin C or X-ray irradiation. Mitomycin C treatment for 2:45 hours was found to effectively prevent myoblast proliferation while cultures which underwent X-ray irradiation (120 kV; 4.0 mA; 12.5 minutes, Faxitron X-ray) eventually began growing again. After mitomycin-C treatment, cells were washed 3 times in PBS and incubated in hES medium.

A line of H9 hES cells containing a pCAG CMV-GFP(Puro) construct (H9-GFP), which constitutively express GFP, was used to distinguish differentiating hES cells from the myoblast feeder cells (**Figure 2.2**). On Day 0 of the differentiation, H9-GFP cells were plated onto the inactivated, differentiated myoblast cultures at a 1:12 dilution in hES medium for 24 hours, followed by serum free medium (SFM, RPMI with 1% insulin transferrin selectin (ITS), Glutamax, NEAA, Penstrep) with 25 ng/mL BMP-4 (PeproTech) for 24 hours, and then SFM without BMP-4 for 48 hours. At this point, the medium was changed to increasing concentrations of HFM conditioned medium in DMEM with Glutamax, NEAA, and Penstrep (Diff- medium). Cells were grown in 7:1, 3:1, then 1:1 Diff-/CM for four days each or until the time point had been reached. Differentiations were stopped after 12, 17, 21, and 28 days.

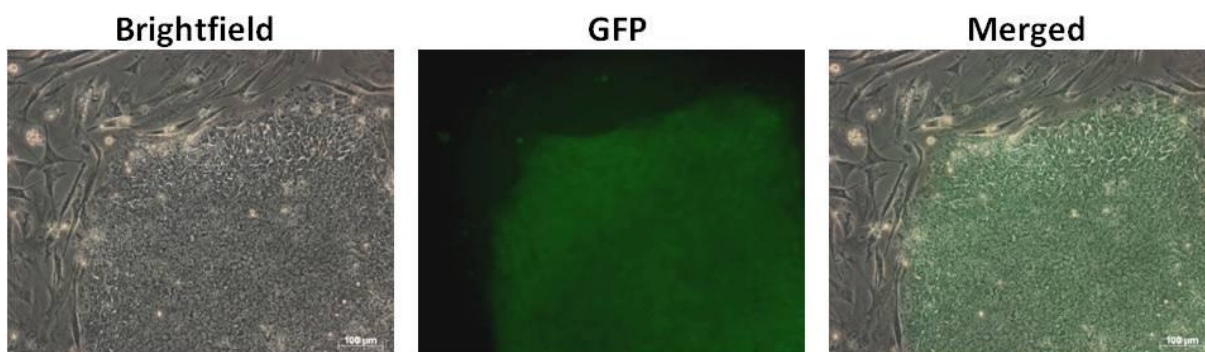


Figure 2.2: H9-GFP Cells. A colony of undifferentiated H9-GFP cells at 10x magnification. GFP expression in the colony is clearly distinguishable from the surrounding MEFs.

2.1.3 Culture and Differentiation of iPS Clone IV Cells

The iPS clone IV cells were generated by transducing adult human dermal fibroblasts with *NANOG*, *OCT4*, *SOX2*, *KLF4*, and *MYC* in retroviral particles (Armstrong, Tilgner et al. 2010). iPS cells were grown and passaged using the same conditions as hES cells. However, it generally took 1-2 days longer than hES cells for iPS cells to grow to the point of passaging.

To differentiate, iPS cells were plated onto new plates without MEF feeders and grown in Diff:CM for 12 (three trials), 16 (one trial), or 20 days (one trial).

2.1.4 Culture of DMD Fibroblast Cells

Fibroblasts from two patients with Duchenne muscular dystrophy were obtained from the Newcastle Biobank. The first sample (F029) came from an 8 year old male patient with a mutation in exon 53 of the *DYSTROPHIN* gene. The second sample (F055) came from a 5 year old male patient with a mutation in exon 68 of the *DYSTROPHIN* gene. Both samples were passage one. Cells were cultured in T25 flasks (Iwaki) in MEF medium and usually passaged every 3-4 days. For passaging, freezing/thawing, and counting, cells were handled using the same protocols described for MEFs.

2.2 Generation of the Pax7P-GFP Construct

In order to detect *PAX7* gene activity for the purpose of using *PAX7* expression to sort differentiating hES cells, a 1.5 kilobase (kb) region of the *PAX7* promoter (Pax7P) was cloned into the pEGFP-1 vector (Clontech) so that GFP would be expressed when the gene was active.

2.2.1 PCR Isolation of the PAX7 Promoter

PCR was used to isolate the fragment of the *PAX7* promoter from human genomic DNA. Using the primers 5'-CTGACTCCTGATCATTTCAGTTGGG-3' and 5'-GCGATCTCTTTCTTTCCGTCTTCT-3' a 1.6 kb portion of the promoter was amplified using the following 50 μ L reaction mixture: 29.25 μ L H₂O, 10 μ L 5x GoTAQ Buffer (Promega), 2.5 μ L dimethyl sulfoxide (DMSO, Finnzyme), 1 μ L of 100 ng/ μ L human genomic DNA, 1 μ L of each primer (100 μ M), 5 μ L of 2 mM dNTPs (New England Biolabs), and 0.25 μ L of GoTAQ DNA polymerase (Promega). The reaction was run in a Mastercycler gradient thermocycler (Eppendorf) with the following cycle steps: 2 minute initial denaturation at 94°C; followed by 30 cycles of a 30 second denaturation step at 94°C, 30 second annealing step at 61°C, and 2 minute elongation step at 72°C; and ending with a 10 minute final elongation step at 72°C before being kept at 4°C until analyzed by gel electrophoresis. The PCR product was then run on a 1% agarose gel containing 0.5 μ g/mL ethidium bromide (Sigma) in 1x Tris-Acetate-EDTA (TAE) buffer. DNA was stained by the ethidium bromide and the gel was visualized using a Gel Doc XR imaging system (Bio-Rad) and QuantityOne software. The band corresponding to the *PAX7* promoter was cut out of the gel with a scalpel and purified using a Gel Purification Kit (Qiagen) following the manufacturer's instructions.

2.2.2 Cloning of the *PAX7* Promoter into the pCR 2.1-TOPO and pEGFP-1 Vectors

The purified *PAX7* promoter was cloned into the pCR 2.1-TOPO vector (Invitrogen) following the manufacturer's instructions. Briefly, 4 μ L of the product from the gel extraction was added to 1 μ L of Salt Solution and 1 μ L of the TOPO vector. The reaction was gently mixed and kept at room temperature for 30 minutes before being used to transform TOP 10 *E. coli* cells (Invitrogen). 5 μ L of the TOPO reaction was added to one vial of bacteria and incubated for 30 minutes on ice. The vials were then submerged in a 42°C water bath for 30 seconds, 250 μ L of S.O.C. Medium (Invitrogen) was added, and the tube was incubated in a 37°C shaker for one hour before being plated on LB Agar plates containing 30 μ g/mL kanamycin (Sigma). Plates were incubated for 12-14 hours to allow colonies to grow. Individual colonies were removed from the plate with a pipette and cultures were grown overnight in 5-10 mL LB Broth containing 30 μ g/mL kanamycin. Glycerol stocks were made from the bacteria cultures by adding 200 μ L of culture to 200 μ L of glycerol and stored at -80°C. The remaining bacteria were centrifuged at 8,000 rpm for 8 minutes to form a pellet and the plasmid DNA was isolated using a QIAprep Spin Miniprep Kit (Qiagen) following the manufacturer's instructions.

The concentration of purified DNA was measured on a Nanodrop spectrophotometer (LabTech) and the Pax7P-TOPO construct was digested with the restriction enzymes Sac I and Pst I (Fermentas) using the following reaction mixture: 37 μ L of H₂O, 5 μ L of 10x Tango Buffer (Fermentas), 3.5 μ L of 300 ng/ μ L DNA (to give a total of 1 μ g of DNA), and 2 μ L of each enzyme. The digestion reaction was

allowed to proceed for 4 hours at 37°C. The product was run on a 1% agarose gel as described above. Digestion with Sac I-Pst I gives a 1.5 kb product that was purified using a Gel Purification Kit (Qiagen). The pEGFP-1 vector was previously cloned into *E. coli* (R. Stewart and L. Lako, unpublished data) and cultured, isolated, and digested with Sac I and Pst I as described. The digested portion of the *PAX7* promoter was ligated to the digested pEGFP-1 vector using T4 DNA Ligase (Promega). The reaction was set up with 4.5 µL of the promoter, 4.5 µL of vector, 1 µL of 10x Ligase Buffer (Promega), and 0.33 µL of T4 DNA Ligase and allowed to run for 3 hours at room temperature. The Pax7P-pEGFP construct was then used to transform TOP 10 *E. coli* cells which were plated, allowed to form colonies, and grown in culture before extracting the DNA using an EndoFree Plasmid Maxi Kit (Qiagen) following the manufacturer's instructions.

To confirm that the Pax7P insert was properly ligated into the pEGFP-1 vector, the purified plasmid was analyzed by PCR using the primer pair 5'-GCTCACATGTTCTTCTGCG-3' and 5'-CATGGCGGACTTGAAGAAGTC-3' which flanks the insert in the vector as well as 5'-GCACAACCTACCCAGCTGATC-3' and 5'-CATGGCGGACTTGAAGAAGTC-3' where the forward primer falls within the Pax7P insert. Proper insertion yielded a band at roughly 1.8 kb using the first pair of primers and 880 base pairs (bp) using the second primer pair. This was then confirmed by sequencing the construct using the first set of the above primers. Sequencing was performed by MWG after being provided with 100 ng/µL of purified plasmid in 15 µL of dH₂O and the above primers.

2.2.3 Nucleofection of the Pax7P-GFP Construct into Adult Human Myoblasts

Prior to nucleofection, the construct was linearized by restriction enzyme digestion. The enzyme Xho I was used to prevent the separation of the promoter and GFP gene, with the following reaction mixture: 22.25 µL H₂O, 3 µL 10x Buffer R (Fermentas), 2 µL DNA (2.77 µg/µL), and 2.75 µL Xho I (10 units/µL, Fermentas). The mixture was incubated at 37°C for 4 hours followed directly by phenol:chloroform purification. For DNA purification, an equal volume of Tris EDTA-saturated phenol:chloroform:isoamyl alcohol (Sigma) was added to the aqueous mixture containing the linearized construct and mixed thoroughly. It was then centrifuged at 2,000 rpm for 5 minutes at room temperature in a tabletop microcentrifuge to separate the aqueous and non-aqueous layers. The top (aqueous) layer was removed to a new tube while care was taken to avoid the interface between layers. To precipitate the DNA, 0.1 volumes of 3 M sodium acetate (pH 5.5) and then 2 volumes of absolute ethanol were added to the separated aqueous layer followed by overnight incubation at -20°C. The DNA was recovered by centrifugation at 10,000 rpm for 15 minutes. The ethanol was removed without disturbing the DNA pellet, and the pellet was washed with 70% ethanol and centrifuged at 10,000 rpm for 5 minutes. The ethanol was removed and the pellet was dried in a sterile tissue culture hood. The construct was resuspended in a small volume of H₂O.

Adult human myoblasts were nucleofected using the NHDF-Adult Nucleofector Kit (Amaxa). A 6-well plate coated with Matrigel (BD Biosciences) was prepared 2 hours prior to nucleofection. Matrigel was kept in 0.5 mL aliquots containing 1:1 Matrigel:KO DMEM. In order to prevent the Matrigel from solidifying, all steps were carried out on ice using chilled pipettes. One aliquot was thawed on ice and added to 5.5 mL of ice cold DMEM, mixed quickly, and used to coat a 6-well plate (with 1 mL of Matrigel solution per well). The 6-well plate was kept at room temperature for several hours to allow for coating before the Matrigel solution was aspirated. The nucleofection solution was prepared by adding 22.2 μL of Supplemental Solution to 100 μL of Solution and allowing it to warm to room temperature. In the meantime, a T25 flask of cells was trypsinized with 0.75 mL Trypsin-EDTA for 4-5 minutes, neutralized with 3-4 mL of medium, centrifuged at 800 rpm for 3 minutes, and washed with 3-4 mL of PBS before being centrifuged a second time. During the second centrifugation, 2 μL of 3.2 $\mu\text{g}/\mu\text{L}$ of DNA (construct) was added to 8 μL of the prepared nucleofection solution. The PBS was aspirated from the cell pellet and the cells were resuspended in 100 μL of nucleofection solution, to which the 10 μL of solution containing the construct was added and mixed by pipetting up and down 3 times. The cell suspension with the construct was then transferred to a cuvette. The cuvette was placed in the Nucleofector machine (Amaxa) and run on program A-024. A white precipitate forms at the top of the cuvette above the cell suspension. The cell suspension was transferred with as little precipitate as possible using a nucleofection pipette from the cuvette to pre-warmed medium in two wells of the 6-well plate. The cells were allowed to settle for 48 hours before being switched to myogenic medium containing 300 $\mu\text{g}/\text{mL}$ neomycin. After several days, cells were analyzed for GFP expression using a FACS Caliber flow cytometer (BD Biosciences).

2.2.4 Nucleofection of the Pax7P-GFP Construct into H9 Cells

The initial method for nucleofecting hES cells required that one 6-well plate worth of colonies were removed in pieces as if passaging. The pieces were allowed to settle in a 15 mL Falcon tube while 22.2 μL of Supplemental Solution was added to 100 μL of Solution using the mES Cell Nucleofector Kit (Amaxa). The medium was then aspirated from the Falcon tube and the hES colony pieces were washed once, briefly, with PBS and centrifuged at 600 rpm for 2 minutes. During this centrifugation, 3 μL of 3.2 $\mu\text{g}/\mu\text{L}$ of DNA (linearized Pax7-GFP construct) was added to 7 μL of the prepared nucleofection solution. The PBS was aspirated, the colony pieces were resuspended in 100 μL of nucleofection solution, and the DNA solution was added and mixed by pipetting up and down 3 times. The suspension was then transferred to a cuvette, placed in the Nucleofector machine, and run on program A-023. The colony pieces were then resuspended in two wells of a 6-well plate containing pre-warmed medium. Colonies were allowed to adhere for 48-72 hours in normal hES medium before being switched to medium containing 100 $\mu\text{g}/\text{mL}$ neomycin. This method did not

yield enough undifferentiated, transfected cells to generate a cell line and a new approach was sought.

The new nucleofection protocol was modified from a recently established procedure for hES cell nucleofection (Hohenstein, Pyle et al. 2008). Two 6-well plates of H9 hES cells were washed twice with PBS and incubated in Trypsin-EDTA (0.5 mL per well) for 5 minutes at 37°C. Cells were then triturated with a 5 mL pipette, 2 mL per well of hES medium was added, and cells were filtered using a 40 µm filter (BD Falcon). The cells were then centrifuged at 800 rpm for 3 minutes, resuspended in 100 µL of prepared nucleofection solution (mES Cell Nucleofector Kit), and incubated at 37°C for 5 minutes. Meanwhile, 1 µL of 3.2 µg/µL DNA was added to 9 µL of nucleofection solution and this was added to the cell suspension following the 5 minute incubation. The cell suspension was then transferred to a cuvette and run on program A-023. After nucleofection, the cells were transferred to 500 µL of pre-warmed RPMI medium and incubated for 5 minutes at 37°C. This was then split between two wells of a 6-well plate containing 2.75 mL hES medium with 30 µL of 1 mM ROCKi (Sigma) for a final concentration of 10 µM and inactive MEF feeder cells. The ROCKi was added to the hES medium on MEF cells one hour prior to seeding with nucleofected H9s and kept in the medium at 10 µM until neomycin was added.

Neomycin was first added at 25 µg/mL 96 hours post-nucleofection, increased to 50 µg/mL at one week post-nucleofection, and finally to 100 µg/mL at 10 days post transfection. At this point, one of the two wells was taken off neomycin and passaged. The cells had reached a confluent monolayer covering the entire well, so strips of cells were removed with a 100 µL pipette tip and transferred to a new plate containing fresh feeders. When healthy new colonies could be detected, the remaining well was also passaged. At this point, the H9 Pax7-GFP cells could be passaged and maintained like normal hES cells (described above). It was found that the most effective way to maintain cell viability and prevent differentiation while on neomycin was to gradually increase the concentration after passaging, but to keep low levels of neomycin on newly passaged cells. Immediately prior to the act of passaging, medium lacking neomycin was added to the cells. When the cells were plated onto new feeders, a ratio of 2:1 hES medium to selection medium (hES medium with 25 ng/mL bFGF and 100 µg/mL neomycin) was used. As the cells grew, the first medium change used 1:1 hES to selection medium and the second medium change (and any subsequent ones) used 100% selection medium.

2.3 Generation and Culture of DMD Induced Pluripotent Stem Cells

2.3.1 Preparation of hES Conditioned Medium

Conditioned medium was prepared and used to grow reprogramming fibroblasts generated by the multi-gene OSKM construct (described below). Immortalized MEFs were grown in T150 flasks. When the cells had reached confluence or near-confluence, they were irradiated according to the following conditions: 120 kV, 4.0 mA, 6 minutes (Faxitron X-ray). The day after irradiation, MEF medium was replaced with hES medium (50 mL per T150) for 24 hours and then collected and replaced with fresh hES medium for up to one week. The collected medium was filtered and supplemented with 1 $\mu\text{g}/\mu\text{L}$ ITS (final concentration) and 0.4 $\mu\text{g}/\mu\text{L}$ bFGF.

2.3.2 Attempted Generation of DMD iPS Lines using Multi-gene OCT4/SOX2/KLF4/MYC (OSKM) Construct

Human embryonic kidney (HEK) 293FT cells (Invitrogen) were cultured in T75 tissue culture flasks (Iwaki) with MEF medium containing Penstrep (Gibco) and 500 $\mu\text{g}/\text{mL}$ neomycin (Geneticin). They were passaged similarly to MEFs at 70-80% confluence every 2-3 days. The cells were loosely attached so medium was changed with extreme care and cells were only trypsinized for 2 minutes when passaging. On Day 1 of the reprogramming procedure, 5×10^6 cells were plated on a 10 cm Lenti Dish (Iwaki) in MEF medium without antibiotics. The next day, the medium was changed to OptiMEM I (5 mL per dish, Gibco) with 25 μM Chloroquine (Sigma) two hours prior to transfection. Next, 9 μg of ViraPower packaging mix (1 $\mu\text{g}/\mu\text{L}$ stock, Invitrogen) was added to 3 μg of the pLenti OSKM expression plasmid and 1.5 mL of OptiMEM I pre-warmed to 37°C in a 1.5 mL Eppendorf tube. In another tube, 36 μL of Lipofectamine 2000 (Invitrogen) was added to 1.5 mL of OptiMEM I. Both were incubated for 5 minutes at room temperature before being combined and incubated for another 20 minutes at room temperature. The mixture was then added to the cells and incubated overnight at 37°C. After 16 hours the medium was removed and replaced with MEF medium for 48 hours.

On Day 4, 50,000 F029 or F055 fibroblasts were plated in one well of a 6-well plate. The next day, the medium on the fibroblasts was changed to MEF medium with 6 $\mu\text{g}/\text{mL}$ polybrene (Sigma). The medium containing the viral particles with the OSKM plasmid was collected from the HEK 293FT cells (approximately 10 mL per 10 cm dish) and centrifuged at 3000 rpm for 15 minutes at 4°C. The supernatant was filtered with 0.45 μm syringe filter (Nalgene). Fresh MEF medium was added to the HEK cells. The medium on the fibroblasts was replaced with the filtered supernatant containing 6

$\mu\text{g}/\text{mL}$ polybrene. In different experiments, either 4.5 mL of supernatant, 1 mL of supernatant and 1 mL of MEF medium (with 6 $\mu\text{g}/\text{mL}$ polybrene), or 2 mL of supernatant and 1 mL of MEF medium was used and the cells were incubated overnight. On Day 6 the medium was collected from the HEK cells, filtered and either stored at -80°C or added to the fibroblasts. The fibroblasts were examined and if most of the cells had died (from 4.5 mL of supernatant), the medium was changed to MEF medium. If the cells looked healthy (1:1 or 2:1 supernatant:MEF medium), the medium was replaced with new supernatant. On Day 7, healthy looking cells were plated onto MEF feeders in 6-well plates at 8,000 cells per well and grown in hES conditioned medium containing 40 ng/mL bFGF. RNA was also collected from a titre well (extra cells were transduced to determine the viral titre) and a lipofectamine control well (all steps were followed as normal, except no OSKM plasmid was added). Transduced fibroblasts were grown for several weeks on MEFs in hES conditioned medium with high bFGF. Cultures were observed regularly to monitor colony formation and track reprogramming, however no hES cell-like colonies were identified.

2.3.3 Generation of DMD iPS Cells from Stemgent OCT4/SOX2/LIN28/NANOG (OSLN)

Reprogramming Lentivirus Set

DMD fibroblasts were reprogrammed using a Stemgent kit with four factors: hOct4-lentivirus, hSox2-lentivirus, hLin28-lentivirus, and hNanog-lentivirus. 1×10^5 F029 or F055 fibroblasts were plated into one well of a 6-well plate and cultured overnight in MEF medium. The next day, the medium was replaced with 1.35 mL of MEF medium containing 6 $\mu\text{g}/\text{mL}$ polybrene. 500 μL of hOct4-lentivirus and 50 μL of hSox2-, hLin28-, and hNanog-lentivirus were added. The cells were incubated overnight to allow for transduction. 24 hours post-transduction, the cells were replated onto MEF feeders in 6-well plates at 8,000 cells per well and grown in MEF medium. 24 hours after re-plating, medium was changed to hES cell medium and replaced each day for 7 days. Cells were subsequently grown in hES medium containing high bFGF and monitored for colony formation and reprogramming. After several weeks, partially reprogrammed colonies were mechanically passaged and plated onto fresh feeders until hES cell-like colonies appeared among the transduced F055 cells (no fully reprogrammed colonies were detected in the F029 cells). The hES-like colony was transferred into one well of a 4-well plate (Nunc) containing MEF feeder cells.

When the colony had grown, it was partially passaged by removing one half to two thirds of the colony to a new well. Once the newly passaged pieces adhered and began to expand they were checked for hES cell morphology. If they appeared not to have differentiated, the remaining portion of the original colony would be divided and passaged. Colonies generally would not be grown on the same MEF feeders for more than 6-7 days. After plating, a new colony was allowed to adhere and grow for 4-5 days before being partially passaged and then grown for another two days before the remaining cells were transferred to new feeders. This was done to ensure that there was always a

source of undifferentiated iPS cells while expansion was occurring. At this stage, collagenase was not used; all passaging was done mechanically with a 200 μ L pipette tip. Once several 4-well plates with healthy, undifferentiated colonies were obtained, cells were transferred to a 6-well plate (usually an entire 4-well plate would be passaged to one well of a 6-well plate). As the F055 iPS clone was being expanded, colonies would be used for immunostaining, qPCR analysis, or subjected to differentiation.

2.3.4 Freezing Down and Thawing F055 iPS Cells

Because of the very small number of colonies, cells were frozen down using open straw vitrification rather than cryovials. The procedure took place inside an IVF hood with all components warmed to 37°C. In a 4-well plate, the first well contained 0.5 mL of ES-HEPES solution (1.56 mL KO DMEM, 400 μ L FBS, and 40 μ L 1M HEPES (Gibco)), the second well contained 0.5 mL 10% vitrification solution (2 mL ES-HEPES, 250 mL Ethylene Glycol (Sigma), and 250 mL DMSO), and the third well contained 0.5 mL 20% vitrification solution (750 μ L ES-HEPES, 750 μ L 1M sucrose stock, 500 μ L Ethylene Glycol, and 500 μ L DMSO). The fourth well was not used. The 1M sucrose stock solution contained 3.42g of sucrose (VWR) in 14 mL of ES-HEPES and 2 mL FBS. The lid of the 4-well plate was removed and a 20 μ L drop of 20% vitrification solution was placed on its underside.

iPS colonies were mechanically separated as if for passaging. In as small of a volume as possible, 4-6 pieces were collected and transferred to the first well of the 4-well plate above. The cells were incubated for 1 minute before being transferred to the second well for 1 minute. At each transfer, care was taken to ensure that the smallest possible volume was used to gather the colony pieces. The pieces were transferred to the third well for 25 seconds and then into the 20 μ L drop. From there, the pieces were collected and pipetted into another, smaller drop (only several μ L) on the underside of the 4-well plate lid. A vitrification straw was used to suck up the drop containing the pieces via capillary action and immediately placed inside a 15 or 50 mL Falcon tube submerged in liquid nitrogen. The process was repeated for several straws which were then transferred to a nitrogen storage canister.

To thaw cells, a straw was removed from liquid nitrogen and the solution thawed almost immediately. In a 4-well plate pre-heated to 37°C, one well contained 0.2M sucrose solution (4 mL ES-HEPES and 1 mL 1M sucrose stock) and the second contained 0.1M sucrose solution (4.5 mL ES-HEPES and 0.5 mL 1M sucrose stock). The straw was placed into the first well and the colonies either flowed out freely or were pushed out using a pipette stuck into the opposite end of the straw. They were incubated for 1 minute then transferred to the second well for 1 minute, being careful to use as little volume as possible to transfer. The pieces were then transferred to a new 4-well plate containing MEF feeder cells and grown in hES medium with high bFGF. Usually 2-3 pieces were plated in each well and allowed to settle for at least 48 hours before the medium was changed.

2.3.5 Differentiation of F055 iPS Cells

F055 iPS cells were differentiated in 4-well plates for 7-14 days in Diff medium. Once cells had differentiated, they were either isolated for qPCR analysis or fixed and permeabilized for intracellular staining of differentiation markers.

2.4 Flow Cytometry and Fluorescence Activated Cell Sorting (FACS)

2.4.1 Staining and Flow Cytometry of Myoblasts

Myoblasts were harvested by trypsinization as described above for myoblast culture. Once pelleted, the supernatant was aspirated and the cells were resuspended in PBS. Cells were counted using a Vi-Cell Cell Viability Analyzer (Beckman Coulter) and $0.5-1.0 \times 10^6$ cells were washed again using a FACS LyseWash (BD Bioscience) which concentrates the cells into 300 μL of PBS. Depending on cell number and viability (which was almost always greater than 90%), 10-15 μL of conjugated mouse anti-human antibodies (BD Pharmingen) against CD56 (PE), CD106 (APC), and CD34 (PerCP-Cy5.5) were added to each sample. Meanwhile, 5 μL per sample of mouse anti-human M-cadherin (abcam) was added to 5 μL of Zenon700 staining reagent (Invitrogen) and incubated in the dark for 5 minutes, followed by 5 μL of blocking reagent and another incubation for 2-3 minutes in the dark. All 15 μL are then added to the cell suspension containing the other antibodies and left at room temperature in the dark for 45-60 minutes, with periodic gentle mixing. The cells were again washed using a FACS LyseWash and analyzed on an LSR II flow cytometer (BD Bioscience) using BD FACSDiva software. The forward versus side scatter of the cells were analyzed to remove debris and dead cells (though the staining procedure generally resulted in greater than 90% viability) while side scatter (height) and side scatter (area) were plotted to eliminate doublets from analysis. Unstained cells were used as a control for autofluorescence. At least 10,000 events were recorded for each sample. Filters used were: M-cadherin 638/730/45, CD106 638/670/14, CD56 535/585/42, and CD34 488/710/50. The results were analyzed using FACSDiva software (BD Bioscience).

2.4.2 Staining and Flow Cytometry of Differentiated hES Cell Cultures

To harvest differentiated hES cells for staining, wells were washed with PBS once and incubated with 1 mL TVP-trypsin (0.025% Trypsin, 1% chicken serum, 1 mM disodium EDTA in PBS) for 3 to 5 minutes until the cells began to dissociate. To assist this process, the TVP-trypsin was pipetted up and down gently using a 1 mL pipette tip. When most of the cells had dissociated (waiting until all cells had fully dissociated resulted in a high amount of cell death), 3 mL of Diff medium (containing FBS) was added to neutralize the trypsin, and the cells were transferred to a 50 mL Falcon tube through a 50 μm filter

(BD Biosciences). The cell suspension was centrifuged at 800 rpm for 4 minutes, the supernatant was aspirated, and the cells were resuspended in PBS and counted using a Vi-Cell Cell Viability Analyzer.

For the initial differentiations, approximately 1×10^6 cells were washed again using a FACS LyseWash, suspending the cells in 300 μ L of PBS. Surface antibodies were added as described above, with the APC conjugated mouse anti-human CD133 (BD Pharmingen) in place of the CD106 antibody.

However, cells were only incubated for 20-30 minutes before an equal volume of Caltag Fix & Perm Kit (Invitrogen) Reagent A (the fixative) was added. Cells were incubated in the dark for an additional 15 minutes, washed with 5 mL Wash Solution (PBS with 5% FBS and 0.1% NaN_3), and centrifuged at 320 RCF for 5 minutes. The supernatant was removed and the cells were resuspended in 100 μ L of Reagent B (the permeabilization solution) and incubated for 20 minutes in the dark before being washed with Wash Solution and centrifuged as described. The supernatant was removed and the cells were resuspended in PBS for the intracellular primary antibody incubation. 10-15 μ L of monoclonal mouse anti-human Pax7 antibody (R&D Systems) was added to the sample and incubated in the dark at room temperature for 30 minutes. The cells were then washed using the FACS LyseWash and 1 μ L of anti-mouse IgG₁-FITC secondary antibody (Sigma) was added. After a 20-30 minute incubation in the dark at room temperature, the cells were washed again and analyzed on an LSR II flow cytometer. The filter used for Pax7 was 407/450/50.

Subsequent stainings using live cells followed the protocol described for myoblasts above, except cells were dissociated with TVP-Trypsin. For two trials of the HFM time course, the conditioned media differentiations, and for the Activin A differentiations, CD133 was used in addition to CD106. Because both antibodies were APC conjugated, samples were split prior to staining, with one half receiving CD133 and CD56 antibodies and the other receiving CD56, CD106, and M-cadherin antibodies. The differentiations testing various types of conditioned media and the BMP4 time course were all stained only with CD56, CD106, and M-cadherin antibodies. The BMP4 time course used a line of H9 hES cells which constitutively expressed GFP, which was also recorded by the flow cytometer. All differentiations were analyzed using an LSR II flow cytometer with the exception of the BMP4 time course, which used a FACSAria Cell Sorter (BD Biosciences). The filter used for GFP was 488/520/20. The same filter was used for CD133 as for CD106 described above. The results were analyzed using FACSDiva software.

2.4.3 FACS of BMP-4 Co-culture and H9 Pax7-GFP Differentiations

Prior to sorting, cells were stained as described above, however usually $7-10 \times 10^6$ cells were used for sorting and the staining procedure was scaled up accordingly. Cells were analyzed and sorted using a FACSAria Cell Sorter at 20 psi with a 100 μ m nozzle. The populations for the BMP-4 Co-culture differentiations included GFP+, M-cadherin+, CD106/CD56+, and CD106+ (CD56-) cells. For the H9

Pax7-GFP differentiations, four populations were obtained: negative cells, GFP+ cells, CD56/GFP+ cells, and CD56/M-cad/GFP+ cells. For the microarray analysis of differentiated H9 Pax7-GFP populations, only negative cells and CD56/GFP+ cells were obtained. Unstained cells were used to obtain the GFP+ populations. Cells were sorted into 1.5 mL eppendorf tubes and centrifuged at 1200 rpm for 5 minutes in a tabletop microcentrifuge (eppendorf). All but 250 μ L of the supernatant was removed and the cells were used for qPCR as described below.

2.4.4 Flow Analysis of MyoD Expression in the BMP4 D21 Differentiation

Cells were harvested using TVP-Trypsin as described above. The same general staining procedure given for the initial differentiation flow cytometry staining was used here. No surface markers were added, the cells were just fixed and permeabilized using the Caltag Fix & Perm Kit (Invitrogen) before adding 5 μ L of the mouse anti-human MyoD antibody (1 mg/mL, abcam) and then the Cy5-conjugated goat anti-mouse IgG2a secondary (1:500, Jackson ImmunoResearch). Cells were analyzed on an LSR II Flow Cytometer. The filter used for the Cy5 secondary was 638/670/14.

2.5 Quantitative Polymerase Chain Reaction Analysis

2.5.1 RNA Isolation and cDNA Preparation

Dissociated cells (myoblasts by trypsinization, differentiated hES cells by TVP-trypsinization, or sorted cells) were washed once with PBS were centrifuged at 1,800 rpm for 5 minutes on a tabletop microcentrifuge (Eppendorf). $0.5-1.0 \times 10^6$ cells from myoblasts or differentiated cultures or as many sorted cells as possible (usually between 30-300,000) were then resuspended with 250 μ L of PBS in a 1.5 mL eppendorf tube, 750 μ L of Trizol LS (Sigma) were added and the mixture was vigorously pipetted until homogeneous. The sample was incubated at room temperature for 5 minutes to ensure complete cell lysis. 200 μ L of chloroform were added to each tube, followed by vigorous shaking for 15 seconds before the layers were allowed to separate for 2-3 minutes at room temperature. The samples were then centrifuged at 12,000 rpm for 15 minutes at 4°C. The top, aqueous layer (roughly 500 μ L), was removed to a new tube and an equal volume of isopropanol was added to precipitate the RNA, mixed gently by inversion, and incubated at room temperature for 10 minutes. The sample was then centrifuged at 12,000 rpm for 15-30 minutes at 4°C to pellet the RNA. The supernatant was then carefully removed and the small, white pellet was washed with 500 μ L of 70% ethanol, followed by centrifugation at 12,000 rpm for 5 minutes at 4°C. All ethanol was removed and the pellet was allowed to air dry at room temperature until it became translucent, at which point it was resuspended in 12-20 μ L of distilled H₂O (dH₂O) and stored at -80°C.

The concentration of RNA samples was measured on a spectrophotometer (Nanodrop) immediately prior to cDNA preparation. Samples were treated with DNase to ensure no contamination of genomic DNA during the PCR reaction. 1 µg of total RNA in 1-8 µL of dH₂O was added to 1 µL of 10x DNase buffer and 1 µL of DNase (Ambion). The solution was brought to 10 µL total with dH₂O and incubated at 37°C for 20-30 minutes. 1 µL of inactivation solution (Ambion) was added and allowed to incubate at room temperature for 5 minutes with periodic gentle mixing. The samples were centrifuged in 0.5 mL eppendorf tubes at 10,000g for 1.5 minutes and the supernatant containing the RNA was removed to a new tube. 1 µL of random oligonucleotide 15-mers (Sigma) and 1.5 µL of dH₂O were added and the sample was incubated at 70°C for 5 minutes then snap frozen on ice for 2-3 minutes. The following was then added to each sample: 5 µL of 5x Superscript III reaction buffer (Invitrogen), 5 µL of 10 mM dNTPs (Promega), 0.5 µL of RNase inhibitors (Invitrogen), and 1 µL of Superscript III Reverse Transcriptase (Invitrogen) to a total reaction volume of 25 µL. The samples were mixed gently and incubated at 37°C for one hour to allow reverse transcription to occur, followed by a 5 minute incubation at 95°C to destroy the reverse transcriptase. Samples were diluted to 100-150 µL with dH₂O and stored at -20°C.

2.5.2 Quantitative Polymerase Chain Reaction (qPCR)

The qPCR reactions were set up using a master mix containing the following: 5 µL SYBR green (Sigma), 0.5 µL forward primers, 0.5 µL reverse primers, and 2 µL dH₂O (per sample). Each sample was run in triplicate. 8 µL of the master mix for each gene was added to each well of a 384-well plate (Applied Biosystems) followed by 2 µL of cDNA. A blank sample containing water instead of cDNA was run in triplicate for each gene. Each plate was sealed with adhesive film (Applied Biosystems) and then centrifuged at 4000 rpm for 5 minutes. The reactions were carried out in a 7900HT Fast Real-Time PCR System (Applied Biosystems) using melting temperatures determined by a temperature gradient run for each primer pair. The reaction was run with the following cycle steps: 1.5 minute initial denaturation at 95°C; followed by 39 cycles of a 30 second denaturation step at 95°C, 30 second annealing step at 52-65°C depending on the primers being used, a 30 second elongation step at 72°C, and a 10 second melting step at 77-88°C depending on the primers; and ending with a 10 minute final elongation step at 75°C followed by 10 minutes at 95°C. The data were recorded using Sequence Detection System (SDS 2.3) software and were analyzed using qBase software. Primer pairs with annealing and melting temperatures within 1°C of each other were run simultaneously. Primers for each gene are given in **Table 4.2**. GAPDH and RPL13A were used as reference genes.

Table 2.2 Primers Used for Quantitative PCR

Gene	Forward Primer	Reverse Primer	AT/MT* (°C)	Amplicon Length
Pluripotency Genes				
<i>GDF3</i>	AAATGTTTGTGTTGCGGTCA	TCTGGCACAGGTGTCTTCAG	65/81	179
<i>KLF4</i>	CCCAATTACCCATCCTTCCT	CGTCCCAGTCACAGTGGTAA	65/86	70
<i>LIN28</i>	TGCACCAGAGTAAGCTGCAC	CTCCTTTTGATCTGCGCTTC	59/84	189
<i>LIN28 ENDO</i>	AGAAATCCACAGCCCTACCC	TGCACCTTATCCCACTTTC	65/81	125
<i>MYC</i>	GAAACTTTGCCATAGCAGC	GTGAAGCTAACGTTGAGGGG	65/85	237
<i>NANOG</i>	GATTTGTGGGCCTGAAGAAA	AAGTGGGTTGTTGCCTTTG	65/81	75
<i>NANOG ENDO</i>	CCAAATTCTCTGCCAGTGAC	CACGTGGTTTGAAACAAGAAA	65/83	260
<i>OCT4</i>	GAGGAGTCCCAGGACATCAA	CATCGGCCTGTGTATATCCC	65/80	100
<i>OCT4 ENDO</i>	AAGCCCTCATTTACCAGG	CTTGAAGCTTAGCCAGGTC	65/87	165
<i>REX1</i>	AACGGGCAAAGACAAGACAC	GCTGACAGTTCTATTTCCGC	52/83	113
<i>SOX2</i>	CAAGATGCACAACCTCGGAGA	TCTCCGTCTCCGACAAAAGT	65/80	68
<i>SOX2 ENDO</i>	TCACATGTCCCAGCACTACC	CCCATTTCCTCGTTTTTCT	65/85	181
<i>TERT</i>	GCGTTTGGTGGATGATTCT	GGCATAGCTGGAGTAGTCGC	65/86	259
Early Differentiation Genes				
<i>AFP</i>	CTTTGGGCTGCTCGCTATGA	ATGGCTTGAAAGTTCGGGTC	54/78	176
<i>BRACHYURY</i>	TCAGCAAAGTCAAGCTCACCA	CCCCAACTCTCACTATGTGGATT	65/80	102
<i>MIXL1</i>	GCTCGAGAATTTGGAACGAG	GTAACCTCGTCACTCCCAA	65/82	265
<i>NESTIN</i>	CAGGAGAAACAGGGCCTACA	TGGGAGCAAAGATCCAAGAC	61/88	243
<i>PAX6</i>	GTCCATCTTTGCTTGGGAAA	TAGCCAGGTTGCGAAGAAGT	52/80	110
Myogenic Genes				
<i>MEF2</i>	CAGGCCGGTAGACTTGGTTCCACCA	CTGCCCGCTTACAGTTCAGCTAT	58/79	120
<i>MYF5</i>	ATGCCCGAATGTAACAGTCTT	GTGATCCGGTCCACTATGTTG	65/78	146
<i>MYOD</i>	GGCCGGACAGGAGAGGGAGG	GGTCTGGCTTCGCCAACC	65/77	139
<i>MYOGENIN</i>	ATGCAGCTCTCACAGCGCTT	CTGTGATGCTGTCCACGA	65/85	146
<i>PAX3</i>	CACCAGGCATGGATTTCCAGCT	TTGGTCAGGAGTCCATTACCTGAG	57/82	109
<i>PAX7</i>	GAACTGACCTCCCACTGAA	CCTCTGTGAGCTTGGTCCTC	65/80	154
Reference Genes				
<i>GAPDH</i>	TGCACCACCAACTGCTTAGC	GGCATGGACTGTGGTCATGAG	53/81	86
<i>RPL13A</i>	CCTGGAGGAGAAGAGGAAAGAGA	TTGAGGACCTCTGTGATTTGTCAA	65/80	126

*AT: Annealing Temperature, MT: Melting Temperature

Samples of differentiated cells were analyzed in triplicate (a given differentiation was repeated twice and three separate 10 μ L reactions were set up for each trial). Values are presented as the average with standard error bars. For DMD iPS cell characterization, three different stages of undifferentiated iPS cells were used and compared to three different samples of undifferentiated H9 cells. In order to monitor gene expression as the line became established and expanded, the results were not averaged. Error bars in these graphs give the standard error from the average of each well analyzed for a given sample. The iPS samples are numbered in the order that they were obtained, with iPS1 being the earliest passage while iPS3 was the latest passage. FHM cells were used as a negative control for pluripotency markers. Differentiated iPS cells were compared to each of the undifferentiated iPS cultures and the undifferentiated H9 cultures.

2.6 Cell Staining Procedures

2.6.1 Immunostaining of Differentiated hES Cells

Differentiated cultures of BMP4 D21 cells were fixed in 4% paraformaldehyde (Sigma) in PBS (pH 7.4) for 15 minutes at room temperature and then washed twice in cold PBS. Cells were then incubated with PBS containing 0.25% Triton X-100 (Sigma) for 10 minutes and then washed three times in PBS for 5 minutes each. The cells were blocked in 1% bovine serum albumin (BSA) in PBST (PBS with 0.1% v/v Tween 20) for 30 minutes to prevent unspecific binding of the antibodies. The rabbit anti-human desmin antibody (abcam) was incubated at 1:200 or 1 $\mu\text{g}/\text{mL}$ and the mouse anti-human M-cadherin antibody (abcam) was incubated at 1:25 or 4 $\mu\text{g}/\text{mL}$ in PBST with 1% BSA for one hour at room temperature. The solution was decanted and cells were washed three times in PBS for 5 minutes each before being incubated with secondary antibodies at a 1:500 dilution in PBS with 1% BSA for one hour in the dark at room temperature. An AlexaFluor 594 goat anti-rabbit IgG (H+L) (Invitrogen) was used for the desmin staining and a Rhodamin Red-X goat anti-mouse IgG (H+L) (Invitrogen) was used for the M-cadherin staining. Nuclei were stained with 4',6-diamidino-2-phenylindole (DAPI) at a final concentration of 0.5 $\mu\text{g}/\text{mL}$ for 3-5 minutes at room temperature before being washed twice with PBS and imaged using a Zeiss Axiovert 200M and AxioVision software (Zeiss).

2.6.2 Immunostaining of Undifferentiated and Differentiated F055 iPS Cells

Staining procedures were carried out in the 4-well plates the cells were cultured in. The fixation, permeabilization, and antibody incubation steps are described above. For undifferentiated cells, mouse anti-human antibodies against Oct4 (IgG1, Millipore), Nanog (IgG₁, BD Pharmingen), SSEA-4 (IgG₃, BD Pharmingen), Tra-1-60 (IgM, BD Pharmingen), and Tra-1-81 (IgM, BD Pharmingen) were used along with FITC-conjugated sheep anti-mouse IgG (whole molecule, Sigma) and Texas Red-conjugated goat anti-mouse IgM (Sigma) secondary antibodies. All primary antibodies were diluted 1:100 with the exception of Nanog, which was diluted 1:50. Secondary antibodies were diluted 1:500. Differentiated cells were stained with mouse anti-human primary antibodies against AFP (IgG_{2A}, Sigma), β 3-tubulin (IgG_{2A}, Covance), and Nkx-2.5 (IgG₁, R&D Systems). AFP and Nkx-2.5 were diluted 1:50 prior to staining while β 3-tubulin was diluted 1:200. The FITC-conjugated sheep anti-mouse IgG (whole molecule, Sigma) secondary antibody was used at 1:500. Nuclei were stained with DAPI.

2.6.3 Alkaline Phosphatase Staining of Undifferentiated F055 iPS Cells

Alkaline phosphatase was stained for using the Alkaline Phosphatase Detection Kit (Millipore) on iPS colonies in one well of a 4-well plate. Cells were fixed with 4% paraformaldehyde for 2 minutes and then washed in PBST. During the wash, the Fast Red Violet (FRV) and Naphthol AS-BI phosphate

solutions were mixed with water in a 2:1:1 ratio (FRV:Naphthol:water). 0.5 mL of the staining mixture was then added to the cells in the 4-well plate and it was left to incubate in the dark at room temperature for 15 minutes. After staining the cells were washed again with PBST and the covered with PBS prior to imaging. Images were taken on a Zeiss microscope and analyzed with AxioVision software.

2.7 Microarray Analysis of Differentiated H9 Pax7-GFP Cells

After isolating RNA from the two sorted populations of differentiated H9 Pax7-GFP cells (negative and CD56/GFP+), the microarray was performed by an in-house technician at the Institute for Human Genetics. The quality of the RNA was analyzed using an Agilent 2100 Bioanalyzer (Agilent Technologies). The RNA was added to wells in a gel of RNA 6000 Nano gel matrix containing RNA 6000 Nano dye on an RNA Nanochip (Agilent) and then underwent electrophoretic separation and was detected by laser induced fluorescence in the Bioanalyzer. The RNA was determined to have a high enough quality and concentration to proceed with the microarray. cDNA was prepared using an Affymetrix two step process: reverse transcription to synthesize First-Strand cDNA followed by Second-Strand cDNA synthesis to convert single-stranded cDNA into a double stranded cDNA template for transcription. The double stranded cDNA then underwent *in vitro* transcription to generate amplified biotin-modified cRNA, which was subsequently fragmented into pieces between 30 and 400 base pairs to prepare for microarray hybridization.

The cRNA was incubated in Hybridization Master Mix while an Affymetrix HG-U133 Plus 2 chip was pre-hybridized with Hybridization Buffer. The buffer was removed and the master mix containing the cRNA was added to the chip to incubate for 16 hours. After incubation, the chip was placed inside the Affymetrix fluidics station for several rounds of washing and staining with streptavidin and the corresponding antibodies. The probe array was then scanned using an Agilent GeneArray Scanner, generating a .dat image which was then analyzed for probe intensity with the Affymetrix Microarray Suite software. The probe intensities were exported as a .CEL file and analyzed using the GeneSpring GX10 software (Agilent).

Chapter 3: Expression of Myogenic Genes and Cell Surface Markers in Adult and Foetal Myoblast Lines

3.1 Introduction

It was crucial to establish a repertoire of satellite cell markers in order to measure the effectiveness of hES cell differentiation and as a method to isolate putative satellite cells from differentiated cultures using FACS. To do this, human adult (17/01 and S31/05) and foetal (FHM and HFM) myoblast lines were obtained and stained for a number of surface markers expressed on satellite cells. It is important to note that the proteins used were not specific to satellite cells, so a combination of different markers would be necessary to ensure a pure population upon sorting. It was also important to gain as much information as possible regarding the myogenic nature of cells labeled by different combinations of proteins. To this end, the different cell lines used were analyzed by qPCR to assess the level of several myogenic genes.

CD56 (NCAM-1, MSK39) is a well established marker of satellite cells and has been used for the immunomagnetic and FACS isolation of satellite cells from muscle tissue (Sinanan, Hunt et al. 2004; Capkovic, Stevenson et al. 2008). It has also been shown to be expressed on myoblasts and myotubes during muscle differentiation, denervation, and is thought to be involved in myoblast fusion (Illa, Leon-Monzon et al. 1992; Charlton, Mohler et al. 2000; Ishido, Uda et al. 2006). Unfortunately, CD56 is also expressed in many other cell types including neurons, neural stem cells, natural killer cells, and certain populations of T-cells (Illa, Leon-Monzon et al. 1992; Mechtersheimer, Staudter et al. 1992; Ronn, Hartz et al. 1998). Because of the strong preference of ES cells for differentiating along the ectoderm lineage, it was important to include markers which would exclude this population, especially given the general use of CD56 to assess neuronal differentiation of hES cell cultures (Pruszek, Sonntag et al. 2007).

Initial hES cell differentiations leading to this study looked for CD56 in combination with CD34 and M-cadherin. CD34 has been shown to be indicative of quiescent satellite cells in mice (Beauchamp, Heslop et al. 2000); however, it is a poor marker for human satellite cells, which was confirmed by flow cytometry analysis in all four myoblasts lines (see below). In contrast, M-cadherin is a highly specific marker for muscle tissue during development and is expressed in adult satellite cells (Moore and Walsh 1993; Irintchev, Zeschnigk et al. 1994). The only other reported site of expression of M-

cadherin is in the granule cell layer of the cerebellum (Rose, Grund et al. 1995). It is expressed during satellite cell activation, becomes up-regulated as differentiation progresses, and is subsequently down-regulated after fusion during myotube maturation (Zeschnigk, Kozian et al. 1995; Kuch, Winnekendonk et al. 1997; Kaufmann, Kirsch et al. 1999).

The combination of CD56 and M-cadherin provided a good foundation for assessing the myogenic character of hES cell differentiation strategies, but as a pair the proteins would label proliferating and differentiating myoblasts in addition to satellite cells. To address this, the surface marker CD106 (VCAM-1) was later included in the staining protocol. CD106 had been shown to be important to secondary myogenesis during embryonic development of the mouse but down-regulated after birth. In adult mice it is only found on satellite cells where it is thought to be involved in recruiting leukocytes to muscle tissue after injury (Jesse, LaChance et al. 1998) and upregulated in quiescent but not proliferating satellite cells (Fukada, Uezumi et al. 2007).

The myoblast lines were also characterized by qPCR to determine the expression levels of the *PAX7*, *MYF5*, *MYOD*, and *MYOGENIN* genes. The most definitive marker of satellite cells is Pax7, which is present in all satellite cells and expressed in proliferating myoblasts until they begin to differentiate (Kassar-Duchossoy, Giacone et al. 2005; Olguin, Yang et al. 2007). Myf5 is expressed in a subset of satellite cells and indicates an early step in the progression of myogenic differentiation (Fukada, Uezumi et al. 2007). MyoD becomes important as proliferating myoblasts begin to differentiate and both MyoD and Myf5 are expressed as differentiation progresses. Finally, myogenin is upregulated once the commitment to differentiate has been made (Smith, Janney et al. 1994; Yablonka-Reuveni and Rivera 1994). These four genes were chosen because they provide a continuous spectrum of myoblast differentiation, from the quiescent satellite cell to the onset and progression of terminal differentiation.

In adult myoblast cultures, overexpression of Pax7 has been shown to down-regulate MyoD and prevent myogenin expression. Pax7 is thought to be important to maintaining satellite cell quiescence by causing proliferating myoblasts to exit the cell cycle (Olguin and Olwin 2004). MyoD activates myogenin expression to signal myogenic commitment. Once this up-regulation of myogenin occurs, Pax7 expression is significantly reduced and differentiating myoblasts withdraw from the cell cycle (Olguin, Yang et al. 2007). During this process, a small percentage of the population of proliferating myoblasts does not commit to differentiation. Instead, they return to quiescence and reoccupy the satellite cell niche. Continued expression of Myf5, but not MyoD is thought to promote this process (Baroffio, Hamann et al. 1996).

Chapter 3 Aims:

To select suitable myoblast cell surface markers for FACS isolation of differentiating hES cells

To compare the expression of cell surface markers amongst different myoblast lines to determine if the surface markers expressed related to the degree of differentiation in the cell lines

3.2 Results

3.2.1 Flow Cytometry Analysis of Myoblast Surface Markers

Each of the adult (17/01 and S31/05) and foetal (FHM and HFM) myoblast lines were stained simultaneously for CD56, CD106, M-cadherin, and CD34 and analyzed by flow cytometry (**Figure 3.1**). The S31/05 cell line seemed to have lost its myogenic character as all four markers were nearly absent in all cells (**Figure 3.1A**). In the other three lines, CD56 was the most widely expressed marker (**Figure 3.1B-D**). It was found in greater than 40% of HFM cells and greater than 70% of 17/01 and FHM cells. CD106 was also present in a large percentage of the 17/01 cells (36.4%) of which almost all were also positive for CD56. But it was only found in 11% of the HFM cell line and less than 2% of FHM cells (**Figure 3.2**). This was surprising considering that CD106 is highly expressed during secondary myogenesis in embryonic development but only found on quiescent satellite cells of the adult. Interestingly, the HFM line had the only significant population of CD106+/CD56- cells.

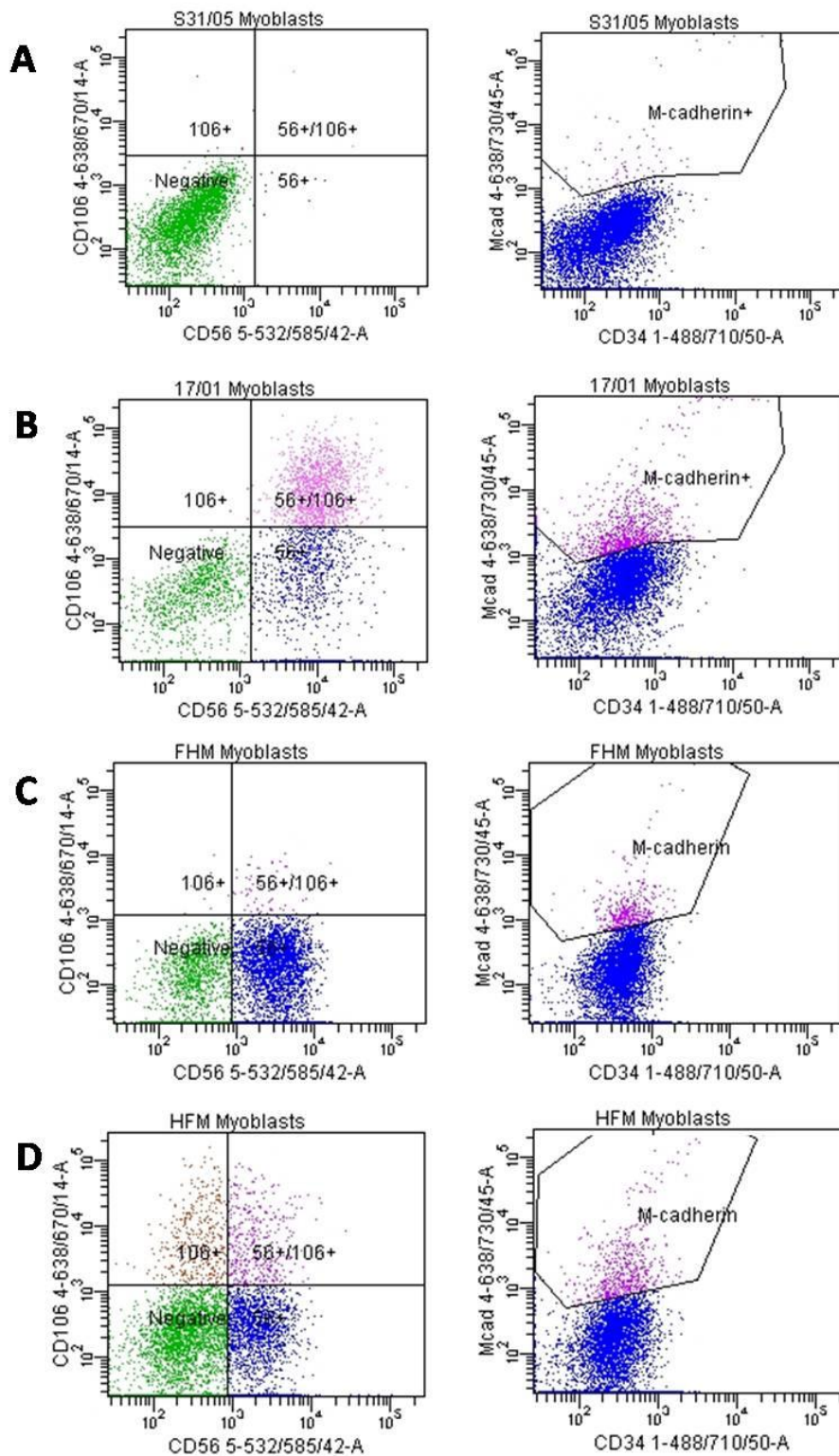


Figure 3.1: Myoblast Analysis by Flow Cytometry. Flow cytometry analysis of satellite cell surface markers in myoblast cell lines. There was very little expression of any surface markers in the S31/05 line (A) and CD34 was absent in all four cell lines. 17/01 cells expressed high levels of CD56 and CD106 and moderate amounts of M-cadherin (B). The FHM line expressed high levels of CD56 but very few cells were CD106 or M-cadherin positive (C). Fewer HFM cells were CD56+ than in the previous two lines and it had a moderate amount of CD106 and M-cadherin expression (D). n=3 for each cell line.

M-cadherin levels were lower than would be expected given its broad expression during myogenic differentiation. It was present in only 15% of 17/01 cells, 4% of FHM cells, and 8% of HFM cells. The majority of M-cadherin+ cells (an average 83% for all three cell lines) were also positive for CD56. In contrast, in the foetal cell lines less than one quarter of M-cadherin+ cells were CD106+, whereas 51% of M-cadherin+ 17/01 cells also expressed CD106. These 17/01 cells also represented the only significant triple positive (CD56+/CD106+/M-cadherin+) population in any of the myoblast lines (Figure 3.2). CD34 was not expressed at a significant level in any of the cell lines.

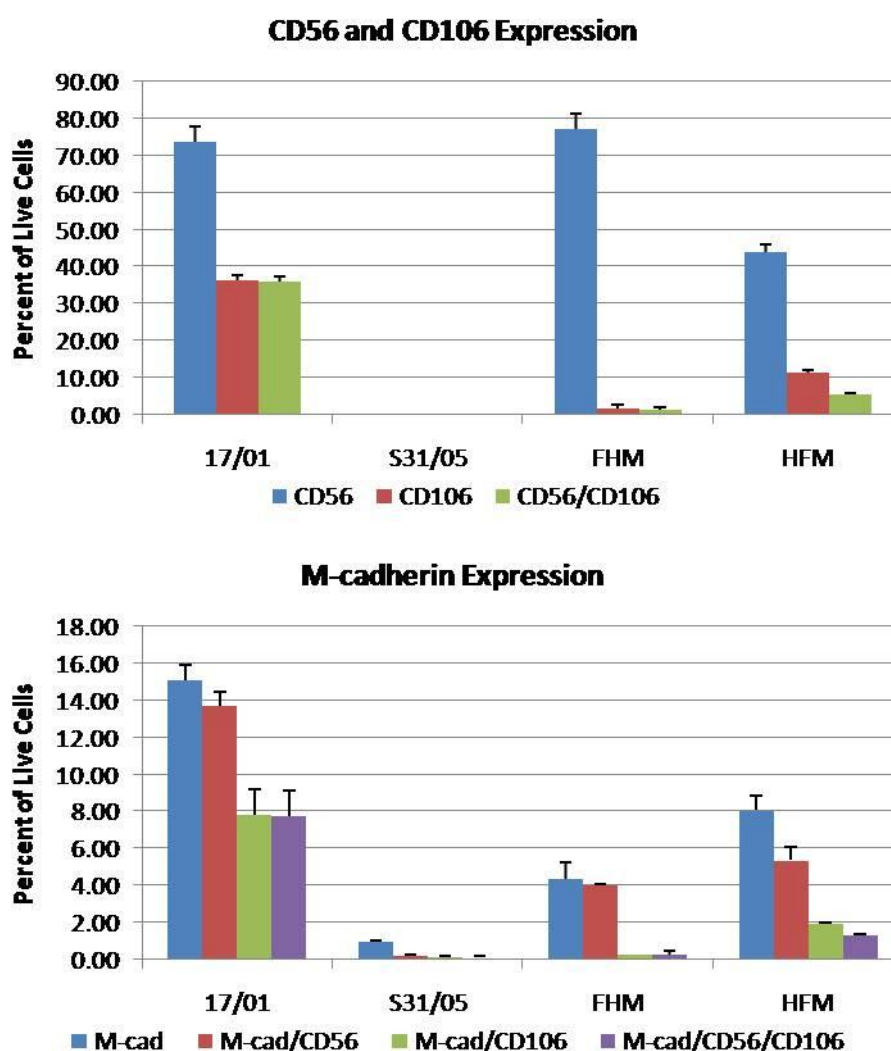


Figure 3.2: Myoblast Analysis by Flow Cytometry (Quantification). Co-expression of CD56, CD106, and M-cadherin in myoblast lines. Both the 17/01 and HFM lines had cells positive for both CD56 and CD106 however only the HFM line had a population of CD106+/CD56- cells (top graph). In the three myogenic lines, most M-cadherin+ cells were also CD56+ while much fewer were positive for CD106. The only substantial population of triple positive cells was in the 17/01 line (bottom). Error bars indicate SEM, n=3 for each cell line.

3.2.2 qPCR Analysis of Myoblast Lines for Myogenic Gene Expression

Further analysis of the myoblasts lines using qPCR confirmed that S31/05 had lost its myogenic character as it expressed extremely low levels of *PAX7*, *MYF5*, *MYOD*, and *MYOGENIN* (Figure 3.3). The two foetal lines expressed significantly higher *PAX7* than 17/01. This may be due to the importance of Pax7 in embryonic muscle development while its expression in the adult is limited to satellite cells and down-regulated as differentiation progresses. Unfortunately *PAX7* expression did not directly correlate with the expression of any of the surface markers examined by flow cytometry as none of the surface markers had higher levels of expression in both foetal lines than in the 17/01 cells. In contrast to *PAX7*, the expression of *MYF5* was highest in the 17/01 line and was similar in the FHM and HFM cells.

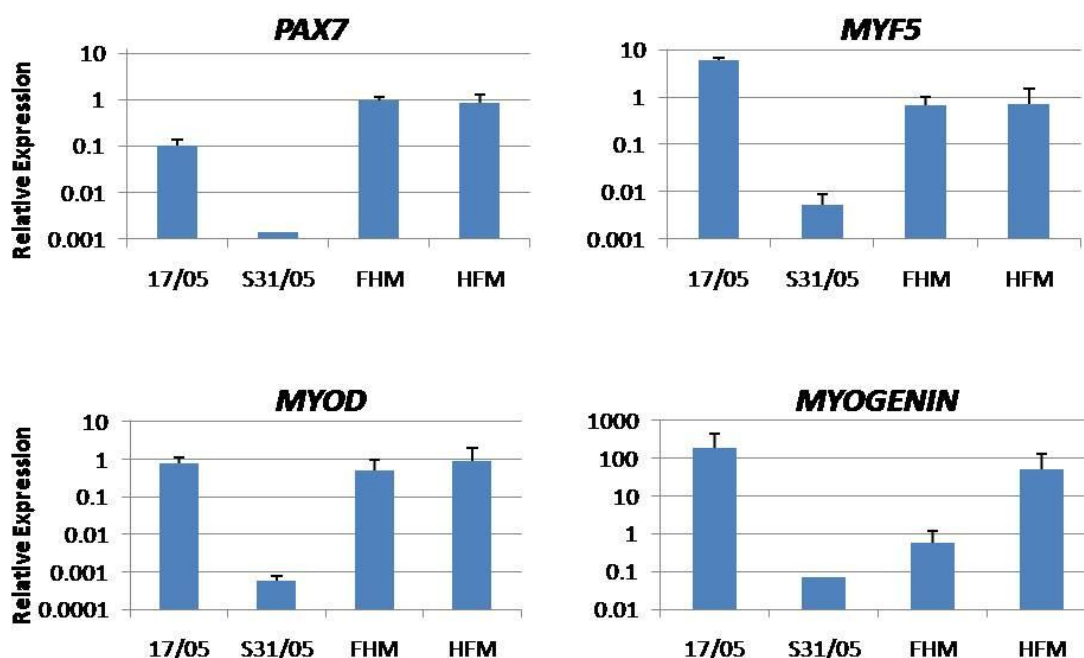


Figure 3.3: Myoblast Analysis by qPCR. qPCR analysis of myogenic genes in myoblast cell lines. Gene expression results confirm the flow cytometry data suggesting that the S31/05 line has lost its myogenic character. Of the remaining three lines, *PAX7* expression is highest in the foetal lines while *MYF5* expression shows the opposite trend. *MYOD* expression is similar in all three lines suggesting that all are equally myogenic in nature. 17/01 cells have the highest level of *MYOGENIN* followed by HFM and FHM cells. n=3 for each cell line.

MYOD expression was not statistically different between the 17/01, FHM, and HFM cells. This indicates that all three cell lines were comparably myogenic in nature, and that any differences in relative gene (or surface marker) expression are due to differences within the myogenic compartment rather than the loss of myogenic character in a cell line (such as the S31/05 line).

MYOGENIN expression was higher in 17/01 and HFM cells and lower in the FHM line. In this respect it seemed to correlate most strongly with the expression of M-cadherin. Both are known to be important during the later phases of myogenic differentiation.

3.3 Discussion

The expression of potential satellite cell surface markers CD56, CD106, and M-cadherin was examined in four different lines of human myoblasts. The expression of different genes important during myogenesis was also examined. One of the four cell lines, S31/05, was found to have lost its myogenic nature. Of the remaining three, all expressed high levels of CD56, while levels of CD106 and M-cadherin varied between cell lines. The three cell lines also showed consistent levels of *MYOD* expression, while *PAX7*, *MYF5*, and *MYOGENIN* gene expression was more variable.

A large difference was seen in the level of the three surface markers among each of the cell lines. While CD56 was always the most highly expressed, it varied from being present in just 45% of HFM cells to 75% of 17/01 and FHM cells. Studies have shown that the level of CD56 expression can change based on the age of the tissue collected as well as variations in myoblast culture conditions (Andersson, Olsen et al. 1993; Lyles, Amin et al. 1993). A high percentage of CD56+ cells were expected as CD56 is present in satellite cells as well as during myoblast differentiation and myocyte fusion. It did not seem to directly correlate with any of the genes examined by qPCR or either of the other surface markers. This may be explained by its ubiquity during myogenesis; most of the other genes and proteins tested are expressed in a stage-specific manner.

Similarly, CD106 levels varied greatly between cell lines with decreasing amounts found in 17/01, HFM, and FHM cells. In the 17/01 and FHM lines (which expressed the highest levels of CD56), nearly all CD106+ cells were CD56+. In the adult, all satellite cells should be CD56+ while only a subset will express CD106, which turns off as satellite cell activation occurs (Fukada, Uezumi et al. 2007). Indeed, it has been observed that all cells which stained positive for CD106 also expressed CD56 (Rosen, Sanes et al. 1992). Similarly, during foetal development, the splice variants of CD56 are known to be expressed in the myotome, on the surface of primary myocytes, and during secondary myogenesis on myoblasts and myotubes (Covault and Sanes 1986; Moore, Thompson et al. 1987; Lyons, Moore et al. 1992) while CD106 is expressed on secondary myoblasts and possibly on secondary myotubes lying alongside primary myotubes (Rosen, Sanes et al. 1992). Based on these expression patterns, it is expected that nearly all CD106+ cells in both adult and foetal lines would also express CD56. Contrary to what previous research suggests, HFM cells showed a decrease in the CD56+ population and had a significant percentage of CD106+/CD56- cells. While one study has shown that CD106 expression decreases when CD56 is overexpressed, most likely due to an increased rate of myoblast fusion

(Fazeli, Wells et al. 1996), there is no evidence of a CD106+/CD56- population of cells during muscle development. It is tempting to speculate that this population has arisen as a result of culture conditions rather than being a novel expression profile of foetal myoblasts.

Given that M-cadherin is expressed in satellite cells and upregulated as they differentiate and fuse, it was surprising that there was so little seen in the three myoblast cultures. This may have been due to the protocol used to culture the cells, which was designed to promote proliferation but not differentiation. A close examination of M-cadherin expression in adult mouse muscle showed that it was found in quiescent satellite cells (M-cadherin+ cells did not incorporate bromodeoxyuridine) from normal muscle and that it was most strongly expressed along the satellite cell-muscle fibre border. After injury, it became localized to myoblasts, and was subsequently down-regulated after myoblast fusion (Irintchev, Zeschnigk et al. 1994). If M-cadherin expression is most strongly activated by the presence of a muscle fibre border (in satellite cells) or during differentiation of myoblasts, then the 17/01, FHM, and HFM cultures would not be expected to express high levels of M-cadherin as they do not contain mature muscle fibres and are not actively differentiating. The majority of M-cadherin+ cells also expressed CD56, which was expected given their overlapping roles during muscle regeneration and the prominence of CD56 in the myoblast cell lines. A much smaller percentage of M-cadherin+ cells co-expressed CD106. In the adult, both M-cadherin and CD106 are known to be expressed on quiescent satellite cells (Irintchev, Zeschnigk et al. 1994; Fukada, Uezumi et al. 2007) and the largest M-cadherin+/CD106+ population is found in the 17/01 line (these cells are also CD56+). While M-cadherin has been observed during embryonic muscle development, its role has not been well characterized. It is thought to indicate a commitment to terminal differentiation of foetal myoblasts (Rose, Rohwedel et al. 1994). The two foetal lines showed a much smaller overlap between M-cadherin and CD106 than the 17/01 line, suggesting that the two proteins are involved in fundamentally different processes.

During muscle development, Pax7 is first expressed in the dermomyotome, followed by the myotome, where nearly 90% of cells are Pax7+ (the vast majority of which co-express Pax3). This population contains most of the proliferating cells during early muscle development and persists until late in development when they take up positions under the basal lamina of muscle fibres, reminiscent of adult satellite cells (Relaix, Rocancourt et al. 2005). It is therefore expected that the two foetal myoblast lines express high levels of PAX7 mRNA, while the adult line expresses significantly less. The Pax7+/Pax3+ population for the most part does not express myogenic determination markers such as Myf5, MyoD, or desmin. Myf5 is important during the onset of embryonic myogenesis. The appearance of myotomal cells is delayed by several days in Myf5-null embryos (Braun, Rudnicki et al. 1992). However, Myf5 expression in mice begins to decline starting around 11.5 dpc as other myogenic factors such as myogenin and MyoD are turned on (Ott, Bober et

al. 1991). This explains the low level of *MYF5* expression in the FHM and HFM cell lines compared to the 17/01 line. During adult regeneration Myf5 is important for the initial proliferation of satellite cells and the establishment of a pool of myoblasts capable of differentiation (Gayraud-Morel, Chretien et al. 2007; Ustanina, Carvajal et al. 2007). Thus it is not surprising that it is expressed at relatively high levels in 17/01 myoblasts grown in conditions to promote proliferation.

Like Myf5, MyoD is important in myoblast determination. In fact, in the absence of either of these proteins, the other seems capable of filling in and allowing myoblast formation and differentiation to occur resulting in apparently normal skeletal muscle (Braun, Rudnicki et al. 1992; Rudnicki, Braun et al. 1992). All three cell lines expressed similar levels of *MYOD*. The relative increase in foetal myoblast *MYOD* expression (compared to *MYF5* expression across all three lines) is most likely due to the fact that MyoD is expressed later in development than Myf5. It was also important to assess the progression of differentiation in the various myoblast cultures and determine if there was a direct relationship with the expression of any surface markers. While Myf5 and MyoD are important in myoblast determination, myogenin is crucial for their differentiation (Brunetti and Goldfine 1990). Knockout studies have shown that myogenin-null mouse embryos contain myoblasts but severely lack differentiated, properly structured muscle fibres (Nabeshima, Hanaoka et al. 1993). *MYOGENIN* expression was highest in the 17/01 and HFM lines and lowest in the FHM line. Different mouse myoblast lines show variable myogenin expression in growth medium but all lines show an increase in myogenin once cultures are switched to differentiation medium (Miller 1990). Thus the differences seen between the three human lines tested may be a result of normal variations or due to errant differentiation in the cultures expressing higher levels of myogenin. High *MYOGENIN* in 17/01 and HFM cultures along with high levels of *MYF5* in the former and *PAX7* in the latter suggest that they contain a broad spectrum of cells along the spectrum of myogenic commitment while the FHM line, containing high *PAX7* but low *MYOGENIN* seems to represent a less mature myogenic population.

PAX7, *MYF5*, *MYOD*, and *MYOGENIN* were chosen because they provided the opportunity to look at different points along the spectrum of myogenic differentiation, from the quiescent satellite cell to the fusing myoblast. The original purpose of this study was to determine the best compilation of surface markers to identify muscle satellite cells. In the adult, this would correlate most strongly to Pax7 and Myf5 expression, and can be excluded by myogenin expression. In the embryo it is more complicated, but Pax7+ progenitors represent proliferative cells with myogenic potential which, for the purposes of transplantation research, are worth studying. These progenitors are also believed to give rise to bona fide satellite cells in adult tissue. Unfortunately, none of the surface markers tested showed a positive correlation with *PAX7* expression. In this regard, CD106 expression was the most surprising. Because it is thought to be expressed strongly in quiescent satellite cells and, unlike CD56 and M-cadherin, does not have a role in myoblast fusion, it was expected to be a good marker for

Pax7 expression and myoblast immaturity. In fact, it displayed a general negative correlation with *PAX7* expression and was most highly expressed in 17/01 cells, which seemed the most differentiated based on gene expression data. Despite this, the combination of CD56, CD106, and M-cadherin should provide a method of identifying and isolating myogenic cells from differentiating hES cultures, as the co-expression of at least two of these proteins ought to be specific to cells in the myogenic lineage.

It would be interesting to further explore the different populations found in the myoblast lines by qPCR analysis and culture characteristics of FACS-separated cells. Specifically, examining how the CD56+/M-cadherin- population differs from the CD56+/M-cadherin+ cells and studying the CD106+/CD56- cells in the HFM line could provide novel insight into the role of these proteins in myogenic differentiation.

Chapter 4: Myogenic Differentiation of hES Cells

4.1 Introduction

There is a therapeutic need for a source of muscle progenitors or muscle satellite cells in order to treat conditions like DMD. Unfortunately, progress using differentiated embryonic stem cells to produce these cells has been limited. Early studies showed that mouse ES cells could differentiate into skeletal muscle cells which were physiologically indistinguishable from normal myocytes (Rohwedel, Maltsev et al. 1994). Additional studies also helped elucidate the role of different genes during myogenic development (discussed in Chapter 1).

More recently, some progress has been made in producing muscle progenitors from mouse embryonic stem cells. In a study by Bhagavati and Xu, mES cells were differentiated for 7 days as EBs and then plated onto cultures of mdx mouse muscle for an additional 4 days before being injected into mdx mice. Their strategy required cell-cell contact between mES and adult muscle derived cells in order for the mES cells to gain myogenic capacity. While they showed that mES cells can form dystrophin+ fibres, the mice were not traced long enough to see if teratomas were formed. Control mES EB cultures using the C2C12 myoblast cell line failed to produce similar results (Bhagavati and Xu 2005). Another group showed that mES cells transfected with human IGF II readily differentiated into cultures containing skeletal muscle cells expressing *myoD*, *myogenin*, *MRF4*, *myf5* and *dystrophin*. However, they did not assess the purity of these myogenic cultures beyond showing that they no longer expressed membrane alkaline phosphatase. Upon transplantation, the cultures were capable of improving muscle regeneration in injured mice (Kamochi, Kurokawa et al. 2006). These studies demonstrated the myogenic and therapeutic capacity of mES cells, but lacked the important step up purifying derived myoblasts in order to eliminate residual undifferentiated cells capable of forming teratomas. This shortcoming was addressed by Darabi et al. However, instead of using a co-culture system to induce mES cell myogenesis, they found it necessary to use a doxycycline-inducible construct to drive Pax3 expression during EB differentiation. Direct injection of these cells into mice resulted in teratoma formation after one month. To remove undifferentiated cells, they were sorted to obtain a platelet derived growth factor receptor-alpha (PDGFR- α)/Flk-1- population thought to be specific to paraxial mesoderm. These cells were highly myogenic, readily engrafted into damaged muscle and improved contractile function (Darabi, Gehlbach et al. 2008; Darabi, Baik et al. 2009). While these studies require the genetic manipulation of transplanted cells in order to promote

myogenesis, Sakurai et al. showed that a PDGFR- α + population could be purified using FACS after differentiating mES cells as a monolayer for 4 days. This population did not express any early markers of myogenesis (such as Pax3, Pax7, Myf5, or MyoD) but was capable of engraftment when injected into injured muscle and gave rise to putative satellite cells (in addition to non-myogenic cells). However, a PDGFR- α -/VEGFR2+ population, characterized as lateral mesoderm, also showed engraftment albeit at a lower efficiency (Sakurai, Okawa et al. 2008). The main flaw in these studies is that they stop *in vitro* differentiation prior to the formation of actual myogenic cells and rely on further differentiation *in vivo*.

Perhaps the most therapeutically useful approach to isolate muscle progenitor cells from differentiating mES cells has been by Chang et al. They used the monoclonal SM/C-2.6 antibody that specifically recognizes mouse satellite cells (Fukada, Higuchi et al. 2004). With this antibody they were able to obtain an enriched population of muscle progenitors directly from mES cells without needing to genetically modify the cell. mES cells were differentiated as EBs for 6 days before being plated for an additional 14 days at which point Pax3, Pax7, Myf5, MyoD, and myogenin staining were all observed. Sorting these cultures based on the expression of the SM/C-2.6 antigen substantially enriched the percentage of Pax7+ and M-cadherin+ cells, and the sorted population was capable of forming muscle fibres *in vitro* (although non-myogenic cells were also present). When transplanted into injured mouse muscle, the SM/C-2.6+ population contributed to long-term engraftment and multiple rounds of muscle regeneration (Chang, Yoshimoto et al. 2009).

Unfortunately human ES cells seem less inclined to form skeletal muscle while differentiating. As a result, less progress has been made towards the isolation of transplantable myogenic precursors. Using a mouse OP9 stromal cell co-culture, Barberi et al. were able to obtain mesenchymal stem cells from differentiating hES cells by sorting for CD73 expression. In a C2C12 co-culture, the CD73+ population was able to form myotubes and expressed MyoD and myogenin (Barberi, Willis et al. 2005). This approach had the major drawback of requiring co-culture with non-human cells in order to promote both the initial differentiation of mesenchymal stem cells and the subsequent myogenic differentiation. In a more direct approach, Zheng et al. attempted to promote myogenic differentiation of hES cells using EBs grown in media varying in the percentage of foetal bovine or horse serum as well as dexamethasone. They also used 5-azacytidine in order to initiate myogenic differentiation. They were able to produce a population of c-Met+ cells that sparsely expressed MyoD (but no Pax7). 5-azacytidine treatment decreased c-Met expression, suggesting that it did not enrich for satellite cells (which are c-Met+) despite increasing Pax7 expression. The cells were negative for other satellite markers, including M-cadherin, NCAM, and Myf5 suggesting that they were largely non-myogenic in nature. However, when injected into injured mouse muscle, they were able to undergo myogenic differentiation and form new myotubes as well as fuse with existing ones

(Zheng, Wang et al. 2006). Barberi et al. later modified their initial strategy to remove any mouse co-culture during the differentiation. hES cells were initially differentiated in serum-free medium at low density to establish a population of CD73+ mesenchymal stem cells isolated using FACS. These CD73+ cells showed a low percentage of skeletal muscle markers but could be further sorted based on the presence of CD56. MyoD was expressed in an average of 60-80% of cell from the CD73+/CD56+ population suggesting it is a largely, if not entirely, myogenic population. These cells showed stable engraftment in injured mouse muscle for up to six months (Barberi, Bradbury et al. 2007). While this strategy generates a population of engraftable myogenic precursors, it requires multiple rounds of FACS sorting and a total of 7-8 weeks of differentiation.

It has been shown that both mouse and human embryonic stem cells will differentiate to skeletal muscle tissue. However, a protocol for the direct, efficient differentiation of muscle satellite cells has not been established in humans.

Chapter 4 Aims:

To develop a strategy of culturing differentiating hES cell that would optimally favour the formation of muscle satellite cells

To analyze and isolate these using flow cytometry and FACS

To demonstrate the myogenic nature of differentiated cells using qPCR and immunostaining for muscle-specific markers

4.2 Results

4.2.1 Monolayer Differentiation using Horse Serum and Conditioned Medium

Cells were initially grown in differentiation medium containing horse serum (see materials and methods) for several days and then switched to 100% conditioned medium from the HFM line of human foetal myoblasts (Differentiation medium for 3 days followed by Conditioned Medium for 7 days was represented as D3CM7). In order to assess the expression of Pax7, a reliable marker of satellite cells, differentiated cells were fixed and permeabilized during the staining process. Cells were also stained for the surface markers CD56, CD133, and M-cadherin (**Figure 4.1**). CD106 had not yet been added to the staining repertoire and CD133 was used in conjunction with CD56 to assess neuronal differentiation (Coskun, Wu et al. 2008).

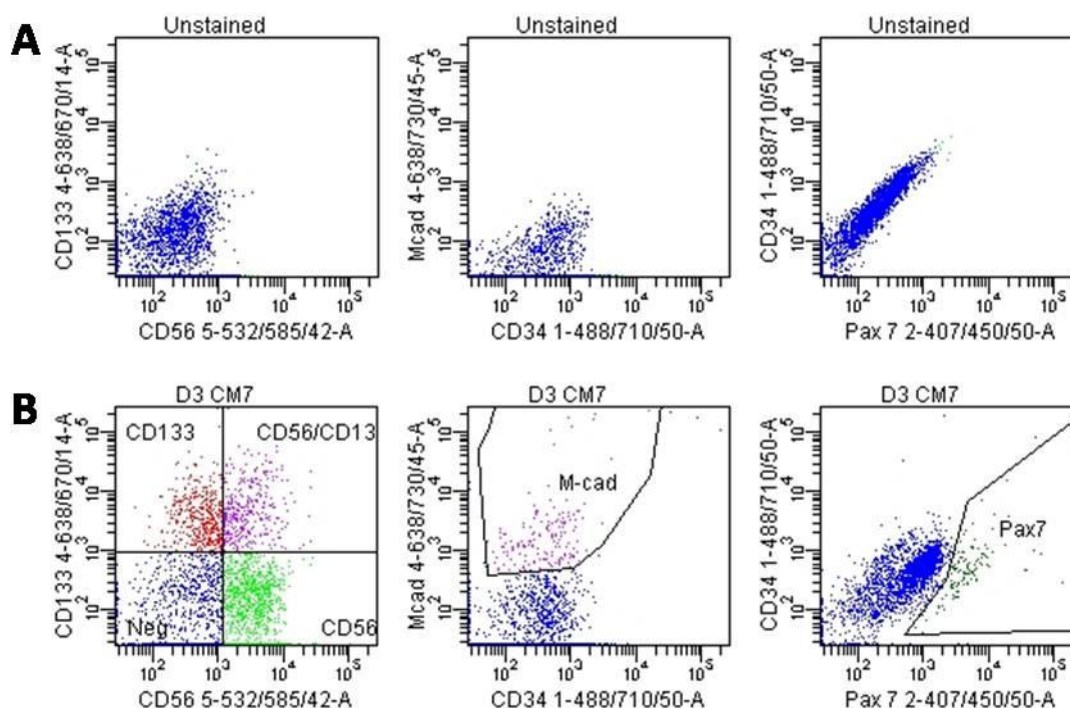


Figure 4.1: Initial Myogenic Differentiation Medium Analysis by Flow Cytometry. Representative dot plots from the flow cytometry analysis of the initial differentiation strategy. (A) Unstained cells were used as a control for autofluorescence in all experiments. (B) Populations of cells stained for CD133, CD56, M-cadherin, and Pax7 are shown along with the gates used to determine population percentages. Dot plots are representative of both trials of multiple time points in the differentiation experiment.

The need to fix and permeabilize cells was a significant drawback in our strategy. While Pax7 is an important marker of satellite cells, no subsequent genetic analysis or culture of sorted cells would be possible once it had been stained for. It was also possible that the fix/perm procedure was having an adverse effect on the surface marker staining. While CD56 showed relatively constant expression between trials, the other markers showed a much greater degree of variability (**Figure 4.2**). Among all the time points of both trials, there were significantly higher levels of CD56 (70% +/- 9.6%) than CD133 (16% +/- 9.8%), M-cadherin (2.1% +/- 1.5%), and Pax7 (2.1% +/- 1.7%). The standard deviation was greater than 60% of the mean percent of live cells for CD133, M-cadherin, and Pax7.

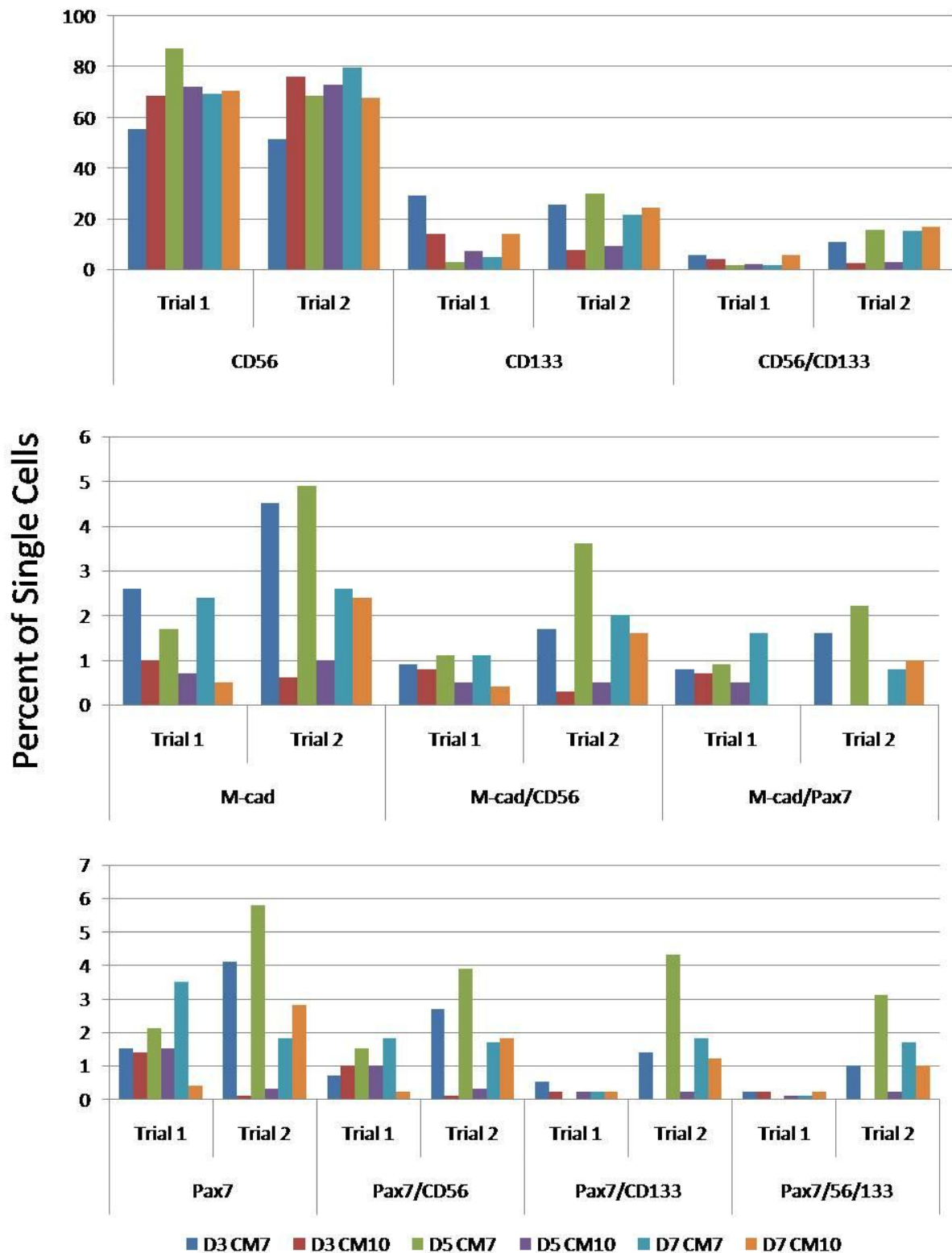


Figure 4.2: Initial Myogenic Differentiation Medium Analysis by Flow Cytometry (Quantification). Consistently high levels of CD56 are seen at all time points. CD133 expression is much lower and more variable between the two trials and the different time points as is M-cadherin and Pax7 expression. Co-expression of satellite cell markers suggests that between 1 and 5% of cells may be myogenic. The high degree of variability was thought to be a product of the fixation and permeabilization procedure, thus only one repeat was conducted before the staining strategy was modified.

4.2.2 Modified Conditioned Medium Differentiation

In an attempt to address these inconsistencies, Pax7 was excluded from subsequent flow cytometry analysis and live cells were stained directly for surface markers without fixation or permeabilization. Instead of switching from Differentiation medium to conditioned medium, cells were grown in 1:1 Diff:CM medium (Differentiation medium containing FBS instead of horse serum and HFM conditioned medium) during the entire experiment. Three different time points were tested: 12, 16, and 20 days. As a control, cells were also grown in 100% Differentiation medium for 12 days. Cells were stained with antibodies against CD56, CD133, CD106, and M-cadherin (**Figure 4.3**).

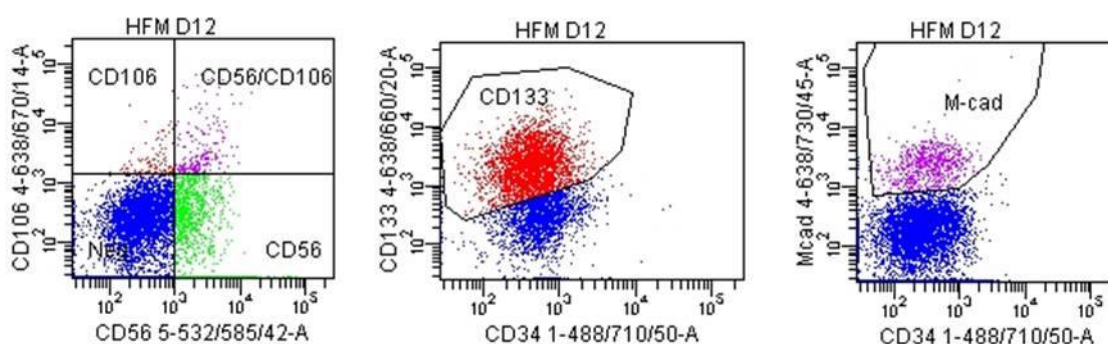
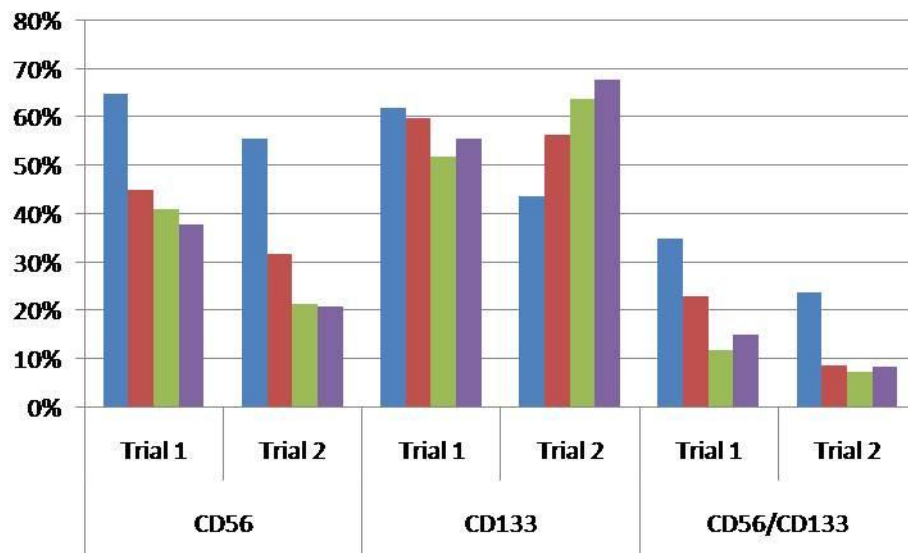


Figure 4.3: Diff:CM Differentiation Analysis by Flow Cytometry. Representative dot plots from the flow cytometry analysis of the HFM time course differentiation. Plots show populations of cells staining for CD106 and CD56 (first plot), CD133 (second plot), and M-cadherin (third plot).

Initial experiments showed that the Diff control cultures had the highest percentages of CD56+ and CD56+/CD133+ cells (**Figure 4.4**), suggesting that the HFM medium decreased the extent of neurogenesis. In order to assess myogenic differentiation, CD106 and M-cadherin were added to the staining protocol and CD133 was removed. CD56 expression remained significantly higher in Diff control cultures than in the HFM cultures and among HFM cultures, it generally decreased as differentiation continued. CD106 levels were similarly low (only 2-5% of cells were positive) in all HFM time points and the Diff control. However, M-cadherin levels were significantly higher in the HFM cultures (around 8% of cells were M-cad+) than in the Diff control (around 4% were M-cad+). There was not a significant difference seen in the CD56+/CD106+ or the M-cad+/CD56+ population between any of the cultures (including the control), however there were more M-cad+/CD106+ cells in the HFM cultures than in the Diff control culture. Triple-positive cells (M-cad+/CD56+/CD106+) were found in all four cultures with the highest average being 0.93% in the HFM day 12 differentiation.



Percentage of Live Cells

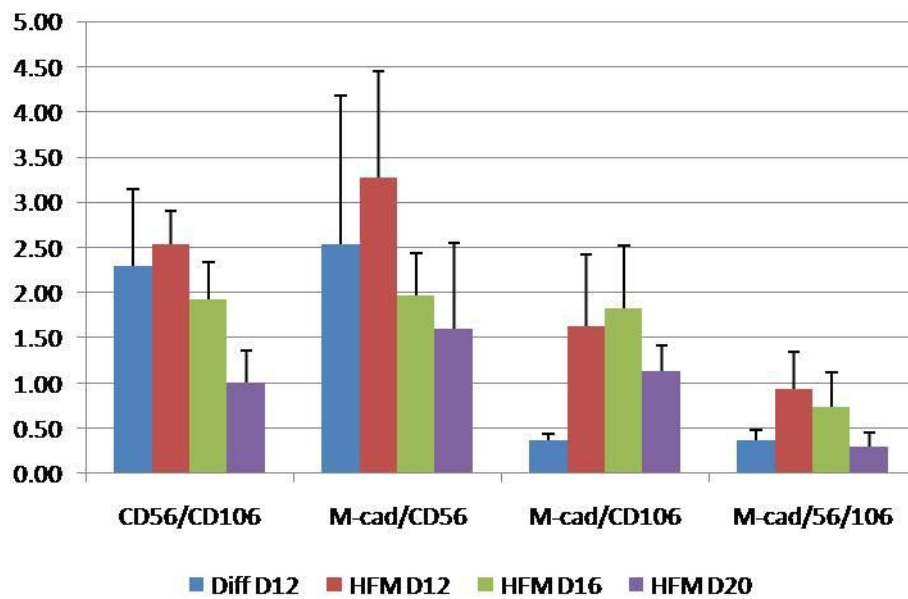
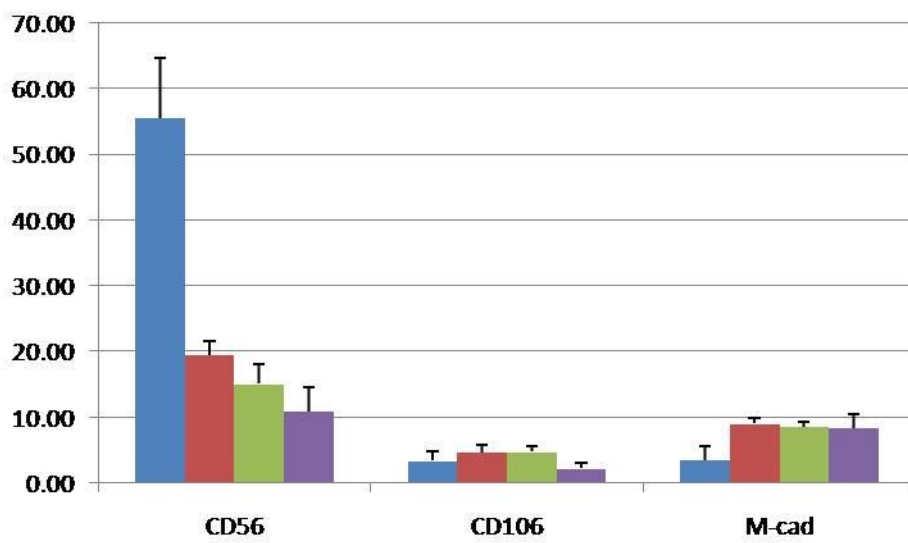


Figure 4.4: Diff:CM Differentiation Time Course Analysis by Flow Cytometry (Quantification). (Top Graph) Cultures grown only in Diff medium (no conditioned medium) showed higher levels of CD56 and CD56/CD133 staining, indicative of neurogenesis, as compared to the cells grown in conditioned medium. All cultures displayed similar levels of CD133 (a broadly expressed stem cell marker). Two trials were conducted. (Middle Graph) Staining for satellite cell markers show similar levels of CD106 between all cultures but a significant increase of M-cadherin expression in the cells grown with conditioned medium. (Bottom Graph) Co-expression of CD56/CD106 and M-cad/CD56 are similar among the different differentiation conditions, however M-cad/CD106 expression is significantly lower in the Diff D12 culture than in the HFM cultures. Very few triple positive cells were seen in any of the cultures, however the highest average was in the HFM D12 differentiation. Middle and Bottom Graphs give the average \pm SEM of three trials.

qPCR was used to analyze the expression of genes involved in myogenesis (**Figure 4.5**). *PAX3* and *PAX7* were most highly expressed in HFM day 12 cultures and decreased as the differentiation length increased. However, *PAX7* expression was highly variable, especially in the HFM day 12 samples. *MEF2* expression did not differ substantially between the three time points; however it was significantly lower in the Diff control. *MYF5* expression increased from 12 to 16 days, but decreased by 20 days of differentiation. It was not detected in the Diff control. In contrast, *MYOD* expression was similar between the Diff control and HFM day 12 cultures. Like *MYF5*, expression peaked after 16 days of differentiation, but with only a slight drop after 20 days.

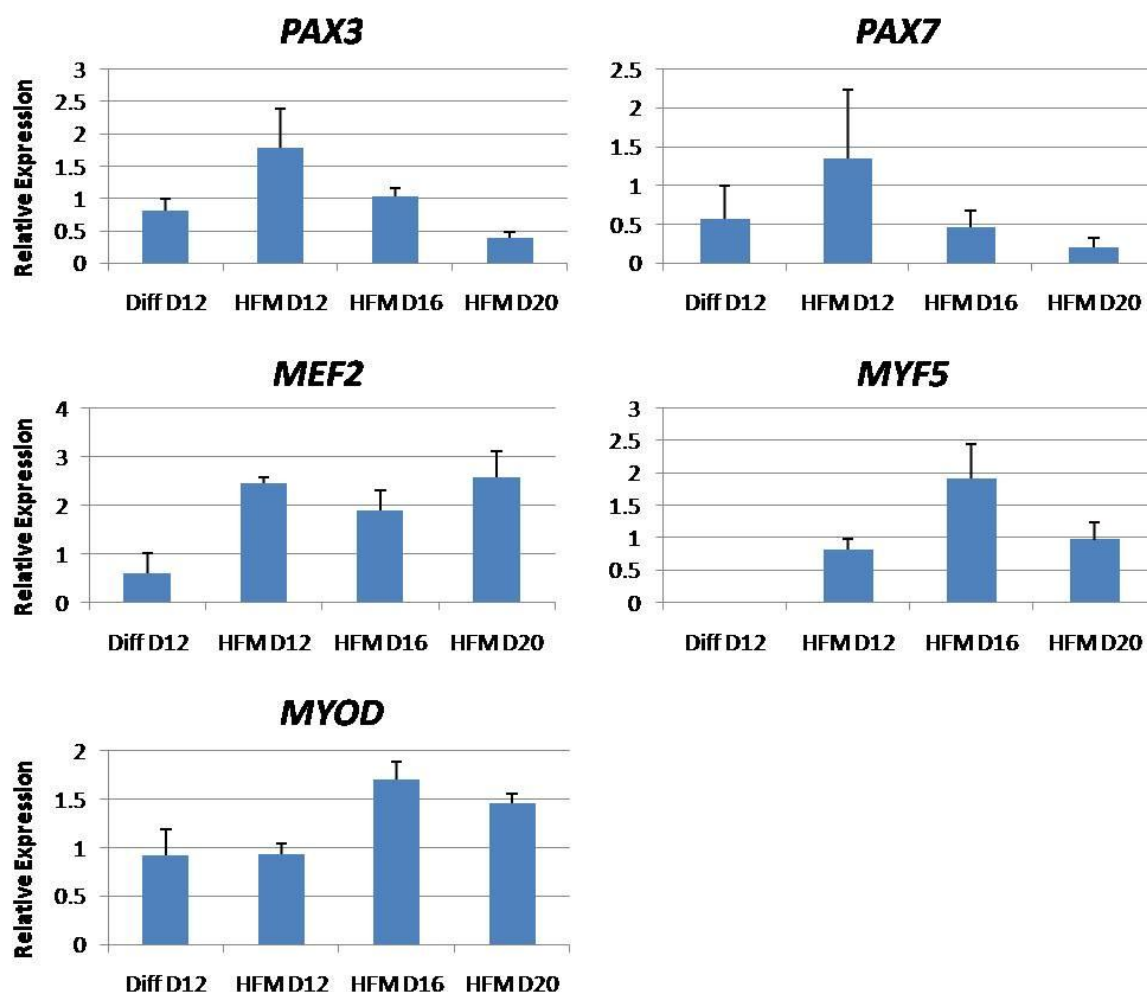


Figure 4.5: Diff:CM Differentiation Analysis by qPCR. The highest level of expression for *PAX3* and *PAX7* occurred after 12 days of differentiation, after which point expression declined steadily. *MEF2* transcript levels were comparable among all three time points of the HFM differentiation, though significantly lower in the Diff control. Expression of both *MYF5* and *MYOD* peaked at 16 days of differentiation, though *MYOD* expression remained high at day 20 while *MYF5* had decreased.

4.2.3 Conditioned Medium from Various Myoblast Lines

Several attempts were made to improve the efficiency of myogenic differentiation in the conditioned medium cultures. In addition to using the HFM cell line to condition medium, the FHM, S31/05 and 17/01 cell lines were used as well. Media conditioned from these other cell lines did not seem to have a significant effect on the differentiation (**Figures 4.6 and 4.7**). While HFM medium seemed to cause slightly higher CD56 expression in both trials, it did not show an increase in CD133+ cells or in the CD56/CD133+ population suggesting that HFM medium did not increase neurogenesis relative to the other conditioned media. None of the media substantially increased the expression of CD106 or M-cadherin. All four media yielded substantially larger populations of CD56+/M-cad+ cells than

CD56+/CD106+ cells. This was most likely due to the higher than normal expression of M-cadherin, especially in the second trial.

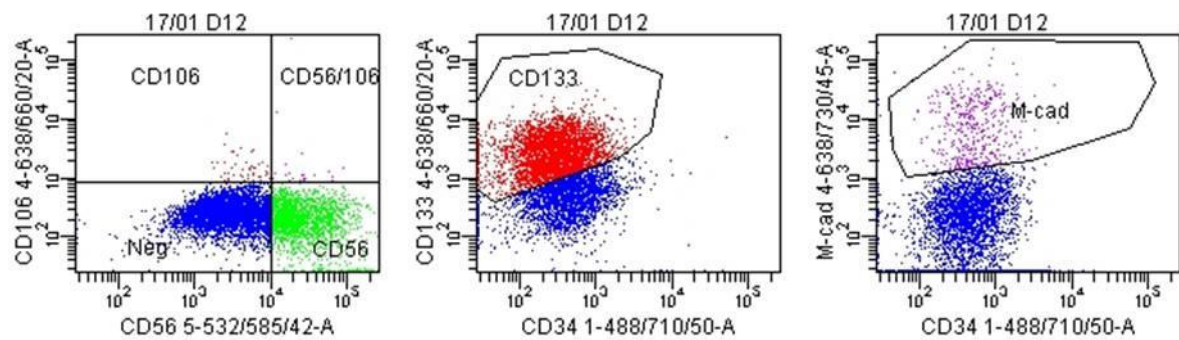


Figure 4.6: Flow Cytometry Analysis of Conditioned Medium from Various Myoblast Lines. Representative dot plots from the flow cytometry analysis of the media conditioned using various myoblast lines. A 12 day differentiation in 17/01 conditioned medium is shown, with populations staining for CD56 and CD106 (first plot), CD133 (second plot), and M-cadherin (third plot).

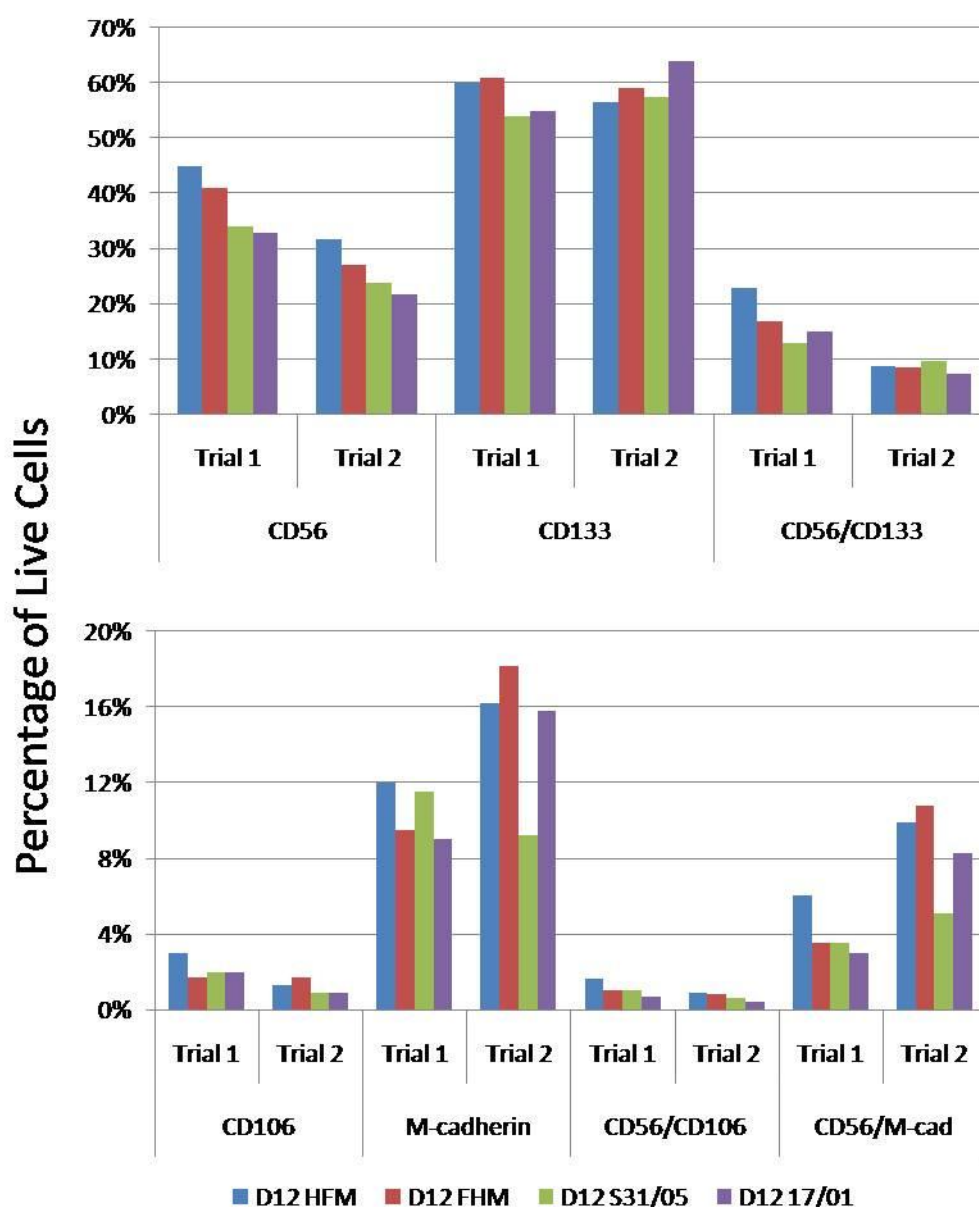


Figure 4.7: Quantification of Flow Cytometry Analysis of Various Conditioned Media. The effect of conditioning medium with various myoblast cell lines on myogenic differentiation. Two foetal (HFM and FHM) and two adult (S31/05 and 17/01) cell lines were compared. (Top Graph) There was not a substantial difference between the cell lines in terms of neurogenesis markers, however HFM conditioned medium yielded the highest expression of CD56 in both trials. However, this did not correlate to a lower level of myogenic markers. (Bottom Graph) All cultures showed comparable levels of CD106 and M-cadherin, in addition to the co-expression of CD56/CD106 and CD56/M-cad. Two trials were conducted for this experiment.

4.2.4 Differentiation with Activin A and Conditioned Medium

Activin A, which had been shown to inhibit ectoderm formation in differentiating ES cell cultures (19279133), was also added to the HFM conditioned medium in order to improve myogenic differentiation. Concentrations of 10, 30, 50, and 100 ng/mL Activin A were found to decrease the percent of cells expressing CD56 in a dose-dependent manner (**Figures 4.8 and 4.9**). However, it

should be noted that only one trial was conducted for the concentrations of 10, 50, and 100 ng/mL, while a second trial for 30 ng/mL showed similar results (data not shown). In addition, increasing levels of Activin A resulted in increased expression of CD133 (but a decrease in the CD56+/CD133+ population). Unfortunately, the presence of Activin A at any concentration did not produce an increase in the expression of CD106 or M-cadherin. As a reference, cultures differentiated in HFM conditioned medium without Activin A had higher levels of M-cadherin and the CD56+/M-cad+ population.

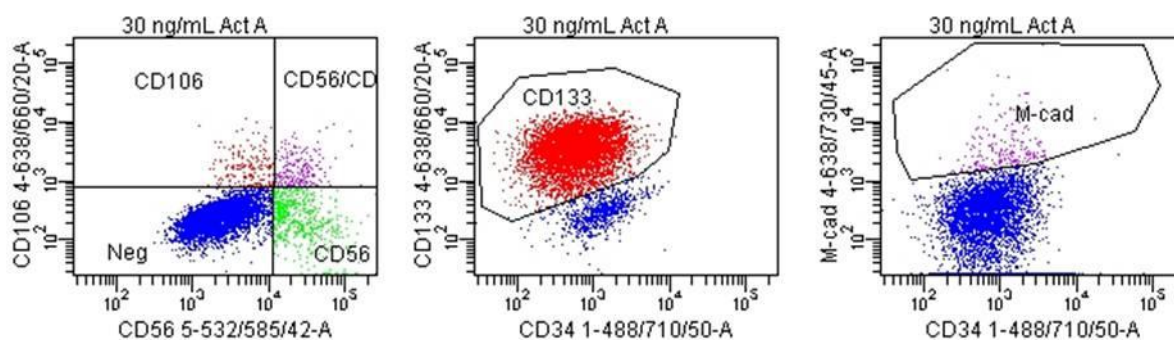


Figure 4.8: Activin A Medium Differentiation Analysis by Flow Cytometry. Representative dot plots from the flow cytometry analysis of the Activin A gradient differentiations. The plots show the results from adding 30 ng/mL of Activin A to the differentiation medium. A significant reduction in the number of cells stained for CD56 can be seen (first plot), while a large increase in CD133 staining is observed (second plot).

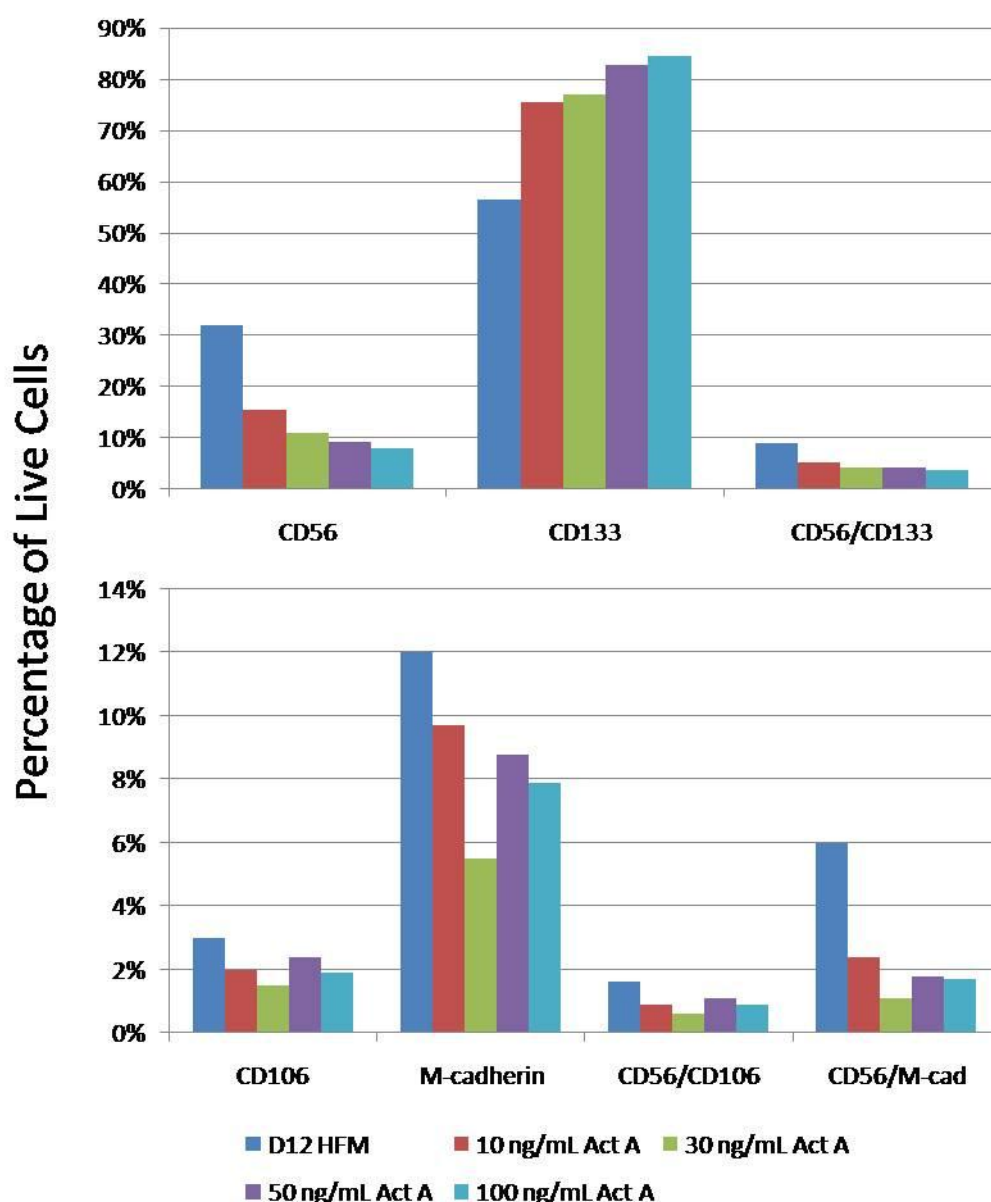


Figure 4.9: Activin A Medium Differentiation Analysis by Flow Cytometry (Quantification). Effect of ectopic expression of Activin A (at concentrations of 10, 30, 50, and 100 ng/mL) on myogenic differentiations. (Top Graph) Activin A was found to reduce CD56 expression and increase CD133 expression in a dose-dependent manner when compared to the HFM D12 differentiation. The percent of cells expressing CD56 decreased by roughly two-thirds, while the expression of CD133 increased by between 10-30%, when Activin A was added to the differentiation medium. (Bottom Graph) Activin A had a much less noticeable effect on CD106 and M-cadherin expression, however M-cadherin and CD56/M-cad expression were higher in the HFM D12 than at any concentration of Activin A. Only one trial was conducted for this experiment.

4.2.5 Myoblast Co-culture and BMP-4 Treatment

A recent study has shown that differentiating hES cells for a short time in serum free medium (SFM) with 25 ng/mL BMP-4 enhances mesoderm formation, though primarily haematopoietic and cardiac differentiation (Zhang, Li et al. 2008). To promote skeletal muscle differentiation using this strategy,

hES cells were grown on a feeder layer of differentiated, mitomycin-C inactivated FHM cells. To distinguish differentiating hES cells from feeder myoblasts, a line of H9 cells constitutively expressing GFP (H9-GFP) was used. Differentiating hES cells were initially plated on myoblasts in hES medium, then SFM, followed by increasing concentrations of conditioned medium with FBS. At all time points, GFP+ cells could be distinguished from the inactivated myoblasts however by day 20 almost all the cells observed were GFP+ (**Figure 4.10**). Four time points were tested: 12 days, 17 days, 21 days, and 28 days after plating. Cells were stained for CD56, M-cadherin, and CD106. Only GFP+ cells (approximately 80% of the cultures) were considered when analyzing the flow cytometry data (**Figure 4.11**). These data were compared to the 12 day HFM differentiation.

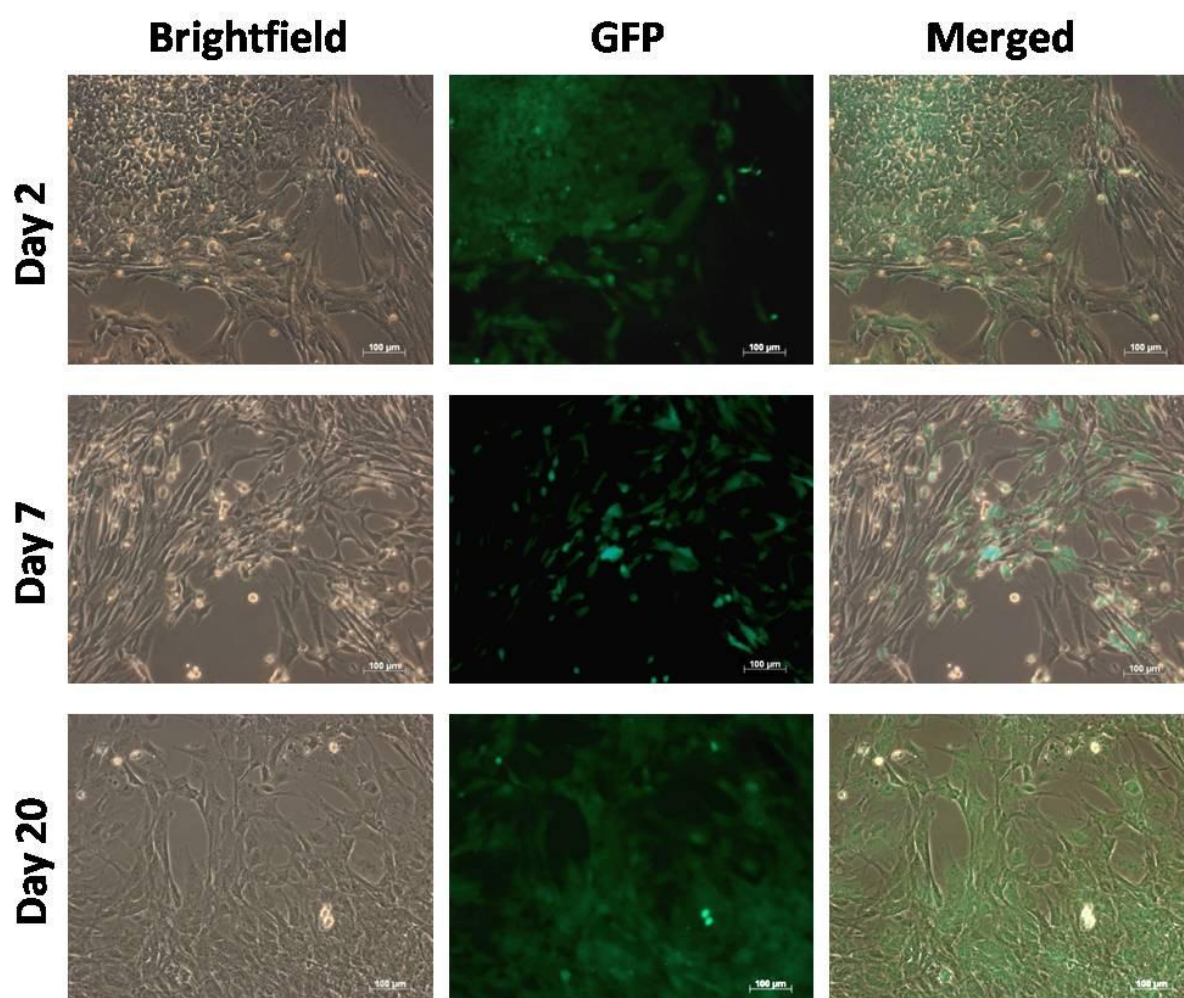


Figure 4.10: H9 Cell GFP Staining during BMP4 Differentiation Experiment. H9-GFP cells differentiating alongside inactivated myoblasts. At day 2, most GFP-positive cells are found in the hES colony that settled after plating, with only a few cells beginning to migrate among the myoblasts. By day 7, GFP-positive cells have further dispersed throughout the myoblast networks and by day 20 the vast majority of the cells are GFP-positive.

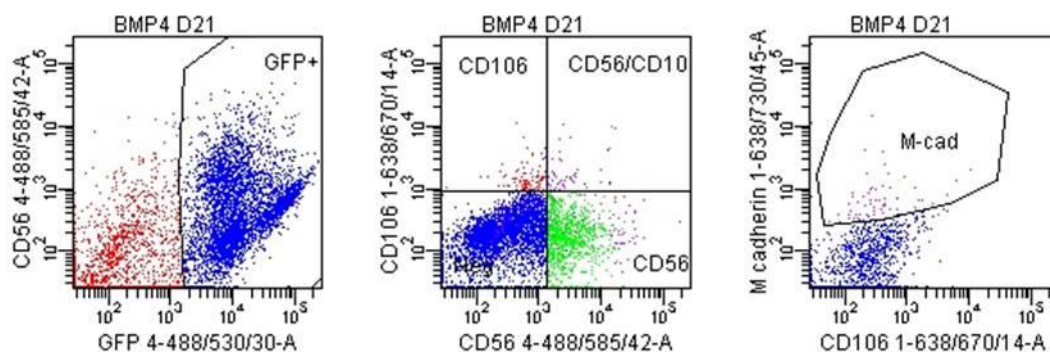


Figure 4.11: BMP4 Differentiation Analysis by Flow Cytometry. Representative dot plots from the flow cytometry analysis of the BMP4 differentiation. Only GFP+ cells were used for analysis and FACS (first plot). GFP+ cells also stained for CD56, CD106 (second plot), and M-cadherin (third plot). Similar gates were used when sorting cells.

CD56 expression varied a good deal between time points, with the highest expression found at day 17 and the lowest at days 12 and 21 (**Figure 4.12**). Surprisingly, all time points expressed significantly more CD56 than HFM D12. CD106 expression was by far the highest in the BMP4 D12 differentiation, however a large degree of variability was observed for that time point: in each of the four trials it was found that 1%, 5.6%, 27.9%, and 28% of the cells expressed CD106. Despite the abnormally high percent of CD106 cells in the last two trials, the other markers tested on those days were not significantly different from other trials or time points. Both the BMP4 D17 and D21 time points had a similar level of CD106 expression as HFM D12, but the BMP4 D28 had significantly less. HFM D12 had the highest level of M-cadherin, around 8%, compared to around 2% for all of the BMP4 differentiations. The co-expression of myogenic markers was also lower among the BMP4 differentiations: rarely more than 1% of the cells were positive for more than one marker, compared to 1 to 3% for HFM D12. The exception was M-cad/CD106 expression in BMP4 D12 cultures, where 1.7% of the cells expressed both markers, very similar to what was seen for HFM D12.

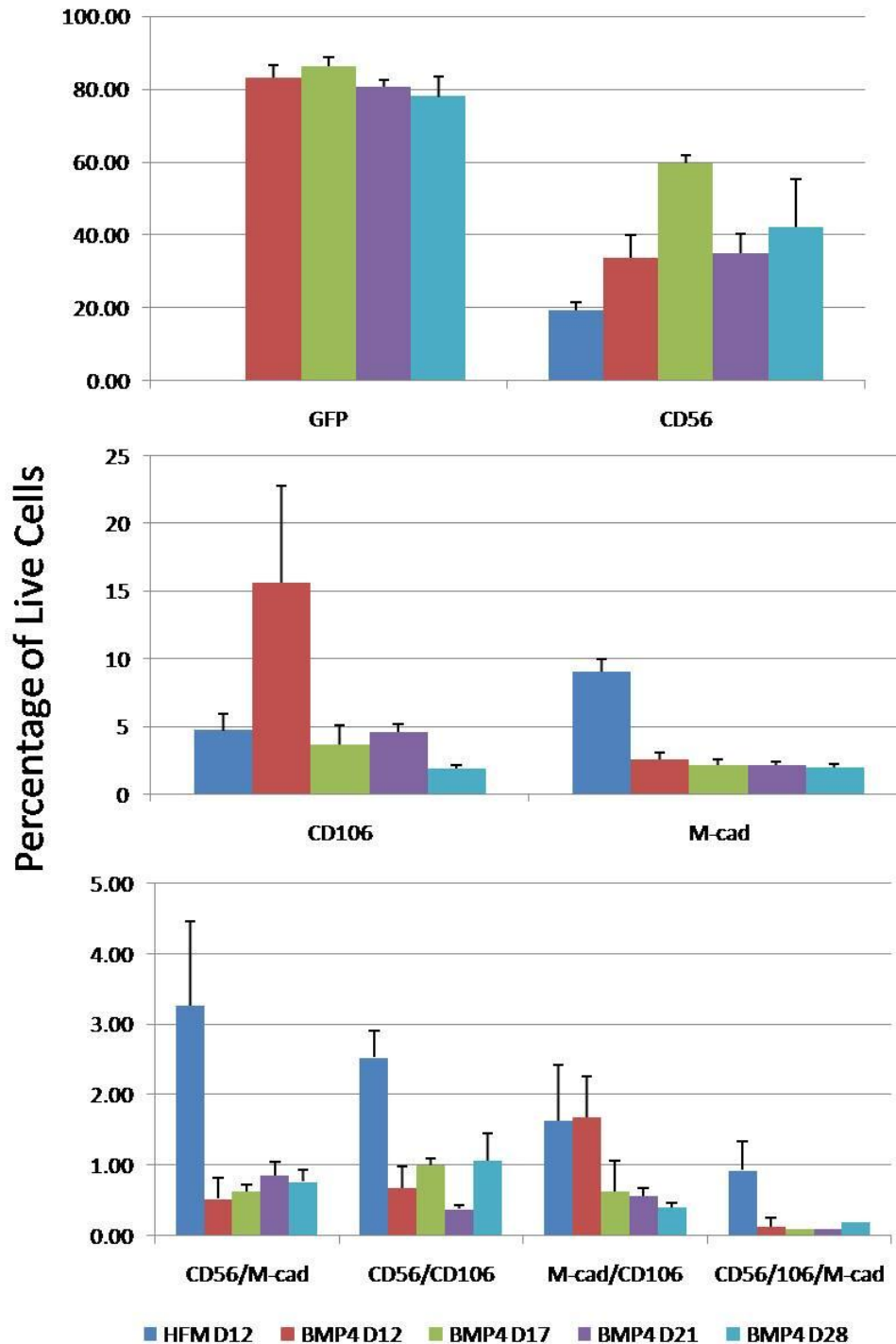


Figure 4.12: BMP4 Differentiation Analysis by Flow Cytometry (Quantification). Expression of GFP in BMP4 differentiation cultures and satellite cell surface markers in GFP+ cells determined by flow cytometry. GFP was expressed in approximately 80% of the cultures. The expression of CD56 was compared between GFP+ BMP4 cells and HFM D12 cells. All of the BMP4 cultures expressed higher levels of CD56 than the HFM D12 cells (Top Graph). The expression of CD106 was comparable between HFM D12 and BMP4 days 17 and 21, with higher levels seen in BMP4 day 12 and lower levels seen in BMP4 day 28. M-cadherin expression was consistently low in all of the BMP4 cultures (Middle Graph). The co-expression of multiple markers was also observed (Bottom Graph). HFM D12 cells were more likely to expression multiple markers than the BMP4 cultures, with the exception of the BMP4 day 12 M-cad/CD106+ population which was comparable to the same population in the HFM D12 culture.

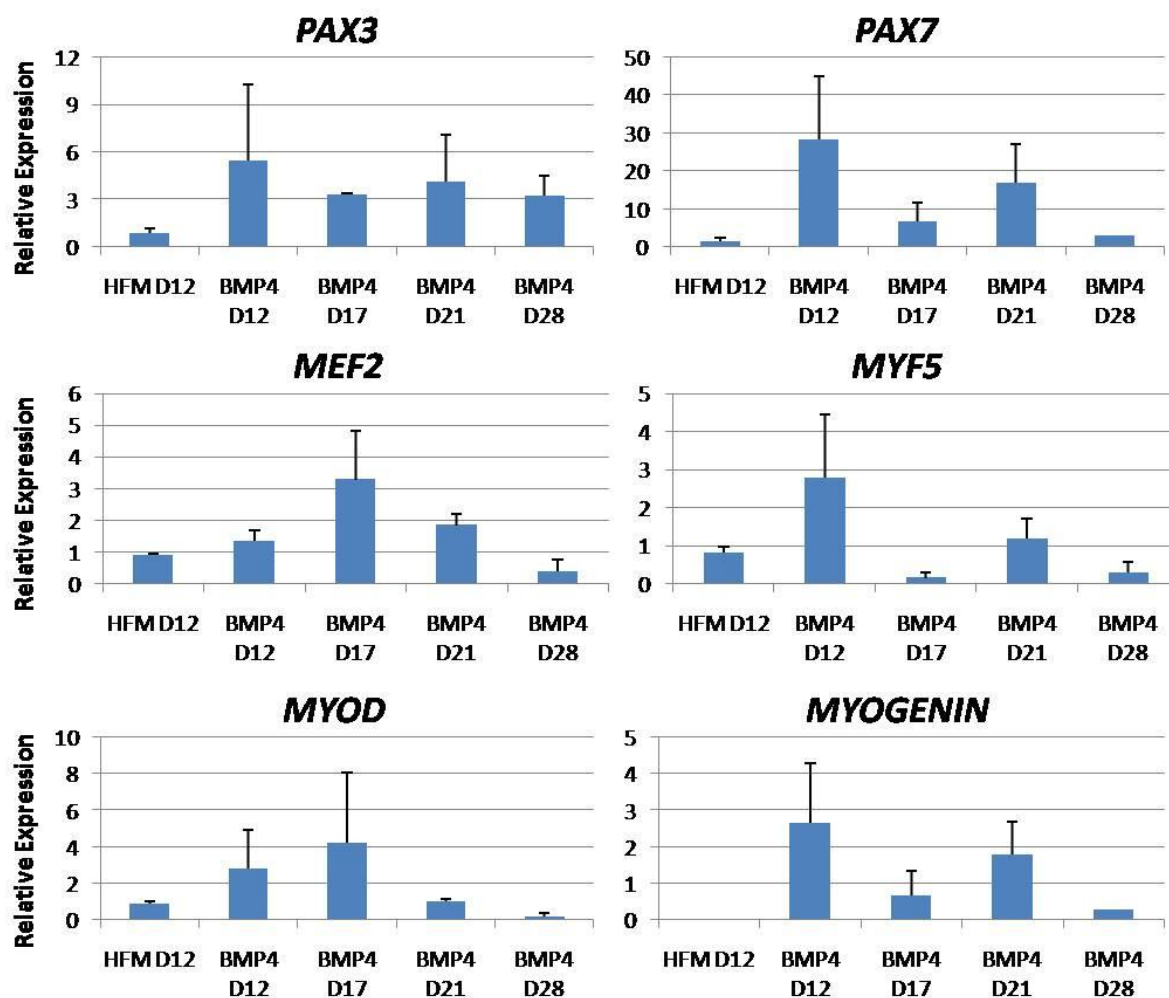


Figure 4.13: BMP4 Differentiation Analysis by qPCR. qPCR analysis from GFP+ cells isolated from the BMP4 differentiations showed an increase in the expression of myogenic genes when compared to the HFM D12 differentiation. *PAX3* and *PAX7* were most highly expressed on days 12 and 21 during the BMP4 differentiation, however these genes also showed a high degree of variability between trials. In contrast, *MEF2* was most highly expressed on day 17, gradually decreasing to a minimum on day 20, with similar results observed of *MYOD*. *MYF5* and *MYOGENIN* expression peaked at day 12, with significant levels also seen at day 21.

Flow cytometry analysis suggested that the HFM D12 differentiation was better at promoting myogenesis than the BMP4 differentiations, but qPCR analysis suggested otherwise. GFP+ cells (only those derived from the H9 GFP line) were isolated using FACS and tested for various myogenic genes (Figure 4.13). While the results varied significantly at certain time points, both *PAX3* and *PAX7* were more highly expressed in BMP4 cultures than the HFM culture. The two genes followed a similar pattern during the BMP4 time course: days 12 and 21 expressed, on average, higher levels while days 17 and 28 expressed lower levels. However, due to the high degree of variability between repeats of the same time point, the differences in expression were generally not statistically significant. *MEF2* was more highly expressed in days 12, 17, and 21 of the BMP4 differentiation than in the HFM D12

culture, with the highest expression occurring at day 17 and then decreasing until day 28. *MYOD* expression was greatest on days 12 and 17 of the BMP4 differentiation, with lower levels seen on day 21 and in the HFM D12 culture. *MYF5* expression was somewhat erratic during the BMP4 time course, with the highest expression on day 12, the lowest on days 17 and 28, and a moderate level on day 21.

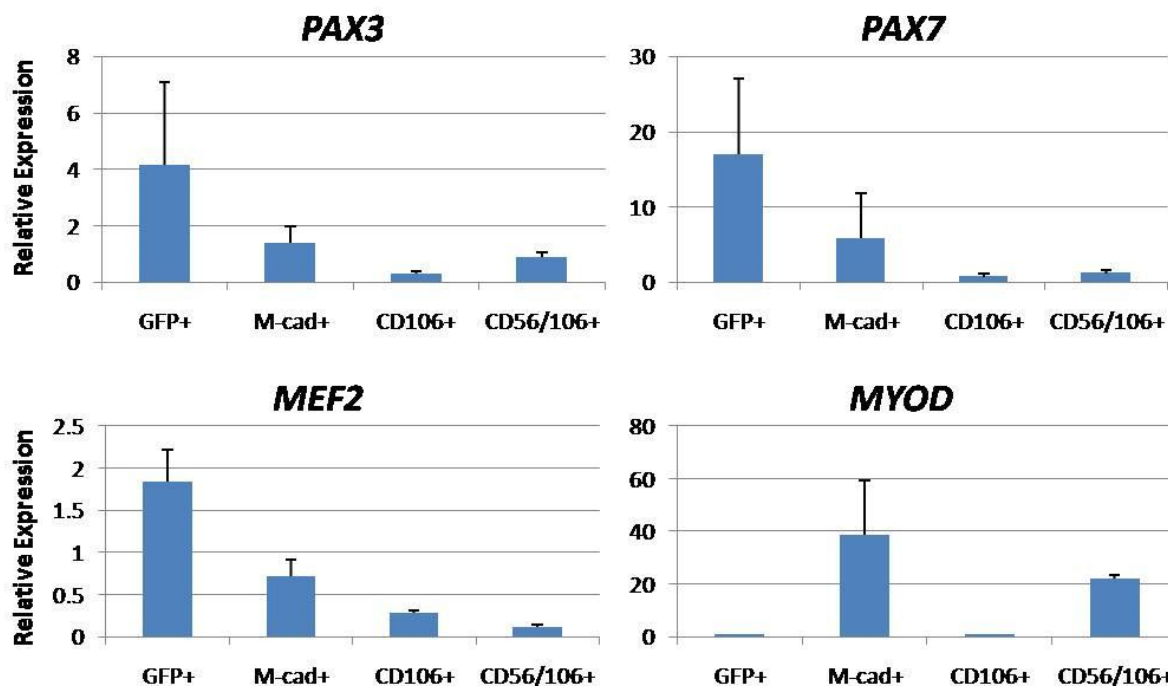


Figure 4.14: BMP4 Differentiation Analysis of Sorted Populations by qPCR. Several different populations of BMP4 day 21 differentiated cells were sorted and analyzed by qPCR. They were compared to the baseline BMP4 results for GFP+ cells. *PAX3*, *PAX7*, and *MEF2* expression were highest in the GFP+ population with significant levels also seen in the M-cad+ cells. However, *MYOD* expression was highest in the M-cad+ and CD56/106+ populations, with only a very small level seen in the GFP+ and the CD106+ cells.

In order to study isolated populations of putative muscle precursors after 21 days of differentiation, cells which were positive for M-cadherin, CD106 (but CD56 negative), and CD56/CD106 were also obtained using FACS and analyzed by qPCR. However, because of the low number of cells in each of these populations, only two trials for each group were tested for the expression of myogenic genes (Figure 4.14). *MYOGENIN* and *MYF5* were excluded because not enough RNA was obtained from the collected cells for reliable qPCR results. The different populations were compared to the average expression obtained for the BMP4 D21 culture (GFP+). All three populations had lower levels of *PAX3* and *PAX7* expression than the GFP+ control. M-cad+ cells had the highest level of *PAX3* expression among the three populations sorted for myoblast markers. Similarly, the GFP+ population had the highest expression of *MEF2*, with the second highest being the M-cad+ cells. However, *MYOD* was

most highly expressed in M-cad⁺ cells and the CD56/CD106⁺ population, suggesting that both consist of largely myogenic cells. The CD106⁺ population expressed low levels of all the genes tested, confirming the need to include other markers (such as CD56) to isolate putative satellite cells.

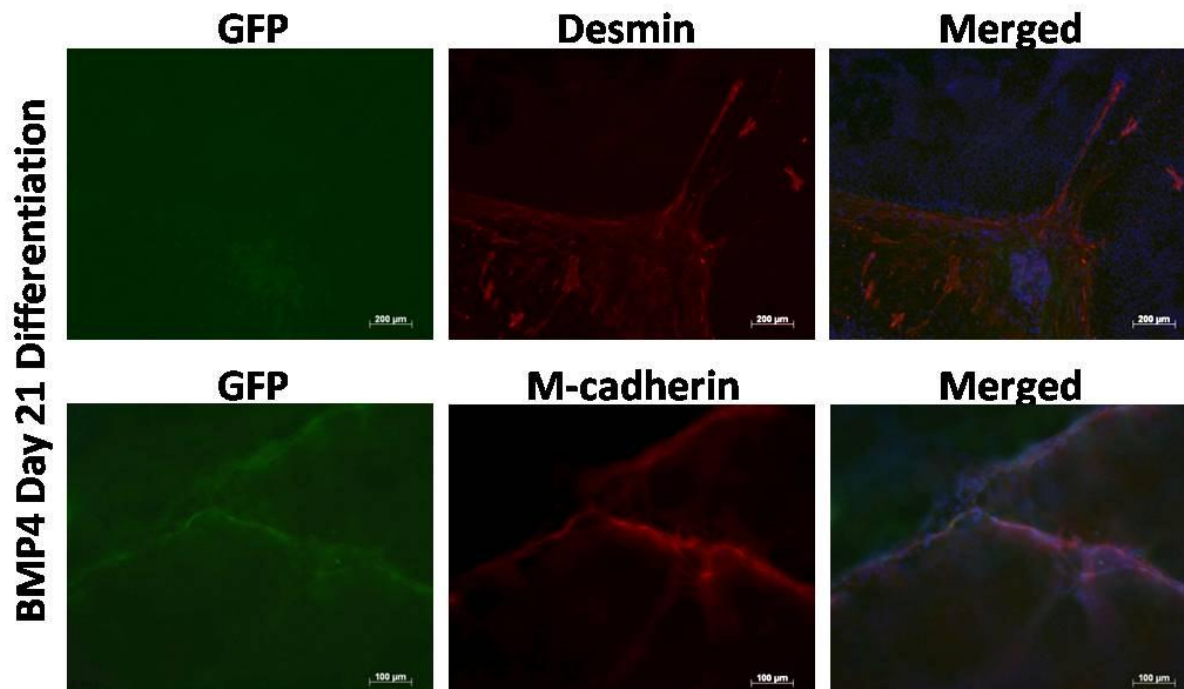


Figure 4.15: BMP4 Differentiation Immunostaining for Desmin and M-Cadherin. Immunostaining of BMP4 day 21 cultures showed GFP-positive cells expressing the intermediate filament marker desmin (top row) as well as the skeletal muscle-specific transmembrane protein M-cadherin (bottom row). Left panels show GFP expression in the differentiation cultures, middle panels show desmin and M-cadherin positive cells stained with AlexaFluor 594 and Rhodamin Red-X secondaries, respectively. The right panels show the merged image along with DAPI staining.

Immunostaining was performed to confirm the presence of myogenic cells in the BMP4 D21 culture (Figure 4.15). Cultures were stained for desmin, a marker of skeletal, cardiac, and smooth muscle cells as well as M-cadherin, which is specific to skeletal muscle. GFP⁺ cells stained positively for both markers, indicating that the cells originated from differentiated hES cells rather than from the myoblast feeder layer. Desmin was expressed much more widely than M-cadherin, most likely due to its presence in non-skeletal muscle cells (such as cardiac and smooth muscle). To further determine the extent of myogenic differentiation, cells were fixed, permeabilized, and stained for MyoD before being analyzed by flow cytometry (Figure 4.16). Of the GFP⁺ cells, it was found that approximately 0.7 % expressed MyoD.

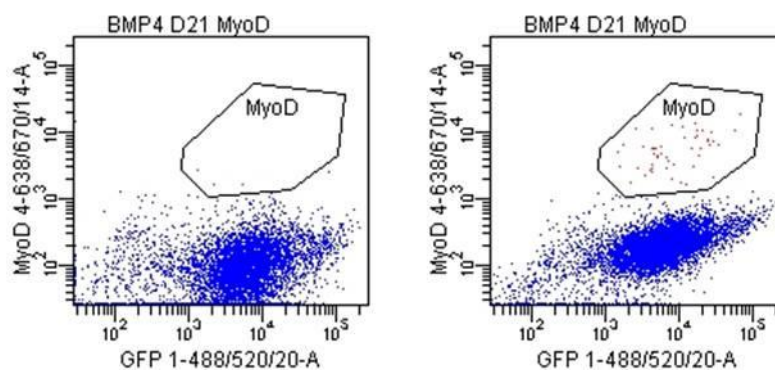


Figure 4.16: BMP4 Differentiation Analysis by Flow Cytometry for MyoD Expression. Flow cytometry analysis of BMP4 day 21 cells stained for MyoD. Unstained cells are seen on the left while MyoD-stained cells are on the right. Approximately 0.7% of GFP+ cells were positive for MyoD.

4.3 Discussion

The initial experiments for this project involved differentiating hES cells as EBs, then disaggregating and plating them for expansion. This route did not seem likely generate useable amounts of myogenic cells and required a great deal of time and effort. To address these shortcomings, a monolayer method of differentiation was designed which proved to be much more expandable than using EBs. However, when allowed to differentiate without external forces, hES cells will predominantly go down the ectoderm lineage. This tendency can be countered by the application of appropriate growth factors, but these approaches can often be expensive and yield only marginally more control of hES cell differentiation. As an alternative, this study primarily used medium conditioned by human foetal myoblasts to promote differentiation of skeletal muscle.

A number of different approaches to isolating satellite cells from differentiating hES cells are described above and summarized in **Table 4**. One consistent problem was finding a reliable surface marker specific to satellite cells (or muscle progenitors) that can be used in FACS. In mice this has been solved by using the SM/C-2.6 antibody. In humans, excellent antibodies are available for CD56 and CD106, two known markers of satellite cells; unfortunately these proteins are also expressed on a number of other cell types produced during hES cell differentiation. In contrast, M-cadherin is specific to the skeletal muscle lineage (though it is expressed throughout myoblast differentiation and fusion), but an effective antibody for flow cytometry has not been produced. Instead, an M-cadherin antibody was used in tandem with a labeling kit that was considerably less reliable than antibodies developed directly for flow cytometry. Direct staining for intracellular markers, specifically Pax7, also had significant drawbacks. The staining was much more variable on cells that had been fixed and permeabilized compared to live cells, and the cells stained for Pax7 could not be used for further analysis such as qPCR. A solution to this problem is discussed in Chapter 5.

The initial differentiation used horse serum which, based on the high expression of CD56, was unsuccessful in promoting mesoderm formation despite its use in several of the studies hoping to generate skeletal muscle from ES cells. hES cells have a natural tendency to differentiate down the ectoderm/neuronal lineage generating a large percentage of CD56+ cells. To determine the extent of neuronal differentiation, either total CD56 expression or CD56/CD133 co-expression was examined. It was assumed that the majority of CD56+ cells were neuronal, however CD133+ cells could be from a non-ectoderm lineage, so as a marker of neural differentiation it was used in tandem with CD56 (Mizrak, Brittan et al. 2008). The initial differentiation strategy also switched to 100% conditioned medium after 3, 5, or 7 days. Inspection of the differentiating cultures revealed a large number of dead, floating cells which were attributed to the use of nutrient-poor conditioned medium.

Table 4: Summary of hES Cell Myogenic Differentiations

Differentiation	Medium Components	Duration	Results
Initial	Diff medium followed by CM	3, 5, or 7 days in Diff; then 7 or 10 days in CM	Lots of cell death, very inconsistent
HFM Diff:CM	Combination of 1:1 Diff:CM from HFM cells	12, 16, or 20 days	Some increase in the expression of myogenic markers, consistent
Myoblast Diff:CM	1:1 Diff:CM from a variety of different myoblast lines	12 days	No significant difference in medium conditioned from different cell lines
Activin A Diff:CM	1:1 Diff:CM with either 10, 30, 50, or 100 ng/mL Act A	10 days in Diff:CM with Act A then 6 days in Diff:CM without Act A	No improvement in myogenic marker expression when compared to just Diff:CM
BMP4 Co-culture	SFM w/ BMP4, SFM w/out BMP4, increasing conc. of HFM CM	1 day in SFM w/ BMP4; 2 days in SFM w/out BMP4; 12, 17, 21, or 28 days inc. conc. of HFM CM	Some improvement in myogenic gene transcription over Diff:CM

Abbreviations: CM – conditioned medium, HFM – human foetal myoblast, SFM – serum-free medium

When the cultures were grown using only 1:1 Diff:CM, cell viability and myogenic differentiation improved. Adding the conditioned medium immediately upon beginning a differentiation was more effective in reducing neurogenesis when compared to using non-conditioned medium containing horse serum. In these experiments, the highest levels of CD56 were seen in the cultures grown only in Diff medium, suggesting that the conditioned medium was positively affecting differentiation. Further, all three HFM time points showed significantly higher expression of M-cadherin compared to the Diff control, which averaged less than 4% of M-cad+ cells in the control culture compared to greater than 8% for the HFM cultures. qPCR analysis further demonstrated the myogenic nature of the differentiated cells. *PAX3* and *PAX7* are both expressed during the earliest stages of myogenesis and were found to be expressed most highly after 12 days of differentiation. After these genes are

expressed in the dermomyotome, the myogenic regulatory factors are turned on and myogenesis proceeds. As expected, *MYF5* and *MYOD* expression peaked after by day 16 when *PAX3/7* was decreasing. Furthermore, *MYOD* expression continued at high levels through day 20 while *MYF5* expression decreased, similar to what is seen during embryonic development. One of the primary advantages of this differentiation is its simplicity: it does not require numerous expensive growth factors or a complicated, lengthy differentiation scheme in order to promote myogenesis. However, the extent of myogenesis was not particularly high. In an attempt to improve this, several changes were made to the differentiation strategy.

Several different myoblast cell lines were used to condition medium for differentiation. It was originally hypothesized that if one line produced substantially more effective medium than another, then it might be possible to isolate the factors which were important in promoting myogenic differentiation. Unfortunately there were not significant differences between the different conditioned media used. While HFM CM showed the highest level of CD56+ cells, the other three media failed to increase the percentage of cells expressing myogenic markers.

Activin A is necessary for the formation of mesoderm (or, more specifically, mesendoderm) during ES cell differentiation (Tada, Era et al. 2005; Sumi, Tsuneyoshi et al. 2008). It has also been shown to help maintain ES cell pluripotency by controlling Nanog expression and thereby preventing neuroectoderm formation (Vallier, Mendjan et al. 2009). While Activin A is generally used in differentiation strategies to promote definitive endoderm formation (D'Amour, Agulnick et al. 2005; Hashemi-Tabar, Orazizadeh et al. 2009), in hES cells this pathway was found to be dependent on the suppression of phosphatidylinositol 3-kinase (McLean, D'Amour et al. 2007). It was therefore hypothesized that Activin A treatment along with exposure to myoblast conditioned medium might promote mesendoderm formation prior to mesoderm and skeletal muscle progenitor cell differentiation.

When Activin A was added to the medium, a dramatic decrease in CD56 expression was observed, consistent with reports that Activin A inhibits ectoderm differentiation. But once again, the decrease in CD56 expression did not correspond to an increase in the expression of myoblast markers. Interestingly, Activin A substantially increased the expression of CD133, a marker of many types of stem cells including haematopoietic, neural, hepatic, prostate, and renal stem cells as well as secretory and epithelial cells (Wu and Wu 2009). Because most studies using Activin A in the differentiation medium are attempting to derive endoderm, it is tempting to speculate that the increase in CD133 expression is the result of hepatic stem cell formation.

BMP-4 is widely used in ES cell differentiation strategies, predominantly to obtain mesoderm-derived tissues and occasionally ectoderm derivatives. After the conversion of ES cells to mesendoderm,

BMP-4 seems necessary for the subsequent production of mesoderm (Sumi, Tsuneyoshi et al. 2008). It has been used to derive cardiomyocytes (Zhang, Li et al. 2008; Takei, Ichikawa et al. 2009), endothelial lineage cells and vascular networks (Boyd, Dhara et al. 2007; Goldman, Feraud et al. 2009), haematopoietic cells (Wang, Cerdan et al. 2006; Zhang, Li et al. 2008), and paraxial mesoderm derivatives (both chondrogenic and myogenic cells, (Nakayama, Duryea et al. 2003; Sakurai, Inami et al. 2009)). It is also used to promote the differentiation of epidermal ectoderm (Yocum, Gratsch et al. 2008), keratinocytes (Coraux, Hilmi et al. 2003), and neural crest cells (Chiba, Kurokawa et al. 2005). Finally, it has been shown that it does not prevent neuroepithelium formation during the initial stages of ES cell differentiation (LaVaute, Yoo et al. 2009). Because of the expansive role BMP-4 has in development, where in many cases subtle differences in concentration produce entirely different tissues, it was important to include additional drivers of myogenic differentiation.

Using BMP-4 to promote mesoderm formation in addition to co-culture with FHM myoblasts and myoblast conditioned medium produced conflicting results. Flow analysis of the myogenic markers suggested that it did not improve myogenic differentiation. HFM D12 produced higher levels of M-cadherin, lower overall levels of CD56, but higher levels of CD56/M-cad and CD56/CD106. However, it should be noted that CD56 is also expressed in the developing chick somite (Duband, Dufour et al. 1987), which may explain why qPCR analysis of myogenic genes showed that most time points during the BMP4 differentiations expressed higher levels of *PAX3*, *PAX7*, *MYOD*, *MYF5*, and *MEF2* than the HFM D12 differentiation. This disparity highlights the difficulty of finding good surface markers to use for flow analysis and FACS.

After cells were sorted for M-cadherin, CD106, and CD56/CD106 expression and compared to GFP+ cells, it was evident that none of the surface markers consistently enriched all populations of myogenic progenitors. While *MYOD* expression was increased in M-cad+ and CD56/CD106 populations, *PAX3*, *PAX7*, and *MEF2* were higher in the GFP+ population. It is worth noting, however, that the three genes expressed more highly in the GFP+ population have the broadest expression during embryonic development: none are specific to skeletal myogenesis. The low level of *MYOD* expression in the GFP+ population suggests that a substantial percent of the *PAX3* and *PAX7* expression may come from non-myogenic cell types.

The differentiation of ES cells towards mesoderm can be seen as a stepwise process of surface marker expression (**Figure 4.17**). Mesendoderm readily forms in the presence of Activin A or Nodal.

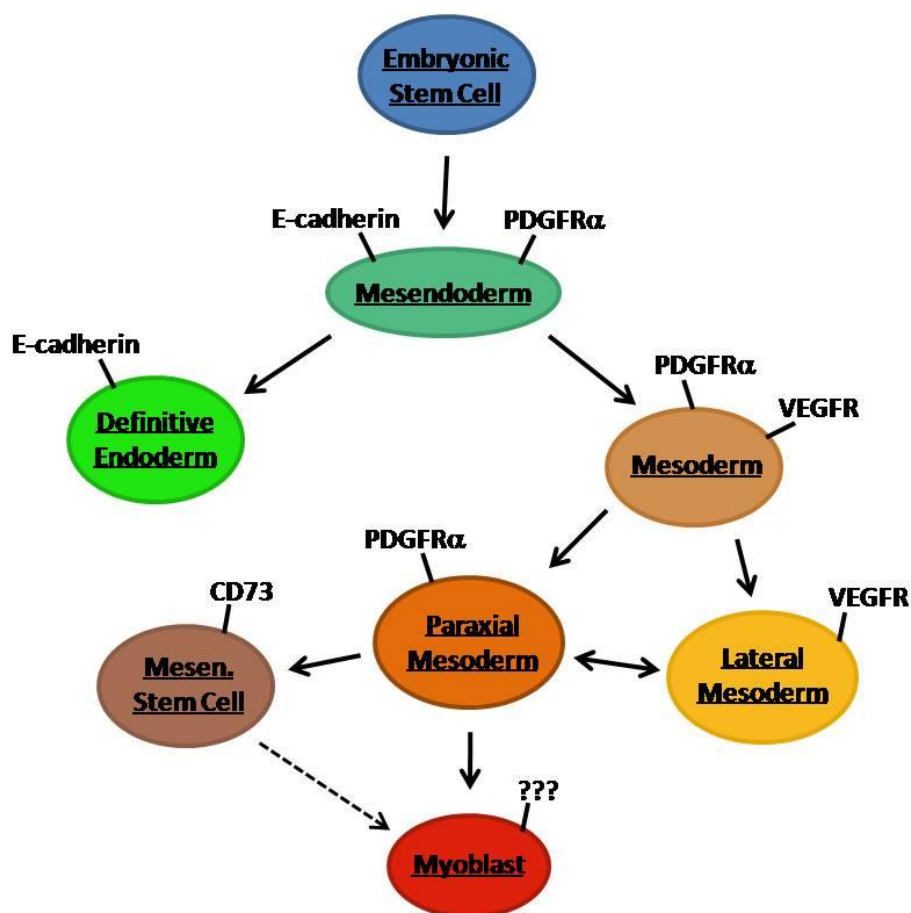


Figure 4.17: Surface Marker Expression during Mesoderm Differentiation. A schematic showing the surface markers expressed during the formation of mesoderm-derived cell types from embryonic stem cells. Note the interconversion between lateral and paraxial mesoderm cells, the ability of CD73+ cells to become myogenic, and the lack of a myoblast-specific surface marker. PDGFR α – platelet derived growth factor receptor-alpha, VEGFR – vascular endothelial growth factor receptor, Mesen. – mesenchymal

These cells are positive for the surface markers E-cadherin (E-cad) and PDGFR α (Tada, Era et al. 2005). This population can then differentiate into definitive endoderm (E-cad+/PDGFR α -) in the presence of Activin A and low serum or mesoderm (E-cad-/PDGFR α +) in the presence of BMP-4 (Sumi, Tsuneyoshi et al. 2008). Further, an unspecified mesoderm population has been described, expressing vascular endothelial growth factor receptor (VEGFR, KDR) and PDGFR α . From this population, both VEGFR-/PDGFR α + and VEGFR+/PDGFR α - cells can be formed and interconvert. They are thought to represent paraxial and lateral plate mesoderm, respectively (Sakurai, Era et al. 2006). Paraxial mesoderm then gives rise to the somites, which go on to form the sclerotome (mesenchymal tissue), myotome, and dermatome. At this point, it has been shown in chick somite explants that high concentrations of BMP-4 act to inhibit the expression of myogenic genes such as *MYF5* and *MYOD*, while Noggin (as a BMP-4 antagonist) has been shown to increase *MYOD* expression but reduce *PAX3* expression. BMP-4 was also shown to increase the lateral plate mesoderm marker *GATA4*, important for myocardial differentiation (Reshef, Maroto et al. 1998). Despite the inhibitory role of BMP-4 on

myogenic differentiation, it remains important for the proper morphogenesis during early myogenesis (Kahane, Ben-Yair et al. 2007). This is somewhat unexpected given the findings that BMP-4 actively promotes paraxial mesoderm formation and the differentiation of chondrogenic and myogenic precursor cells (Nakayama, Duryea et al. 2003; Sakurai, Inami et al. 2009). However, it suggests that myogenic differentiation might be improved by adding Noggin after BMP-4, although this technique has been shown to also increase production of cardiomyocytes (Zhang, Li et al. 2008).

Efficiently generating myogenic cells from a direct differentiation of hES cells has proven to be difficult. While it is possible to conduct a step-wise process from pluripotent cells to mesendoderm (using Activin A) and then to mesoderm (using BMP-4), the specification of paraxial mesoderm and then myogenic cells has remained elusive. At best, some differentiation strategies can produce myogenic cells as by-products in a heterogeneous population. For instance, it is likely that the CD73+ population isolated by Barberi et al. (Barberi, Willis et al. 2005; Barberi, Bradbury et al. 2007) represents cells from the sclerotome, given their expression of mesenchymal markers and their differentiation capacity. While they show that these cells can become myogenic under certain culture conditions, ideally a similar strategy could isolate putative myotomal cells from the same stage in development. However, because so much of early embryonic development depends on subtle concentration gradients of growth factors from numerous sources in a three dimensional embryo, more research is needed before controlled differentiation is proven to be an effective way to derive myogenic stem cells.

Chapter 5: Isolation of Differentiated hES Cells Using a Pax7-GFP Reporter Construct

5.1 Introduction

Pax7 is expressed during the development of both the nervous and muscular systems. The first study describing its expression pattern showed that it is found in the dorsal part of the neural tube; the developing brain, specifically the mesencephalon; and the olfactory epithelium. It is also expressed in the dermomyotome and later the myotome and developing skeletal muscle of the trunk and limbs. However, Pax7 was absent from dermatome-derived tissues as well as cardiac and smooth muscle (Jostes, Walther et al. 1990). More specifically, Pax7 is expressed in the central region of the dermomyotome, while Pax3 is expressed in the epaxial and hypaxial regions. Pax3 is also expressed in the cells migrating from the somites to establish limb musculature, while Pax7 is not expressed in the limb until muscles have begun to form. Pax7 is expressed in the branchial arches, though Pax3 is not, and later in the facial muscles. However, muscles from the developing limb and face do not seem to be affected when Pax7 is absent (Relaix, Rocancourt et al. 2004).

Initial studies of Pax7^{-/-} mice reported that while muscle organization and development were unaffected, postnatal growth of skeletal muscle was severely restricted. This was attributed to the complete absence of satellite cells in null mice. Additionally, side population stem cells isolated from Pax7^{-/-} muscle were more inclined to form haematopoietic colonies than those from wildtype muscle, suggesting that Pax7 is important in adult muscle determination (Seale, Sabourin et al. 2000). However, later reports claim that Pax7^{-/-} mice do not have an obvious muscle phenotype beyond a significantly reduced bodyweight. The small percentage of pups which survived to adulthood was further examined, and it was found that muscle stem cells were still active in two month old mice. However, while satellite cells could be identified in Pax7^{-/-} mice, it was at a much lower number than heterozygous littermates. The number of satellite cells was drastically reduced as the mice aged and, compared to heterozygous cells, isolated satellite cells from null mice also produced fewer MyoD⁺ and desmin⁺ cells when cultured. Pax7^{-/-} mice also showed a reduced capacity to regenerate damaged muscle *in vivo* (Oustanina, Hause et al. 2004).

More recently, Lepper et al. have further examined the role of Pax7 during adult muscle regeneration using conditional gene inactivation in transgenic mice. In adult mice, inactivation of the *Pax7* gene did not cause a reduction in satellite cell number or a decrease in expression of typical surface markers such as M-cadherin. Upon muscle injury, these Pax7^{-/-} satellite cells were capable of

normally contributing to muscle regeneration as well as proliferating and reoccupying the satellite cell niche. In doing so, they did not lose their myogenic capacity. Thus, in the adult, Pax7 is not necessary for satellite cell survival, proliferation, differentiation, or return to quiescence. In contrast, in juvenile mice (7-21 days old), Pax7 inactivation did noticeably decrease regeneration and prevented the normal return of satellite cells to a quiescent state in the satellite cell niche. It was concluded that during early post-natal development, satellite cells undergo a fundamental change whereby Pax7 is no longer necessary for their maintenance and that embryonic myoblasts have fundamentally different genetic requirements than adult satellite cells (Lepper, Conway et al. 2009).

Pax7 is found in the vast majority of satellite cells, defined by their anatomical position (Reimann, Brimah et al. 2004). Quiescent satellite cells express Pax7 but not markers such as MyoD or myogenin. However, when satellite cells are activated and begin to proliferate, the vast majority of cells co-express Pax7 and MyoD. Transcriptional activity of Pax7 is observed in these activated cells. As myoblasts begin to differentiate and fuse, Pax7 is down-regulated and myogenin begins to be expressed. However, a population of Pax7+/MyoD- cells arises from the population of Pax7+/MyoD+ myoblasts. These cells become quiescent and associate with newly formed myofibres (Zammit, Golding et al. 2004; Zammit, Relaix et al. 2006).

Pax7 is ideally suited to be a satellite cell marker because of its ubiquity and specificity: it is expressed in nearly all satellite cells and is down-regulated once myoblasts begin to differentiate. Consequently, Pax7 is often used to identify satellite cells in muscle tissue (Allouh, Yablonka-Reuveni et al. 2008; Kirkpatrick, Allouh et al. 2008) and has recently been employed to isolate satellite cells by FACS (Bosnakovski, Xu et al. 2008). However, for the purpose of isolating putative satellite cells from differentiating hES cells, it should be noted that Pax7 is not a perfect marker. Most adult studies focus on dissected muscle tissue with relatively few non-myogenic cells. Unfortunately, Pax7 is more widely expressed during embryonic development than in the adult, allowing for contamination of additional cell types if other markers are not used. Despite the fact that Pax7 expression in differentiating cultures of hES cells does not guarantee the presence of myogenic tissue, it remains one of the most selective markers of satellite cells.

Chapter 5 Aims:

To develop a genetic construct which, when transfected into hES cells, would express GFP under the control of the *PAX7* gene promoter

To test the Pax7P-GFP construct in myoblasts known to express *PAX7*

To develop a refined protocol for the efficient transfection of the Pax7P-GFP construct into undifferentiated hES cells using Nucleofection technology

To sort cells differentiated using the strategies discussed in Chapter 4 based on their expression of GFP and to analyze these cells using qPCR

5.2 Results

5.2.1 Creation of the Pax7P-GFP Construct

A 1.5 kilobase region of the *PAX7* promoter (called Pax7P) was isolated by PCR and cloned into the pEGFP-1 vector (Figure 5.1).

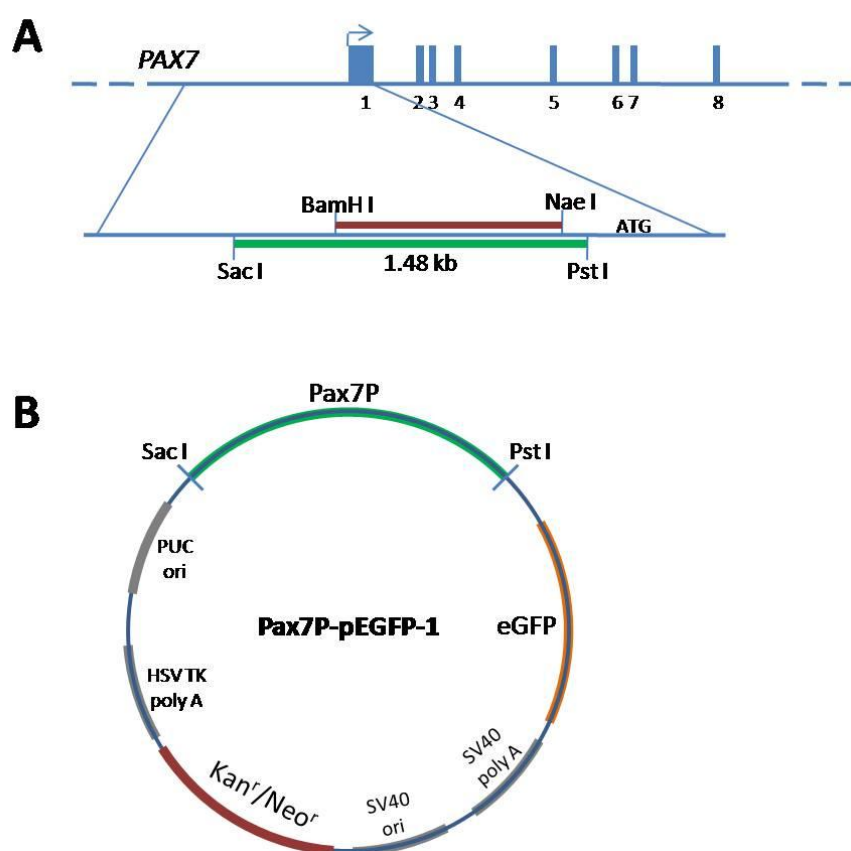


Figure 5.1: Generation of the Pax7P-GFP Construct. (A) Schematic of the *PAX7* gene and the region of the promoter, marked in green, isolated to drive GFP expression in the pEGFP-1 vector. The enzymes *Sac* I and *Pst* I were used to excise the promoter from the purified PCR product. As a comparison, the region of the promoter used in Syagailo et al. is marked in red (Syagailo, Okladnova et al. 2002). (B) The region of the *PAX7* promoter (green) ligated into the pEGFP-1 vector. The promoter drives eGFP (orange) expression while an SV40 promoter drives expression of the kanamycin/neomycin resistance gene (red).

In a previous attempt to generate such a construct, the region of the promoter used in Syagailo et al. was found not to drive GFP expression in differentiating hES cells. As a result, for this study, a

broader region was selected. While many constructs have a high likelihood of being epigenetically silenced once transfected into hES cells (Stewart, Yang et al. 2008), previous experience had shown that the pEGFP-1 vector was somewhat resistant to this tendency, thus it was chosen as the vector to enable GFP expression. Once the construct was generated, it was sequenced around the insertion site to ensure the proper position of the *PAX7* promoter in the vector (**Figure 5.2**). It was found that the regions sequenced both before and after the insertion correctly corresponded to the theoretical sequence determined using the vector sequence and that of the *PAX7* promoter.

Fwd Pax7P	----- CCTGGCCTTTTGTGGCCTTTTGTCTCACATGTTCTTTCTGCGTTATCCCCTGATTCTGT	60
Fwd Pax7P	----AACCGTATTACCGCCATGCATTAGTTATTACTAGCGCTACCGGACTCAGATCTCGA GGATAACCGTATTACCGCCATGCATTAGTTATTACTAGCGCTACCGGACTCAGATCTCGA	56 120
	← pEGFP-1	
Fwd Pax7P	GCTCAGAGTTGGTGAGTTCAGAGCTGTATCAAGTCTTGACGGGCTCCCTCCCTCCCATTT GCTCAGAGTTGGTGAGTTCAGAGCTGTATCAAGTCTTGACGGGCTCCCTCCCTCCCATTT	116 180
	PAX7P →	
Fwd Pax7P	CCCACCTCTTTGGGCCCCCAGATCCTCACACCAGCACCAACTCCCTGTAAACCCAACTAC CCCACCTCTTTGGGCCCCCAGATCCTCACACCAGCACCAACTCCCTGTAAACCCAACTAC	176 240
Fwd Pax7P	CTGCTGGAAAGGAGTTATAGCCCCGGCCTGGGGGCTGAGGAGGACGGCGGGCTGGAG CTGCTGGAAAGGAGTTATAGCCCCGGCCTGGGGGCTGAGGAGGACGGCGGGCTGGAG	236 300
Rev Pax7P	-----GCAAACACCCACCTCACCCCCCTCCCCAGCTTCTGG CGTCGCCACCTTCCCTCCCCCAACCTCCAACCCACCTCACCCCCCTCCCCAGCTTCTGG	37 300
Rev Pax7P	ACGCGTTTGACTGCAGTCGACGGTACCGCGGGCCCGGGATCCACCGGTCGCCACCATGGT ACGCGTTTGACTGCAGTCGACGGTACCGCGGGCCCGGGATCCACCGGTCGCCACCATGGT	97 360
	← PAX7P pEGFP-1 →	
Rev Pax7P	GAGCAAGGGCGAGGAGCTGTTACCCGGGTGGTGCCCATCCTGGTCGAGCTGGACGGCGA GAGCAAGGGCGAGGAGCTGTTACCCGGGTGGTGCCCATCCTGGTCGAGCTGGACGGCGA	157 420
Rev Pax7P	CGTAAACGGCCACAAGTTCAGCGTGTCCGGCGAGGGCGAGGGCGATGCCACCTACGGCAA CGTAAACGGCCACAAGTTCAGCGTGTCCGGCGAGGGCGAGGGCGATGCCACCTACGGCAA	217 480
Rev Pax7P	GCTGACCCTGAAGTTCATCTGCACCACCGGCAAGCTGCCCGTGCCCTGGCCCCACCCTCGT GCTGACCCTGAAGTTCATCTGCACCACCGGCAAGCTGCCCGTGCCCTGGCCCCACCCTCGT	277 540

Figure 5.2: Sequencing the Pax7P-GFP Construct. Overlap between the sequencing results from the forward primer 5'-GCTCACATGTTCTTTCTGCG-3' (Fwd) and the reverse complement of the reverse primer 5'-CATGGCGGACTTGAAGAAGTC-3' (Rev) aligned with theoretical sequence of the *PAX7* promoter ligated into the pEGFP-1 vector (Pax7P). Highlighted areas show the restriction sites for Sac I (blue) and Pst I (red) used for the insertion. Sequence overlap on both sides of the insertion sites demonstrates the successful ligation.

In order to test the vector's ability to drive GFP expression when the *PAX7* gene is active, the Pax7P-GFP construct was nucleofected into adult human myoblasts. After several days on antibiotic selection, the cells were harvested and analyzed by flow cytometry (**Figure 5.3**). Approximately 5% of the cells showed substantial GFP expression, consistent with Pax7 immunostaining results for the same cell line (J. Morgan, unpublished). This strongly suggested that GFP expression faithfully represented *PAX7* gene activity.

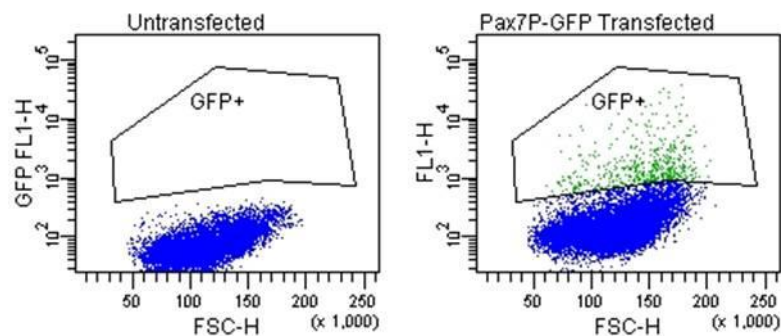


Figure 5.3: Pax7P-GFP Construct Validation by Flow Cytometry. GFP expression in non-transfected (left) and Pax7P-GFP transfected (right) adult human myoblasts analyzed by flow cytometry. Approximately 5% of the cells are GFP+ in the transfected myoblasts.

5.2.2 Generation of the H9 Pax7-GFP Cell Line

A new protocol was developed for the nucleofection of H9 hES cells with the Pax7P-GFP construct based on the method described by Hohenstein et al. The detailed protocol is described in Chapter 2 Materials and Methods. Briefly, single cells were harvested by trypsinization and resuspended in a small amount of mES nucleofection solution, incubated for 5 minutes at 37°C, and 3 µg of the linearized construct was added. The cells were electroporated in a Nucleofector and plated at very high density (one 6-well dish of hES cells were harvested and plated into one well of a 6-well dish) onto MEFs with hES medium containing 10 µM ROCK inhibitor (ROCKi, Y-27632). ROCKi was kept in the medium for 96 hours post-transfection, at which point increasing concentrations of neomycin were added over the following 6 days. The cells were then maintained by passaging normally, with increasing levels of neomycin added after each passage to ensure that only cells that had accepted the Pax7P-GFP construct survived.

5.2.3 Differentiation of H9 Pax7-GFP Cells

H9 Pax7-GFP cells were differentiated in HFM conditioned medium (Diff:CM) for 6, 12, 16, and 20 days to ensure that the new cell line generated comparable results after myogenic differentiation when compared to non-genetically modified H9s. An earlier (6 day) time point was included to better monitor the time at which Pax7 expression was highest. Once again, cells were stained for myogenic surface markers and analyzed by flow cytometry (Figure 5.4).

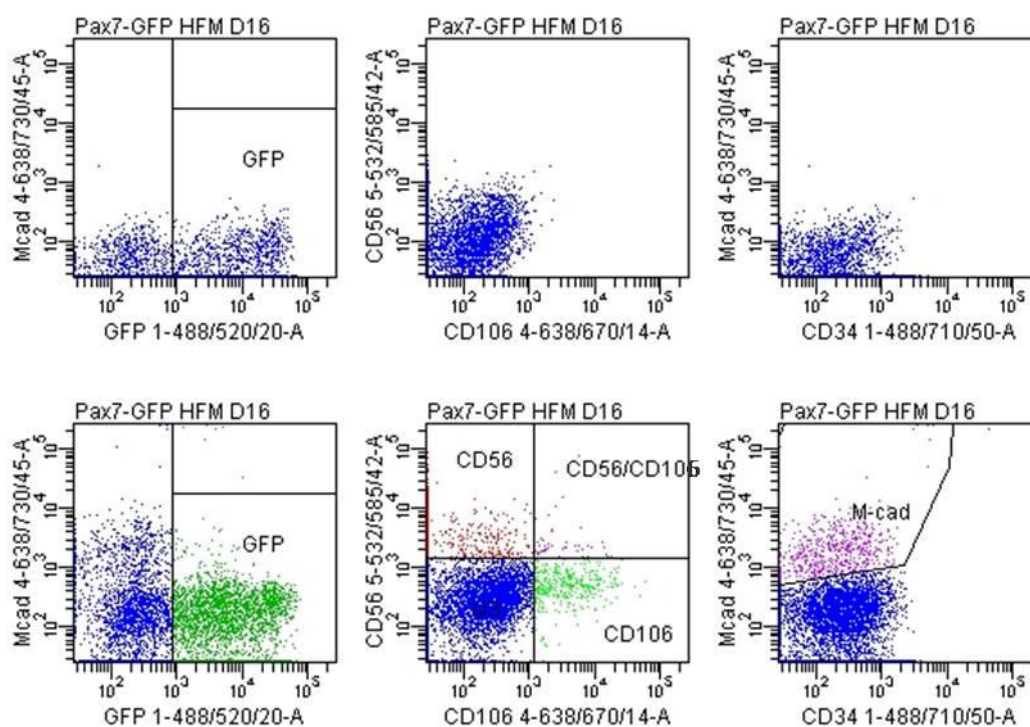


Figure 5.4: Differentiated Pax7GFP Cells Analyzed by Flow Cytometry. Representative dot plots from the flow cytometry analysis of Pax7-GFP HFM differentiation cultures are shown. Unstained cells were used as a control (top row). Cells were analyzed for GFP expression (bottom left) and stained for CD56, CD106 (bottom middle), and M-cadherin (bottom right). GFP was more widely expressed than anticipated, while the surface markers showed similar levels of expression as previous HFM differentiations.

GFP was much more highly expressed than anticipated. As the differentiation progressed, GFP expression decreased from around 80% of the total live cell population at day 6 to 55% at day 20 (Figure 5.5). In addition, the normal expression of the myogenic markers (CD56, CD106, and M-cadherin) was examined alone and with GFP to determine which populations expressed the highest levels of Pax7. Surprisingly, GFP was most highly expressed in CD106+ cells, with on average 86% +/- 5% of the cells (at all time points) positive for both markers. In contrast, only 54% +/- 10% of CD56+ cells also expressed GFP, with co-expression decreasing from 68% at day 6 to 44% at day 20. M-cadherin+ cells showed the lowest percent of GFP co-expression (30% +/- 19%), again with co-expression decreasing as differentiation time increased. The Pax7-GFP line was comparable to normal H9 cells when differentiated in HFM CM, although with a slightly higher level of CD106 and slightly lower levels of CD56 and M-cadherin expression.

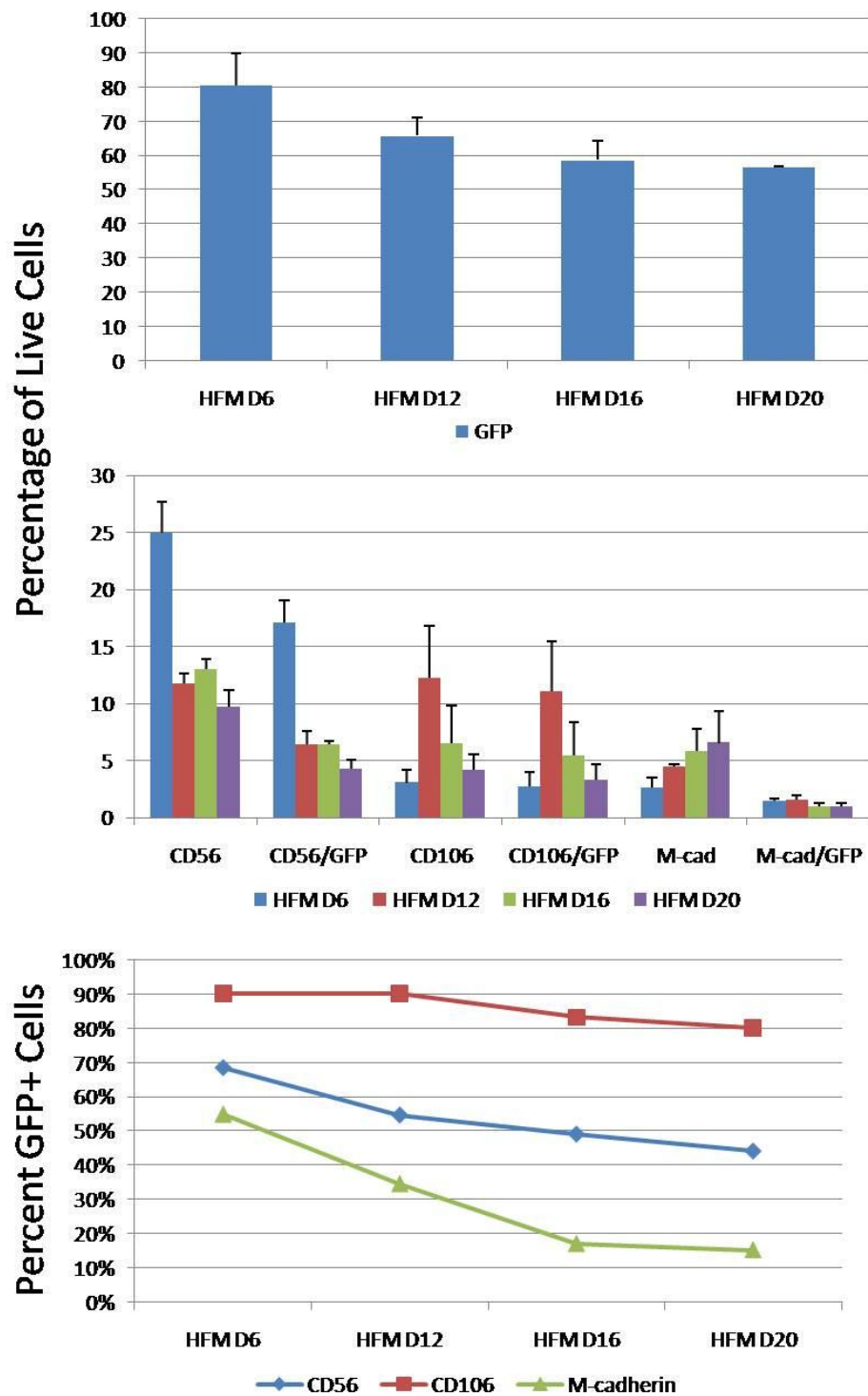


Figure 5.5: Expression Dynamics of Differentiated Pax7GFP Cells. For all four time points, the total GFP expression (top graph) and the expression of CD56, CD106, and M-cadherin as well as their co-expression with GFP (middle graph) are shown. The bottom graph illustrates the percent of GFP+ cells in each of the populations of CD56+, CD106+, and M-cadherin+ cells. The CD106 population has the highest percentage of GFP+ cells followed by the CD56 and M-cadherin populations. In all three populations, GFP expression decreases as the differentiation progressed to 20 days.

The co-expression of satellite cell markers with and without GFP expression was also recorded (Figure 5.6). The CD56/CD106 population had the highest percentage of GFP+ cells (65% +/- 17%) followed by the CD106/M-cad population (56% +/- 11%). As noted above, the relative expression of GFP in these populations tended to decrease as differentiation continued.

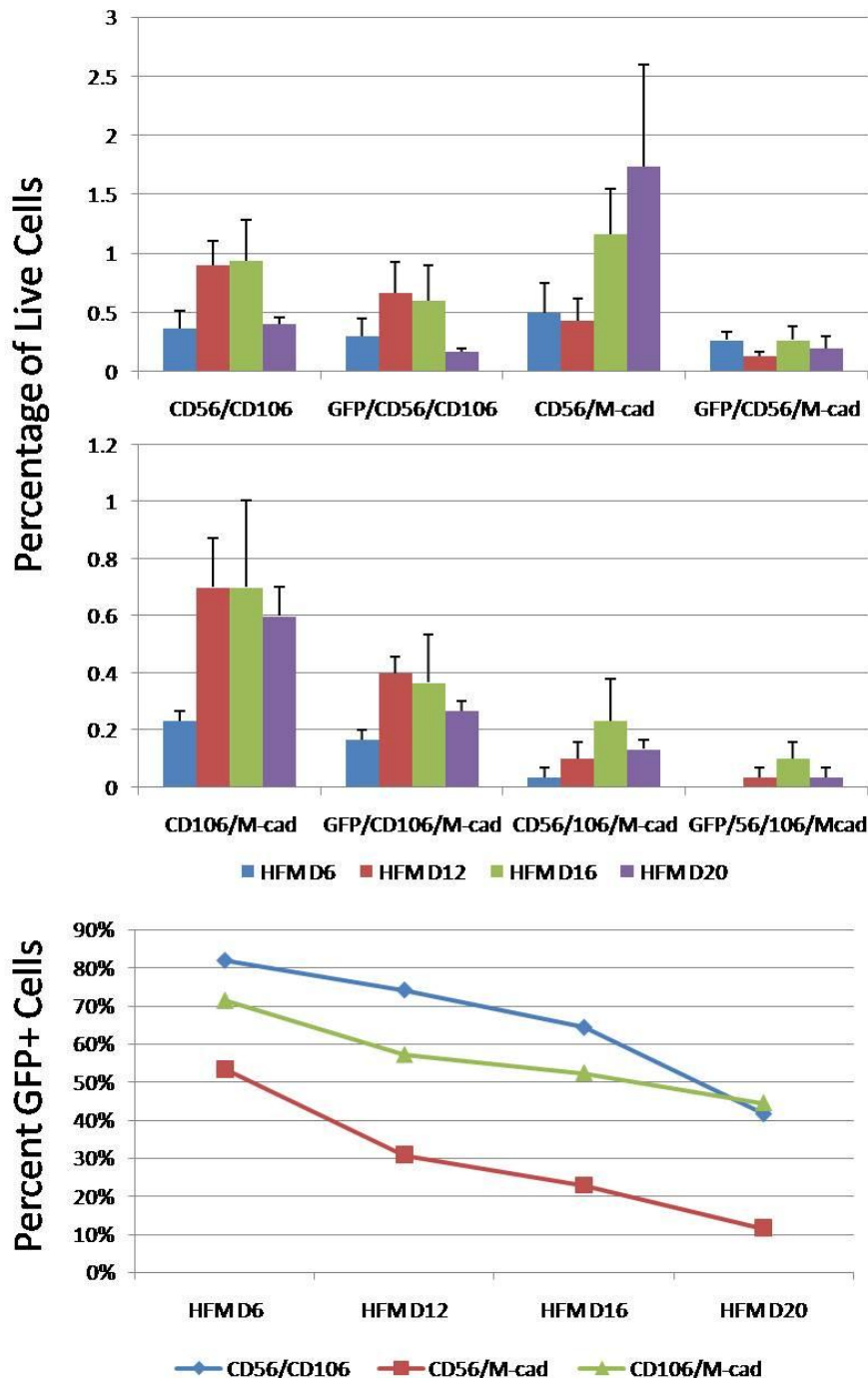


Figure 5.6: Analysis of Marker Co-expression in Differentiated Pax7GFP Cells. Comparison of different populations positive for multiple satellite cell markers and GFP (Top and Middle Graphs). Each of the four time points is shown for a given population and then compared to the same population also expressing GFP. The populations containing CD106 (CD56/CD106+ and CD106/M-cad+) tended to have the highest percentage of GFP+ cells (Bottom Graph). GFP expression also decreased in each of the populations as differentiation progressed.

In addition to flow cytometry analysis, differentiation of the H9 Pax7-GFP line was also analyzed by qPCR (**Figure 5.7**). Because it had previously been shown that using conditioned medium enhanced myogenic differentiation when compared to generic differentiation medium, in this experiment undifferentiated H9 cells were used as a control. qPCR analysis of differentiated cultures showed that *BRACHYURY* expression was highest at day 6, with only very low levels expressed at any other time point. *PAX3*, *MYF5*, and *MYOD* expression all peaked at day 12 and then began to drop steadily from days 16 to 20, with unexpectedly low levels of all three markers at day 20. These data strongly suggested that the number of myogenic cells was highest around day 12, thus it was the day used for sorting specific populations of potential satellite cells. However, this is somewhat different from previous qPCR results from HFM differentiations which showed that *MYOD* and *MYF5* expression was highest at day 16.

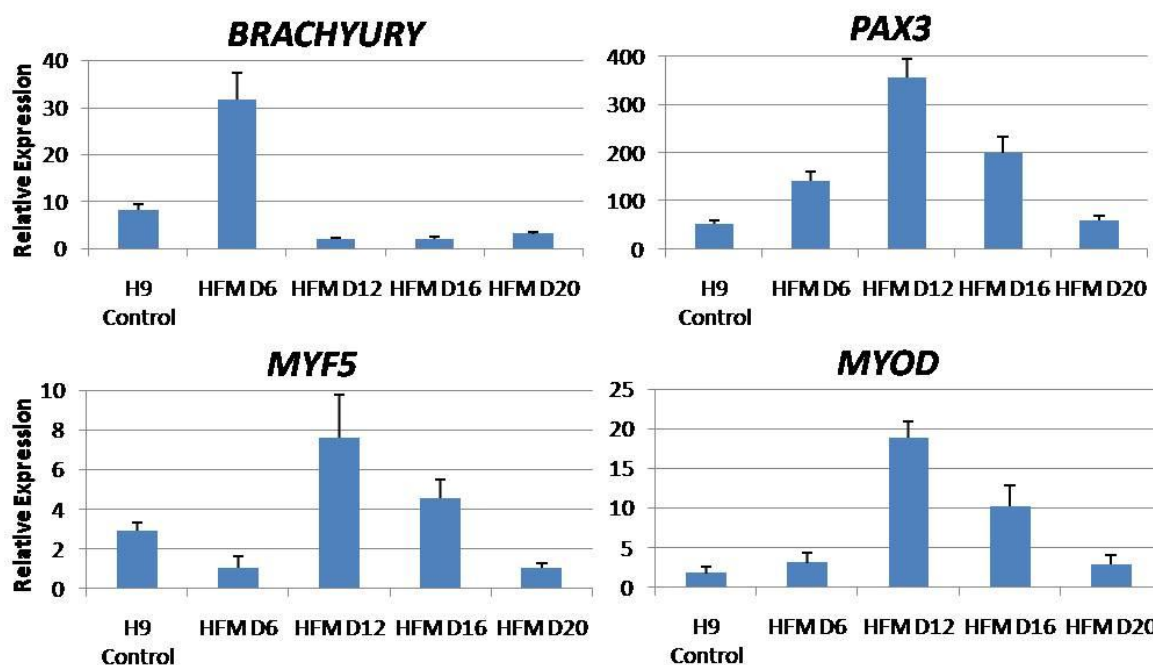


Figure 5.7: Pax7GFP Cell Differentiation Analysis by qPCR. qPCR analysis of the Pax7-GFP HFM differentiations show that the expression of *BRACHYURY* peaks at day 6 and is expressed only at very low levels at other time points and in the undifferentiated H9 control cells. In contrast, myogenic genes such as *PAX3*, *MYF5*, and *MYOD* are all most highly expressed after 12 days of differentiation and then begin to decrease until day 20.

5.2.4 FACS of Differentiated H9 Pax7-GFP Cells

Several of the populations were sorted to determine if the Pax7-GFP construct improved the isolation of myogenic cells. Cells which were negative for GFP and all surface markers were used as a control and a general population of GFP+ cells was also sorted, regardless of their surface marker expression. Finally, two potential myoblast populations, the CD56/GFP dual positive and CD56/M-

cad/GFP triple positive cells, were isolated. The numbers of cells sorted for each population are given in Table 3. The expression of four genes was examined by qPCR (**Figure 5.8**): *NESTIN*, indicating neurogenic cells, *PAX3* (expressed during both neurogenesis and myogenesis), *MYF5*, and *MYOD*. Unfortunately, the very small number of CD56/M-cad/GFP cells prevented a complete qPCR analysis and only *NESTIN* and *MYOD* were tested. Negative cells expressed relatively low levels of all four genes, with no detectable *MYF5* expression. GFP+ cells expressed the highest levels of *PAX3* and *MYF5*, but also *NESTIN*, suggesting that while it contained myogenic cells, it was a mixed population with a substantial amount of neuronal cells, which may also be contributing to the high expression of *PAX3*. *MYOD* was undetectable in this population. In contrast, the CD56/GFP cells expressed low levels of *NESTIN*, but moderate levels of *PAX3*, *MYF5*, and *MYOD* indicating a substantially enriched myogenic population. The highest expression of *MYOD* was seen in the CD56/M-cad/GFP population, which also had a very low level of *NESTIN*. However, because of the limited number of cells that could be obtained by FACS, this population seems unpromising as a source of potential satellite cells.

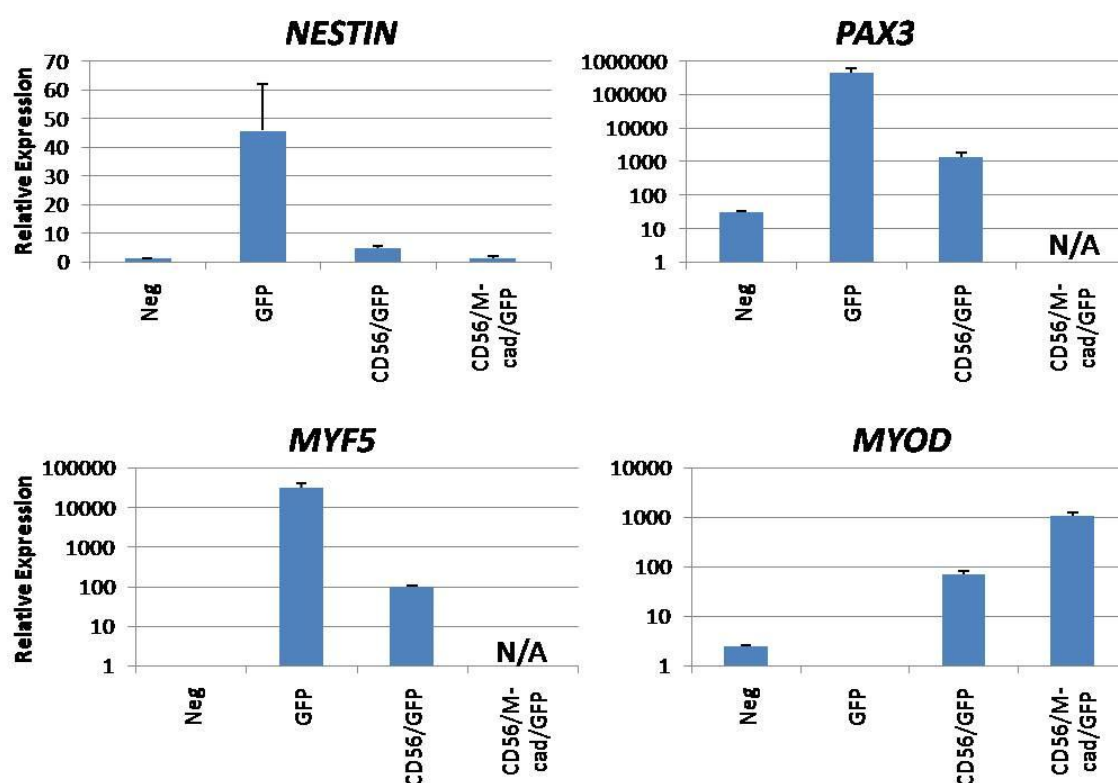


Figure 5.8: Pax7GFP Cell Differentiation Analysis of Sorted Populations by qPCR. qPCR analysis of sorted populations for *NESTIN*, *PAX3*, *MYF5*, and *MYOD* expression. *NESTIN* is most highly expressed in the GFP+ population, indicating that it has a significant percent of neurogenic cells. *PAX3* and *MYF5* expression are also highest in the GFP+ population, suggesting that it also contains myogenic cells, although no *MYOD* transcript was detectable. In contrast, the CD56/GFP+ population expresses low levels of *NESTIN* but moderate levels of *PAX3*, *MYF5*, and *MYOD*. The CD56/M-cad/GFP+ population did not contain enough cells to test for *PAX3* and *MYF5*, but it did express the highest level of *MYOD* in all four populations.

Two populations were sorted for Affymetrix microarray analysis: negatives cells as a control and the CD56/GFP positive cells. The results are presented as the extent of up- or down-regulation of various genes in the positive (CD56+/GFP+) population as compared to the negative (CD56-/GFP-) cells (**Figure 5.9**). Surprisingly, very few myogenic genes were found to be up-regulated in the CD56/GFP cells: *MYF5*, *FOXK1*, *MYOD*, *MYOGENIN*, *M-CADHERIN*, and *PAX7* all had comparable levels of expression between the two populations. Two genes expressed in myogenic cells were up-regulated in the CD56/GFP population: *CD56* and *PAX3*. However, both of these are also expressed during neurogenesis, as well as other genes found to be at least 10-fold up-regulated such as *PAX6*, *ENC1*, *LIX1*, *LGI1*, *CDH6*, *MAP2*, and *NOGGIN*. These genes were also found to be at least 5-fold up-regulated when the CD56+/GFP+ population was compared to microarray results from undifferentiated H9 cells (obtained from S. Yung, unpublished data). Most significantly, the fact that GFP+ cells did not show an increase in *PAX7* expression when compared to GFP- cells implied that there was a fundamental flaw in the H9 Pax7-GFP cell line.

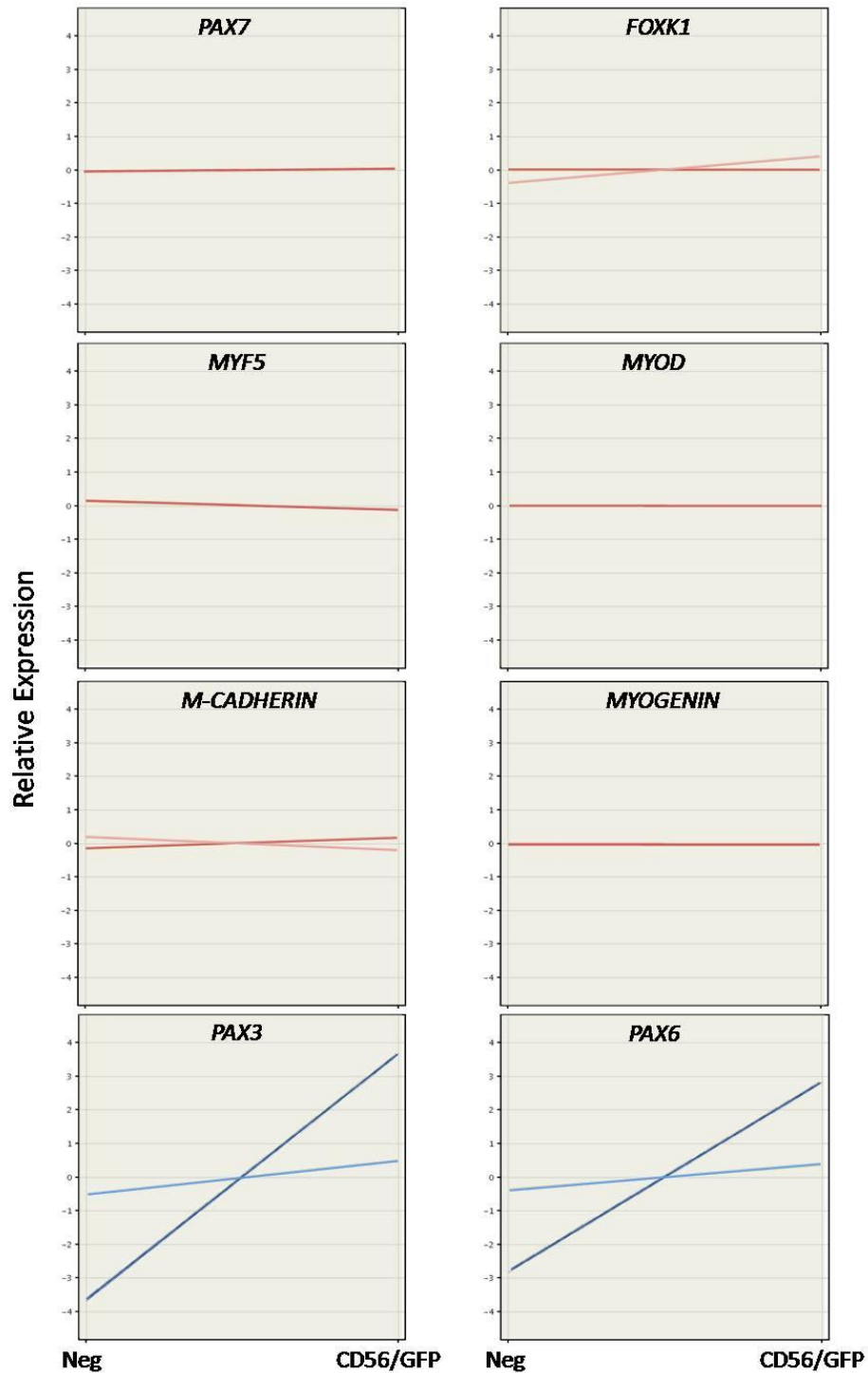


Figure 5.9: Microarray Analysis of Sorted Differentiated Pax7GFP Cells. Microarray results were chosen for selected genes expressed during myogenesis and neuroectoderm differentiation. A positive sloped line indicates that the gene is more highly expressed in the CD56/GFP+ population than the Negative population. Most genes marking myogenic differentiation (*MYF5*, *MYOD*, *MYOGENIN*) or satellite cells (*PAX7*, *FOXK1*, *M-CADHERIN*) were not more highly expressed in the CD56/GFP+ population than the Negative control cells (top three rows). *PAX3* did show an increase in expression, however, like *PAX6* and many of the other up-regulated genes, it is expressed during neuroectoderm formation (bottom row).

To address the inconsistency found between Pax7 expression and GFP expression, differentiated Pax7-GFP cells were sorted into three populations: GFP-negative cells, GFP-positive cells, and GFP-highly positive cells (**Figure 5.10**). The populations were then analyzed by qPCR for *PAX7* gene expression. Ironically, the GFP-negative population displayed the highest relative expression of *PAX7*. The GFP+ and GFP++ cells showed only 50-60% of the level of expression of GFP-negative cells. This further confirmed that the Pax7-GFP construct was not accurately representing *PAX7* gene activity.

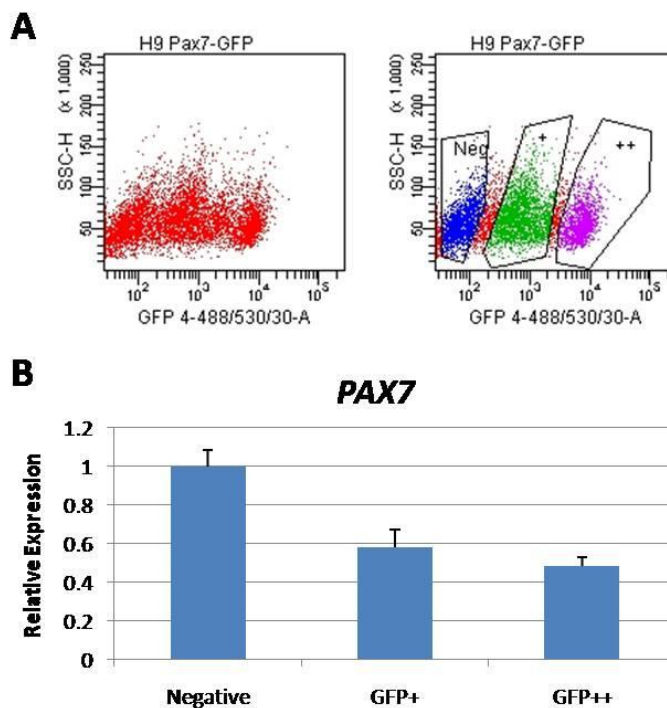


Figure 5.10: Evaluation of Pax7 Expression in Pax7GFP Cells. (A) FACS analysis of different populations of GFP negative and positive cells. Left Graph shows the range of GFP expression while the right graph shows the gates used to sort negative (Blue), moderately positive (Green), and brightly positive (Purple) cells. (B) qPCR analysis of *PAX7* in the sorted populations. GFP-negative cells showed the highest expression of *PAX7* while GFP+ and GFP++ cells expressed similarly low levels.

5.3 Discussion

In order to assess *PAX7* gene activity by flow cytometry of live cells, a genetic construct was created where GFP expression was driven by the *PAX7* promoter. This construct was then nucleofected into hES cells which, after selection, underwent the myogenic differentiation scheme described in Chapter 4. Differentiated cells were analyzed and sorted based on their expression of GFP, CD56, and M-cadherin. Unfortunately, it was ultimately found that the construct did not accurately reflect *PAX7* expression.

The first several attempts to generate the H9 Pax7-GFP line used an earlier protocol and were unsuccessful, largely due to the lack of colony survival after nucleofection. However, the first attempt at the new method generated colonies that were robust enough to survive continued selection under neomycin and a subsequent trial confirmed these results. The new protocol was more efficient both in terms of the number of cells which up-took the construct and in improved survivability and recovery of the cells after nucleofection and under selection. The procedure did not seem to have an adverse effect on the cells' ability to differentiate, as the Pax7-GFP line showed similar surface marker expression as normal H9s when subjected to the myogenic differentiation strategy.

GFP expression in myoblasts seemed to validate the construct, as the percentage of GFP+ cells was very close to what was predicted from Pax7 immunostaining. The first warning that GFP expression did not correlate to Pax7 expression was the high number of GFP+ cells observed during the initial flow cytometry analysis. While it seemed unlikely that Pax7 would be present in 80% of the cells at day 6 of the differentiation, it was not entirely improbable because Pax7 is expressed during neural development in addition to somitogenesis and myogenesis. It was also surprising that the CD106+ population expressed the highest percentage of GFP+ cells. CD106 also labels endothelial cells, smooth muscle cells, and certain types of stem cells, none of which should express Pax7. Thus the only subset of cells within the CD106+ population that should co-express Pax7 is satellite cells. In contrast, all M-cadherin+ cells ought to be myogenic, yet a much smaller proportion of this population co-expressed Pax7. Additionally, the populations of cells which co-expressed multiple markers would be expected to express higher levels of Pax7 because they are more likely to contain bona fide satellite cells. However, none of these expressed more GFP than the CD106+ population.

Despite the evidence suggesting the Pax7-GFP construct may not have been faithfully representing *PAX7* gene activity, it was crucial to examine isolated populations obtained by FACS. While CD106 showed a higher percentage of GFP+ cells, a sorted CD106+ population from BMP4 differentiated cells only expressed very low levels of myogenic transcripts (discussed in Chapter 4). Further, CD56 was found to be more highly expressed in foetal myoblasts (discussed in Chapter 3) and was thought to have a more reliable antibody for sorting. It is also expressed in both quiescent and activated satellite cells, unlike CD106 (Fukada, Uezumi et al. 2007). Thus the initial populations sorted included negative cells, GFP+ (CD56-/M-cad-) cells, CD56+/GFP+ cells, and CD56+/M-cad+/GFP+ cells. The qPCR analysis generated substantially different results from the microarray. When analyzed by qPCR, myogenic genes such as *PAX3*, *MYF5*, and *MYOD* were found to be more highly expressed in the CD56/GFP population than the negative population but of these, only *PAX3* was similarly upregulated in the microarray. The microarray results suggested that the CD56/GFP population was largely ectodermal and essentially devoid of any increase in myogenic gene expression when compared to negative or hES cells. This was partially supported by the presence of *NESTIN* transcript in the

CD56/GFP population analyzed by qPCR, but the difference in myogenic gene expression between the two methods of comparison remains irreconcilable. The neurogenic nature of the CD56/GFP population highlights the importance of including additional surface markers such as CD106 or M-cadherin when isolating potential satellite cells and, correspondingly, the need for more efficient methods of myogenic differentiation.

One significant restraint during the generation of the H9 Pax7-GFP cell line was the persistent inability to find *PAX7* primers that worked with the qPCR conditions used in these experiments. Working primers were only generated after the microarray had been performed, when it became clearer that GFP expression did not correspond to *PAX7* activity. With these, it was possible to conclusively show the non-specificity of the Pax7-GFP construct. Unfortunately, the nature of the construct's expression remained elusive. The primary problem when introducing constructs into hES cells by transfection is their eventual silencing, whereas the Pax7-GFP construct was overactive. However, it is difficult to attribute this activity to general "leakiness," primarily because the construct was not consistently expressed among different populations of differentiated cells (for instance, CD106+ cells were much more likely to express GFP than M-cadherin+ cells). It is also worth noting that the insertion was random and varied since the Pax7-GFP cell line was not generated by selecting clones but by continued antibiotic selection. Therefore anomalies in GFP expression should not be attributed to the construct insertion site. It is therefore tempting to speculate that the region of the *PAX7* promoter cloned into the vector acted as a functional promoter, but not in the same manner as the endogenous *PAX7* promoter and, by chance, was significantly more active in CD106+ cells than in the other populations examined. This could also explain the observation that GFP expression tended to decrease over time. One possible reason for the decreased expression could be that the construct was lost from dividing cells; however constant antibiotic selection during differentiation should have prevented this. Another possibility is that as cells differentiated they began to silence the promoter in the construct, with the notable exception of CD106+ cells, which continued to express high levels of GFP even after 20 days of differentiation.

Chapter 6: Myogenic Differentiation of iPS Cells and Generation of a DMD iPS Cell Line

6.1 Introduction

The induction of pluripotency in differentiated cells by the introduction of a small set of genes expressed in ES cells was first achieved by Takahashi and Yamanaka in 2006. They initially tested 24 factors believed to be important in maintaining pluripotency by transducing them into MEFs containing a neomycin resistance gene knocked into one of the exons of the mES cell-specific gene *Fbx15*. Any cells that began to reprogram (and express *Fbx15*) would become resistant to neomycin. Individually, none of the factors were enough to generate resistant clones, however when all 24 factors were transduced neomycin-resistant colonies appeared, some of which exhibited mES cell-like morphology and expressed ES cell markers. After testing which of the 24 factors could be excluded without affecting neomycin-resistant colony formation, four factors were found to be sufficient for the generation of induced pluripotent stem (iPS) cells: *Oct4*, *Sox2*, *c-Myc*, and *Klf4*. The cells were found to be capable of producing teratomas containing cells from all three germ layers when injected into immunocompromised mice and could generate chimeric embryos after being introduced to blastocysts by microinjection, demonstrating their pluripotency (Takahashi and Yamanaka 2006).

The same four factors were later proven to be capable of generating iPS cells from adult human dermal fibroblasts by retroviral transduction. The iPS cells were tested by immunocytochemistry and found to express hES cell surface markers (SSEA3/4, TRA-1-60/81) and NANOG. Western blot and qPCR analysis showed they expressed *OCT4*, *SOX2*, *NANOG*, *REX1*, *TERT*, *KLF4*, and *MYC* among other ES cell markers. The iPS cells were also capable of differentiating into cells from all three germ layers *in vitro* and in teratomas (Takahashi, Tanabe et al. 2007). Similar results were obtained when human foetal and foreskin fibroblasts were transduced using lentiviral vectors with *OCT4*, *LIN28*, *NANOG*, and *SOX2* (Yu, Vodyanik et al. 2007), demonstrating a degree of flexibility in the viral vector, genes, and cell types transduced. Due to the high therapeutic relevance of iPS cell generation, a great deal of effort was spent exploring clinically acceptable methods of reprogramming. One of the main concerns was the stable integration of viral constructs containing oncogenes such as *Myc*. Indeed, in a study comparing tumorigenesis in chimeric mice containing iPS cells generated with and without *Myc*, those with *Myc* had a much higher incidence of tumour-associated death (Nakagawa, Koyanagi et al. 2008). Since the initial efforts to generate and characterize iPS cells with integrating retro- and

lentivirus vectors, other studies have also achieved reprogramming using inducible lentivirus vectors (Stadtfield, Maherali et al. 2008), non-integrating adenovirus vectors (Stadtfield, Nagaya et al. 2008), transient transfection (Okita, Nakagawa et al. 2008), non-integrating episomal vectors (Yu, Hu et al. 2009), transposon-based systems (Yusa, Rad et al. 2009), and ectopic recombinant protein treatment (Zhou, Wu et al. 2009) among others.

Perhaps the most promising and advantageous feature of iPS cell technology is the ability to generate what are, in effect, patient-specific ES cell lines. In the relatively short time since the first iPS cells were generated by Takahashi and Yamanaka, a number of studies have sought to capitalize on the possible therapeutic uses of iPS cells. In 2007, Hanna et al. generated several iPS lines from mice and showed that the reprogrammed cells were as capable of haematopoietic differentiation as mES cells and could achieve haematopoietic reconstitution of irradiated mice. They then repeated this work using cells from a mouse model of sickle cell anemia. Once iPS cells had been generated, they corrected the sickle cell mutation using a gene-targeting construct containing the wild-type allele and were able to treat the sickle cell defect in affected mice (Hanna, Wernig et al. 2007). Wernig et al. showed that iPS cells were capable of neuronal differentiation and, more specifically, could form dopamine neurons under the same conditions used to differentiate mES cells. Neural precursors derived from iPS cells were transplanted into developing mouse embryos and could migrate extensively and differentiate into functional neurons *in vivo*. More significantly, improvements were seen in a rat model of Parkinson's disease when iPS-derived dopamine neurons were injected into the midbrain (Wernig, Zhao et al. 2008).

While these studies are promising, there was some question as to whether iPS cells could be efficiently generated from elderly human patients with various diseases. Dimos et al. showed that dermal fibroblasts from a skin biopsy of an 82 year old patient with amyotrophic lateral sclerosis (ALS) could be reprogrammed using retroviral transduction of *OCT4*, *SOX2*, *KLF4*, and *MYC*. They went on to show that these cells could differentiate into motor neurons and glia, two cell types affected by and important to the progression of ALS (Dimos, Rodolfa et al. 2008). In addition to the direct therapeutic relevance of iPS cell generation, the possibility of modeling the pathology of certain diseases *in vitro* also exists. Ebert et al. were able to obtain iPS cells from a young patient with spinal muscular atrophy (SMA), a disease which leads to the degeneration of certain motor neurons. While animal models of SMA exist, they lack one of the genes thought to be important in disease progression. Using the iPS cells generated from an SMA patient, this study showed that they could be differentiated to motor neurons that were phenotypically different than wild-type cells and responded to drugs designed to treat SMA (Ebert, Yu et al. 2009). Further along these lines, Park et al. developed iPS cells from a number of patients with various diseases including adenosine deaminase deficiency-related severe combined immunodeficiency (ADA-SCID), Shwachman-Bodian-

Diamond syndrome, Gaucher disease type III, Duchenne and Becker muscular dystrophy, Parkinson's disease, Huntington's disease, juvenile-onset type 1 diabetes mellitus, Down syndrome, and a carrier of Lesch-Nyhan syndrome (Park, Arora et al. 2008).

The next step in the progression towards therapeutically relevant iPS cells is to generate cells from a patient with a genetic defect and then correct the mutation. Fanconi anemia (FA) is the most common of the inherited bone marrow failures and is characterized by a decline in haematopoietic stem cells and limited production of peripheral blood cells. Fibroblasts from FA patients were obtained and their mutation was corrected. The cells were then used to generate iPS cells that were capable of normal haematopoietic differentiation and appeared to be disease free when compared to differentiated wild-type iPS or hES cells and healthy mononuclear bone marrow cells (Raya, Rodriguez-Piza et al. 2009). Very recently, a similar approach was taken to generate corrected iPS cells from a DMD patient. The genetic defect (a deletion of exons 4-43 of the *DYSTROPHIN* gene) was corrected by transferring a human artificial chromosome (HAC) containing the full length *DYSTROPHIN* gene into the fibroblasts using microcell-mediated chromosome transfer. The fibroblasts were then reprogrammed and injected into SCID mice to test for teratoma formation. Muscle tissue expressing human dystrophin was detected in the teratomas, demonstrating that the HAC was capable of restoring dystrophin expression and that the iPS cells were capable of myogenic differentiation (Kazuki, Hiratsuka et al. 2010).

While this work proves that mutated genes in cells from patients with DMD can be corrected prior to iPS generation, much more work remains to be done. DMD iPS cells need to be subjected to myogenic differentiation (as opposed to incidental muscle tissue formation from teratomas) and studied both *in vitro* and in transplantation models *in vivo*. Their behavior should also be compared to non-disease iPS cells and hES cells.

Chapter 6 Aims:

To test the strategy for myogenic differentiation developed in Chapter 4 using previously generated iPS cells and compare them with differentiated hES cells

To generate a line of iPS cells using fibroblasts obtained from a patient with Duchenne muscular dystrophy

6.2 Results

6.2.1 Myogenic Differentiation of iPS Cells

In order to test the ability of the previously established iPS cell line (iPS clone IV, **Figure 6.1**) to undergo myogenic differentiation, iPS cells were differentiated in HFM Diff:CM for 12, 16, and 20 days and compared to H9 cells differentiated under the same conditions described in Chapter 4.



Figure 6.1: iPS Clone IV Cells. A colony of iPS Clone IV cells on MEF feeders at (A) 10x, (B) 20x, and (C) 40x magnification showing hES cell-like morphology and colony structure.

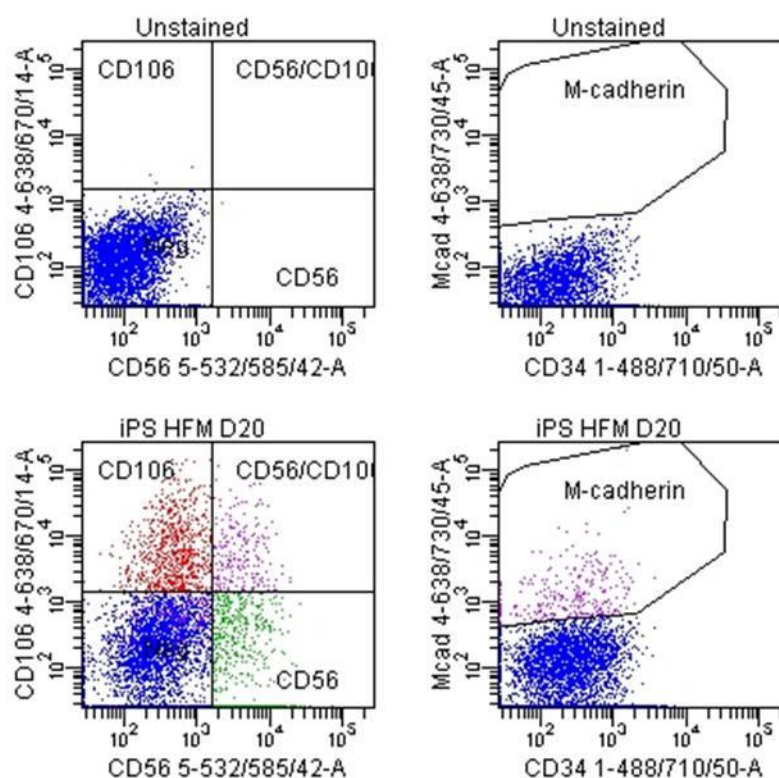


Figure 6.2: Myogenic iPS Differentiation Analysis by Flow Cytometry. Flow cytometry analysis of iPS clone IV cells differentiated in Diff:CM. Data for day 20 of the differentiation is representative of all time points. (Top Row) Unstained cells were used as a control for autofluorescence. (Bottom Row) Cells were stained for CD56 and CD106 (Left Plot) as well as M-cadherin (Right Plot). CD106 expression was surprisingly high, while expression M-cadherin was significantly lower than hES cell differentiations.

The cells were then analyzed by flow cytometry for the expression of CD56, CD106, and M-cadherin (**Figure 6.2**). Three trials were conducted for the 12 day time point, however, only one trial was conducted for days 16 and 20. Differentiated iPS cells showed substantially higher levels of CD106 expression than hES cells (38.2 +/- 7.5% compared to 4.8 +/- 2.1%, $p = 0.02$) as well as higher CD56/CD106 co-expression (20.1 +/- 6.3% compared to 2.5 +/- 0.6%, $p = 0.04$) when differentiated under the same conditions for 12 days (**Figure 6.3**). The expression of CD56 was approximately 2 to 3 times greater in the iPS cells and a nearly 4-fold increase in CD106+ cells was seen. However, M-cadherin expression in the iPS cells was only half the level or less than that seen in differentiated hES cell cultures. Most of the populations of cells co-expressing multiple markers (excluding CD56/CD106+ cells) were comparable between the two cell types.

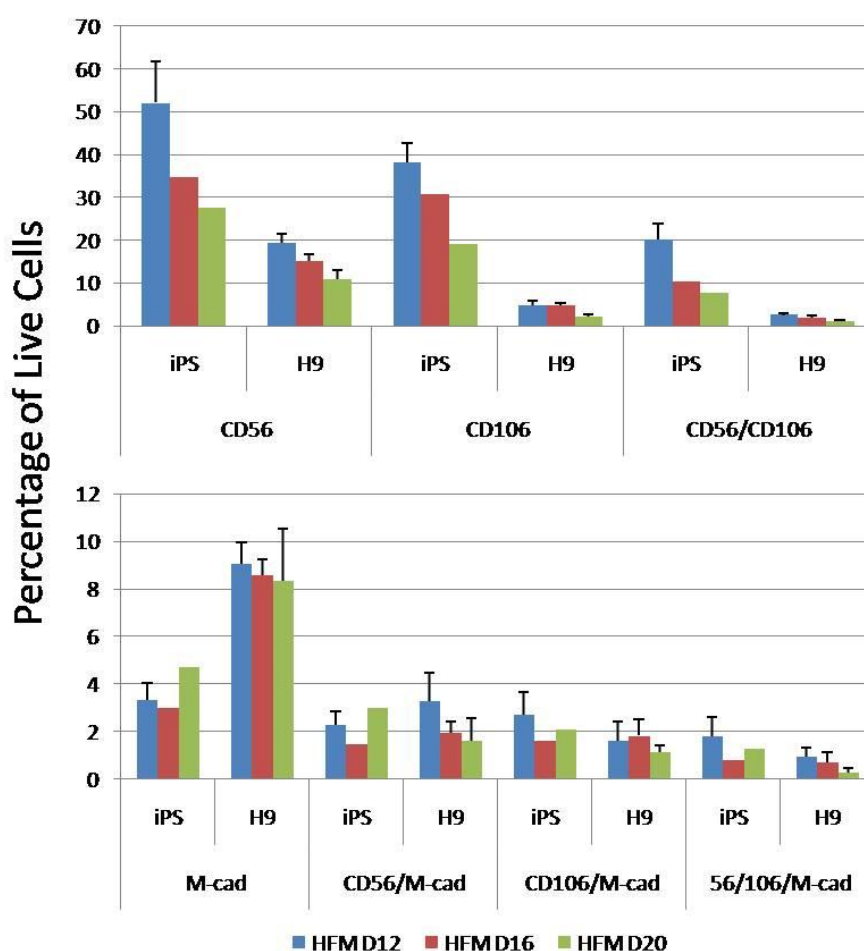


Figure 6.3: Comparison of Flow Cytometry Data after Myogenic Differentiation of iPS and H9 Cells. The iPS cells showed significantly higher levels of CD56 and CD106 as well as the CD56/CD106 dual positive population (Top Graph). However, they expressed significantly lower levels of M-cadherin (Bottom Graph). Other dual and triple positive populations were comparable between the two cell types. Only one trial was conducted for iPS D16 and D20. All other time points were performed in triplicate.

The expression of several myogenic genes in differentiated iPS cells was analyzed by qPCR at each time point and compared to differentiated H9 cells (**Figure 6.4**). At each time point, *PAX3* expression was higher in the iPS cultures than in the hES cultures, while *PAX7* expression was similar between the two. In contrast, *MEF2* expression was generally higher in the hES cultures than in the iPS differentiations. Only low levels of *MYF5* were expressed in any of the iPS time points, with no transcript being detectable at day 16. While this might suggest that the cells were predominantly non-myogenic, the differentiated iPS cultures expressed comparable levels of *MYOD* to the hES cultures.

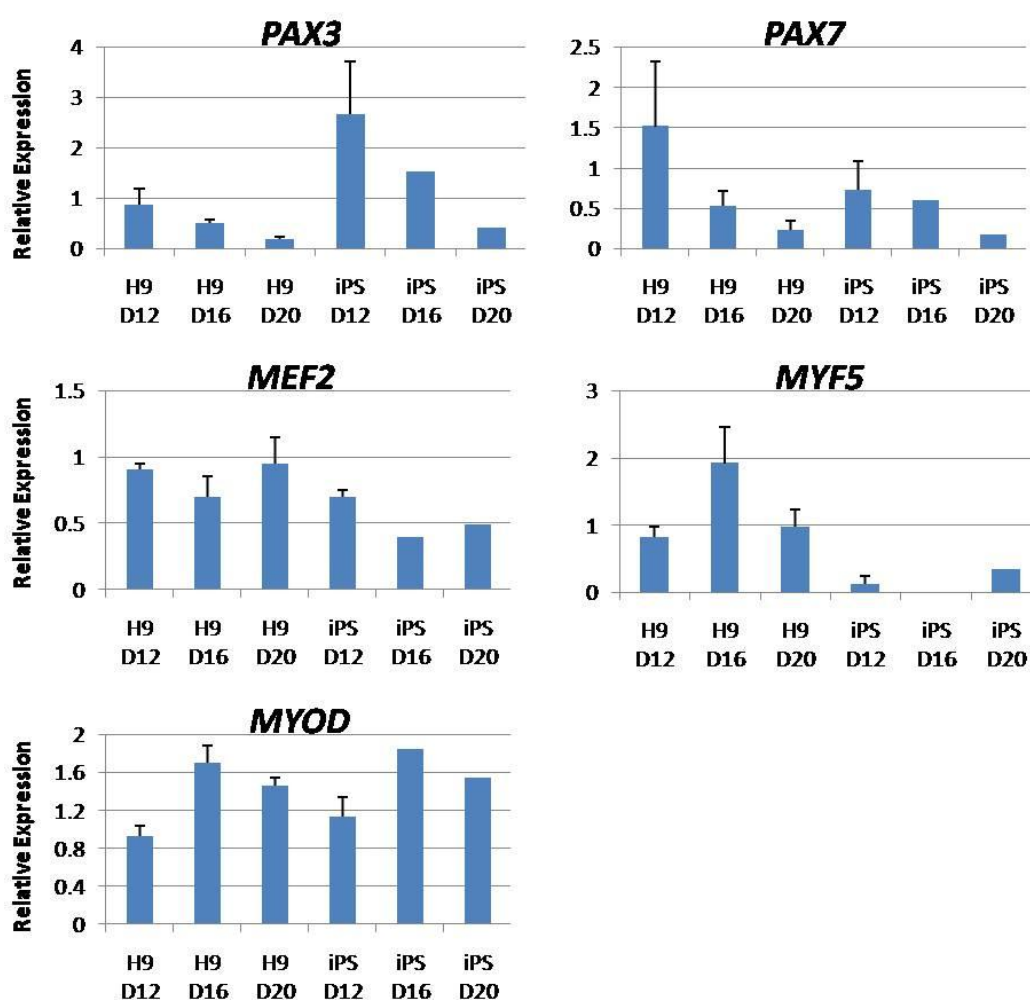


Figure 6.4: iPS Cell Myogenic Differentiation Analysis by qPCR. The qPCR analysis of differentiated iPS cells was compared to differentiated H9s. *PAX3* was more highly expressed in the iPS cultures, while *PAX7* did not show a significant difference in expression. The iPS cultures expressed slightly lower *MEF2* but very low levels of *MYF5* (with none detectable at day 16). Considering the large difference in *MYF5* expression, it was somewhat surprising that *MYOD* expression was similar between the two cell types.

6.2.2 Generation of a DMD iPS Cell Line

Fibroblast cells were obtained from two male patients, aged 5 (F055) and 8 years (F029), with Duchenne muscular dystrophy. The cells were expanded and, as early as possible, subjected to viral transduction to initiate reprogramming. Early attempts used a single pLenti expression plasmid containing *OCT4*, *SOX2*, *KLF4*, and *MYC*. The expression plasmid was transfected into HEK 293FT cells for virus production, the viral supernatant was collected and applied to cultures of the DMD fibroblasts. The transduced cells were then plated at low density (approximately 8,000 cells per well of a 6-well plate) onto MEFs to allow for colony formation. Unfortunately, this protocol did not result in complete reprogramming (**Figure 6.5**).

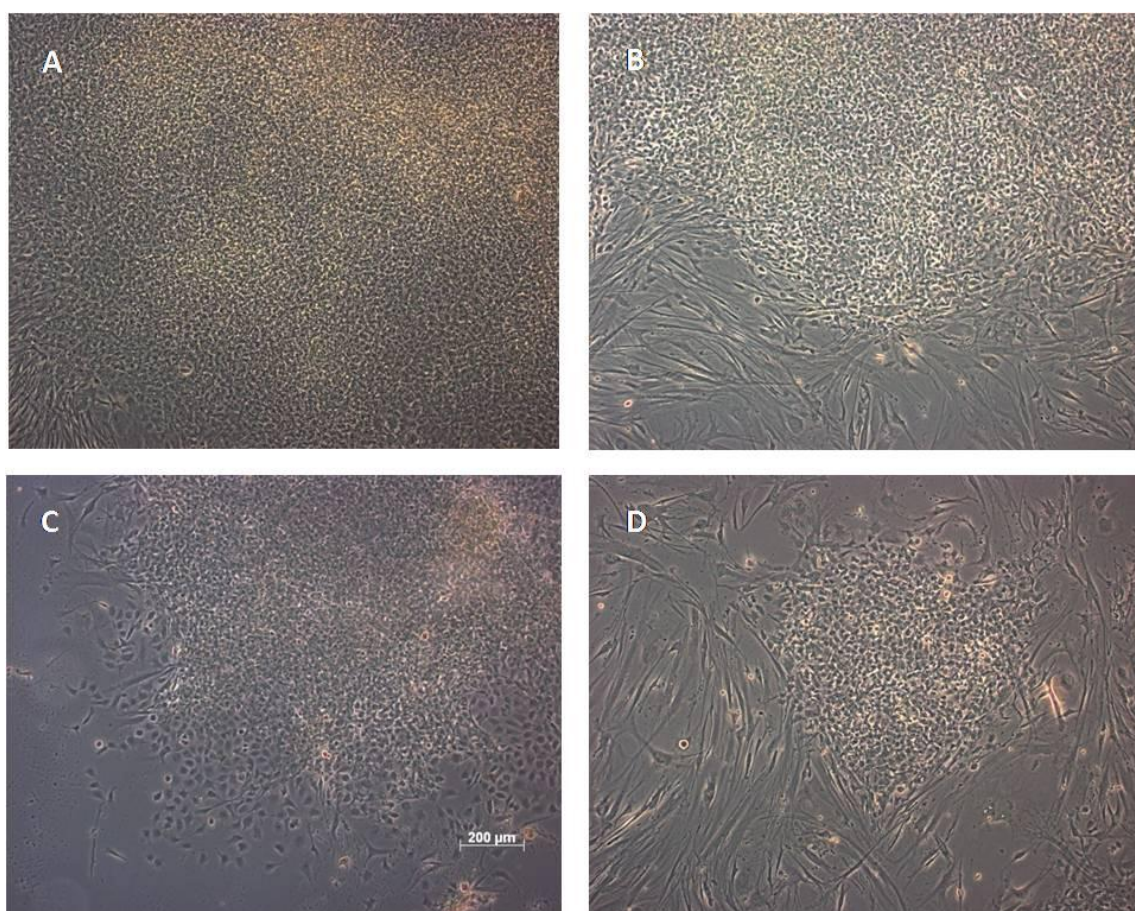


Figure 6.5: OSKM Construct Failed to Reprogramme DMD Fibroblasts. Only incomplete reprogramming of F055 fibroblast cells was observed after transduction with the OSKM construct. Cells in large colonies with a very distinct morphology could be observed after 16 days (A) and 19 days (B) on MEF feeders. After removing MEFs surrounding colonies, a new type of proliferating cells could be seen 21 days plating (C). Even as late as 25 days post plating, small colonies of partially reprogrammed cells could be found. However, no hES cell-like colonies were observed. All pictures were taken at 5x magnification. A 200 μm scale bar can be seen in (C).

Subsequent attempts used the Stemgent Reprogramming Lentivirus Set containing human *OCT4*, *LIN28*, *NANOG*, and *SOX2*. Twenty-four hours after viral transduction, cells were replated and cultured on MEF feeder cells for several weeks during which time some of the cells underwent morphological changes and began to form colonies (**Figure 6.6**). Eventually a small, hES cell-like colony appeared among the transduced F055 cells. The colony was passaged onto fresh feeders (**Figure 6.7**) and expanded to test for the expression of pluripotency genes and differentiation potential.

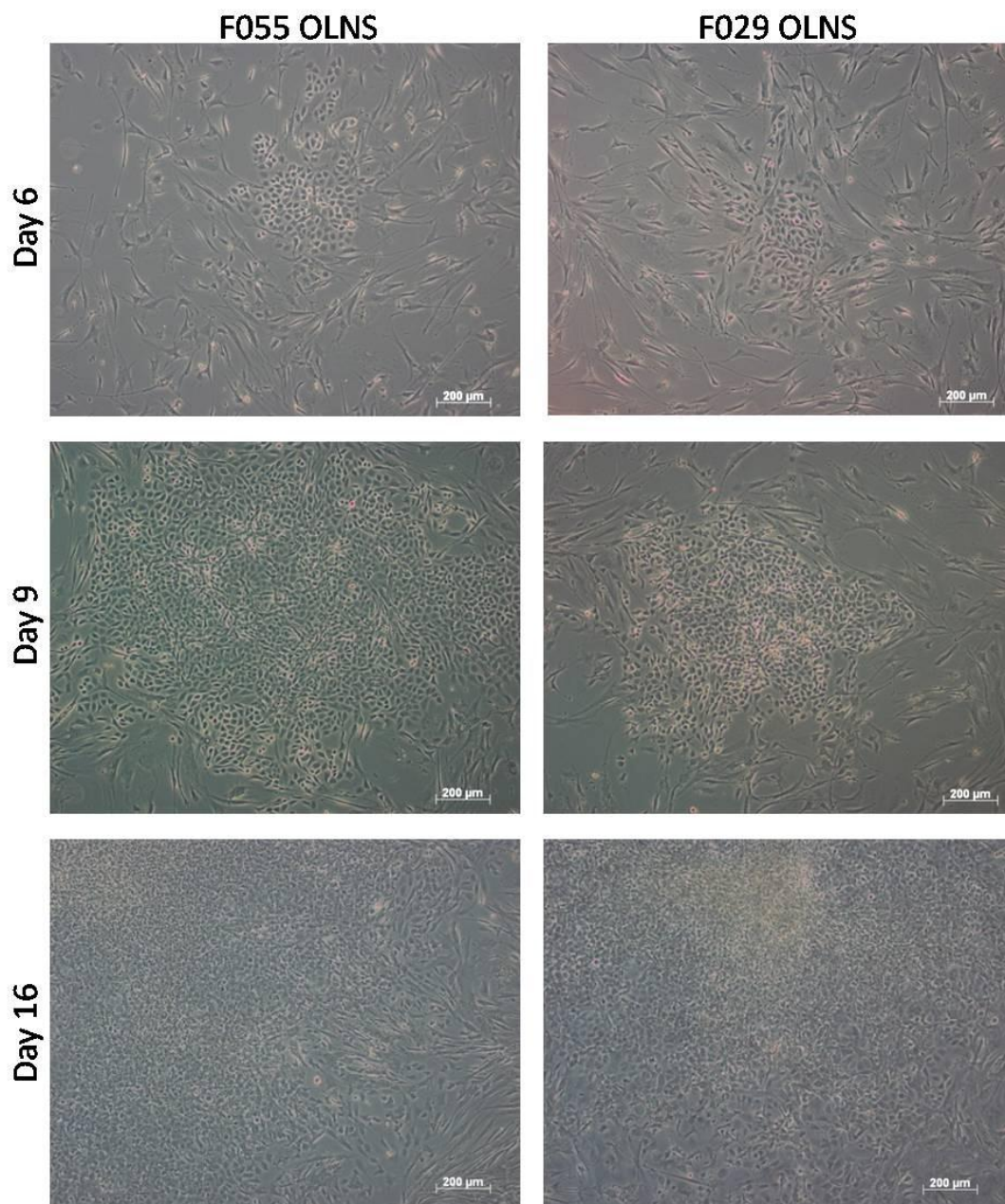


Figure 6.6: Reprogramming DMD Fibroblasts after Transduction with *OCT4*, *LIN28*, *NANOG*, and *SOX2*. Images were taken 6, 9, and 16 days after plating on MEF feeders. The left column shows transduced F055 fibroblasts while the right column shows F029 fibroblasts. Early colonies can be seen by day 6 (top row) and continue to expand through day 16 (bottom rule). Morphological changes, predominantly a decrease in cell size, can be seen as the colonies expand. Pictures were taken at 5x magnification.

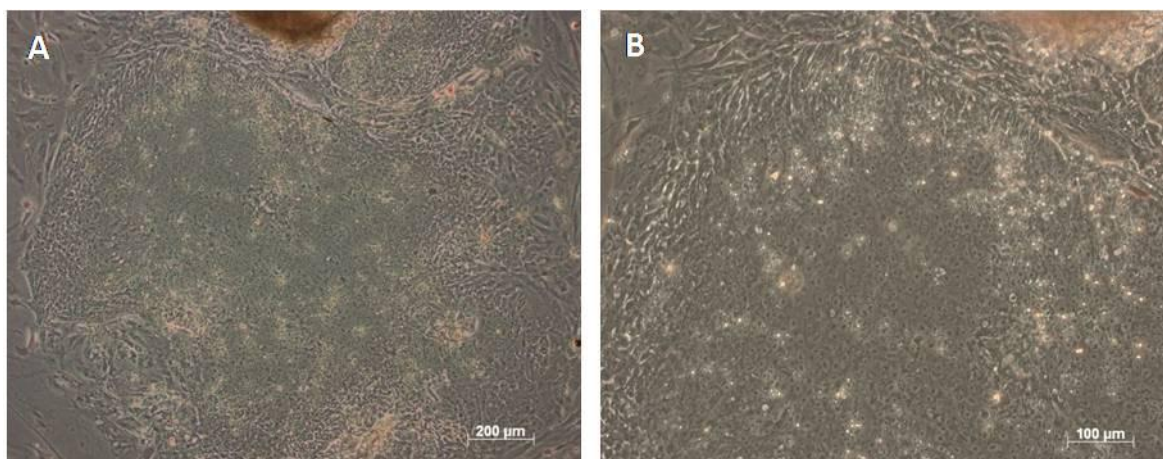


Figure 6.7: F055 iPS Cell Colony. An early colony of fully reprogrammed cells from transduced F055 fibroblasts showing hES cell morphology at 5x (A) and 10x (B) magnification. Round cells can be seen with a large, central nucleolus and a small cytoplasm surrounded by differentiated cells and MEF feeders.

Undifferentiated colonies were stained for the expression of OCT4, NANOG, SSEA4, TRA-1-60, TRA-1-81, and alkaline phosphatase (**Figure 6.8**). The cells were positive for all of the pluripotency markers tested, while feeder cells and differentiated cells were negative.

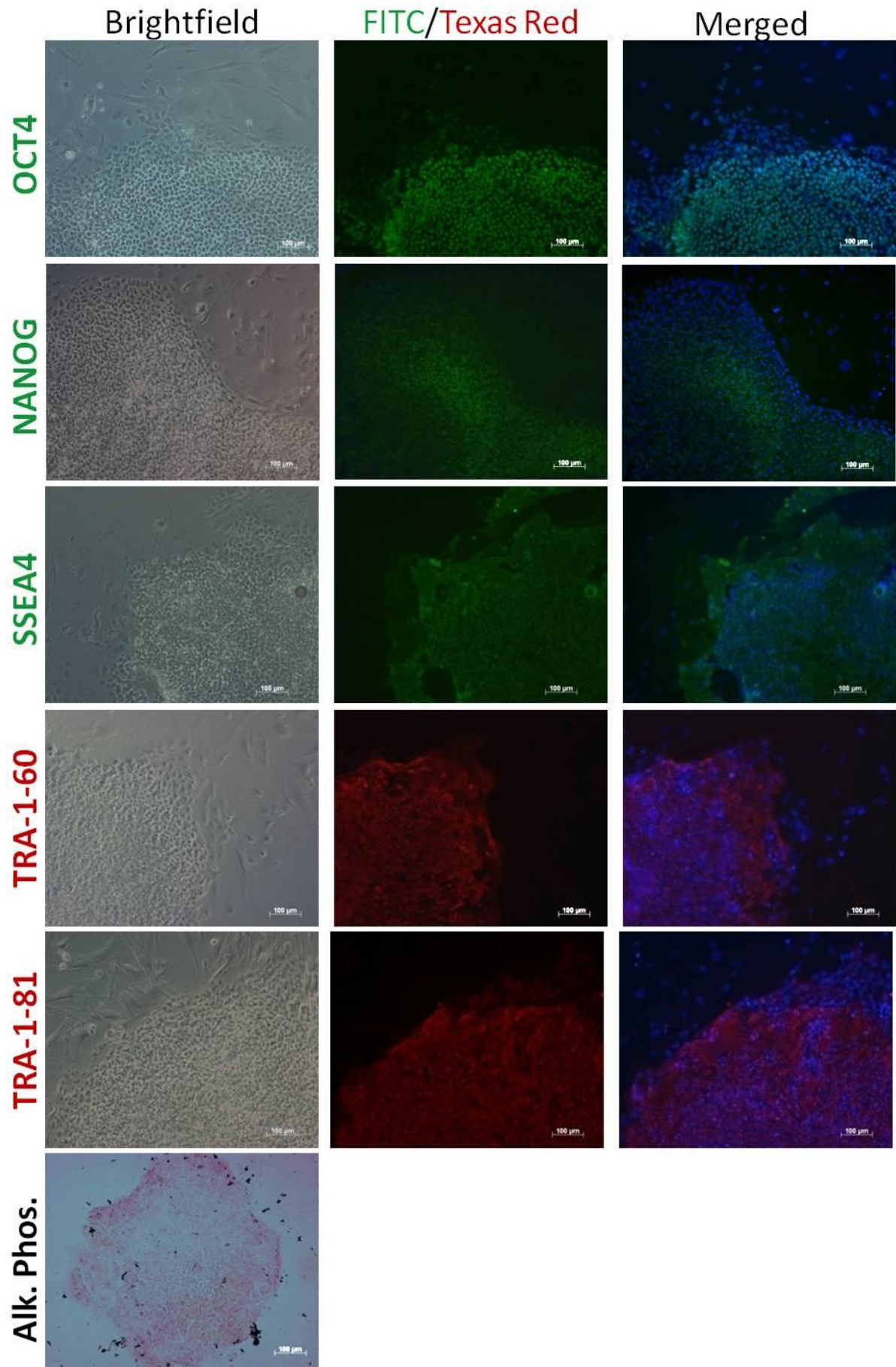


Figure 6.8: Immunostaining of F055 iPS Cells. Colonies of F055 iPS cells were stained for markers of pluripotency. The left column shows brightfield images of the colonies, the middle column shows the cells stained for each protein, and the right column shows the merged image of the marker and DAPI. The colonies showed strong expression of the pluripotency genes OCT4 and NANOG as well as the surface markers SSEA4, TRA-1-60, and TRA-1-81. Cells also stained positive for alkaline phosphatase activity (bottom row).

To further establish their pluripotency, F055 iPS cells from three time points during their expansion were analyzed by qPCR and compared to H9 cells (as a positive control) and FHM cells (as a negative control) for *NANOG*, *OCT4*, *LIN28*, *SOX2*, *TERT*, *MYC*, *GDF3*, *KLF4*, and *REX1* (**Figure 6.9**). With the exception of *REX1*, the F055 iPS cells expressed either similar or higher levels (*OCT4*, *NANOG*, and *KLF4*) than the H9 cells.

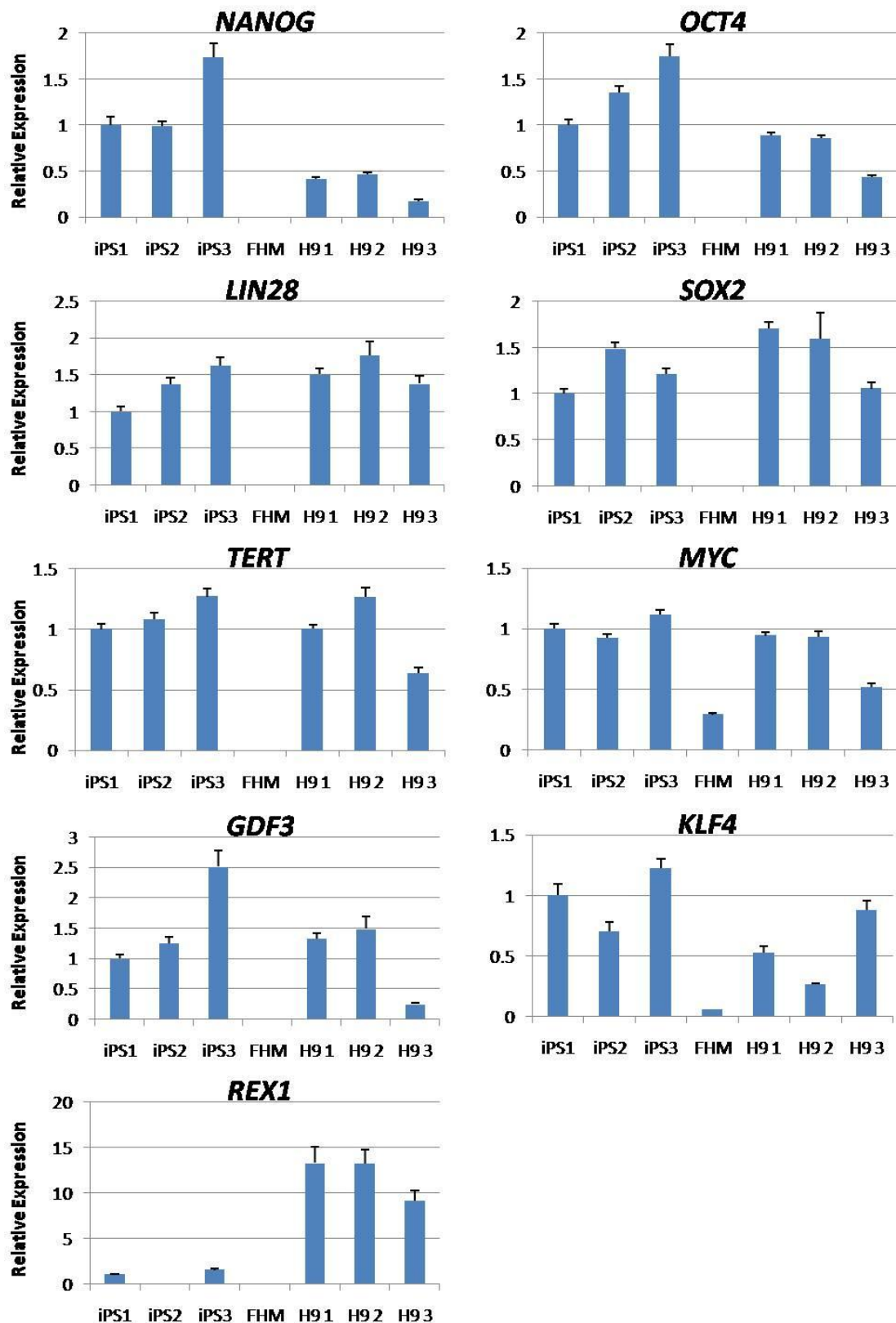


Figure 6.9: Analysis of F055 iPS Cell Pluripotency by qPCR. The expression of pluripotency-related genes was analyzed by qPCR and compared between three different samples of F055 iPS cells and H9s. FHM cells were used as a negative control. *NANOG*, *OCT4*, *KLF4*, and *GDF3* transcripts were all more highly expressed in the iPS cells than the H9s. Similar levels of *LIN28*, *SOX2*, *TERT*, and *MYC* were seen in both cell types. However, *REX1* was much more highly expressed in H9s than the iPS line.

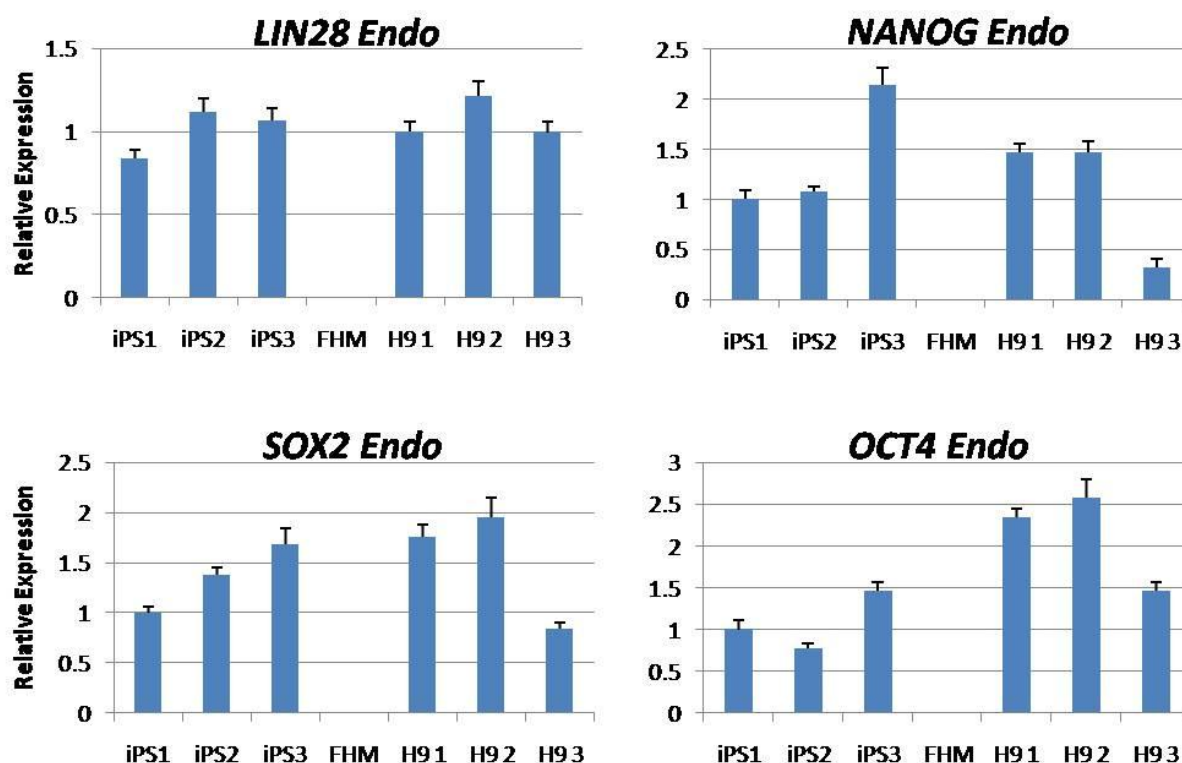


Figure 6.10: Endogenous Transcript Analysis of F055 iPS Cells by qPCR. In order to distinguish between total mRNA expression and endogenous expression, primers were designed to amplify only endogenous transcript for *LIN28*, *NANOG*, *SOX2*, and *OCT4*. Expression levels of *LIN28*, *NANOG*, and *SOX2* were comparable between the F055 iPS line and H9 cells, however *OCT4* levels were lower in the iPS cells. Endogenous expression of each gene was also found to be higher in the iPS3 sample (the latest sample tested) than in earlier iPS samples.

In order to control for exogenous expression from the viral transgenes, cells were also analyzed for *OCT4* Endo, *LIN28* Endo, *NANOG* Endo, and *SOX2* Endo using additional primers designed to only amplify endogenous transcripts (**Figure 6.10**). F055 iPS cells expressed similar levels of endogenous *LIN28*, *NANOG*, and *SOX2* and only slightly lower levels of endogenous *OCT4* than the H9 controls. Consistent with previous experience, as the cells were expanded over time (from iPS1 to iPS3), levels of the endogenous genes generally increased. Because of intellectual property concerns, primers specific to the exogenous genes could not be obtained. A comparison of pluripotency marker expression between the F055 iPS line and H9 cells can be found in **Table 6**.

Table 6: Pluripotency Marker Expression in F055 iPS and H9 Cells

Marker	F055 iPS Cells	H9 Cells
Immunostaining		
OCT4	+++	NT*
NANOG	++	NT
SSEA4	+++	NT
TRA-1-60	+++	NT
TRA-1-81	+++	NT
ALK. PHOS.	++	NT
qPCR		
OCT4 (Endo)	+++ (++)	++ (+++)
NANOG (Endo)	+++ (+++)	+ (+++)
SOX2 (Endo)	+++ (+++)	+++ (+++)
LIN28 (Endo)	+++ (+++)	+++ (+++)
TERT	+++	+++
MYC	+++	+++
GDF3	+++	+++
KLF4	+++	++
REX1	+	+++

*NT: not tested

6.2.3 Differentiation Potential of F055 iPS Cells

After having demonstrated the expression of key pluripotency markers, it was necessary to establish the ability of the F055 iPS cell line to differentiate down all three germ layers. To do this, cells were differentiated in Diff Medium (described in Chapter 2) containing 20% FBS for 7-14 days and stained for α -fetoprotein (AFP, endoderm), β 3-tubulin (ectoderm), and Nkx-2.5 (mesoderm, **Figure 6.11**). In differentiated cultures, cells staining for each of the markers could be found, demonstrating the ability of the F055 iPS cell line to differentiate down all three germ layers.

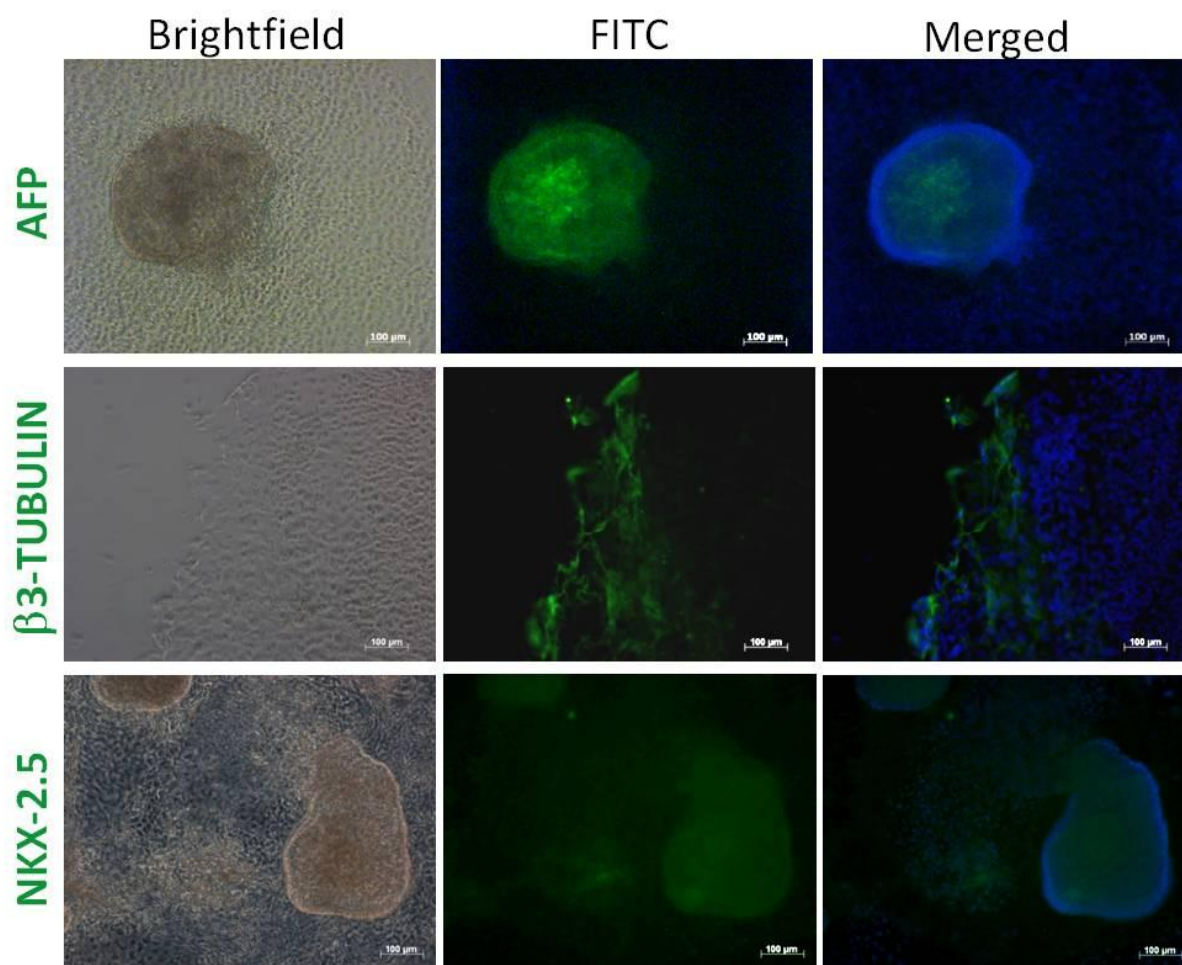


Figure 6.11: Immunostaining of Differentiated F055 iPS Cells. F055 iPS cells were differentiated and stained for markers of each germ layer to test for pluripotency. Cells were positive for AFP (top row, endoderm), β 3-TUBULIN (middle row, ectoderm), and weakly positive for NKX-2.5 (bottom row, mesoderm). Brightfield images of the differentiated cells are shown at 10x magnification (left column). The three proteins were stained green (middle column) while nuclei were stained with DAPI (merged, right column).

To further establish the cells ability to differentiate, lineage-specific genes were analyzed by qPCR (**Figure 6.12**). Differentiated cultures were tested for *NESTIN* and *PAX6* (predominantly ectoderm), *AFP* (endoderm), and *BRACHYURY* and *MIXL1* (mesendoderm/mesoderm). As a comparison, gene expression in undifferentiated F055 iPS cells and undifferentiated H9 cells was also examined. *NESTIN* and *PAX6* were slightly more highly expressed in the differentiated cells than the undifferentiated iPS cells. However, undifferentiated H9 cells expressed higher levels of these genes than the differentiated culture, suggesting that in the H9 cultures some unintended differentiation had occurred. In contrast, *AFP* and *BRACHYURY* were much more highly expressed in the differentiated cells than any of the undifferentiated cultures. *MIXL1* was also substantially up-regulated in the differentiated cells.

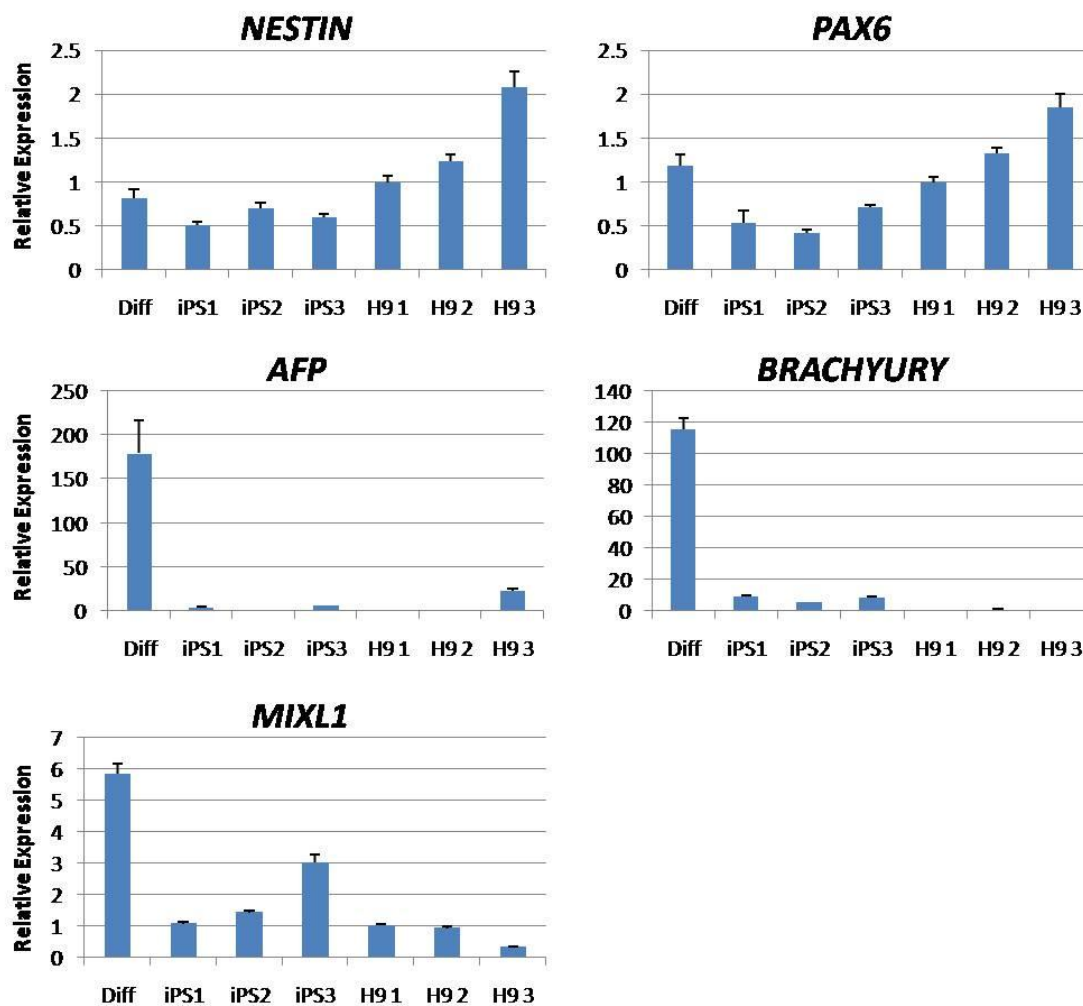


Figure 6.12: F055 iPS Cell Differentiation Analysis by qPCR. Differentiated F055 iPS cultures (Diff) were also analyzed by qPCR for genes involved in early lineage formation and compared to undifferentiated F055 iPS cells and H9 cells. Both ectoderm markers (*NESTIN* and *PAX6*) were expressed at higher levels in some of the H9 samples than the differentiated iPS cells, however the Diff sample expressed higher levels of *PAX6* than the undifferentiated iPS cells. *AFP* and *BRACHYURY* were expressed much more highly in the differentiated cultures than any other samples and *MIXL1* expression was significantly increased.

6.3 Discussion

In order to establish the myogenic nature of iPS cells, non-DMD iPS cells were differentiated using myoblast conditioned medium as described in Chapter 4 and compared to differentiated H9 cells. In addition, a line of iPS cells from a DMD patient was also generated by lentiviral transduction of *OCT4*, *LIN28*, *NANOG*, and *SOX2* and tested for pluripotency-related genes and the ability to differentiate down all three germ layers.

The iPS line used in the myogenic differentiations had previously been shown to be capable of pluripotent differentiation (Armstrong, Tilgner et al. 2010). However, its ability to undergo myogenic differentiation had not been tested. When differentiated under the conditions used to derive muscle satellite cells, the iPS line behaved quite differently from H9 cells. Differentiated iPS cells expressed higher levels of both CD56 (generally indicating neuroectoderm differentiation) and CD106 (predominantly an endothelial cell marker) than H9 cells at similar time points. The high percentage of CD56/CD106+ cells suggests a substantial number of myogenic precursors among the iPS cultures, unfortunately the relatively low M-cadherin expression somewhat contradicts this.

qPCR data showed that differentiated H9 cells expressed much higher levels of *MYF5* than the iPS cultures, though *MYOD* expression was similar between the two cell types. While these two genes are not necessarily co-expressed during myogenesis, it was surprising that such a disparity existed between the expression levels of *MYF5* and *MYOD* in iPS cells. While the iPS cells showed substantial differences in myogenic gene and surface cell marker expression compared to H9 cells, they appear to be similar in their ability to undergo myogenic differentiation. It is possible that each favors a different type of myogenic precursor, CD56/CD106+ cells from the iPS differentiation and M-cadherin+ cells from the H9 cultures, and that these separate populations account for the differences in gene expression. It is also likely that there are some differences in the genetic background of H9 cells compared to the iPS cells or it is possible that the iPS cells had not undergone complete reprogramming, either of which could result in some of the differences seen in myogenic populations.

Developing an iPS cell line from patients with DMD and subjecting them to myogenic differentiation would allow an *in vitro* study of a diseased model of early myogenesis. It would also make it possible to test possible therapeutic interventions centering on correcting the mutated *DYSTROPHIN* gene and generating transplantable myogenic precursors. To these ends, the F055 iPS cell line was created by transducing fibroblasts from a patient with DMD with *OCT4*, *LIN28*, *NANOG*, and *SOX2* and tested to ensure that it represented a truly pluripotent cell type. The International Stem Cell Initiative established some of the defining molecular characteristics of hES cells, including the expression of surface markers SSEA4, TRA-1-60, and TRA-1-80, alkaline phosphatase, and *NANOG*, *OCT4*, and *GDF3* (Adewumi, Aflatoonian et al. 2007). Immunostaining of F055 iPS cells confirmed the expression of all the markers listed except *GDF3*, while qPCR analysis verified the expression of *NANOG*, *OCT4*, and *GDF3* among many other pluripotency-related genes.

KLF4 is important in maintaining pluripotency and is a common factor used to reprogram cells for the generation of iPS cell lines. Inhibition of *KLF4* by siRNA was found to promote ES cell differentiation.

It is believed to be a regulator of NANOG expression and has been shown to bind to the *NANOG* promoter (Adewumi, Aflatoonian et al. 2007). *KLF4* was more highly expressed in the F055 iPS cells than in the H9 controls. GDF3 is a member of the TGF β superfamily that has distinct roles during mouse and human ES cell differentiation which are thought to be related to its inhibition of BMPs. In humans, GDF3 treatment maintains expression of other pluripotency genes even under differentiating conditions (Levine and Brivanlou 2006). As discussed above, it is an important marker of hES cells and is strongly expressed in undifferentiated F055 iPS cells. Other genes were tested that have important roles in ES cell biology that extend beyond the maintenance of pluripotency. *MYC* and *TERT* are both expressed in undifferentiated ES cells and are thought to have dual functions in preventing the commitment to differentiation (Cartwright, McLean et al. 2005; Yang, Przyborski et al. 2008) and helping establish cell immortality, where MYC is capable of inducing *TERT* expression (Wang, Xie et al. 1998). Knockdown of either of the proteins results in increased differentiation. *LIN28* is thought to act at the level of mRNA translation as an important regulator of differentiation. However, unlike *MYC* and *TERT*, knockdown studies showed that *LIN28* is dispensable for the maintenance of pluripotency while overexpression actually increases differentiation at low cell densities and (Darr and Benvenisty 2009). All three of these genes show similar levels of expression between the F055 iPS cells and the undifferentiated H9s.

One of the genes examined had a much lower level of expression in the F055 iPS cells than in the H9 control: *REX1*. *REX1* is often considered one of the basic markers of undifferentiated pluripotent hES cells (Brivanlou, Gage et al. 2003), although mouse ES cells cultures are heterogeneous for *Rex1* expression and *Rex1+* and *Rex1-* cells can interconvert (Toyooka, Shimosato et al. 2008). It was subsequently hypothesized that *Rex1+* cells were related to the ICM while *Rex1-* cells were related to the epiblast and primitive ectoderm, all of which were found in normal mES cultures. Additional studies of *Rex1*-knockout cell lines demonstrated that *Rex1* was not necessary for self-renewal of ES cells and did not alter the expression of pluripotency factors such as *Oct4*, *Nanog*, and *Sox2*. However, *Rex1*^{-/-} cells were found to differentiate more readily when exposed to retinoic acid than wildtype controls (Scotland, Chen et al. 2009). A recent study has suggested that bona fide iPS cells will express TRA-1-60 and SSEA4 while reprogramming, while cells that do not complete the reprogramming process may still express genes such as *OCT4*, *SOX2*, *NANOG*, and *GDF3*, but are unable to differentiate down all three germ layers and show a decreased cellularity (Chan, Ratanasirintrao et al. 2009). The study also identified *REX1* as an important marker of a truly pluripotent iPS cell line. However, the ability of the F055 iPS cell line to expand and differentiate down all three germ layers strongly indicates that it is a legitimate iPS cell line.

To ensure that the expression levels of *OCT4*, *LIN28*, *NANOG*, and *SOX2* were from endogenous gene expression and not from the viral vectors, new primers were designed to exclusively amplify

endogenous transcript as opposed to total mRNA. It has previously been reported that as iPS cells are cultured they start to silence viral genes and increase the expression of endogenous genes (Yamanaka and Blau). This trend can be seen in the DMD iPS line as earlier passages (iPS1, Figure 6.10) generally express lower levels of the endogenous genes than later passages (iPS3). Both *LIN28* and *SOX2* showed very similar results for the endogenous-only mRNA expression and the total mRNA expression, indicating that the viral genes had been silenced in the F055 iPS cells and the endogenous genes were being expressed at normal levels. Interestingly, while both *OCT4* and *NANOG* total mRNA expression was higher in the iPS cells than the H9 cells, when the endogenous-only expression was tested iPS cells expressed similar levels of *NANOG* to H9 cells but somewhat lower levels of *OCT4*. This suggests that some *OCT4* and *NANOG* transcripts are still coming from the viral vector and that while endogenous *NANOG* expression has been fully activated in the iPS cells, endogenous *OCT4* expression may not be.

After determining that the F055 iPS cells expressed the expected pluripotency markers, it was important to show that they behaved as pluripotent stem cells and differentiated down all three germ layers. The gold standard to test this is to inject cells into immunocompromised mice and examine the resultant teratomas for cells from each lineage. Unfortunately time and the small number of cells available did not permit this, so instead cells were differentiated *in vitro* and stained for markers indicative of one germ layer. AFP is expressed in the visceral endoderm early in development and the foetal liver (Dziadek and Adamson 1978; Dziadek and Andrews 1983). Because of its exclusive expression in endoderm-derived tissues it is commonly used to establish the differentiation of pluripotent cells to endoderm (Zeng, Miura et al. 2004). The F055 iPS line stained strongly for AFP and showed a very high increase in mRNA expression upon differentiation. The genes *MIXL1* and *BRACHYURY* are often used as mesoderm markers, though they are actually present in mesendoderm and are important during early endoderm/mesoderm specification (Hart, Hartley et al. 2002; Izumi, Era et al. 2007). The F055 iPS cells show a strong up-regulation of *BRACHYURY* and a moderate up-regulation of *MIXL1* upon differentiation. This, along with the strong expression of *AFP*, suggests that the F055 iPS cells may have a strong tendency to differentiation towards mesendoderm rather than ectoderm.

Differentiated cells also stained for NKX-2.5, a transcription factor important in specifying the cardiogenic field and indicative of mesoderm formation (Sadler 2003). Two genes were used to determine ectoderm formation: *PAX6*, which is important during eye development, and *NESTIN*, a common marker of neural progenitor cells, though it is expressed in many other cells (Tsonis and Fuentes 2006; Jin, Liu et al. 2009). Unsurprisingly, when the expression of *PAX6* and *NESTIN* was examined by qPCR, only a slight increase in expression could be seen upon differentiation. In fact, in both cases the genes were more highly expressed in one of the undifferentiated H9 controls than in

the differentiated F055 iPS culture. However, positive staining for β 3-tubulin confirmed that the F055 iPS cells could differentiate to lineages derived from ectoderm (Zeng, Miura et al. 2004).

Further experiments are needed to fully characterize the F055 iPS cell line. Most notably, cells must be injected into immunocompromised mice to test for teratoma formation (and to ensure that all three germ layers are represented). They should also be analyzed to ensure a normal karyotype, express DNA methylation patterns and histone modifications similar to ES cells, and further expanded to ensure their long term self-renewal. For therapeutic purposes, the mutated *DYSTROPHIN* gene could then be corrected (or replaced with a working version) and the cells could be subjected to myogenic differentiation to be tested for their ability to form functional myofibres *in vitro* and *in vivo* using animal models of muscle regeneration or muscular dystrophy.

Chapter 7: Conclusions

Several methods for the directed differentiation of hES cells towards myogenic progenitor or satellite cells have been presented. The chief driving force in these experiments has been the use of medium conditioned by human myoblasts in the differentiating cultures. In addition, cell signaling molecules Activin A and BMP-4 were used in attempts to promote the early formation of mesoderm from undifferentiated cells. Initial plating densities of differentiating hES cells were also varied, and in one experiment, differentiating cells were co-cultured with inactivated foetal myoblasts. Gene expression analysis for myogenic markers such as PAX7, PAX3, MYOD, MYF5, and MYOGENIN was performed by qPCR and suggested that the use of conditioned medium moderately increased the number of myogenic cells in differentiated cultures.

The next important step in this work is the culture and further characterisation of isolated myogenic cells. It would be important to establish their ability to undergo *in vitro* myogenesis resulting in multinucleated myofibres. The cells could also be stained for intracellular markers of satellite cells and myoblasts such as PAX7, MYOD, MYF5, and MYOGENIN and for markers of differentiated skeletal muscle fibres. If used for animal transplant experiments, culture conditions that promoted expansion but prevented differentiation would need to be developed. Initial transplantation studies could be carried out in SCID mice using a model of muscle injury to demonstrate the ability of isolated satellite cells to regenerate damaged muscle *in vivo*.

Finding signaling molecules that promote the formation of skeletal muscle tissue via paraxial mesoderm remains an important area for future research. While the conditioned medium used in the described experiments proved more effective than standard differentiation protocols, the percent of total cells in differentiated culture that unambiguously expressed myogenic markers remained low. To improve upon this, the use of additional growth factors could be employed. For instance, as discussed in Chapter 4, Activin A could be used to promote mesendoderm formation, followed by BMP-4 to promote paraxial mesoderm development with Noggin used to subsequently antagonize BMP-4 and induce myogenesis. Wnts and Sonic hedge hog are also known to activate myogenic regulatory factor expression during development (Cossu and Biressi 2005) and have also been shown to be important during adult muscle regeneration (Polesskaya, Seale et al. 2003). These factors provide a number of alternative approaches to the directed differentiation of myogenic cells. However, the use of multiple signaling proteins quickly becomes expensive when compared to the use of conditioned medium.

The selection of cell-surface markers to label and isolate putative satellite cells was an equally important component of this project. Without a well-validated repertoire of surface markers, myogenic cells in differentiated cultures could not be purified and used for cell-replacement therapy. Several human adult and foetal myoblast cell lines were analyzed by flow cytometry to determine which proteins should be employed: it was found that CD56, CD106, and M-cadherin were consistently expressed in a subset of cells in three out of the four myoblast lines, the fourth line having been determined by qPCR to have lost its myogenic nature. A substantial literature precedent also supported the use of these proteins as markers of satellite cells.

Ideally, a single marker could be used to isolate satellite cells such as the mouse SM/C-2.6 antibody. Unfortunately, such an antibody for human satellite cells has not been identified. As satellite cells become more thoroughly characterised, it is possible that a highly selective, highly specific marker will be found. Unfortunately both CD56 and CD106 have low specificity (other cell types also express them) while M-cadherin is not particularly selective (reports vary as to whether or not all satellite cells, especially quiescent ones, express M-cadherin). These issues can also be resolved by improving the percent of the differentiating cells which become myogenic, thereby reducing possible sources of contamination from other cell types. It would also be feasible to add an earlier round of cell sorting, similar to Barberi et al. 2005, who sorted for CD73 expression and then subsequently sorted for CD56 expression to obtain a population of myogenic cells. An early sort with PDGFR- α would select for a variety of mesendoderm or mesoderm populations, eliminating definitive endoderm and ectoderm cells, and a population of PDGFR- α + / VEGFR- cells could specifically isolate paraxial mesoderm. These cells might then be further cultured in myogenic conditioned medium. This approach was used by Sakurai et al. 2008 in differentiating mouse ES cells. They directly injected the PDGFR- α + cells and found that the cells contributed to muscle regeneration. The drawback to this sort of approach is that it would substantially complicate the protocol and still does not guarantee full conversion to myogenic cells.

Even with an improvement in the percentage of myogenic cells that can be obtained from differentiating hES cells, a substantial scale-up of hES cell culture would be required in order to use this approach therapeutically in patients with DMD. While the culture techniques described in this work might be sufficient for a single muscle site injection (assuming an improvement in the efficiency of myogenic differentiation), they would be insufficient for a therapeutic regimen that required multiple site injections. For this, it might be necessary to explore the use of novel undifferentiated hES cell culture methods, such as the work described by Steiner et al. 2010 where hES cell colonies were grown and propagated in suspension cultures. In addition, the early steps of hES cell differentiation might be carried out in suspension cultures. There is a long precedent for differentiating mouse and human ES cells as EBs both in the presence and absence of signaling

molecules to promote the development of a given lineage. These methods could be used for the early establishment of mesoderm followed by plating and expansion in pro-myogenic medium until a substantial number of satellite cells were obtained. Unfortunately any large scale growth and directed differentiation of hES cells will be quite expensive, especially if multiple recombinant signaling molecules are needed during differentiation. The same concern exists for differentiation procedures that require multiple rounds of FACS: large quantities of expensive antibodies will be needed to purify cells for each round, substantially increases the cost of such experiments.

Finally, the myogenic differentiation strategy was tested in iPS cells and compared with H9 cells. Not surprisingly, a difference was seen between the two lines, highlighting the importance of studying iPS cells along side of hES cells. In addition, a new iPS cell line was generated using fibroblasts from a patient with DMD. Both qPCR analysis and immunostaining strongly suggested that the DMD iPS cells were a pluripotent cell line, showing both a broad array of pluripotency markers and the ability to differentiate down all three germ lines. However, further culture is still needed to prove the immortality of these cells and they must be tested for teratoma formation in mice. Studying myogenic differentiation in these cells would allow for proof-of-concept experiments where the mutated DYSTROPHIN gene could be repaired and the cells subsequently differentiated into satellite cells. Transplanting these cells in animal models would be important to both establish their myogenic potential and ensure that they remain differentiated, despite having gone through viral reprogramming.

References

- Adewumi, O., B. Aflatoonian, et al. (2007). "Characterization of human embryonic stem cell lines by the International Stem Cell Initiative." *Nat Biotechnol* **25**(7): 803-16.
- Allouh, M. Z., Z. Yablonka-Reuveni, et al. (2008). "Pax7 reveals a greater frequency and concentration of satellite cells at the ends of growing skeletal muscle fibers." *J Histochem Cytochem* **56**(1): 77-87.
- Ambrosetti, D. C., C. Basilico, et al. (1997). "Synergistic activation of the fibroblast growth factor 4 enhancer by Sox2 and Oct-3 depends on protein-protein interactions facilitated by a specific spatial arrangement of factor binding sites." *Mol Cell Biol* **17**(11): 6321-9.
- Andermarcher, E., M. A. Surani, et al. (1996). "Co-expression of the HGF/SF and c-met genes during early mouse embryogenesis precedes reciprocal expression in adjacent tissues during organogenesis." *Dev Genet* **18**(3): 254-66.
- Andersson, A. M., M. Olsen, et al. (1993). "Age-related changes in expression of the neural cell adhesion molecule in skeletal muscle: a comparative study of newborn, adult and aged rats." *Biochem J* **290** (Pt 3): 641-8.
- Armstrong, L., K. Tilgner, et al. (2010). "Human induced pluripotent stem cell lines show stress defense mechanisms and mitochondrial regulation similar to those of human embryonic stem cells." *Stem Cells* **28**(4): 661-73.
- Asakura, A., P. Seale, et al. (2002). "Myogenic specification of side population cells in skeletal muscle." *J Cell Biol* **159**(1): 123-34.
- Avilion, A. A., S. K. Nicolis, et al. (2003). "Multipotent cell lineages in early mouse development depend on SOX2 function." *Genes Dev* **17**(1): 126-40.
- Balcerzak, D., S. Poussard, et al. (1995). "An antisense oligodeoxyribonucleotide to m-calpain mRNA inhibits myoblast fusion." *J Cell Sci* **108** (Pt 5): 2077-82.
- Barberi, T., M. Bradbury, et al. (2007). "Derivation of engraftable skeletal myoblasts from human embryonic stem cells." *Nat Med* **13**(5): 642-8.
- Barberi, T., L. M. Willis, et al. (2005). "Derivation of multipotent mesenchymal precursors from human embryonic stem cells." *PLoS Med* **2**(6): e161.
- Baroffio, A., M. Hamann, et al. (1996). "Identification of self-renewing myoblasts in the progeny of single human muscle satellite cells." *Differentiation* **60**(1): 47-57.
- Beauchamp, J. R., L. Heslop, et al. (2000). "Expression of CD34 and Myf5 defines the majority of quiescent adult skeletal muscle satellite cells." *J Cell Biol* **151**(6): 1221-34.
- Bhagavati, S. and W. Xu (2005). "Generation of skeletal muscle from transplanted embryonic stem cells in dystrophic mice." *Biochem Biophys Res Commun* **333**(2): 644-9.
- Blau, H. M., C. P. Chiu, et al. (1983). "Cytoplasmic activation of human nuclear genes in stable heterocaryons." *Cell* **32**(4): 1171-80.
- Blau, H. M., C. Webster, et al. (1983). "Defective myoblasts identified in Duchenne muscular dystrophy." *Proc Natl Acad Sci U S A* **80**(15): 4856-60.
- Bosnakovski, D., Z. Xu, et al. (2008). "Prospective isolation of skeletal muscle stem cells with a Pax7 reporter." *Stem Cells* **26**(12): 3194-204.
- Boyd, N. L., S. K. Dhara, et al. (2007). "BMP4 promotes formation of primitive vascular networks in human embryonic stem cell-derived embryoid bodies." *Exp Biol Med (Maywood)* **232**(6): 833-43.
- Boyer, L. A., T. I. Lee, et al. (2005). "Core transcriptional regulatory circuitry in human embryonic stem cells." *Cell* **122**(6): 947-56.
- Brambrink, T., R. Foreman, et al. (2008). "Sequential expression of pluripotency markers during direct reprogramming of mouse somatic cells." *Cell Stem Cell* **2**(2): 151-9.

- Braun, T. and H. H. Arnold (1994). "ES-cells carrying two inactivated myf-5 alleles form skeletal muscle cells: activation of an alternative myf-5-independent differentiation pathway." *Dev Biol* **164**(1): 24-36.
- Braun, T., M. A. Rudnicki, et al. (1992). "Targeted inactivation of the muscle regulatory gene Myf-5 results in abnormal rib development and perinatal death." *Cell* **71**(3): 369-82.
- Briggs, R. and T. J. King (1952). "Transplantation of Living Nuclei From Blastula Cells into Enucleated Frogs' Eggs." *Proc Natl Acad Sci U S A* **38**(5): 455-63.
- Brivanlou, A. H., F. H. Gage, et al. (2003). "Stem cells. Setting standards for human embryonic stem cells." *Science* **300**(5621): 913-6.
- Brunetti, A. and I. D. Goldfine (1990). "Differential effects of fibroblast growth factor on insulin receptor and muscle specific protein gene expression in BC3H-1 myocytes." *Mol Endocrinol* **4**(6): 880-5.
- Buckingham, M. (2006). "Myogenic progenitor cells and skeletal myogenesis in vertebrates." *Curr Opin Genet Dev* **16**(5): 525-32.
- Buckingham, M., L. Bajard, et al. (2003). "The formation of skeletal muscle: from somite to limb." *J Anat* **202**(1): 59-68.
- Capkovic, K. L., S. Stevenson, et al. (2008). "Neural cell adhesion molecule (NCAM) marks adult myogenic cells committed to differentiation." *Exp Cell Res* **314**(7): 1553-65.
- Caron, L., F. Bost, et al. (2005). "A new role for the oncogenic high-mobility group A2 transcription factor in myogenesis of embryonic stem cells." *Oncogene* **24**(41): 6281-91.
- Cartwright, P., C. McLean, et al. (2005). "LIF/STAT3 controls ES cell self-renewal and pluripotency by a Myc-dependent mechanism." *Development* **132**(5): 885-96.
- Chambers, I., D. Colby, et al. (2003). "Functional expression cloning of Nanog, a pluripotency sustaining factor in embryonic stem cells." *Cell* **113**(5): 643-55.
- Chan, E. M., S. Ratanasirintrao, et al. (2009). "Live cell imaging distinguishes bona fide human iPS cells from partially reprogrammed cells." *Nat Biotechnol* **27**(11): 1033-7.
- Chan, J., K. O'Donoghue, et al. (2006). "Galectin-1 induces skeletal muscle differentiation in human fetal mesenchymal stem cells and increases muscle regeneration." *Stem Cells* **24**(8): 1879-91.
- Chang, H., M. Yoshimoto, et al. (2009). "Generation of transplantable, functional satellite-like cells from mouse embryonic stem cells." *FASEB J* **23**(6): 1907-19.
- Charge, S. B. and M. A. Rudnicki (2004). "Cellular and molecular regulation of muscle regeneration." *Physiol Rev* **84**(1): 209-38.
- Charlton, C. A., W. A. Mohler, et al. (2000). "Neural cell adhesion molecule (NCAM) and myoblast fusion." *Dev Biol* **221**(1): 112-9.
- Chen, J. C. and D. J. Goldhamer (2003). "Skeletal muscle stem cells." *Reprod Biol Endocrinol* **1**: 101.
- Chiba, S., M. S. Kurokawa, et al. (2005). "Noggin and basic FGF were implicated in forebrain fate and caudal fate, respectively, of the neural tube-like structures emerging in mouse ES cell culture." *Exp Brain Res* **163**(1): 86-99.
- Collins, C. A., I. Olsen, et al. (2005). "Stem cell function, self-renewal, and behavioral heterogeneity of cells from the adult muscle satellite cell niche." *Cell* **122**(2): 289-301.
- Conboy, M. J., A. O. Karasov, et al. (2007). "High incidence of non-random template strand segregation and asymmetric fate determination in dividing stem cells and their progeny." *PLoS Biol* **5**(5): e102.
- Coraux, C., C. Hilmi, et al. (2003). "Reconstituted skin from murine embryonic stem cells." *Curr Biol* **13**(10): 849-53.
- Cornelison, D. D., M. S. Filla, et al. (2001). "Syndecan-3 and syndecan-4 specifically mark skeletal muscle satellite cells and are implicated in satellite cell maintenance and muscle regeneration." *Dev Biol* **239**(1): 79-94.
- Cornelison, D. D., B. B. Olwin, et al. (2000). "MyoD(-/-) satellite cells in single-fiber culture are differentiation defective and MRF4 deficient." *Dev Biol* **224**(2): 122-37.
- Cornelison, D. D., S. A. Wilcox-Adelman, et al. (2004). "Essential and separable roles for Syndecan-3 and Syndecan-4 in skeletal muscle development and regeneration." *Genes Dev* **18**(18): 2231-6.

- Cornelison, D. D. and B. J. Wold (1997). "Single-cell analysis of regulatory gene expression in quiescent and activated mouse skeletal muscle satellite cells." *Dev Biol* **191**(2): 270-83.
- Coskun, V., H. Wu, et al. (2008). "CD133+ neural stem cells in the ependyma of mammalian postnatal forebrain." *Proc Natl Acad Sci U S A* **105**(3): 1026-31.
- Cossu, G. and S. Biressi (2005). "Satellite cells, myoblasts and other occasional myogenic progenitors: possible origin, phenotypic features and role in muscle regeneration." *Semin Cell Dev Biol* **16**(4-5): 623-31.
- Covault, J. and J. R. Sanes (1986). "Distribution of N-CAM in synaptic and extrasynaptic portions of developing and adult skeletal muscle." *J Cell Biol* **102**(3): 716-30.
- D'Amour, K. A., A. D. Agulnick, et al. (2005). "Efficient differentiation of human embryonic stem cells to definitive endoderm." *Nat Biotechnol* **23**(12): 1534-41.
- Darabi, R., J. Baik, et al. (2009). "Engraftment of embryonic stem cell-derived myogenic progenitors in a dominant model of muscular dystrophy." *Exp Neurol* **220**(1): 212-6.
- Darabi, R., K. Gehlbach, et al. (2008). "Functional skeletal muscle regeneration from differentiating embryonic stem cells." *Nat Med* **14**(2): 134-43.
- Darr, H. and N. Benvenisty (2009). "Genetic analysis of the role of the reprogramming gene LIN-28 in human embryonic stem cells." *Stem Cells* **27**(2): 352-62.
- Davidson, R. L., B. Ephrussi, et al. (1966). "Regulation of pigment synthesis in mammalian cells, as studied by somatic hybridization." *Proc Natl Acad Sci U S A* **56**(5): 1437-40.
- Decary, S., V. Mouly, et al. (1996). "Telomere length as a tool to monitor satellite cell amplification for cell-mediated gene therapy." *Hum Gene Ther* **7**(11): 1347-50.
- Desbordes, S. C., D. G. Placantonakis, et al. (2008). "High-throughput screening assay for the identification of compounds regulating self-renewal and differentiation in human embryonic stem cells." *Cell Stem Cell* **2**(6): 602-12.
- Dezawa, M., H. Ishikawa, et al. (2005). "Bone marrow stromal cells generate muscle cells and repair muscle degeneration." *Science* **309**(5732): 314-7.
- Dhawan, J. and T. A. Rando (2005). "Stem cells in postnatal myogenesis: molecular mechanisms of satellite cell quiescence, activation and replenishment." *Trends Cell Biol* **15**(12): 666-73.
- Dimos, J. T., K. T. Rodolfa, et al. (2008). "Induced pluripotent stem cells generated from patients with ALS can be differentiated into motor neurons." *Science* **321**(5893): 1218-21.
- Donalies, M., M. Cramer, et al. (1991). "Expression of M-cadherin, a member of the cadherin multigene family, correlates with differentiation of skeletal muscle cells." *Proc Natl Acad Sci U S A* **88**(18): 8024-8.
- Draper, J. S., H. D. Moore, et al. (2004). "Culture and characterization of human embryonic stem cells." *Stem Cells Dev* **13**(4): 325-36.
- Duband, J. L., S. Dufour, et al. (1987). "Adhesion molecules during somitogenesis in the avian embryo." *J Cell Biol* **104**(5): 1361-74.
- Dziadek, M. and E. Adamson (1978). "Localization and synthesis of alphafoetoprotein in post-implantation mouse embryos." *J Embryol Exp Morphol* **43**: 289-313.
- Dziadek, M. A. and G. K. Andrews (1983). "Tissue specificity of alpha-fetoprotein messenger RNA expression during mouse embryogenesis." *EMBO J* **2**(4): 549-54.
- Ebert, A. D., J. Yu, et al. (2009). "Induced pluripotent stem cells from a spinal muscular atrophy patient." *Nature* **457**(7227): 277-80.
- Emery, A. E. (2002). "The muscular dystrophies." *Lancet* **359**(9307): 687-95.
- Evans, M. J. and M. H. Kaufman (1981). "Establishment in culture of pluripotential cells from mouse embryos." *Nature* **292**(5819): 154-6.
- Fassler, R. and M. Meyer (1995). "Consequences of lack of beta 1 integrin gene expression in mice." *Genes Dev* **9**(15): 1896-908.
- Fazeli, S., D. J. Wells, et al. (1996). "Altered secondary myogenesis in transgenic animals expressing the neural cell adhesion molecule under the control of a skeletal muscle alpha-actin promoter." *J Cell Biol* **135**(1): 241-51.

- Fukada, S., S. Higuchi, et al. (2004). "Purification and cell-surface marker characterization of quiescent satellite cells from murine skeletal muscle by a novel monoclonal antibody." Exp Cell Res **296**(2): 245-55.
- Fukada, S., Y. Miyagoe-Suzuki, et al. (2002). "Muscle regeneration by reconstitution with bone marrow or fetal liver cells from green fluorescent protein-gene transgenic mice." J Cell Sci **115**(Pt 6): 1285-93.
- Fukada, S., A. Uezumi, et al. (2007). "Molecular signature of quiescent satellite cells in adult skeletal muscle." Stem Cells **25**(10): 2448-59.
- Garry, D. J., A. Meeson, et al. (2000). "Myogenic stem cell function is impaired in mice lacking the forkhead/winged helix protein MNF." Proc Natl Acad Sci U S A **97**(10): 5416-21.
- Gayraud-Morel, B., F. Chretien, et al. (2007). "A role for the myogenic determination gene Myf5 in adult regenerative myogenesis." Dev Biol **312**(1): 13-28.
- Gehring, W. J. (1996). "The master control gene for morphogenesis and evolution of the eye." Genes Cells **1**(1): 11-5.
- Ginis, I., Y. Luo, et al. (2004). "Differences between human and mouse embryonic stem cells." Dev Biol **269**(2): 360-80.
- Goldman, O., O. Feraud, et al. (2009). "A boost of BMP4 accelerates the commitment of human embryonic stem cells to the endothelial lineage." Stem Cells **27**(8): 1750-9.
- Gros, J., M. Manceau, et al. (2005). "A common somitic origin for embryonic muscle progenitors and satellite cells." Nature **435**(7044): 954-8.
- Gurdon, J. B. (1962). "The developmental capacity of nuclei taken from intestinal epithelium cells of feeding tadpoles." J Embryol Exp Morphol **10**: 622-40.
- Gussoni, E., Y. Soneoka, et al. (1999). "Dystrophin expression in the mdx mouse restored by stem cell transplantation." Nature **401**(6751): 390-4.
- Hanna, J., M. Wernig, et al. (2007). "Treatment of sickle cell anemia mouse model with iPS cells generated from autologous skin." Science **318**(5858): 1920-3.
- Hansen-Smith, F. M. and B. M. Carlson (1979). "Cellular responses to free grafting of the extensor digitorum longus muscle of the rat." J Neurol Sci **41**(2): 149-73.
- Harris, H., O. J. Miller, et al. (1969). "Suppression of malignancy by cell fusion." Nature **223**(5204): 363-8.
- Hart, A. H., L. Hartley, et al. (2002). "Mixl1 is required for axial mesendoderm morphogenesis and patterning in the murine embryo." Development **129**(15): 3597-608.
- Hasegawa, K., J. E. Pomeroy, et al. (2010). "Current technology for the derivation of pluripotent stem cell lines from human embryos." Cell Stem Cell **6**(6): 521-31.
- Hashemi-Tabar, M., M. Orazizadeh, et al. (2009). "Kinetics of gene expression during exposure of mouse stem cells to activin A." Pak J Biol Sci **12**(4): 324-31.
- Hasty, P., A. Bradley, et al. (1993). "Muscle deficiency and neonatal death in mice with a targeted mutation in the myogenin gene." Nature **364**(6437): 501-6.
- Hawke, T. J., N. Jiang, et al. (2003). "Absence of p21CIP rescues myogenic progenitor cell proliferative and regenerative capacity in Foxk1 null mice." J Biol Chem **278**(6): 4015-20.
- Hohenstein, K. A., A. D. Pyle, et al. (2008). "Nucleofection mediates high-efficiency stable gene knockdown and transgene expression in human embryonic stem cells." Stem Cells **26**(6): 1436-43.
- Hyslop, L. A., L. Armstrong, et al. (2005). "Human embryonic stem cells: biology and clinical implications." Expert Rev Mol Med **7**(19): 1-21.
- Illa, I., M. Leon-Monzon, et al. (1992). "Regenerating and denervated human muscle fibers and satellite cells express neural cell adhesion molecule recognized by monoclonal antibodies to natural killer cells." Ann Neurol **31**(1): 46-52.
- Irintchev, A., M. Zeschnigk, et al. (1994). "Expression pattern of M-cadherin in normal, denervated, and regenerating mouse muscles." Dev Dyn **199**(4): 326-37.
- Ishido, M., M. Uda, et al. (2006). "Alterations of M-cadherin, neural cell adhesion molecule and beta-catenin expression in satellite cells during overload-induced skeletal muscle hypertrophy." Acta Physiol (Oxf) **187**(3): 407-18.

- Izumi, N., T. Era, et al. (2007). "Dissecting the molecular hierarchy for mesendoderm differentiation through a combination of embryonic stem cell culture and RNA interference." *Stem Cells* **25**(7): 1664-74.
- James, D., A. J. Levine, et al. (2005). "TGFbeta/activin/nodal signaling is necessary for the maintenance of pluripotency in human embryonic stem cells." *Development* **132**(6): 1273-82.
- Jesse, T. L., R. LaChance, et al. (1998). "Interferon regulatory factor-2 is a transcriptional activator in muscle where it regulates expression of vascular cell adhesion molecule-1." *J Cell Biol* **140**(5): 1265-76.
- Jin, Z., L. Liu, et al. (2009). "Different transcription factors regulate nestin gene expression during P19 cell neural differentiation and central nervous system development." *J Biol Chem* **284**(12): 8160-73.
- Johnson, S. E. and R. E. Allen (1995). "Activation of skeletal muscle satellite cells and the role of fibroblast growth factor receptors." *Exp Cell Res* **219**(2): 449-53.
- Jostes, B., C. Walther, et al. (1990). "The murine paired box gene, Pax7, is expressed specifically during the development of the nervous and muscular system." *Mech Dev* **33**(1): 27-37.
- Kahane, N., R. Ben-Yair, et al. (2007). "Medial pioneer fibers pattern the morphogenesis of early myoblasts derived from the lateral somite." *Dev Biol* **305**(2): 439-50.
- Kamochi, H., M. S. Kurokawa, et al. (2006). "Transplantation of myocyte precursors derived from embryonic stem cells transfected with IGFII gene in a mouse model of muscle injury." *Transplantation* **82**(4): 516-26.
- Kassar-Duchossoy, L., E. Giaccone, et al. (2005). "Pax3/Pax7 mark a novel population of primitive myogenic cells during development." *Genes Dev* **19**(12): 1426-31.
- Kaufmann, U., J. Kirsch, et al. (1999). "The M-cadherin catenin complex interacts with microtubules in skeletal muscle cells: implications for the fusion of myoblasts." *J Cell Sci* **112** (Pt 1): 55-68.
- Kazuki, Y., M. Hiratsuka, et al. (2010). "Complete genetic correction of ips cells from Duchenne muscular dystrophy." *Mol Ther* **18**(2): 386-93.
- Kirkpatrick, L. J., M. Z. Allouh, et al. (2008). "Pax7 shows higher satellite cell frequencies and concentrations within intrafusal fibers of muscle spindles." *J Histochem Cytochem* **56**(9): 831-40.
- Kopp, J. L., B. D. Ormsbee, et al. (2008). "Small increases in the level of Sox2 trigger the differentiation of mouse embryonic stem cells." *Stem Cells* **26**(4): 903-11.
- Kuang, S., K. Kuroda, et al. (2007). "Asymmetric self-renewal and commitment of satellite stem cells in muscle." *Cell* **129**(5): 999-1010.
- Kuch, C., D. Winnekenonk, et al. (1997). "M-cadherin-mediated cell adhesion and complex formation with the catenins in myogenic mouse cells." *Exp Cell Res* **232**(2): 331-8.
- Kwak, K. B., S. S. Chung, et al. (1993). "Increase in the level of m-calpain correlates with the elevated cleavage of filamin during myogenic differentiation of embryonic muscle cells." *Biochim Biophys Acta* **1175**(3): 243-9.
- LaVaute, T. M., Y. D. Yoo, et al. (2009). "Regulation of neural specification from human embryonic stem cells by BMP and FGF." *Stem Cells* **27**(8): 1741-9.
- Law, P. K., T. G. Goodwin, et al. (1997). "Human gene therapy with myoblast transfer." *Transplant Proc* **29**(4): 2234-7.
- Lepper, C., S. J. Conway, et al. (2009). "Adult satellite cells and embryonic muscle progenitors have distinct genetic requirements." *Nature* **460**(7255): 627-31.
- Levine, A. J. and A. H. Brivanlou (2006). "GDF3, a BMP inhibitor, regulates cell fate in stem cells and early embryos." *Development* **133**(2): 209-16.
- Lluis, F., E. Perdiguero, et al. (2006). "Regulation of skeletal muscle gene expression by p38 MAP kinases." *Trends Cell Biol* **16**(1): 36-44.
- Ludwig, T. E., M. E. Levenstein, et al. (2006). "Derivation of human embryonic stem cells in defined conditions." *Nat Biotechnol* **24**(2): 185-7.
- Lyles, J. M., W. Amin, et al. (1993). "Regulation of NCAM by growth factors in serum-free myotube cultures." *J Neurosci Res* **34**(3): 273-86.

- Lyons, G. E., R. Moore, et al. (1992). "Expression of NCAM isoforms during skeletal myogenesis in the mouse embryo." *Dev Dyn* **194**(2): 94-104.
- Martin, G. R. (1981). "Isolation of a pluripotent cell line from early mouse embryos cultured in medium conditioned by teratocarcinoma stem cells." *Proc Natl Acad Sci U S A* **78**(12): 7634-8.
- Matsumura, K. and K. P. Campbell (1994). "Dystrophin-glycoprotein complex: its role in the molecular pathogenesis of muscular dystrophies." *Muscle Nerve* **17**(1): 2-15.
- Mauro, A. (1961). "Satellite cell of skeletal muscle fibers." *J Biophys Biochem Cytol* **9**: 493-5.
- McLean, A. B., K. A. D'Amour, et al. (2007). "Activin efficiently specifies definitive endoderm from human embryonic stem cells only when phosphatidylinositol 3-kinase signaling is suppressed." *Stem Cells* **25**(1): 29-38.
- Mechtersheimer, G., M. Staudter, et al. (1992). "Expression of the natural killer (NK) cell-associated antigen CD56(Leu-19), which is identical to the 140-kDa isoform of N-CAM, in neural and skeletal muscle cells and tumors derived therefrom." *Ann N Y Acad Sci* **650**: 311-6.
- Megenev, L. A., B. Kablar, et al. (1996). "MyoD is required for myogenic stem cell function in adult skeletal muscle." *Genes Dev* **10**(10): 1173-83.
- Mendell, J. R., J. T. Kissel, et al. (1995). "Myoblast transfer in the treatment of Duchenne's muscular dystrophy." *N Engl J Med* **333**(13): 832-8.
- Mikkelsen, T. S., J. Hanna, et al. (2008). "Dissecting direct reprogramming through integrative genomic analysis." *Nature* **454**(7200): 49-55.
- Miller, J. B. (1990). "Myogenic programs of mouse muscle cell lines: expression of myosin heavy chain isoforms, MyoD1, and myogenin." *J Cell Biol* **111**(3): 1149-59.
- Miller, K. J., D. Thaloor, et al. (2000). "Hepatocyte growth factor affects satellite cell activation and differentiation in regenerating skeletal muscle." *Am J Physiol Cell Physiol* **278**(1): C174-81.
- Miller, R. G., K. R. Sharma, et al. (1997). "Myoblast implantation in Duchenne muscular dystrophy: the San Francisco study." *Muscle Nerve* **20**(4): 469-78.
- Minasi, M. G., M. Riminucci, et al. (2002). "The meso-angioblast: a multipotent, self-renewing cell that originates from the dorsal aorta and differentiates into most mesodermal tissues." *Development* **129**(11): 2773-83.
- Mitsui, K., Y. Tokuzawa, et al. (2003). "The homeoprotein Nanog is required for maintenance of pluripotency in mouse epiblast and ES cells." *Cell* **113**(5): 631-42.
- Mizrak, D., M. Brittan, et al. (2008). "CD133: molecule of the moment." *J Pathol* **214**(1): 3-9.
- Montarras, D., J. Morgan, et al. (2005). "Direct isolation of satellite cells for skeletal muscle regeneration." *Science* **309**(5743): 2064-7.
- Moore, R. and F. S. Walsh (1993). "The cell adhesion molecule M-cadherin is specifically expressed in developing and regenerating, but not denervated skeletal muscle." *Development* **117**(4): 1409-20.
- Moore, S. E., J. Thompson, et al. (1987). "Skeletal muscle neural cell adhesion molecule (N-CAM): changes in protein and mRNA species during myogenesis of muscle cell lines." *J Cell Biol* **105**(3): 1377-86.
- Morgan, J. E., D. J. Watt, et al. (1988). "Partial correction of an inherited biochemical defect of skeletal muscle by grafts of normal muscle precursor cells." *J Neurol Sci* **86**(2-3): 137-47.
- Myer, A., E. N. Olson, et al. (2001). "MyoD cannot compensate for the absence of myogenin during skeletal muscle differentiation in murine embryonic stem cells." *Dev Biol* **229**(2): 340-50.
- Nabeshima, Y., K. Hanaoka, et al. (1993). "Myogenin gene disruption results in perinatal lethality because of severe muscle defect." *Nature* **364**(6437): 532-5.
- Nakagawa, M., M. Koyanagi, et al. (2008). "Generation of induced pluripotent stem cells without Myc from mouse and human fibroblasts." *Nat Biotechnol* **26**(1): 101-6.
- Nakayama, N., D. Duryea, et al. (2003). "Macroscopic cartilage formation with embryonic stem-cell-derived mesodermal progenitor cells." *J Cell Sci* **116**(Pt 10): 2015-28.
- Negróni, E., G. S. Butler-Browne, et al. (2006). "Myogenic stem cells: regeneration and cell therapy in human skeletal muscle." *Pathol Biol (Paris)* **54**(2): 100-8.
- Nichols, J., B. Zevnik, et al. (1998). "Formation of pluripotent stem cells in the mammalian embryo depends on the POU transcription factor Oct4." *Cell* **95**(3): 379-91.

- Niwa, H., T. Burdon, et al. (1998). "Self-renewal of pluripotent embryonic stem cells is mediated via activation of STAT3." *Genes Dev* **12**(13): 2048-60.
- Niwa, H., J. Miyazaki, et al. (2000). "Quantitative expression of Oct-3/4 defines differentiation, dedifferentiation or self-renewal of ES cells." *Nat Genet* **24**(4): 372-6.
- Okita, K., M. Nakagawa, et al. (2008). "Generation of mouse induced pluripotent stem cells without viral vectors." *Science* **322**(5903): 949-53.
- Olguin, H. C. and B. B. Olwin (2004). "Pax-7 up-regulation inhibits myogenesis and cell cycle progression in satellite cells: a potential mechanism for self-renewal." *Dev Biol* **275**(2): 375-88.
- Olguin, H. C., Z. Yang, et al. (2007). "Reciprocal inhibition between Pax7 and muscle regulatory factors modulates myogenic cell fate determination." *J Cell Biol* **177**(5): 769-79.
- Ott, M. O., E. Bober, et al. (1991). "Early expression of the myogenic regulatory gene, myf-5, in precursor cells of skeletal muscle in the mouse embryo." *Development* **111**(4): 1097-107.
- Oustanina, S., G. Hause, et al. (2004). "Pax7 directs postnatal renewal and propagation of myogenic satellite cells but not their specification." *EMBO J* **23**(16): 3430-9.
- Park, I. H., N. Arora, et al. (2008). "Disease-specific induced pluripotent stem cells." *Cell* **134**(5): 877-86.
- Partridge, T., Q. L. Lu, et al. (1998). "Is myoblast transplantation effective?" *Nat Med* **4**(11): 1208-9.
- Partridge, T. A., J. E. Morgan, et al. (1989). "Conversion of mdx myofibres from dystrophin-negative to -positive by injection of normal myoblasts." *Nature* **337**(6203): 176-9.
- Peault, B., M. Rudnicki, et al. (2007). "Stem and progenitor cells in skeletal muscle development, maintenance, and therapy." *Mol Ther* **15**(5): 867-77.
- Pesce, M. and H. R. Scholer (2001). "Oct-4: gatekeeper in the beginnings of mammalian development." *Stem Cells* **19**(4): 271-8.
- Polesskaya, A., P. Seale, et al. (2003). "Wnt signaling induces the myogenic specification of resident CD45+ adult stem cells during muscle regeneration." *Cell* **113**(7): 841-52.
- Prelle, K., A. M. Wobus, et al. (2000). "Overexpression of insulin-like growth factor-II in mouse embryonic stem cells promotes myogenic differentiation." *Biochem Biophys Res Commun* **277**(3): 631-8.
- Price, F. D., K. Kuroda, et al. (2007). "Stem cell based therapies to treat muscular dystrophy." *Biochim Biophys Acta* **1772**(2): 272-83.
- Pruszek, J., K. C. Sonntag, et al. (2007). "Markers and methods for cell sorting of human embryonic stem cell-derived neural cell populations." *Stem Cells* **25**(9): 2257-68.
- Radley, H. G., A. De Luca, et al. (2007). "Duchenne muscular dystrophy: focus on pharmaceutical and nutritional interventions." *Int J Biochem Cell Biol* **39**(3): 469-77.
- Ralston, A. and J. Rossant (2010). "The genetics of induced pluripotency." *Reproduction* **139**(1): 35-44.
- Raya, A., I. Rodriguez-Piza, et al. (2009). "Disease-corrected haematopoietic progenitors from Fanconi anaemia induced pluripotent stem cells." *Nature* **460**(7251): 53-9.
- Reimann, J., K. Brimah, et al. (2004). "Pax7 distribution in human skeletal muscle biopsies and myogenic tissue cultures." *Cell Tissue Res* **315**(2): 233-42.
- Relaix, F., D. Rocancourt, et al. (2004). "Divergent functions of murine Pax3 and Pax7 in limb muscle development." *Genes Dev* **18**(9): 1088-105.
- Relaix, F., D. Rocancourt, et al. (2005). "A Pax3/Pax7-dependent population of skeletal muscle progenitor cells." *Nature* **435**(7044): 948-53.
- Reshef, R., M. Maroto, et al. (1998). "Regulation of dorsal somitic cell fates: BMPs and Noggin control the timing and pattern of myogenic regulator expression." *Genes Dev* **12**(3): 290-303.
- Rohwedel, J., K. Guan, et al. (1998). "Loss of beta1 integrin function results in a retardation of myogenic, but an acceleration of neuronal, differentiation of embryonic stem cells in vitro." *Dev Biol* **201**(2): 167-84.
- Rohwedel, J., V. Horak, et al. (1995). "M-twist expression inhibits mouse embryonic stem cell-derived myogenic differentiation in vitro." *Exp Cell Res* **220**(1): 92-100.

- Rohwedel, J., V. Maltsev, et al. (1994). "Muscle cell differentiation of embryonic stem cells reflects myogenesis in vivo: developmentally regulated expression of myogenic determination genes and functional expression of ionic currents." *Dev Biol* **164**(1): 87-101.
- Ronn, L. C., B. P. Hartz, et al. (1998). "The neural cell adhesion molecule (NCAM) in development and plasticity of the nervous system." *Exp Gerontol* **33**(7-8): 853-64.
- Rose, O., C. Grund, et al. (1995). "Contactus adherens, a special type of plaque-bearing adhering junction containing M-cadherin, in the granule cell layer of the cerebellar glomerulus." *Proc Natl Acad Sci U S A* **92**(13): 6022-6.
- Rose, O., J. Rohwedel, et al. (1994). "Expression of M-cadherin protein in myogenic cells during prenatal mouse development and differentiation of embryonic stem cells in culture." *Dev Dyn* **201**(3): 245-59.
- Rosen, G. D., J. R. Sanes, et al. (1992). "Roles for the integrin VLA-4 and its counter receptor VCAM-1 in myogenesis." *Cell* **69**(7): 1107-19.
- Rudnicki, M. A., T. Braun, et al. (1992). "Inactivation of MyoD in mice leads to up-regulation of the myogenic HLH gene Myf-5 and results in apparently normal muscle development." *Cell* **71**(3): 383-90.
- Sabourin, L. A., A. Girgis-Gabardo, et al. (1999). "Reduced differentiation potential of primary MyoD-/- myogenic cells derived from adult skeletal muscle." *J Cell Biol* **144**(4): 631-43.
- Sadler, T. W. (2003). *Langman's Medical Embryology*, Lippincott Williams & Wilkins.
- Sakurai, H., T. Era, et al. (2006). "In vitro modeling of paraxial and lateral mesoderm differentiation reveals early reversibility." *Stem Cells* **24**(3): 575-86.
- Sakurai, H., Y. Inami, et al. (2009). "Bidirectional induction toward paraxial mesodermal derivatives from mouse ES cells in chemically defined medium." *Stem Cell Res* **3**(2-3): 157-69.
- Sakurai, H., Y. Okawa, et al. (2008). "Paraxial mesodermal progenitors derived from mouse embryonic stem cells contribute to muscle regeneration via differentiation into muscle satellite cells." *Stem Cells* **26**(7): 1865-73.
- Sampaolesi, M., S. Blot, et al. (2006). "Mesoangioblast stem cells ameliorate muscle function in dystrophic dogs." *Nature* **444**(7119): 574-9.
- Sampaolesi, M., Y. Torrente, et al. (2003). "Cell therapy of alpha-sarcoglycan null dystrophic mice through intra-arterial delivery of mesoangioblasts." *Science* **301**(5632): 487-92.
- Sato, N., L. Meijer, et al. (2004). "Maintenance of pluripotency in human and mouse embryonic stem cells through activation of Wnt signaling by a pharmacological GSK-3-specific inhibitor." *Nat Med* **10**(1): 55-63.
- Schneuwly, S., R. Klemenz, et al. (1987). "Redesigning the body plan of *Drosophila* by ectopic expression of the homoeotic gene *Antennapedia*." *Nature* **325**(6107): 816-8.
- Schultz, E. (1996). "Satellite cell proliferative compartments in growing skeletal muscles." *Dev Biol* **175**(1): 84-94.
- Scotland, K. B., S. Chen, et al. (2009). "Analysis of Rex1 (zfp42) function in embryonic stem cell differentiation." *Dev Dyn* **238**(8): 1863-77.
- Seale, P., L. A. Sabourin, et al. (2000). "Pax7 is required for the specification of myogenic satellite cells." *Cell* **102**(6): 777-86.
- Shi, X. and D. J. Garry (2006). "Muscle stem cells in development, regeneration, and disease." *Genes Dev* **20**(13): 1692-708.
- Sinanan, A. C., N. P. Hunt, et al. (2004). "Human adult craniofacial muscle-derived cells: neural-cell adhesion-molecule (NCAM; CD56)-expressing cells appear to contain multipotential stem cells." *Biotechnol Appl Biochem* **40**(Pt 1): 25-34.
- Smith, C. K., 2nd, M. J. Janney, et al. (1994). "Temporal expression of myogenic regulatory genes during activation, proliferation, and differentiation of rat skeletal muscle satellite cells." *J Cell Physiol* **159**(2): 379-85.
- Smythe, G. M., M. J. Davies, et al. (2001). "Absence of desmin slightly prolongs myoblast proliferation and delays fusion in vivo in regenerating grafts of skeletal muscle." *Cell Tissue Res* **304**(2): 287-94.

- Stadtfield, M., N. Maherali, et al. (2008). "Defining molecular cornerstones during fibroblast to iPS cell reprogramming in mouse." *Cell Stem Cell* **2**(3): 230-40.
- Stadtfield, M., M. Nagaya, et al. (2008). "Induced pluripotent stem cells generated without viral integration." *Science* **322**(5903): 945-9.
- Steiner, D., H. Khaner, et al. (2010). "Derivation, propagation and controlled differentiation of human embryonic stem cells in suspension." *Nat Biotechnol* **28**(4): 361-4.
- Stephens, L. E., A. E. Sutherland, et al. (1995). "Deletion of beta 1 integrins in mice results in inner cell mass failure and peri-implantation lethality." *Genes Dev* **9**(15): 1883-95.
- Stewart, C. E., P. L. James, et al. (1996). "Overexpression of insulin-like growth factor-II induces accelerated myoblast differentiation." *J Cell Physiol* **169**(1): 23-32.
- Stewart, C. E. and P. Rotwein (1996). "Insulin-like growth factor-II is an autocrine survival factor for differentiating myoblasts." *J Biol Chem* **271**(19): 11330-8.
- Stewart, R., C. Yang, et al. (2008). "Silencing of the expression of pluripotent driven-reporter genes stably transfected into human pluripotent cells." *Regen Med* **3**(4): 505-22.
- Sumariwalla, V. M. and W. H. Klein (2001). "Similar myogenic functions for myogenin and MRF4 but not MyoD in differentiated murine embryonic stem cells." *Genesis* **30**(4): 239-49.
- Sumi, T., N. Tsuneyoshi, et al. (2008). "Defining early lineage specification of human embryonic stem cells by the orchestrated balance of canonical Wnt/beta-catenin, Activin/Nodal and BMP signaling." *Development* **135**(17): 2969-79.
- Syagailo, Y. V., O. Okladnova, et al. (2002). "Structural and functional characterization of the human PAX7 5'-flanking regulatory region." *Gene* **294**(1-2): 259-68.
- Tada, M., T. Tada, et al. (1997). "Embryonic germ cells induce epigenetic reprogramming of somatic nucleus in hybrid cells." *EMBO J* **16**(21): 6510-20.
- Tada, M., Y. Takahama, et al. (2001). "Nuclear reprogramming of somatic cells by in vitro hybridization with ES cells." *Curr Biol* **11**(19): 1553-8.
- Tada, S., T. Era, et al. (2005). "Characterization of mesendoderm: a diverging point of the definitive endoderm and mesoderm in embryonic stem cell differentiation culture." *Development* **132**(19): 4363-74.
- Takahashi, K., K. Tanabe, et al. (2007). "Induction of pluripotent stem cells from adult human fibroblasts by defined factors." *Cell* **131**(5): 861-72.
- Takahashi, K. and S. Yamanaka (2006). "Induction of pluripotent stem cells from mouse embryonic and adult fibroblast cultures by defined factors." *Cell* **126**(4): 663-76.
- Takei, S., H. Ichikawa, et al. (2009). "Bone morphogenetic protein-4 promotes induction of cardiomyocytes from human embryonic stem cells in serum-based embryoid body development." *Am J Physiol Heart Circ Physiol* **296**(6): H1793-803.
- Tanabe, Y., K. Esaki, et al. (1986). "Skeletal muscle pathology in X chromosome-linked muscular dystrophy (mdx) mouse." *Acta Neuropathol* **69**(1-2): 91-5.
- Tatsumi, R. and R. E. Allen (2004). "Active hepatocyte growth factor is present in skeletal muscle extracellular matrix." *Muscle Nerve* **30**(5): 654-8.
- Tatsumi, R., J. E. Anderson, et al. (1998). "HGF/SF is present in normal adult skeletal muscle and is capable of activating satellite cells." *Dev Biol* **194**(1): 114-28.
- Temm-Grove, C. J., D. Wert, et al. (1999). "Microinjection of calpastatin inhibits fusion in myoblasts." *Exp Cell Res* **247**(1): 293-303.
- Tesar, P. J., J. G. Chenoweth, et al. (2007). "New cell lines from mouse epiblast share defining features with human embryonic stem cells." *Nature* **448**(7150): 196-9.
- Thomson, J. A., J. Itskovitz-Eldor, et al. (1998). "Embryonic stem cell lines derived from human blastocysts." *Science* **282**(5391): 1145-7.
- Torrente, Y., M. Belicchi, et al. (2004). "Human circulating AC133(+) stem cells restore dystrophin expression and ameliorate function in dystrophic skeletal muscle." *J Clin Invest* **114**(2): 182-95.
- Toyooka, Y., D. Shimosato, et al. (2008). "Identification and characterization of subpopulations in undifferentiated ES cell culture." *Development* **135**(5): 909-18.

- Tsonis, P. A. and E. J. Fuentes (2006). "Focus on molecules: Pax-6, the eye master." *Exp Eye Res* **83**(2): 233-4.
- Ustanina, S., J. Carvajal, et al. (2007). "The myogenic factor Myf5 supports efficient skeletal muscle regeneration by enabling transient myoblast amplification." *Stem Cells* **25**(8): 2006-16.
- Vaittinen, S., R. Lukka, et al. (2001). "The expression of intermediate filament protein nestin as related to vimentin and desmin in regenerating skeletal muscle." *J Neuropathol Exp Neurol* **60**(6): 588-97.
- Vallier, L., S. Mendjan, et al. (2009). "Activin/Nodal signalling maintains pluripotency by controlling Nanog expression." *Development* **136**(8): 1339-49.
- Wagner, K. E. and M. C. Vemuri (2010). "Serum-free and feeder-free culture expansion of human embryonic stem cells." *Methods Mol Biol* **584**: 109-19.
- Wakayama, T., A. C. Perry, et al. (1998). "Full-term development of mice from enucleated oocytes injected with cumulus cell nuclei." *Nature* **394**(6691): 369-74.
- Wang, J., L. Y. Xie, et al. (1998). "Myc activates telomerase." *Genes Dev* **12**(12): 1769-74.
- Wang, L., C. Cerdan, et al. (2006). "Derivation and characterization of hematopoietic cells from human embryonic stem cells." *Methods Mol Biol* **331**: 179-200.
- Watt, D. J., K. Lambert, et al. (1982). "Incorporation of donor muscle precursor cells into an area of muscle regeneration in the host mouse." *J Neurol Sci* **57**(2-3): 319-31.
- Weitzer, G., D. J. Milner, et al. (1995). "Cytoskeletal control of myogenesis: a desmin null mutation blocks the myogenic pathway during embryonic stem cell differentiation." *Dev Biol* **172**(2): 422-39.
- Wernig, M., J. P. Zhao, et al. (2008). "Neurons derived from reprogrammed fibroblasts functionally integrate into the fetal brain and improve symptoms of rats with Parkinson's disease." *Proc Natl Acad Sci U S A* **105**(15): 5856-61.
- Wilmut, I., A. E. Schnieke, et al. (1997). "Viable offspring derived from fetal and adult mammalian cells." *Nature* **385**(6619): 810-3.
- Wozniak, A. C. and J. E. Anderson (2007). "Nitric oxide-dependence of satellite stem cell activation and quiescence on normal skeletal muscle fibers." *Dev Dyn* **236**(1): 240-50.
- Wu, Y. and P. Y. Wu (2009). "CD133 as a marker for cancer stem cells: progresses and concerns." *Stem Cells Dev* **18**(8): 1127-34.
- Yablonka-Reuveni, Z. and A. J. Rivera (1994). "Temporal expression of regulatory and structural muscle proteins during myogenesis of satellite cells on isolated adult rat fibers." *Dev Biol* **164**(2): 588-603.
- Yamanaka, S. and H. M. Blau "Nuclear reprogramming to a pluripotent state by three approaches." *Nature* **465**(7299): 704-12.
- Yang, C., S. Przyborski, et al. (2008). "A key role for telomerase reverse transcriptase unit in modulating human embryonic stem cell proliferation, cell cycle dynamics, and in vitro differentiation." *Stem Cells* **26**(4): 850-63.
- Ying, Q. L., J. Nichols, et al. (2003). "BMP induction of Id proteins suppresses differentiation and sustains embryonic stem cell self-renewal in collaboration with STAT3." *Cell* **115**(3): 281-92.
- Yocum, A. K., T. E. Gratsch, et al. (2008). "Coupled global and targeted proteomics of human embryonic stem cells during induced differentiation." *Mol Cell Proteomics* **7**(4): 750-67.
- Yu, J., K. Hu, et al. (2009). "Human induced pluripotent stem cells free of vector and transgene sequences." *Science* **324**(5928): 797-801.
- Yu, J. and J. A. Thomson (2008). "Pluripotent stem cell lines." *Genes Dev* **22**(15): 1987-97.
- Yu, J., M. A. Vodyanik, et al. (2007). "Induced pluripotent stem cell lines derived from human somatic cells." *Science* **318**(5858): 1917-20.
- Yuan, H., N. Corbi, et al. (1995). "Developmental-specific activity of the FGF-4 enhancer requires the synergistic action of Sox2 and Oct-3." *Genes Dev* **9**(21): 2635-45.
- Yusa, K., R. Rad, et al. (2009). "Generation of transgene-free induced pluripotent mouse stem cells by the piggyBac transposon." *Nat Methods* **6**(5): 363-9.
- Zammit, P. S., J. P. Golding, et al. (2004). "Muscle satellite cells adopt divergent fates: a mechanism for self-renewal?" *J Cell Biol* **166**(3): 347-57.

- Zammit, P. S., T. A. Partridge, et al. (2006). "The skeletal muscle satellite cell: the stem cell that came in from the cold." *J Histochem Cytochem* **54**(11): 1177-91.
- Zammit, P. S., F. Relaix, et al. (2006). "Pax7 and myogenic progression in skeletal muscle satellite cells." *J Cell Sci* **119**(Pt 9): 1824-32.
- Zeng, X., T. Miura, et al. (2004). "Properties of pluripotent human embryonic stem cells BG01 and BG02." *Stem Cells* **22**(3): 292-312.
- Zeschnigk, M., D. Kozian, et al. (1995). "Involvement of M-cadherin in terminal differentiation of skeletal muscle cells." *J Cell Sci* **108 (Pt 9)**: 2973-81.
- Zhang, P., J. Li, et al. (2008). "Short-term BMP-4 treatment initiates mesoderm induction in human embryonic stem cells." *Blood* **111**(4): 1933-41.
- Zheng, J. K., Y. Wang, et al. (2006). "Skeletal myogenesis by human embryonic stem cells." *Cell Res* **16**(8): 713-22.
- Zhou, H., S. Wu, et al. (2009). "Generation of induced pluripotent stem cells using recombinant proteins." *Cell Stem Cell* **4**(5): 381-4.